



## **Terms and Conditions of Use of Digitised Theses from Trinity College Library Dublin**

### **Copyright statement**

All material supplied by Trinity College Library is protected by copyright (under the Copyright and Related Rights Act, 2000 as amended) and other relevant Intellectual Property Rights. By accessing and using a Digitised Thesis from Trinity College Library you acknowledge that all Intellectual Property Rights in any Works supplied are the sole and exclusive property of the copyright and/or other IPR holder. Specific copyright holders may not be explicitly identified. Use of materials from other sources within a thesis should not be construed as a claim over them.

A non-exclusive, non-transferable licence is hereby granted to those using or reproducing, in whole or in part, the material for valid purposes, providing the copyright owners are acknowledged using the normal conventions. Where specific permission to use material is required, this is identified and such permission must be sought from the copyright holder or agency cited.

### **Liability statement**

By using a Digitised Thesis, I accept that Trinity College Dublin bears no legal responsibility for the accuracy, legality or comprehensiveness of materials contained within the thesis, and that Trinity College Dublin accepts no liability for indirect, consequential, or incidental, damages or losses arising from use of the thesis for whatever reason. Information located in a thesis may be subject to specific use constraints, details of which may not be explicitly described. It is the responsibility of potential and actual users to be aware of such constraints and to abide by them. By making use of material from a digitised thesis, you accept these copyright and disclaimer provisions. Where it is brought to the attention of Trinity College Library that there may be a breach of copyright or other restraint, it is the policy to withdraw or take down access to a thesis while the issue is being resolved.

### **Access Agreement**

By using a Digitised Thesis from Trinity College Library you are bound by the following Terms & Conditions. Please read them carefully.

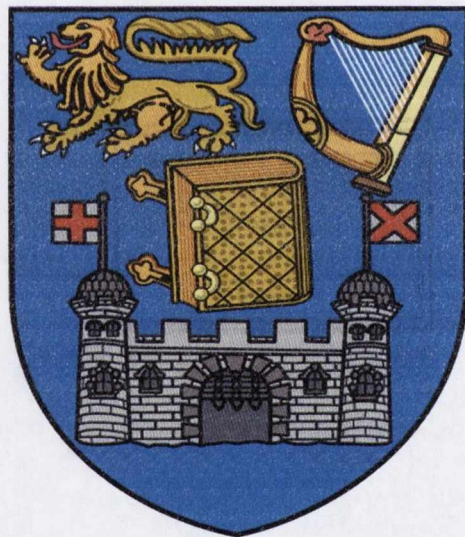
I have read and I understand the following statement: All material supplied via a Digitised Thesis from Trinity College Library is protected by copyright and other intellectual property rights, and duplication or sale of all or part of any of a thesis is not permitted, except that material may be duplicated by you for your research use or for educational purposes in electronic or print form providing the copyright owners are acknowledged using the normal conventions. You must obtain permission for any other use. Electronic or print copies may not be offered, whether for sale or otherwise to anyone. This copy has been supplied on the understanding that it is copyright material and that no quotation from the thesis may be published without proper acknowledgement.

# **The Role of MyD88 in Embryonal Carcinoma Stem Cells**

**Gomaa M. A. Sulaiman**

**02155451**

**Department of Histopathology and Morbid Anatomy,  
School of Medicine  
University of Dublin,  
Trinity College**



**A thesis submitted to Trinity College,  
University of Dublin  
For the degree of  
Doctor of Philosophy  
September 2015**

**Under the supervision of Professor John O'Leary**

**And**

**Dr. Michael Gallagher**

**TRINITY LIBRARY**  
08 MAR 2017  
**DUBLIN**

*Thesis 11177*

# Table of Contents

<b>Table of Contents</b> .....	i
<b>List of Figures</b> .....	x
<b>List of Tables</b> .....	xiv
<b>List of Supplementary Tables</b> .....	xv
<b>Abbreviations</b> .....	xvi
<b>List of Publications</b> .....	xix
<b>Declaration</b> .....	xx
<b>Dedication</b> .....	xxi
<b>Acknowledgements</b> .....	xxii
<b>Abstract</b> .....	xxiv
<b>1 General Introduction</b>	
1.1 Overview.....	1
1.2 Stem Cells are Arranged as Hierarchies.....	2
1.3 Pluripotent Stem Cells.....	4
1.4 Tumour Production is Initiated and Driven by Cancer Stem Cells.....	8
1.5 The Embryonal Carcinoma Cancer Stem Cell Model.....	9
1.6 Retinoic Acid Signaling and NTera2 Embryonal Carcinoma Cell Differentiation.....	11
1.7. Toll-Like Receptor Signaling.....	13
1.8. Myeloid Differentiation Response Gene 88 (MyD88).....	15
1.9. MyD88 Data Previously Generated by our Group.....	17
1.10. Aims and Hypotheses.....	18

## 2 Materials and Methods

2.1 Cell Culture.....	19
2.1.1 Cell Counting.....	19
2.1.2. Conditioned Media Experiments.....	20
2.2 Differentiation Protocols.....	20
2.2.1 Retinoic Acid.....	20
2.2.2 Endoderm Differentiation Kit.....	21
2.2.3. Mesoderm Differentiation Kit.....	21
2.2.4. Ectoderm Differentiation Kit.....	21
2.2.5 Detection of Differentiation via Alkaline Phosphatase Assay.....	21
2.3 siRNA Transfections.....	22
2.3.1 Transfection of 2102Ep cells in a 24-well plates.....	22
2.3.1.1 Forward transfection.....	22
2.3.1.2 Reverse transfection.....	22
2.3.1.3 Reverse transfection followed by Forward transfection.....	22
2.4 MyD88 Peptide Inhibition in 2102Ep cells.....	23
2.4.1 MyD88 Peptide Inhibitor Treatment.....	23
2.4.2 Validation of MyD88 Peptide Inhibition via Interleukin-1 beta Treatment.....	23
2.5 TaqMan qPCR Analysis.....	24
2.6 Flow cytometry.....	24
2.7 Fluorescence Activated Cell Sorting (FACS).....	24
2.8 Statistical Analysis (Flow Cytometry and qPCR).....	25

3.4.2. A Technical Comment on the use of siRNAs.....	55
3.5 Conclusion.....	55
<b>4. MyD88 is a Retinoic Acid Differentiation Gatekeeper in 2102Ep hEC cells.</b>	
4.1 Introduction.....	57
4.1.1. Cripto-1 Expression Marks Two Sub-Populations of NTERA2 Pluripotent Embryonal Carcinoma Cells.....	58
4.1.2. Is MyD88 a Retinoic Acid Differentiation Gatekeeper in Embryonal Carcinoma CSCs?.....	59
4.1.3. Is MyD88 an Absolute Differentiation Gatekeeper in Embryonal Carcinoma CSCs?.....	60
4.1.4 Aims and Hypothesis .....	63
4.2 Materials and Methods.....	63
4.3 Results	
4.3.1 NTERA2 cells treated with RA can be distinguished by SSEA4, Oct4, Sox2 and Nanog expression. Highly Express SSEA4 in the Undifferentiated State.....	64
4.3.2 Force-Differentiated 2102Ep cells can be distinguished by SSEA4 and Oct4, Sox2, Nanog expression.....	66
4.3.3. Loss of MyD88 Does Not Effect 2102Ep SSEA4 expression.....	68
4.3.4. 2102Ep cells contain 2 sub-populations, only one of which differentiates in MyD88PepInh +RA conditions.....	69
4.3.5. Separated SSEA4 <sup>Pos</sup> and SSEA4 <sup>Neg</sup> MyD88PepInh+RA Treated	

2.9 Whole-Genome Gene Expression Array Analysis.....	25
2.10 microRNA Expression Array Analysis.....	28
2.11 Gene Array Data Analysis	
2.11.1. Affymetrix Data Analysis.....	29
2.11.2. miRNA-Target Interaction Analysis.....	30
2.11.3. Pathway Analysis.....	30
<b>3. Peptide Inhibition of MyD88 Leads to Differentiation of 2102Ep cells</b>	
3.1.1. Introduction.....	31
3.1.2. Demonstrating Stem Cell Differentiation.....	31
3.1.3. Inhibition of MyD88 via Peptide Inhibitor.....	34
3.1.4. Aims and Hypothesis.....	35
3.2. Materials and Methods.....	35
3.3. Results.....	36
3.3.1. siRNA is an unsuitable approach for knockdown of MyD88 in 2102Ep Cells.....	36
3.3.2. Loss of MyD88 does not Affect Oct4-Sox2-Nanog Expression.....	42
3.3.3. siRNA-Knockdown of MyD88 does not Permit Differentiation of 2102Ep Cells in Response to Retinoic Acid.....	43
3.3.4. MyD88 Peptide Inhibitor Facilitates Retinoic Acid-Induced Differentiation of 2102Ep Cells.....	45
3.4. Discussion.....	51
3.4.1. The Relationship Between Self-Renewal and Differentiation.....	51

5.2 Materials and Methods.....	95
5.3 Results.....	96
5.3.1. Defining the MyD88 Inhibition Mechanism: Comparison of MyD88PepInh and CtrlPepInh Treated 2102Ep cells.....	96
5.3.1.1. An Overview of Gene Array Analysis of the MyD88 Inhibition Mechanism.....	96
5.3.1.2. Loss of MyD88 Affects HOX, Taste Receptor and Olfactory Receptor Genes.....	98
5.3.1.3. Inhibition of MyD88 does not Affect Expression of Pluripotency Markers Oct4-Sox2 Nanog.....	99
5.3.1.4. Inhibition of MyD88 Appears to Activate MyD88-Independent TLR Signalling.....	100
5.3.1.5. MyD88 Inhibition Does Not Alter RA Signaling Genes.....	100
5.3.1.6. MyD88 Regulates Taste and Olfactory Receptor Gene Expression.....	100
5.3.1.7. Loss of MyD88 Activates HOX Gene Expression.....	101
5.3.1.8. Summary of MyD88 Inhibition Data.....	102
5.3.2. Identification of the MyD88 Inhibition Facilitated RA Differentiation Mechanism: Comparison of MyD88PepInh Treated and SSEA4 <sup>Neg</sup> Cells.....	103
5.3.2.1. Loss of MyD88 in the Presence of RA Facilitates Differentiation of 2102Ep cells via Upregulation of RA Signaling.....	103
5.3.2.2. Inhibition of MyD88 in Combination with RA Treatment Appears to	



2102Ep cells Express Oct4-Sox2-Nanog at High and Low Levels Respectively.....	71
4.3.6. MyD88 Inhibition Facilitates Non-RA Lineage Differentiation Mechanisms.....	73
4.3.7. Differentiated Ntera2 Cells Secrete Factors That are Sufficient to Differentiate Undifferentiated Ntera2 Cells.....	77
4.3.8. Can the 2102Ep Sub-Populations be Isolated via De-Differentiation...	80
4.4 Discussion.....	82
4.4.1 MyD88 is a Differentiation Gatekeeper in Pluripotent Cells.....	83
4.4.2 MyD88 is a Novel Upstream Regulator of Oct4-Sox2-Nanog.....	84
4.4.3 Loss of MyD88 Facilitates Transition to a Primed Self-Renewal State.....	85
4.4.4 Proposed model of MyD88-regulated differentiation in 2102Ep Cells.....	85

## **5 MyD88 Inhibition Facilitates Differentiation of 2102Ep Cells Through Activation of Retinoic Acid Signaling**

5.1. Introduction	
5.1.1 Overview.....	88
5.1.2 Hox Genes are Key Developmental/Differentiation Regulators.....	89
5.1.3 Taste Receptor Family 2.....	90
5.1.4 Olfactory Receptors.....	91
5.1.5. MicroRNAs.....	93
5.1.6. Aims & Hypotheses.....	95

Further Activate MyD88-Independent TLR Signaling.....	105
5.3.2.3. MyD88 Inhibition Permits 2102Ep Activation of RA Signaling in Response to RA.....	105
5.3.2.4. Inhibition of MyD88 in Combination with RA Treatment Appears to Rescue Taste and Olfactory Receptor Gene Expression.....	106
5.3.2.5. Loss of MyD88 Facilitates Upregulation of HOX Genes During RA Treatment.....	107
5.3.2.6. Summary of SSEA4 <sup>Neg</sup> Differentiation Data.....	107
5.3.3. MicroRNA Array Analysis Identifies Several Cancer and Stem Cell Differentiation miRs Associated with MyD88 Inhibition.....	108
5.3.4. SR <sup>PR</sup> Differentiation is/is not similar, but not identical, to RA-Induced NTera2 Differentiation.....	111
5.3.5. Identification of Putative SR <sup>PR</sup> Markers.....	112
5.4 Discussion.....	115
5.4.1 MyD88 Promotes Nullipotency by Preventing the 2102Ep Response to RA.....	116
5.4.2. MyD88 Promotes Nullipotency By Inhibiting HOXA/D Family Gene Expression.....	117
5.4.3. Taste and Olfactory Receptors Are Novel Regulators of Nullipotency /Pluripotency.....	118
5.4.4 MyD88-Independent TLR Signaling Drives Differentiation of 2102Ep Cells.....	120
5.4.5. Future Work: Isolation of SR <sup>PR</sup> cells.....	121

5.5 Conclusion.....	122
<b>6 General Discussions</b>	
6.1 Overview.....	124
6.2 MyD88 is a Novel Upstream Regulator of Oct4-Sox2-Nanog.....	125
6.3 Differentiation from Pluripotent Cells is not a Single-Coupled Process.....	126
6.4 A New Model of NTera2 Differentiation.....	128
6.5. Are the 2102Ep Sub-Populations a Stem-Progenitor Cell Hierarchy?.....	129
6.6 Differentiation Gate-Keepers May Facilitate Differentiation-Resistance in CSCs.....	130
6.7 The Potential Importance of MyD88 to Regenerative Medicine.....	132
<b>References</b> .....	134
<b>Appendix 1</b> .....	142
<b>Appendix 2</b> .....	144

## List of Figures

Figure 1.1 Stem Cell division.....	3
Figure 1.2 Hematopoietic stem cell differentiation.....	4
Figure 1.3. The Ground State Model of ES Differentiation.....	7
Figure 1.4. The Competition Model of ES Differentiation.....	7
Figure 1.5. Tumour-Initiation by CSCs.....	9
Figure 1.6. The Retinoic Acid Signaling Pathway.....	13
Figure 1.7. Toll-like Receptor (TLR) Signalling Pathway.....	16
Figure 2.1 Work Flow of Whole-Genome Gene Expression Array Analysis.....	27
Figure 2.2 Work Flow of Whole-Genome MicroRNA Expression Array Analysis.....	29
Figure 3.1. Typical undifferentiated and differentiated morphologies of 2102Ep cells.....	32
Figure 3.2. Mode of Action of MyD88 Peptide Inhibitor.....	35
Figure 3.3 Knockdown of MyD88 in 2102Ep Cells Using Different siRNA Concentrations.....	37
Figure 3.4 Knockdown of MyD88 in 2102Ep Cells Assessed At Different Concentrations Over Time.....	38
Figure 3.5. Liopfectamine RNAiMax improves MyD88 knockdown in 2102Ep cells.....	39
Figure 3.6. 'OptiMEM' media further enhances transfection efficiency.....	40
Figure 3.7. Transfection of 2012Ep cells with siMyD88 using Lipofectamine RNAi max in OptiMEM media.....	41

Figure 3.8. A comparison of reverse and forward+reverse transfection approaches.....	42
<u>Figure 3.9.</u> The effect of knocking down MyD88 on Oct4-Sox2-Nanog Expression in 2102EP cells.....	43
<u>Figure 3.10.</u> Pre-Treatment of 2102Ep cells with Retinoic Acid does not Affect Knockdown Efficiency.....	44
<u>Figure 3.11.</u> The Addition of Retinoic Acid to siMyD88 Transfected Cells does not Induce Differentiation via Changes in Oct4, Sox2, Nanog Expression.....	44
Figure 3.12. The MyD88 Peptide Inhibitor Inhibits MyD88-dependent TLR Signaling.....	46
<u>Figure 3.13.</u> MyD88PepInh+RA Treatment Induces a Differentiation Phenotype.....	47
<u>Figure 3.14.</u> MyD88PepInh+RA Treatment Inhibits Growth of 2102Ep cells.....	47
<u>Figure 3.15.</u> MyD88PepInh+RA Treatment Reduces Oct4-Sox2-Nanog Expression.....	48
<u>Figure 3.16.</u> Alkaline Phosphatase (AP) Expression Indicates that MyD88PepInh+RA Treated 2102Ep cells are in an Undifferentiated State.....	49
<u>Figure 3.17.</u> MyD88PepInh+RA Treated 2102Ep cells appear as 2 sub-populations.....	50
<u>Figure 3.18.</u> The Relationship Between Self-Renewal and Differentiation.....	52
<u>Figure 3.19.</u> Loss of MyD88 Facilitates Transition to an Intermediate Stem Cell State.....	53
<u>Figure 3.20.</u> The 'Ground State' Model of Pluripotency.....	54

Figure 4.1. The Competition Model of Human Embryonic Stem Cell	
Differentiation.....	62
Figure 4.2. Three Parameters Used in Flow Cytometry Analysis.....	65
Figure 4.3. NTera2 Cells Highly Express SSEA4 in the Undifferentiated State.....	65
Figure 4.4. SSEA4 Expression Does Not Discriminate Between 2102Ep Cells in -RA	
versus +RA Conditions.....	67
Figure 4.5. SSEA4 Expression Discriminates Undifferentiated and Differentiated	
2102Ep Cells.....	67
Figure 4.6. Loss of MyD88 Does Not Effect SSEA4 Expression in 2102Ep Cells....	68
Figure 4.7. CtrlPepInh Treated 2102Ep Cells Similarly Highly Express SSEA4 in -RA	
and +RA Conditions.....	70
Figure 4.8. Validation of the Two Sub-Population Hypothesis.....	70
Figure 4.9. Separation and Molecular Analysis of the Two 2102Ep	
Sub-Populations.....	72
Figure 4.10. MyD88 inhibition Does not Effect Cellular Morphology of 2102Ep Cells	
in Lineage Differentiation Conditions.....	75
Figure 4.11. MyD88 inhibition Effects SSEA4 Expression in 2102Ep Cells in	
Endoderm Lineage Differentiation Conditions.....	75
Figure 4.12. MyD88 inhibition Effects SSEA4 Expression in 2102Ep Cells in	
Ectoderm Differentiation Conditions.....	76
Figure 4.13. MyD88 inhibition Effects SSEA4 Expression in 2102Ep Cells in	
Mesoderm Differentiation Conditions.....	77
Figure 4.14. NTera2 Cells Secrete Stem Cell State Specific Factors That Promote	

Figure 4.14 Self-Renewal and Differentiation.....	79
Figure 4.15 DiffConn Media Induces Differentiation of MyD88PepInh-treated 2102Ep.....	80
Figure 4.16. Primed Self-Renewing State 2102Ep Cells can be Isolated via De- Differentiation.....	82
Figure 4.17. Early Model of MyD88-Regulation Differentiation.....	87
Figure 4.18. Proposed Model of MyD88-Regulation Differentiation.....	87
Figure 5.1. Hox Gene Family Organisation.....	90
Figure 5.2. The Taste Sensation Signaling Pathway.....	91
Figure 5.3. Olfactory Receptor Signaling.....	93
Figure 5.4. MicroRNA Biogenesis.....	95
Figure 5.5. Overview of Gene Expression Array Analysis in Chapter 5.....	97
Figure 5.6. Gene Expression Array Analysis of MyD88PepInh and CtrlPepInh Samples.....	98
Figure 5.7. Gene Expression Array Analysis of MyD88PepInh and SSEA4 <sup>Neg</sup> .....	104
Figure 5.8. MicroRNA Expression Array Analysis of MyD88PepInh and CtrlPepInh Samples.....	109
Figure 5.9. Proposed Model of Differentiation Regulated by MyD88-Independent TLR Signaling.....	120
Figure 5.10. Validation of Putative SR <sup>PR</sup> cells.....	122
Figure 6.1. A Unified Model of RA-Induced Differentiation of NTera2 hEC Cells...	129
Figure 6.2 The Primed Self-Renewal State Stem Cell Hierarchy Model.....	130

## List of Tables

Table 5.1. Comparison of MyD88 PepInh Samples to Control PepInh treated	
Samples.....	99
Table 5.2. Taste and Olfactory Receptors altered in MyD88PepInh	
versus Ctrl.....	101
Table 5.3. HOX genes altered in MyD88PepInh versus Ctrl.....	
	102
Table 5.4. Comparison of SSEA4 <sup>Neg</sup> Samples to MyD88 PepInh	
treated samples.....	104
Table 5.5. Downregulation of Oct4, Sox2 and Nanog in SSEA4 <sup>Neg</sup> cells.....	
	104
Table 5.6. TLR genes altered in SSEA4 <sup>Neg</sup> cells versus MyD88PepInh	
treated cells.....	105
Table 5.7. RA signaling genes altered in SSEA4 <sup>Neg</sup> cells versus MyD88PepInh	
treated cells.....	106
Table 5.8. HOX genes altered in SSEA4 <sup>Neg</sup> cells versus MyD88PepInh	
treated cells.....	107
Table 5.9. Top miRNAs upregulated in MyD88 PepInh treated cells.....	
	110
Table 5.10 Top miRNAs downregulated in MyD88 PepInh treated cells.....	
	111
Table 5.11 Identification of putative SR <sup>PR</sup> Markers (upregulated in SR <sup>PR</sup> cells).....	
	113
Table 5.12. Identification of putative SR <sup>PR</sup> Markers (downregulated in	
SR <sup>PR</sup> cells.....	114



## List of Supplementary Tables

**Table S1.** Full genelist for MyD88PepInh versus Ctrl PepInh Experiment.

**Table S2.** Full DAVID analysis output for MyD88PepInh versus Ctrl PepInh Experiment.

**Table S3.** Full gene list for MyD88 PepInh versus SSEA4<sup>Neg</sup> Experiment.

**Table S4.** Full DAVID analysis output for MyD88PepInh versus SSEA4<sup>Neg</sup> Experiment.

**Table S5.** Full gene list for SSEA4<sup>Neg</sup> versus SSEA4<sup>Pos</sup> versus Experiment.

**Table S6.** Full microRNA genelist for MyD88PepInh versus CtrlPepInh Experiment.

## Abbreviations

- AC3: Type 3 Adenylyl Cyclase
- AD: Asymmetric Division
- AP: Alkaline Phosphatase
- BdUR: Bromodeoxyuridine
- cDNA: Complementary DNA
- CNGC: Cyclic Nucleotide-Gated Channel
- CR-1: 'Cripto-1' Gene
- CRABPs: Cellular RA Binding Proteins
- CRBPs: Cellular Retinol Binding Proteins
- cRNA: Biotinylated RNA synthesised from cDNA
- CSC: Cancer Stem Cell
- CYP26: Cytochrome p450 Family 26
- DMEM: Dulbecco's Modified Eagle Medium
- DMSO: Dimethyl Sulfoxide
- EC: Embryonal carcinoma (cells)
- EGF: Epidermal Growth Factor
- ELISA: Enzyme-Linked Immunosorbent Assay
- EOC: Epithelial ovarian carcinoma
- EpiSC: Epiblast-like stem cell
- ES: Embryonic stem (cells)
- EZH: Enhancer of Zest Homologue
- FACS: Florescent-Activated Cell Sorting
- FBS: Foetal Bovine Serum
- FGF: Fibroblast Growth Factor
- GAPDH: Glyceraldehyde 3-phosphate dehydrogenase
- GPCRs: G protein-coupled receptors

GSIs: Gamma Secretase Inhibitors  
hEC: Human Embryonal Carcinoma  
hES: Human Embryonic Stem (cells)  
HGF: Hepatocyte Growth Factor  
Hh: Hedgehog  
HMBA: Hexamethylene Bisacetamide  
HSC: Haematopoietic Stem Cell  
IL: InterLeukin  
IL-1 $\beta$ : Interleukin –one beta  
IPS: Induced Pluripotent Stem  
IRF: Interferon Regulatory Factor  
LPS: LipoPolySaccharide  
mES: Mouse Embryonic Stem (Cell)  
miRNA: Micro RNA  
mRNA: messenger RNA  
MTI: miRNA-Target Interaction  
MyD88: Myeloid Differentiation Primary Response Gene 88  
MSC: Mesenchymal Stem Cell  
NF- $\kappa$ B: Nuclear Factor kappa light polypeptide gene enhancer in B cells  
NGF: Neural Growth Factor  
ORs: Olfactory Receptors  
OSNs: Olfactory Sensory Neurons  
PAMPs: Pathogen Associated Molecular Patterns  
PBS: Phosphate Buffered Salin  
PcG: Polycomb group  
Phospho I- $\kappa$ B $\alpha$ : Phosphoylated I-Kappa-B-alpha  
PKA : protein kinase A

PI: Propidium Iodide

PRRs: Pattern Recognition Receptors

q-PCR: Quantitative Polymerase Chain Reaction

RA: Retinoic Acid (*all-trans*)

RALDH: Retinaldehyde Dehydrogenase

RAR: Retinoic Acid Receptor:

RARE: Retinoic Acid response element

RBPs: Retinol Binding Proteins

RDH: Retinol Dehydrogenase

RISC: RNA-Induced Silencing Complex

RXR: Retinoid X Receptor

shRNA: Short Hairpin RNA

siRNA: Small Interfering RNA

Shh: Sonic Hedgehog

SR: Self-Renewal

SR<sup>PR</sup>: Primed Self-Renewal

SSEA4: Stage Specific Embryonic Antigen 4

STRA6: Stimulated by RA 6

TGF- $\beta$ : Transforming Growth Factor-beta

TIR: Toll/Interleukin-1 Receptor

TLR: Toll-Like Receptor

TNF- $\alpha$ : Tumour Necrosis Factor –Alpha

TRs: Taste Receptors

UTR: 3' Untranslated Region

## List of Publications

### Publications

Sulaiman et al. MyD88 is a Differentiation Gatekeeper in Human, Pluripotent Embryonal Carcinoma Stem Cells **2016** (In prep)

### Meetings

Sulaiman et al. MyD88 is a Differentiation Gatekeeper in Nullipotent Embryonal Carcinoma Stem Cells. United States and Canadian Association of Pathologists (USCAP) Annual Meeting **2015**.

Sulaiman et al. Inhibition of MyD88 Facilitates Primed-State transition During Differentiation of Nullipotent Embryonal Carcinoma Cancer Stem Cells. Pathology Society of Great Britain and Ireland (PathSoc) Annual Meeting, **2015**.

Sulaiman et al. Inhibition of MyD88 Facilitates Primed-State transition During Differentiation of Nullipotent Embryonal Carcinoma Cancer Stem Cells. Irish Association of Cancer Researchers (IA-CR) Annual Meeting, **2015**.

Sulaiman et al. Inhibition of MyD88 Permits Forced-Differentiation of Nullipotent Embryonal Carcinoma Cancer Stem Cells. IA-CR Annual Meeting **2014**.

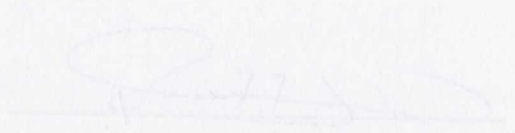
Sulaiman et al. Secretion of Specific Toll-Like Receptor Signaling Proteins in the Response of Embryonal Carcinoma Cancer Stem Cells to Differentiation, Hypoxia and Chemotherapy. IA-CR Annual Meeting **2013**.

## Declaration

I declare that this is my own work and has not been submitted previously for a PhD degree at this or any other university. I agree that the library may lend or copy this thesis on request.



## Dedication

A handwritten signature in blue ink, appearing to be 'Gomez Suliman', written over a horizontal line.

Gomez Suliman

**This work is dedicate to the soul of my mother in law Embarka Rahumah,  
whose leaving deeply saddened us**

## Acknowledgements

Firstly I would like to express my sincerest gratitude to My Supervisor Professor John O'Leary for his support, encouragement and for giving me the opportunity to carry out this research.

I would like deeply to express my very big thanks and appreciation to My Second Supervisor Dr. Michael Gallagher for his patience, support, encouragement, technical advice and for instructing me in the way of writing the thesis. Mic, without God and your unlimited help and support, carrying out this project could not be possible.

Also I would like to express my thanks to all of my colleagues in the Coombe Women's and St James Hospital, especially to Dr. Cathy Spillane for her help with the gene and microRNA array analysis, and to my PhD mates Claudia Gasch and Mark Bates

I would especially like to thank all of Dr. Eamon Breen for his help with the Flow Cytometry and FACS, Dr. Gordon Blackshields for his help with the bioinformatics analyses. Sincere thanks also goes to My closest friend Mehdi Ahmed and his wife Francis for their help and support and to Professor Salem Mudallel for all of his helpful advice.

I wish to express my gratitude and deepest thanks to my brothers and sisters in law for everything,

A huge thanks with love goes to my parents Azeza and Emhemmed, who always ask God to help me prosper, and to my brothers and sisters. I am forever indebted to you.

I would like to express my particularly gratitude and thanks to my wife Salwa for all her help, without whom all would have been so much more difficult, and my big deep love is expressed to my children Laith, Mohammed, Dana, Dina and Taim.

Finally I ask God to have mercy on my mother in law, to forgive her and allow her to rest in peace



## Abstract

Tumour-initiating cells are known to share some properties with stem cells. These so called 'Cancer Stem Cells' (CSCs) are highly tumourigenic in the undifferentiated state, a property that is lost upon CSC differentiation. For many years, our group has studied CSC differentiation in a nullipotent embryonal carcinoma CSC cell line (2102Ep), which can resist differentiation to produce highly-aggressive tumours. Previous work in the lab highlighted a potential role for Toll-Like Receptor (TLR) Signaling mediator protein Myeloid Differentiation Response Gene 88 (MyD88) in the mechanism through which 2102Ep cells resist differentiation. This led to a hypothesis that manipulation of MyD88 may allow forced-differentiation of 2102Ep cells to remove their tumorigenic potential. However, in previous studies, this mechanism was only observed sporadically. This indicated that an improved MyD88 knockdown/inhibition protocol was required for elucidation of the MyD88 regulated differentiation mechanism. Addressing this, the initial aim of this project was to develop an experimental model through which the role of MyD88 in 2102Ep differentiation-resistance could be studied. The project subsequently aimed to fully characterize this mechanism towards an improved understanding of differentiation-resistance in CSCs.

This thesis describes how an experimental model was established, through which loss of MyD88 was shown to facilitate differentiation of 2102Ep cells. Specifically, loss of MyD88 opened 2102Ep cells to differentiation in response to the morphogen 'retinoic acid' (RA). A differentiation phenotype was clearly observed but was not accompanied by appropriate changes in stem cell markers. This inconsistency led to a new hypothesis that the 2102Ep cell line contained 2 sub-populations.

The thesis subsequently describes how these 2 sub-populations were isolated via flow cytometry for undifferentiated pluripotent stem cell marker Stage Specific Embryonic Antigen 4 (SSEA4). The first sub-population appears to be fully nullipotent and capable of resisting differentiation. The second sub-population can differentiate in response to RA-treatment, via a standard Oct4-Sox2-Nanog mechanism, once MyD88 function is ablated. This indicates the presence of a two-step differentiation mechanism, which is unusual in terms of stem cell biology. The

novel sub-population identified, appears to move into a new 'Primed Self-Renewal (SR<sup>PR</sup>) State' following loss of MyD88, a concept that has been mostly only hypothesized. Mechanistically, this role is shown to relate to the secretion of self-renewal and differentiation promoting factors by these cells via MyD88-dependent and MyD88-independent TLR Signaling respectively. The data indicate that this is the normal differentiation response of pluripotent cells to RA, which is somehow inhibited in 2102Ep cells. In additional experiments, it is shown that MyD88 is not RA-specific, as its inhibition facilitates differentiation in response to other differentiation stimuli.

The thesis concludes with gene array characterisation of the molecular events regulated by A) MyD88 and B) loss of MyD88 in combination with RA. This analysis revealed that the primary role of MyD88 in the undifferentiated state is inhibition of Hox gene expression. Upon loss of MyD88, Hox gene expression is increased, which appears to define the SR<sup>PR</sup> state, which can now respond to RA via activation of the RA signaling pathway.

In conclusion, this project has identified MyD88 as a novel Differentiation Gate-Keeper in pluripotent and nullipotent embryonal carcinoma cells. The data suggests that targeting of specific differentiation gate-keepers in other malignancies may increase the efficiency of forced-differentiation in the clinic. Additionally, as a potential regulator of non-malignant pluripotent cells, it is proposed that inhibition of MyD88 may increase the efficiency of directed differentiation of non-malignant pluripotent cells in regenerative medicine.

# Chapter 1

## General Introduction

### 1.1. Overview

The mechanisms through which Cancer Stem Cells (CSCs) promote their undifferentiated 'self-renewal' state and promote or resist differentiation are of huge interest to CSC researchers. This is due to the well-established observation that CSCs can generate tumours while in an undifferentiated state but lose this ability upon differentiation. All cancers maintain a population of CSCs in the tumour by employing mechanisms to resist differentiation stimuli, which are ever-present in the tumour micro-environment. If these mechanisms could be understood, it should be possible to develop novel anti-cancer therapies based on pushing CSCs in to a non-tumourigenic differentiated state. These so called 'Forced Differentiation' approaches are of huge interest to CSC researchers. One interesting CSC model through which this concept can be studied is the nullipotent 2102Ep Embryonal Carcinoma CSC line, which can completely resist all differentiation stimuli to produce highly aggressive tumours. This cell line has been of interest to our research group for many years.

Previous work in our research group demonstrated that loss of the Myeloid Differentiation Response Gene 88 (MyD88) protein appeared to open 2102Ep cells up to differentiation stimuli that these cells otherwise fully resist. However, this mechanism was only observed sporadically, despite considerable efforts to clarify the mechanism. The primary aim of this study was to address this problem by developing a consistent experimental model through which the role of MyD88 in differentiation-resistance could be assessed. Having achieved this, the project further aimed to fully characterise the mechanism with a view towards informing our efforts to develop Force-Differentiation of CSCs as a clinically relevant treatment.

Initially, a small interfering RNA (siRNA) approach was employed and achieved up to 90% knockdown of MyD88. However, the leaky nature of the siRNA approach proved problematic, as the residual 10% expression was sufficient to maintain 2102Ep nullipotency. Subsequently, a Peptide Inhibitor approach was employed, which inhibits MyD88 protein function rather than expression. This approach was highly efficient in permitting 2102Ep differentiation. However, despite the obvious

differentiated cell phenotype displayed by the cells, suspicion arose when well-characterised markers of differentiation remained unaltered. A flow cytometry approach subsequently identified two sub-populations within the 2102Ep cell line, one of which is susceptible to differentiation upon loss of MyD88. As this project continued towards its conclusion, the precise mechanism involved was elucidated through gene expression array analysis. This data demonstrated that loss of MyD88 is essential for differentiation of embryonal carcinoma cells. Specifically, MyD88 determines these cells' ability to activate differentiation signaling pathways. This is a highly-novel mechanism that suggests that stem cells do not differentiate as generally understood and will be of considerable importance in our efforts to better understand CSC Force-Differentiation en route to CSC targeting in the clinic. Additionally, this mechanism may be relevant to regenerative medicine efforts involving engineering of new cells and tissues from pluripotent cells.

In this Chapter, a general introduction to the subject area of stem cells and CSCs will be provided. This will be followed by a description of the model system used, the differentiation pathway involved and the role of the key protein in our mechanism 'MyD88'. Subsequently, the demonstration of a role for MyD88 in differentiation will be described in Chapter 3, the identification of two sub-populations described in Chapter 4 and the molecular characterisation of the mechanism described in Chapter 5. Finally, the implications of our work for stem cell and CSC biology will be discussed in Chapter 6.

## **1.2 Stem Cells are Arranged as Hierarchies**

While CSCs are the main subject of this thesis, it is important to first describe some principles of stem cell biology, so that the CSC work can be better understood. Our group has recently published comprehensive commentaries and reviews of stem cell and CSC theory, to which the reader is referred for citation of general stem cell and CSC theory (Ffrench et al 2014, 2015). Stem cells are defined as having three properties not shared by somatic cells (Ffrench et al 2015, 2014). First, stem cells have the capacity for long-term proliferation in the undifferentiated state, a process referred to as 'self-renewal' (SR) in stem cell biology. Secondly, these immature stem cells can produce specialised mature cells by a process known as differentiation. Depending on the body's requirements, stem cells can produce two

undifferentiated cells through SR or two differentiated cells through differentiation. Additionally, stem cells often produce one undifferentiated cell and one differentiated cell simultaneously, in a process referred to as 'asymmetric division' (AD) (Figure 1.1).

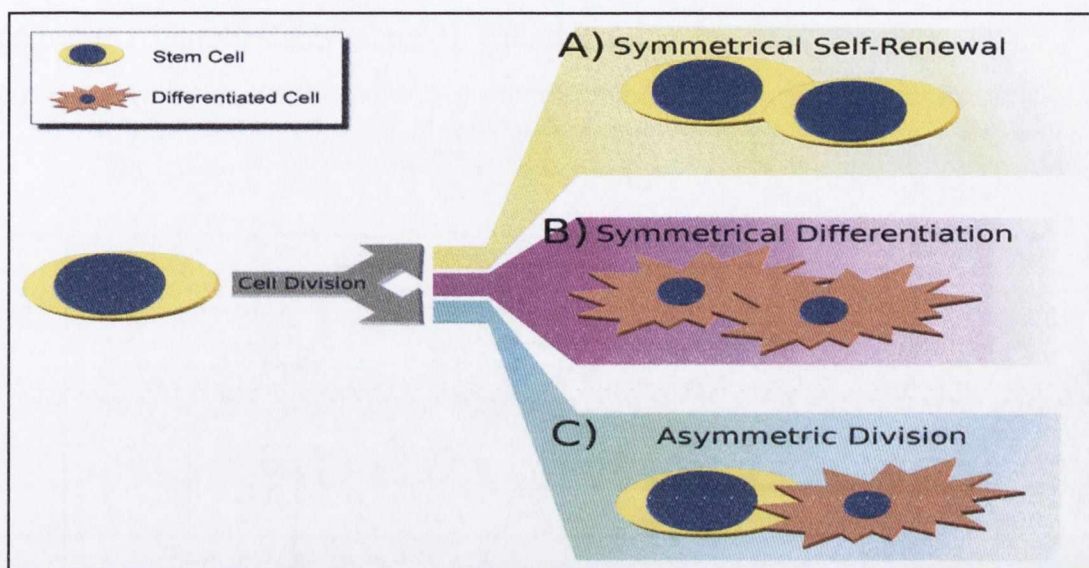


**Figure 1.1 Stem Cell division.** The image illustrates the ways in which stem cells can divide. Stem cells can divide by symmetric division to produce (A) two stem cells via a process termed 'self-renew' and (B) two more mature, specialized cells via a process termed 'differentiation'. C) Often, stem cells can produce one stem cell and one differentiated cell simultaneously, in a process referred to as 'asymmetric division' (Ffrench et al 2015).

Thirdly, stem cells use extensive rounds of SR and differentiation to produce *de novo* tissues in the embryo and to grow or repair existing tissues post-embryonically. Stem cells are primarily characterised by their potency, a term used to refer to the number of cell and tissue types they can produce. Most stem cells are 'multipotent', which describes their ability to produce several types of related stem cell. For example, multipotent haematopoietic stem cells (HSCs) can produce all of the different types of blood cell in the body (Copley et al 2012). In contrast, the rare 'pluripotent' stem cell is capable of producing cells representative of all three germ layers. For example, pluripotent embryonic stem (ES) cells can produce all of the tissues found in the embryo (Evans and Kaufman 1981, Thomson et al 1998).

In recent years it has become clear that stem cells produce their differentiated progeny through one or more intermediaries known as 'Progenitor' cells. Progenitors are themselves stem cells, but are less potent than the parent stem cell that produces them (Ffrench et al 2014, 2015). The best-studied example of this is the HSC, which produces blood cells in the bone marrow. It is now understood that

HSCs produce a number of progenitors that are committed to the production of either myeloid or lymphoid cells via differentiation (Bonnet and Dick 1997, Copley et al 2012, Figure 1.2). The Stem-Progenitor-Differentiated cell model has complicated stem cell analysis and, in particular, the identification and isolation of novel stem cells. This is because it is now understood that most tissues contain multiple different stem and progenitor cells acting independently and inter-dependently. Unfortunately for CSC researchers, tumour tissue is similarly complicated, as will be discussed below.

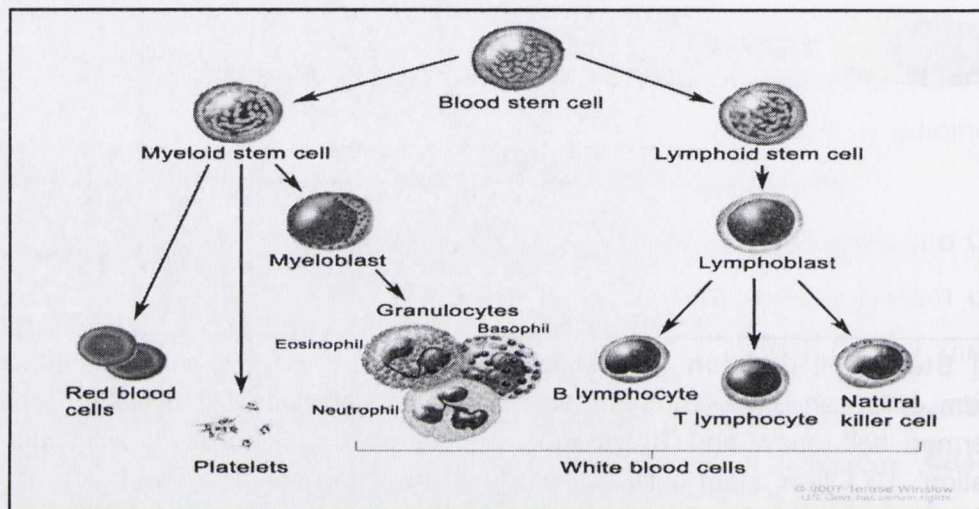


**Figure 1.2 Hematopoietic stem cell differentiation.** In recent years, stem cells have been shown to be organized in stem-progenitor-differentiated cell hierarchies. In the example shown, the hematopoietic or blood stem cells produce red or white blood cells through myeloid or lymphoid progenitors respectively ([www.cancer.gov](http://www.cancer.gov)).

### **1.3 Pluripotent Stem Cells**

The Embryonal Carcinoma (EC) CSC model employed in this project is the oldest and best characterised pluripotent stem cell model (Andrews 2002, Andrews et al 2005). Pluripotent stem cells can differentiate into cells representing all three germ layers (endoderm, mesoderm and ectoderm). To date, three types of pluripotent stem cell have been described, two 'naturally'-occurring and one synthetic. Pluripotent human EC cells are derived from EC tumours and are described in detail below (Section 1.5). Pluripotent human ES cells are derived from the inner cell mass of the developing embryo blastocyst (Thompson et al 1998). The discovery and isolation of ES cells was welcomed with both controversy and celebration (Evans

2011). This was due to the fact that ES cells offered great possibilities for the artificial generation of new cells and organs for regenerative medicine, but the generation of an ES cell line presents ethical concerns, as it involves the 'destruction' of a human embryo. These concerns led to the synthetic production of pluripotent stem cells known as 'induced pluripotent stem' (iPS) cells in 2007 (Takahashi et al 2007), for which Yamanaka Shinya was awarded the Noble Prize in 2011. As such, the only known pluripotent cells are EC, ES and iPS cells.

Mechanistically, pluripotency is determined by three master regulators known as Oct4, Sox2 and Nanog (Matin et al 2004, Vencken et al 2014, Chen et al 2007, Ffrench et al 2015). Oct4, Sox2 and Nanog are a complex of proteins that act as the mechanistic overseers of EC and ES cells (Andrews 2002, Andrews et al 2005, Silva and Smith 2008). High expression of Oct4, Sox2 and Nanog maintains the SR state and blocks differentiation mechanisms (Matin et al 2004, Vencken et al 2014, Chen et al 2007, Ffrench et al 2015, Silva and Smith 2008, Loh and Lim 2011). Loss of any one of these genes is sufficient to initiate a cascade that results in down-regulation of all three and spontaneous differentiation (Matin et al 2004, Vencken et al 2014, Chen et al 2007, Ffrench et al 2015). In contrast, over-expression of any of these three can result in maintenance of the SR state (Matin et al 2004, Vencken et al 2014, Chen et al 2007, Loh and Lim 2011). Additionally, over-expression of combinations of proteins including Oct4-Sox2-Nanog, can transition adult cells into an iPSC state (Takahashi et al 2007). The most powerful of the three is Nanog, which is reflected in the naming of the gene after the 'Tir na n'Og' (Land of Eternal Youth) Irish legend (Chambers et al 2003). Oct4-Sox2-Nanog status is so important that a 'differentiation from pluripotent cell' mechanism that does not involve loss of the complex has never been described. One caveat to this is the expression of Sox2 in EC cells. We and others have demonstrated that, paradoxically, loss of Sox2 force-differentiates EC cells but these cells' standard differentiation response often takes place without loss of Sox2 expression (Andrews 2002, Andrews et al 2005, Vencken et al 2014). In terms of ES and EC cell research, Oct4-Sox2-Nanog are the key proteins of interest. While much is understood of the mechanisms acting downstream of Oct4-Sox2-Nanog, very little is known of the mechanisms acting upstream. As we will describe, in this study we have identified MyD88 as a novel upstream regulator of the Oct4-

Sox2-Nanog mechanism, a finding that will be of much interest to the field of stem cell research.

Pluripotency is, of course, a property of the SR state only. Two models have been proposed for maintenance of the pluripotent SR state. The first 'Ground State' model has been proposed by Austin Smith in mouse ES (mES) cells. This model proposes that mES cells exist in a ground or 'naive' state, which can transition to an Epiblast-like stem cell (EpiSC) state that is primed for differentiation. In this model, A) mES cells express Fibroblast Growth Factor (FGF) and MAPK signaling to transition to the Epiblast-like 'EpiSC' state and B) EpiSC express stemness signaling transduction pathways to facilitate differentiation (Silva and Smith 2008, Figure 1.3). These stemness signaling pathways include Transforming Growth Factor-beta (TGF- $\beta$ ), Hedgehog (Hh), Notch, Snail and Wnt pathways, all of which are known to be widely involved in the differentiation mechanisms of various types of stem cell (Reviewed in Ffrench et al 2015). In contrast, Bing Lim has proposed a 'Competition Model' for maintenance of the human ES SR state. In this model, Bing Lim proposes that key pluripotency factors such as Oct4, Sox2 and Nanog each promote differentiation of one specific lineage while inhibiting the differentiation of another. In this way, these key factors compete with one another to influence lineage differentiation. Bing Lim proposes that this competition results in a homeostasis being reached, where all inhibition and promotion events are cancelled out, resulting in a stable pluripotent SR state (Loh and Lim 2011, Figure 1.4). Differences between these models are debated and are most likely due to mES and hES cells representing cells derived from slightly earlier and later stage embryos. Regardless of the validity of either mechanism, it is important that our understanding of the mechanism of exit from the pluripotent SR state during early differentiation is improved.



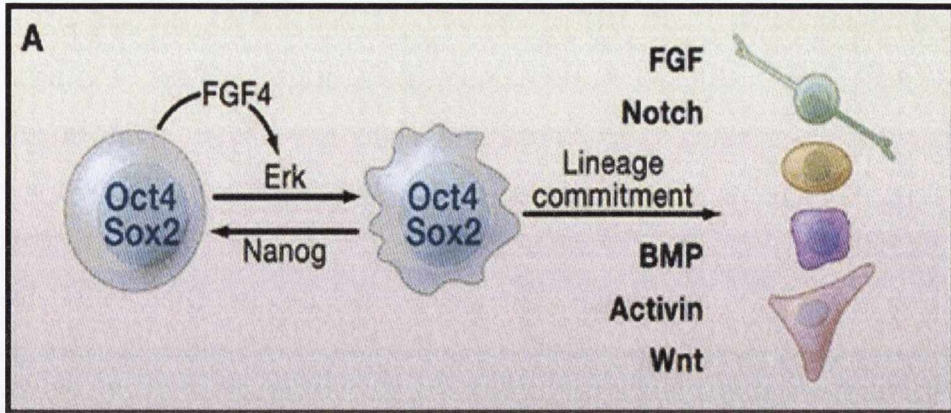


Figure 1.3. **The Ground State Model of ES Differentiation.** In this model, mES cells exist *in vivo* in a ground state that expresses high levels of Oct4-Sox2-Nanog. Through FGF and Erk signaling, these cells transition to an EpiSC state, which is primed for lineage differentiation. This lineage differentiation is dependent upon stemness signaling pathways such as Notch, TGF- $\beta$  (BMP) and Wnt (Silva and Smith 2008).

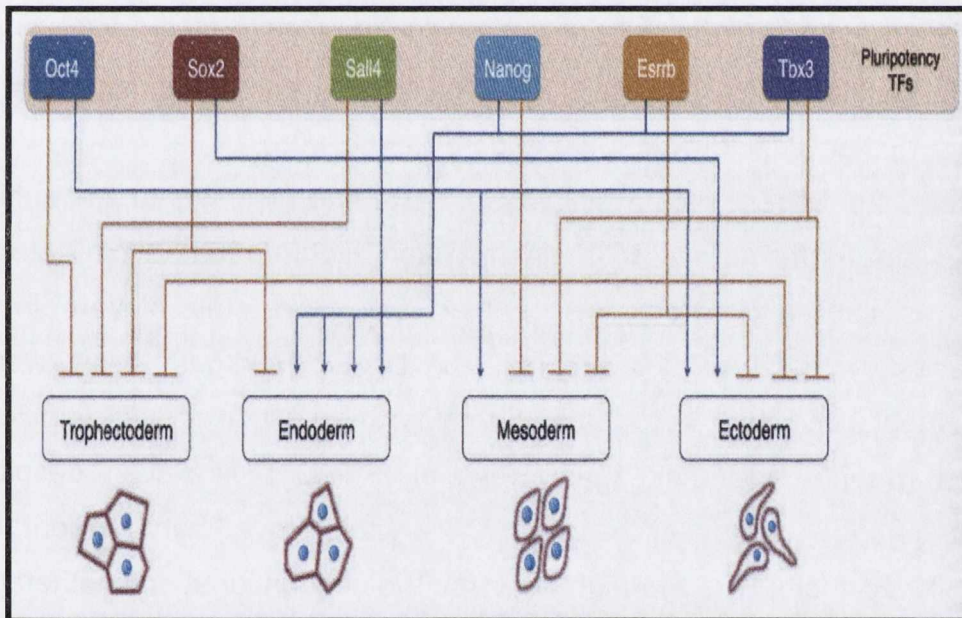


Figure 1.4. **The Competition Model of ES Differentiation.** This model proposes that key pluripotency factors such as Oct4-Sox2-Nanog each regulate one specific lineage differentiation while inhibiting another. This results in a competitive homeostasis being achieved, which results in a stable pluripotent SR state (Loh and Lim 2011).

## **1.4 Tumour Production is Initiated and Driven by Cancer Stem Cells**

It is now well-established that tumour-initiating cells share some of the properties of stem cells (French et al 2015, 2014). In response, these cells have become commonly and collectively known as CSCs. Contemporary CSC Theory proposes that cancers contain a relatively small population of CSCs, which can self-renew and differentiate in a parallel fashion to stem cells (Bonnet and Dick 1997, Reya et al 2001). CSCs can produce tissues with similar potency to non-malignant stem cells from the same area of the body (Kleinsmith and Pierce 1964, Andrews et al 1982, Al-Hajj et al 2003). An interesting comparison of relevance to this thesis is that of pluripotent ES cells and pluripotent EC cells, the latter of which includes the 2102Ep model of study in this project. ES and EC cells are barely distinguishable in their undifferentiated states and produce similar tissue types through similar mechanisms during differentiation (Andrews et al 2002, Andrews 2005, Josephson et al 2007). However, the organization of the embryo produced by ES cells is radically different from the 'organisationally deranged' teratoma (three-germ layer malignant tumour) produced by EC cells (Andrews 2002, Andrews et al 2005).

In terms of tumourigenesis, single CSCs have been shown to be sufficient to regenerate malignancies *in vivo* (Kleinsmith and Pierce 1964, Al-Hajj et al 2003). The obvious implication from this is that CSCs are key players in primary tumourigenesis and metastasis and must be targeted as part of an overall anti-cancer strategy, and that their persistence post-intervention is sufficient to explain recurrence (Bonnet and Dick 1997, Reya et al 2001). However, despite being obvious targets for anti-cancer therapies, CSCs have proved very resilient. It is now well-established that CSCs are highly-resistant to conventional chemotherapies and radiation-therapies (French et al 2015, 2014). Additionally, the similarity between stem cells and CSCs from the same region of the body makes it very difficult to target CSCs without damaging the non-malignant stem cell pool, a side-effect that would have devastating growth and repair consequences for the patient. Efforts to target CSCs require a substantial increase in our understanding of CSC biology. Of particular interest to CSC researchers are the mechanisms through which CSCs resist differentiation to retain a pool of undifferentiated CSCs during tumourigenesis. If this pool could be targeted, it is believed that CSC-driven primary, metastatic and recurrent disease would be substantially compromised. This is due to the over-riding

principle that CSC tumourigenic potential is lost upon their differentiation. As will be described in detail later, Forced-Differentiation of CSCs is one of the key interests of our group and aims of this study.

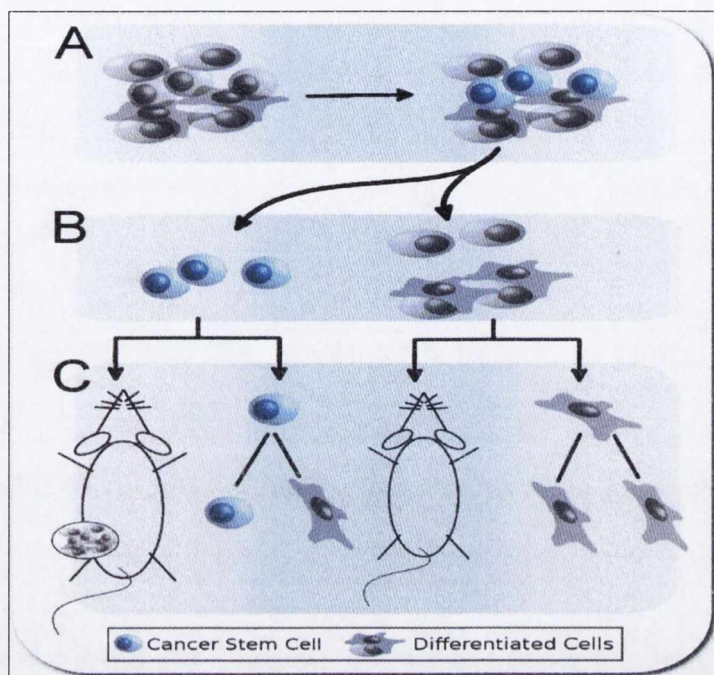


**Figure 1.5. Tumour-Initiation by CSCs.** This image illustrates that CSCs are tumourigenic and can efficiently generate tumours when introduced into immune-compromised mice in low numbers. In contrast, differentiated cells lose their tumourigenic potential and do not form tumours in immune-compromised mice. As such, forced-differentiation is a potential approach through which CSCs may be targeted in the clinic (Ffrench et al 2014).

## 1.5 The Embryonal Carcinoma Cancer Stem Cell Model

The CSC model used in this study is the Embryonal Carcinoma (EC) model. Embryonal Carcinomas are a subset of germ cell tumours, which are the malignant counterpart of pluripotent ES cells (Andrews et al 2005). Previous work has shown overall similarity between EC CSCs and ES cells by microarray comparison of ES cells with two EC CSC lines with normal karyotype, namely 2102Ep and NTera2 (Duran et al 2001, Josephson et al 2007). NTera2 is a pluripotent EC CSC line derived from a human teratocarcinoma (well-differentiated malignant teratoma, (Andrews et al 1980, Andrews et al 1984a, Andrews 1984, Andrews 2002, Andrews et al 2005). In culture, NTera2 cells can be grown in a stable undifferentiated state and be induced to differentiate down several different lineages in response to morphogens such as all-*trans* retinoic acid (RA), bromodeoxyuridine (BrdU) and hexamethylene bisacetamide (HMBA) (Andrews et al 1980, Andrews 1984, Andrews et al 1990). 2102Ep is a nullipotent EC CSC line derived from a human embryonal

carcinoma (an undifferentiated malignant teratoma, Andrews et al 1980, 1982, 1984b, Kannagi et al 1983, Andrews 2002, Andrews et al 2005). NTera2 and ES cells are commonly used to model and identify the subtle differences between the mechanisms of differentiation from malignant and non-malignant pluripotent cells. Additionally, 2102Ep is employed as a model of differentiation resistance. For example, our group has identified several gene signatures associated with 2102Ep differentiation resistance and shown that they are highly expressed in patient tumour samples (Gallagher et al 2009, 2012). In an additional study, our group identified MyD88 as a key player in NTera2 differentiation and a prognostic indicator of patient outcome in ovarian cancer (d'Adhemar et al 2014).

During this project, a group of five molecular markers are used as readouts when determining or confirming the self-renewal (undifferentiated) or differentiation status of EC CSCs. These five markers, Stage-Specific Embryonic Antigen 4 (SSEA4), Alkaline Phosphatase (AP), Oct4, Sox2 and Nanog, are very well established in pluripotent stem cell biology (Andrews et al 1980, 1982, 1984b, 2005, Kannagi et al 1983, Andrews 2002, Ffrench et al 2014, 2015). SSEA4 and AP are non-functional (in terms of a stem cell role) markers specifically expressed by nullipotent and pluripotent EC CSCs and ES cells and not expressed in adult cells (Andrews et al 1980, 1982, 1984b, 2005, Kannagi et al 1983, Andrews 2002, Stefkova et al 2015). Both SSEA4 and AP have become popular readouts for nullipotent and pluripotent cell analysis. SSEA4 was originally described from epitope screening studies in murine embryos (Solter and Knowles 1979). As SSEA4 is not a functional requirement for stem cells, it has been most commonly employed as a flow cytometry readout, due to its high cell-surface expression on undifferentiated and low expression on differentiated EC CSCs and ES cells. As the name suggests, AP is a phosphatase that functions optimally in alkaline environments. AP is expressed from as early as two cells in the mouse embryo and is equally expressed in all embryonic cells until the early blastocyst, at which point it is exclusively expressed by the pluripotent cells in the inner cell mass (Stefkova et al 2015). Commercially-available AP kits have become popular tools for Elisa or staining based assays, which can quickly confirm stem cell status without the requirement for expensive equipment. The gold standard test for differentiation status is loss of expression of Oct4, Sox2 and Nanog (Matin et al 2004, Vencken et al 2014, Chen et al 2007, Ffrench et al

2014, 2015). While all three transcription factors regulate as a complex, Nanog appears to be more independent while Oct4-Sox2 operate as a heterodimer (Rizzino 2013). In our experience, loss of Oct4-Sox2-Nanog in EC cells begins within three days of differentiation beginning (Gallagher et al 2009, Gallagher et al 2012, d'Adhemar et al 2014). This can be exploited through assessment of Oct4, Sox2 and Nanog status using qPCR. Together, these five markers provide strong indications of the stem cell status of NTera2 and 2102Ep cells.

## **1.6 Retinoic Acid Signaling and NTera2 Embryonal Carcinoma Cell Differentiation**

In this project, EC CSCs are differentiated by addition of all-*trans* Retinoic Acid (RA). Retinoic acid is the most important derivative of liposoluble vitamin A or Retinol, which plays a major role in a number of biological processes such as development, cell proliferation, differentiation, and apoptosis. Retinoic acid acts as a ligand for the RA signal transduction pathway, which has been long known to play roles in embryonic anterior/posterior patterning regulation via Hox genes (Chambon 1996, Marletaz et al 2006, Das et al 2014). Cells respond to high or low concentrations of RA differently. For example, cells at the posterior end of *Xenopus laevis* embryos respond to higher concentrations of RA, while lower concentrations regulate the anterior end (Simeone et al 1991). The most common form of RA found in the body is all-*trans* RA, which has been exploited as a differentiation tool in pluripotent stem cell biology. Retinoic Acid has also been shown to induce 'NTera2' human EC CSCs to differentiate into neuron-like cells (Andrews et al 1984a, Andrews 1984). Since the 1980s, RA-induced differentiation has been extensively characterised in this model, which has led to the identification of key regulatory molecules in ES cells (Reviewed in Andrews 2002, Andrews et al 2005). For example, RA directly binds to and activates HOX genes as part of a cascade that ultimately facilitates differentiation through downregulation of Oct4-Sox2-Nanog and SSEA4 (Mallo and Alonso 2013). Today, RA-differentiation of NTera2 cells is commonly used as an easily cultured model for ES cell differentiation. RA is also commonly used to model differentiation of ES cells (Andrews 2002). Additionally, over-expressing RA receptors in somatic cells enhances RA signaling, which permits reprogramming into iPS cells (Wei Wang et al 2011).

In experimental conditions, RA is generally provided to cells in its *all-trans* RA form. This is a derivative of Vitamin A (Retinol) taken in via the diet, which is the main ligand for RA signal transduction. Retinoic Acid signaling is a complex pathway that involves both signal transduction and biochemical/bio-conversion processes (Chambon 1996, Paschaki et al 2013, Das et al 2014, Cunningham and Deuter 2015, Figure 1.6). Signal transduction begins with the binding of retinols to Retinol Binding Proteins (RBPs) outside the cell. This retinol-RBP complex binds the RBP receptor STRA6 (Stimulated by RA 6), which facilitates uptake of retinol in to the cell via diffusion. Retinols bind Cellular Retinol Binding Proteins (CRBPs), which facilitate the conversion of some retinols to retinal by retinol dehydrogenase (RDH). Retinal is then oxidised by retinaldehyde dehydrogenase (RALDH) to produce RA, which is bound in the cell by Cellular RA Binding Proteins (CRABPs). This complex is transported to the nucleus of the cell where it is received by and complexes with the nuclear receptor heterodimer RAR/RXR (RA Receptor/Retinoid X Receptor). These complexes bind to RA response element (RARE) sequences within the DNA of target genes, upon which they act as transcription factors. Examples of RA target genes include *Rarb*, *Oct4* and *Hox* genes *a1*, *a3*, *a4*, *b1*, *b3*, *b4*, *b5*, *c4*, and *d4* (Cunningham and Deuster 2015). This leads to changes in the expression of RA target genes, which triggers a cascade that leads to differentiation of the cell. For example, in pluripotent cells, RA treatment results in a cascade that downregulates *Oct4-Sox2-Nanog*-driven differentiation. Finally, excess RA is presented to cytochrome p450 family 26 (CYP26) enzymes for degradation.

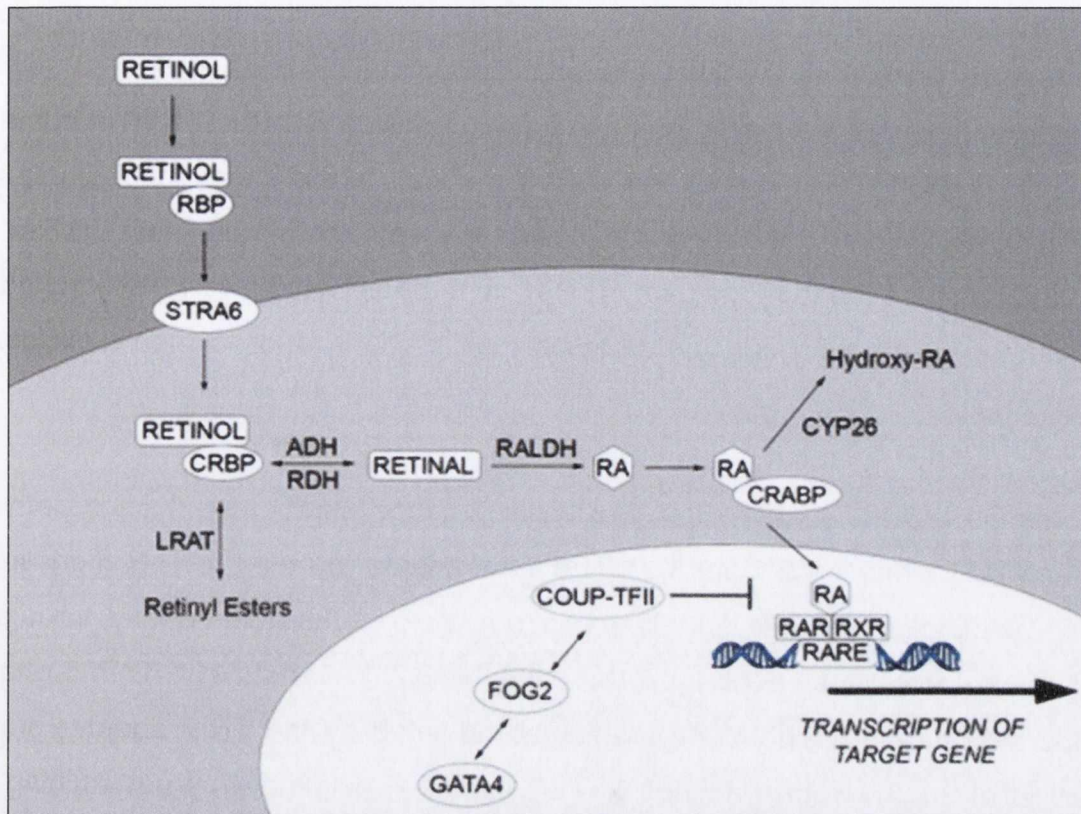


**Figure 1.6. The Retinoic Acid Signaling Pathway.** Vitamin A derivatives including retinol and retinoic acid (RA) act as ligands to the RA signaling pathway. Outside the cell, retinols bind to retinol binding proteins (RBPs), which facilitates diffusion in to the cell via the cell surface receptor STRA6 (Stimulated by RA 6). Once inside the cell, retinol is converted to retinal by retinol dehydrogenase (RDH) and then retinoic acid by retinaldehyde dehydrogenase (RALDH), processes that are chaperoned by Cellular retinol BP (CRBP) and cellular RABP (CRABP). RA-CRABP complexes enter the nucleus of the cell, where they complex with the nuclear receptor heterodimer RAR/RXR (RA receptors/Retinoid X receptors), which facilitates binding to RA response elements (RAREs) within the DNA sequences of target genes. Once bound, this complex acts as a transcription factor, which activates a cascade resulting in development and/or differentiation events ([www.cdh.wikia.com](http://www.cdh.wikia.com)).

## **1.7. Toll-Like Receptor Signaling**

Toll like Receptors (TLRs) are transmembrane proteins that are best understood in their important role in the early innate immune system, where they sense microorganisms and endogenous danger signals (Hemanshu Patel et al 2012). In this project, the elucidation of a role for TLR signaling in differentiation will be described, which re-visits their less studied, original description as developmental regulators. Toll receptors were identified in the 1980s as essential receptors for the establishment of dorso-ventral patterning in developing embryos by the isolation of

the corresponding mutants in *Drosophila melanogaster* (Hashimoto et al 1988). Subsequently, TLRs were identified in humans and mice (Takeda et al 2003), where 10 human and 12 murine members have been identified (**TLR1 -TLR10** in humans, and **TLR1 -TLR9, TLR11, TLR12** and **TLR13** in mice). In the intervening years, little research has been reported in relation to the role of TLRs in development/differentiation. Instead, TLRs have been extensively researched in innate immunity, which is considered to be their primary (and, to many, exclusive) role.

TLRs are the receptors at the top of a well-described signal transduction pathway known as TLR Signaling (Figure 1.7). The main adapter protein for TLR Signaling is MyD88 (Section 1.8). TLR Signaling can operate MyD88-dependently through a series of intermediaries (IRAK4, IRAK1, and IRAK2). Alternatively, TLR Signaling can operate MyD88-independently, which is mediated by the TRIF adapter protein (O'Neill et al 2013). Both branches of TLR signaling culminate by determining the profile of pro-inflammatory chemokines and cytokines secreted by the cell (Lu et al 2008, Kawai et al 1999). Specifically, the function of TLR signaling is to activate NF- $\kappa$ B, which results in the production and secretion of pro-inflammatory chemokines and cytokines that respond to the (pathogenic) stimulus (O'Neill et al 2013).

TLRs consist of three major domains, a leucine rich extra cellular domain, a transmembrane domain, and a cytoplasmic TIR domain (Yamamoto and Takeda 2010). In immunity, TLRs have been functionally defined as pattern recognition receptors (PRRs), recognizing a variety of pathogen-associated microbial patterns (PAMPs), such as lipopolysaccharide (LPS), lipoprotein and nucleic acids (Akira et al 2006, Beutler et al 2007, Yamamoto and Takeda 2010). TLRs can be broadly divided into different groups according to the subcellular site of ligand recognition. TLRs 1, 2, 4, 5, and 6 are localized at the plasma membrane, where they detect molecules displayed on the surface of various pathogens. TLRs 3, 7, 8, 9, 11, 12, and 13 are localized to various endosomal compartments, where most detect microbial nucleic acids. (Barton and Kagan 2009, Bonham et al 2014). Recent work has identified ligands for TLR11, TLR12 and TLR13 that were previously unknown (DiGioia and Zanoni 2015). A relationship between TLR signaling and stem cell biology has not been widely described. However, in recent years it has been noted



that TLR3 expression is associated with increased efficiency in producing iPS cells from adult cells (Lee et al 2012). Very recently, it has been shown that TLR3 is a key regulator of stem cell-driven regeneration of hair-containing-skin cells following wounding (Nelson et al 2015). However, the results described in this thesis are, to our knowledge, the first mechanistic indications for a role for TLR signaling in differentiation of pluripotent cells.

### **1.8. Myeloid Differentiation Response Gene 88 (MyD88)**

During initial characterization of the differentiation and differentiation-resistance mechanisms of NTera2 and 2102Ep EC CSCs respectively by our group, the MyD88 gene was highlighted. MyD88 is downregulated upon differentiation of NTera2 cells but maintained at a higher level of expression in 2102Ep cells resisting differentiation (d'Adhemar et al 2014). Myeloid Differentiation Primary Response Gene 88 (MyD88) is almost exclusively known for its role as the main adapter protein and mediator of TLR Signaling (Medzhitov et al 1997, Janssens and Beyaert 2002). Due to its well-established association with innate immunity, the discovery of a differentiation role for MyD88 could be considered surprising. However, MyD88 was originally characterized as a myeloid differentiation regulator in mouse studies (Liebermann and Hoffman 2002, Lord et al 1990). Pluripotent stem cell differentiation is essentially the same process as embryonic development and as such many stem cell differentiation genes were originally identified as developmental regulators long before the establishment of stem cell models in culture. In fact, the 'D' in MyD88 stands for 'Differentiation', which reflects its potential stem cell role.

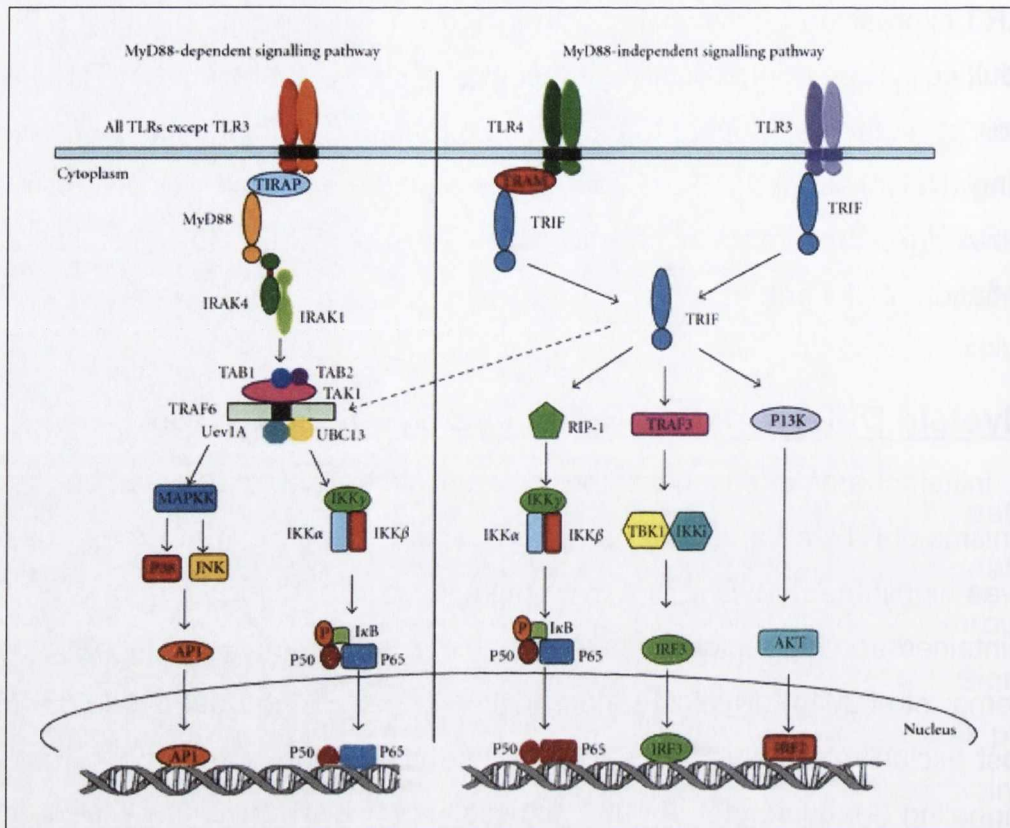


**Figure 1.7. Toll-like Receptor (TLR) Signalling Pathway.** All TLR signalling is mediated by the intracellular adaptor protein MyD88 dependent pathway except TLR 3, which acts MyD88 independently using the TRIF pathway, which is also known as TICAM1. (Left panel) The MyD88-dependent TLR Signalling pathways recruits a signalling complex composed of IRAK1, IRAK4 and TRAF6. This leads to induction of MAPKK and IKK complexes, which results in activation and nuclear translocation of AP-1 and NF- $\kappa$ B to triggers the production of pro-inflammatory cytokines. (Right panel). MyD88-independent Signalling uses TRIF to activate the IKK complexes through RIP1. TRIF can also interact with TRAF3 and the phosphatidylinositol 3-kinase (PI3K)-AKT pathway resulting in the nuclear translocation of IRF3 and IRF2. TRIF can further potentially interact with TLR4, leading to an associate with TRAF6 to activate AP-1 and NF- $\kappa$ B (Patel et al 2012).

MyD88 has been very poorly studied outside of its role in TLR signaling. Instead, researchers have focused on other aspects of TLR signaling such as the function of different TLRs and the populations of chemokines and cytokines produced by the pathway (O'Neill et al 2013). In cancer, MyD88 has been described by our group and others as a prognostic indicator in ovarian cancer. One reported ovarian CSC model is based upon isolation of cells expressing high levels of MyD88 (Kelly et al 2006). In this model, Type 1 epithelial ovarian cancer (EOC) cells are MyD88<sup>Low</sup> and considered to be non-stem cells, while Type 2 EOCs are MyD88<sup>High</sup> and considered to be CSCs. However, the work described in this thesis is the first mechanistic report of a role for MyD88 in pluripotent differentiation.

## **1.9. MyD88 Data Previously Generated by our Group**

Our group developed our discovery of the connection between MyD88 and EC CSCs into two parallel projects. In the first, MyD88 was studied in ovarian cancer as ECs can arise in the ovary. This project demonstrated an important association between high MyD88 expression and poor prognosis/outcome in a large cohort of Irish ovarian cancer patient tumour samples (d'Adhemar et al 2014). In parallel, a project was initiated to characterize the role of MyD88 in EC CSCs (Cooke 2013). To date, work by a previous student in the lab demonstrated that MyD88 expression levels were altered during the response of EC CSCs to differentiation, hypoxia and chemotherapy treatments and that these responses were different in NTera2 and 2102Ep cells (Cooke 2013). During the course of the previous student's work, a potential link between loss of MyD88 and 2102Ep forced differentiation was uncovered. However, 2102Ep cells differentiated only very rarely and a consistent protocol through which the MyD88 mechanism could be identified remained elusive. For example, MyD88 knockdown and control samples did not cluster at all in terms of gene expression array analysis. Due to these types of problems, elucidation of the mechanism proved impossible during the scope of the previous student's project. This potential link between MyD88 and 2102Ep differentiation was very exciting and, addressing this, the project was continued and became the subject of the PhD project described in this thesis.

## **1.10. Aims and Hypotheses**

This project is built upon previous work indicating a role for MyD88 in the differentiation of NTera2 cells and the differentiation-resistance of 2102Ep cells. In 2102Ep cells, the MyD88 differentiation mechanism involves two-steps: loss of MyD88 and subsequent addition of differentiation morphogen RA. The MyD88-RA driven mechanism was only observed sporadically: differentiation appeared to occur randomly, rarely, and with no relationship to the percentage knockdown achieved by the siRNA treatment. Addressing this, it was hypothesized that development of an improved protocol would allow elucidation of the role of MyD88 in these cells. Work addressing this hypothesis is described in Chapter 3. Subsequently, the MyD88 differentiation mechanism was further characterised in Chapters 4 and 5.

The primary hypothesis of this thesis was that MyD88 was a differentiation gatekeeper for RA-induced differentiation. Second, it was hypothesised that MyD88 might be a differentiation gatekeeper for other lineage differentiation mechanisms. Third, it was hypothesised that MyD88 was a novel upstream regulator of the Oct4-Sox2-Nanog complex. Fourth, it was hypothesised that MyD88 carried out its function by regulating the production and secretion of TLR signaling chemokines and cytokines by the cells. Fifth, it was hypothesised that gene and microRNA array analysis could be used to characterise the MyD88 differentiation molecular mechanism. Ultimately, it was hypothesised that this collective analysis could A) provide new insight in to how a pool of CSCs can be maintained during tumorigenesis and B) how pluripotent cells exit the self-renewal state prior to lineage differentiation.

Addressing these hypotheses, the first aim of the project was to develop a consistent MyD88 knockdown/inhibition protocol. Secondly, the project aimed to characterise the MyD88 mechanism at a biological and molecular level. Thirdly, the project aimed to demonstrate whether MyD88 was RA-specific or regulated other lineage-differentiation mechanisms. Finally, the project aimed to assess the effect of MyD88-regulated secreted factors on the stem cell status of hEC cells.

## Chapter 2.

### Materials and Methods

#### 2.1 Cell Culture

Two sister embryonal carcinoma (EC) cell lines were used in this study, 2102Ep and NTera2. Nullipotent 2102Ep cells were originally derived from a human testicular teratocarcinoma, and resist retinoic acid (RA) differentiation to form very aggressive, undifferentiated embryonal carcinoma tumours (Andrews 2002, Andrews et al 2005). NTera2 cells are pluripotent and differentiate in response to 10 $\mu$ M RA to form well-differentiated embryonal carcinoma tumours known as teratocarcinomas (Andrews 2002, Andrews et al 2005). Both cell lines were kind gifts from Professor Peter Andrews, Sheffield University and were grown in human EC ('hEC') media [Dulbecco's Modified Eagle Medium DMEM media with L-Glutamine (Sigma) supplemented with 10% Fetal Bovine Serum (FBS) (Sigma) and 5% penicillin-streptomycin (Sigma)]. Cell lines were established from 1ml stock frozen samples stored in liquid nitrogen. Frozen cells were quickly warmed to room temperature, transferred to a 15 ml tube containing hEC media and centrifuged for 5 minutes at 1000 rpm. After this the supernatant was removed and the pellet resuspended in hEC media and seeded in T-25cm<sup>2</sup>, and then to aT-75cm<sup>2</sup> cell culture flask upon nearing confluence (Sarstedt Ltd U.S.A). All cell culture was carried out in a humidified 5% CO<sup>2</sup> atmosphere at 37°C. Cells were passaged every three days, or as required, by removing the old media and washing the cells with 1X phosphate buffered saline (PBS) (Sigma). Cells were then harvested via cell scrapping (NTera2) or 5-15 minute incubation in preheated 0.25 % trypsin/EDTA (2102Ep, Sigma). Harvested cells were into 15 ml tube, centrifuged for 5 minutes at 1000 rpm, the supernatant removed and the cell pellet resuspended and replated in hEC media.

##### 2.1.1 Cell Counting

For all experiments, hEC cells were counted using a hemocytometer (Sigma). Harvested cell pellets were resuspended in 3mls of hEC media and 50 $\mu$ l of the cell suspension transferred in to a 1.5ml tube. This solution was diluted in 150 $\mu$ l of hEC media after which 200 $\mu$ l 0.4% trypan blue was added (total dilution=1:8). 10 $\mu$ l from

this solution was applied to each of the two side of the haemocytometer, and non-blue cells occupying the four corner squares of the haemacytometer counted. The total cell numbers from multiple counts were then averaged, and the number multiplied by the dilution factor and then by 2,500. This yielded the number of cells per ml.

### **2.1.2. Conditioned Media Experiments**

For the conditioned media experiments, Ntera2 cells were differentiated with RA for 7 or 14 days as described below (Section 2.2.1). After this, media containing RA was removed from cells, which were washed in PBS and plated in hEC media containing no RA. Undifferentiated cells were incubated in hEC media as described above. Cells were incubated in hEC media for 7 days. Each day, conditioned media was removed to storage at 4°C and fresh media added. Each day, conditioned media was pooled with the conditioned media from the other days, to create a 7 day pooled sample. Media was then passed through a 0.2µm polyethersulfone filter (Vwr international) to remove cellular debris and again stored at 4°C until used. For the actual conditioned media experiment, undifferentiated Ntera2 cells were seeded at a density of 180,00 cells per well in 6 well plates. 2mls of the appropriate conditioned or control media was then added to the wells. Cells were monitored and moved up to larger flasks as appropriate. Cells were then harvested for flow cytometry analysis as described below.

## **2.2 Differentiation Protocols**

### **2.2.1 Retinoic Acid**

All *trans* Retinoic Acid (RA) was added to the cells as previously described (Gallagher et al 2009, 2012, d'Adhemar et al 2014). Briefly, RA (Sigma), which is prepared in solution in DMSO (Sigma), was added to cells upon plating at standard cell numbers at a concentration of  $10^{-5}$  M. This concentration was chosen as it has been used historically as the standard RA concentration for these cells. This allowed direct comparison to previously published data. Media containing RA was replenished as required.

### **2.2.2 Endoderm Differentiation Kit**

The StemXvivo™ Endoderm Kit was purchased from R&D Systems. It is designed to drive Human pluripotent and induced pluripotent stem cells to differentiate into definitive endoderm via incubation in specially formulated media supplements. 300,000 cells were seeded in 6 well plate in hEC media and allowed to adhere overnight. Subsequently, the media was removed and the cells washed with preheated hEC media, after which 2ml of 'Differentiation Medium I' was added. This was prepared freshly according to the manufacturer's instruction. On the following day, media was removed and replaced with 'Differentiation Media II', which was changed daily for 6 days. Media II was prepared, aliquoted and stored at 4°C according to the manufacturer's instruction. After three days, cells were moved up to the T-25 flask. On day 7, cells were harvested and analysed using flow cytometry and qPCR analyses. All the experiments performed in triplicate. Where MyD88 Peptide Inhibitor was included in this protocol (Section 2.4), plated cells were treated with the MyD88PepInh for 6 hours prior to the addition of the Differentiation Medias. Subsequently, MyD88PepInh was included in the new media that was replaced daily.

### **2.2.3. Mesoderm Differentiation Kit**

The StemXvivo™ Mesoderm Kit was purchased from R&D Systems. Cells were treated as outlined above (2.2.2). In this case, differentiation was induced by treating cells with 'Mesoderm Differentiation Base Media', which was prepared freshly as described in manufactures protocol. Mesoderm differentiation base media was changed daily as described above (Section 2.2.2).

### **2.2.4. Ectoderm Differentiation Kit**

The StemXvivo™ Ectoderm Kit was purchase from R&D Systems) was used. Cells were treated as outlined above (2.2.2). In this case, differentiation was induced by treating cells with 2ml of 'Ectoderm Differentiation Media', which was prepared fresh according to the manufactures protocol. Ectoderm Differentiation media was changed daily as described above (Section 2.2.2).

### **2.2.5 Detection of Differentiation via Alkaline Phosphatase Assay**

Alkaline phosphatase (AP) is a cell surface gene highly expressed in undifferentiated embryonic stem (ES) cells and decreased upon differentiation, which can be used as

a marker to assess the differentiation state in 2101Ep cells. Post-experiment cells were harvested, counted and equal numbers of cells assessed for alkaline phosphatase (AP) expression using the Quantitative Alkaline Phosphatase ES Characterization Kit (Millipore) as per manufacturer's instructions. Post-assay, cells absorbance was measured at 405nm and transformed into AP expression values by comparison to standards supplied in the kit.

## **2.3 siRNA Transfections**

### **2.3.1 Transfection of 2102Ep cells in a 24-well plates**

#### **2.3.1.1 Forward transfection**

24 well plates were seeded with 50,000-56,000 (previously optimised by our group: Vencken et al 2014) 2102Ep cells maintained in hEC media without antibiotics and allowed to adhere over-night. Old media was removed and 500 µl of 'Opti-MEM' media added. A final concentration of 7.5nM siRNA was diluted in 50µl of Opti-MEM and mixed with 1.8 µl of lipofectamin RNAiMAX diluted in 50 µl of Opti-MEM and incubated at room temperature for 5 minutes. The mixture was then applied to the cells. After 4 hours, transfection media was removed and replaced with hEC media without antibiotics, and incubated for the required time. All experiments were performed in triplicate. All three siRNAs used were pre-designed (Life Technologies. siMyD88#1 ID S9138: siMyD88#2 ID S9136: siNeg ID 4390843).

#### **2.3.1.2 Reverse transfection**

A mixture of 7.5nm (final concentration) MyD88 siRNA and 1.5 µl of lipofectamine RNAiMax was diluted in 100 µl of Opti-MEM and applied to each well of 24 well plate. After 5 minutes of room temperature incubation, 50,000-56,000 2102Ep cells, pre-diluted in 500µl of hEC media or 500 µl of Opti-MEM, were applied to each well and incubated for the required time. All experiments were performed in triplicate.

#### **2.3.1.3 Reverse transfection followed by Forward transfection**

During an online search for additional transfection options, the suggestion of a combined reverse followed by forward transfection was noted ([www.personomics.com](http://www.personomics.com)). While this had not been previously tested in hEC cells, the



unsatisfactory outcome from reverse and forward transfections in this study led to the decision to attempt this combined approach. In this protocol, cells were transfected as described in Section 2.3.1.2 over-night then followed by forward transfection as described in Section 2.3.1.1.

## **2.4 MyD88 Peptide Inhibition in 2102Ep cells**

### **2.4.1 MyD88 Peptide Inhibitor Treatment**

The MyD88 Peptide Inhibitor (PepInh) drug (InvivoGen) acts by blocking homo-dimerisation of MyD88, which inhibits the proteins normal function (Derossi et al 1994, Ioiarro et al 2005, Toshchakov et al 2005). 2102Ep cells were seeded at a density of 50,000-56,000 cells per well in a 24 –well plate or 168,000 cells per well in a 6-well plate in standard hEC media without the addition of antibiotics, and allowed to adhere overnight, as described above. Subsequently, 5 $\mu$ M MyD88 PepInh or the Control PepInh supplied by the company was added to the cells for 6 hours. If required, at this point RA was added to a final concentration of 10<sup>-5</sup>M. Media containing inhibitor drugs or controls and  $\pm$ RA as appropriate was changed every day for the number of days required.

### **2.4.2 Validation of MyD88 Peptide Inhibition via Interleukin-1 Treatment**

Cells were prepared as described above and plated in a 96 well plate at a concentration of 56,000 cells per well. Cells were then treated with MyD88 PepInh (5 $\mu$ M) or Control PepInh (5 $\mu$ M) overnight. The following day, media was removed and new media containing the appropriate PepInh added. Cells were incubated for 6 hours before being treated with 30ng/ml Interleukin-1 (IL-1 $\beta$ , InvivoGen) for 30 minutes. IL-1 $\beta$  can only act MyD88-dependently and as such is a measure of MyD88-dependent TLR signaling (Section 1.7). Activation of MyD88-dependent signaling was detected as the presence of phosphorylated I- $\kappa$ B $\alpha$ , which is the active component of NF $\kappa$ B. Phospho I- $\kappa$ B $\alpha$  was detected using the 'PhosphoTracer I- $\kappa$ B $\alpha$  Total ELISA Kit' (Abcam), as per manufacturer's instructions. Fluorescence was measured at 595nm using a Tecan Sunrise 96 well Microplate Reader.

## **2.5 TaqMan qPCR Analysis**

Cells were washed with PBS and either A) lysed directly from the cell culture plate using RNA lysis buffer or B) pelleted, supernatant removed and the pellet stored at -80°C until use. RNA was isolated using the mirVANA kit (Ambion) as per manufacturer's instruction, and RNA concentration and quality assessed using a nanodrop. cDNA synthesis was carried out using the cDNA Archive Kit, and qPCR performed using pre-designed TaqMan assays on the 7900 PCR thermocycler all as per manufacturer's instructions (all components from Life Technologies). Gene expression data is expressed as percentage gene expression relative to the stated normalizer control using the  $2^{-ddCt}$  method (Livak and Schmittgen 2001).

## **2.6 Flow cytometry**

2102Ep cells were washed twice in PBS, detached from the cell culture plate using 0.25% trypsin/EDTA (Sigma), pelleted, re-suspended in PBS and counted by using a hemocytometer, all as described above. In each set of assays, three samples were required; Autofluorescence, Isotype Control and SSEA4 stained samples. For each sample, 1 million cells were re-suspended in 100µl PBS. The autofluorescence sample was left unstained. 10µl of PE-conjugated mouse IgG3 anti-SSEA4 antibody (R and D Systems) and 10µl of an isotype control PE-labeled antibody (R and D Systems) were added to the respective samples, vortexed and incubated for 30 min at 4°C. Following this incubation, cells were washed and pelleted and re-suspended in 1 ml of PBS. Flow cytometry was performed on a Cyan ADP Flow Cytometer (Beckman Coulter). Samples were excited using a 488nm laser and detected between 575/25nm. Doublets were excluded using the pulse width parameter and dead cells were excluded using propidium iodide staining (Invitrogen); Excited = 488nm; detected = 680/30nm). Flow cytometry was carried out at the TCD facilities in the Institute of Molecular Medicine (IMM), St James Hospital, Dublin 8 and the Trinity Biomedical Sciences Institute (TBSI), Pearse Street, Dublin 8.

## **2.7 Fluorescence Activated Cell Sorting (FACS)**

Separation and isolation of the two 2102Ep sub-populations was performed by flow-cytometry based FACS sorting. Cells were stained with SSEA4 as above, using 2102Ep cells force-differentiated by transfection with a siRNA for Sox2 as a differentiated 2101Ep control, as previously described (Vencken et al 2014). SSEA4 positive and SSEA4 negative cells were collected in separate 1.5 ml tubes containing PBS and maintained on ice. Cells were subsequently processed for qPCR analysis as described above. FACS was carried out at the Trinity Biomedical Sciences Institute (TBSI), Pearse Street, Dublin 8.

## **2.8 Statistical Analysis (Flow Cytometry and qPCR)**

Statistical analysis for expression arrays is described in the expression array section (Section 2.9). All other statistical analyses were performed using the 'GraphPad prism 6' analytical software program. The student's two-tailed t-test were used to compare between two groups and the data represent the mean of biological triplicates samples (n=3) and expressed as mean and standard deviation and the P. values of 0.05 were considered statistically significant.

## **2.9 Whole-Genome Gene Expression Array Analysis**

In this study Gene expression analysis arrays was carried out using Affymetrix GeneChip® HuGene 2.0 Sense Target (ST) arrays. Prior to analysis, RNA was isolated as described above and the concentration and quality of the RNA samples assessed using NanoDrop2000 and Agilent Bioanalyzer 2100. Sample preparation was spread over a 3 day workflow, which is outlined in Figure 2.1. Sample preparation was carried out using the Whole Transcript (WT) Plus reagent Kit (Applied Biosystems, Life Technologies). Serial dilution of poly-A control for 150ng of total RNA was prepared and 2µl of the 4<sup>th</sup> dilution was spiked with the total RNA for a final volume of 5µl. This was then used to synthesize First-strand cDNA by adding 5µl of the total RNA to 5µl of First-strand cDNA master mix (4µl of first-strand buffer and 1µl of first-strand enzyme) for a final volume of 10µl, and incubated in a thermal cycler. This produces a single-strand cDNA sample with a T7 promoter at the 5' end

by priming the total RNA with primers containing T7 promoter sequence.

After this, single-stranded cDNA was converted to double-strand cDNA by using DNA polymerase and RNA H to simultaneously degrade the RNA and synthesis double-strand cDNA, which experimentally acts as a template for transcription. In this reaction, 20 $\mu$ l of second-strand master mix (18 $\mu$ l second-strand buffer and 2 $\mu$ l of second-strand enzyme) was added to each 10 $\mu$ l sample of single-stranded cDNA, for a total volume of 30 $\mu$ l, and incubated in a thermal cycler.

The resultant double-strand cDNA was used as a template in an 'in-vitro transcription' (IVT) reaction to synthesise antisense RNA (cRNA) using T7RNA polymerase. In this reaction, 30 $\mu$ l of IVT master mix (24 $\mu$  IVT Buffer and 6 $\mu$ l of IVT enzyme) was transferred to each 30 $\mu$ l sample of second-strand cDNA samples for a total volume of 60 $\mu$ l. This was then incubated for 16hr in a thermal cycler using specific cRNA synthesis program. The synthesised cRNA was purified to remove salts, enzymes, inorganic phosphates and unincorporated nucleotides by a magnetic purification beads protocol using a magnetic stand, and then used as a template to synthesise 2<sup>nd</sup> - cycle single-strand cDNA. In this procedure, 100 $\mu$ l of the purification bead sample was added to each 60 $\mu$ l cRNA sample, and transferred to U-bottom plate. Several additional steps including washing, incubating, pipetting, vortexing and shaking were performed. The concentration and purity of the cRNA was measured using a NanoDrop 2000.

15 $\mu$ g of the resultant cRNA was used as a template to synthesise '2<sup>nd</sup> cycle single-strand cDNA'. In this reaction, 24 $\mu$ l cRNA (15 $\mu$ g) samples were combined with 4 $\mu$ l of 2<sup>nd</sup> - cycle primer and incubated in a thermal cycler. Next, a '2<sup>nd</sup> cycle single strand-cDNA master mix' was prepared, 12 $\mu$ l of which was added to each 28 $\mu$ l cRNA 2<sup>nd</sup> cycle primer. After this incubation, 4 $\mu$ l of RNase H was added to each sample, which hydrolyses cRNA to leave only single-strand cDNA. The resultant cDNA samples were then stored over night at -20°C. The following day, samples were purified using magnetic beads as described above and according to the manufacturer's instructions. The concentration of the sample was determined as previously described and the samples fragmented and labelled using the WT Terminal Labeling Kit 30 RXW as per manufacturer's instructions. Samples were hybridized to GeneChips as per manufacturer's instructions and subsequently washed using a

dedicated fluidics station 450 (Affymetrix) and AGCC Fluidics Control Software (Affymetrix Inc.) Finally, samples were scanned using GeneChip® Operating software in Affymetrix GeneChip® Scanner 3000 and quality control was assessed as per manufacturer's instructions.

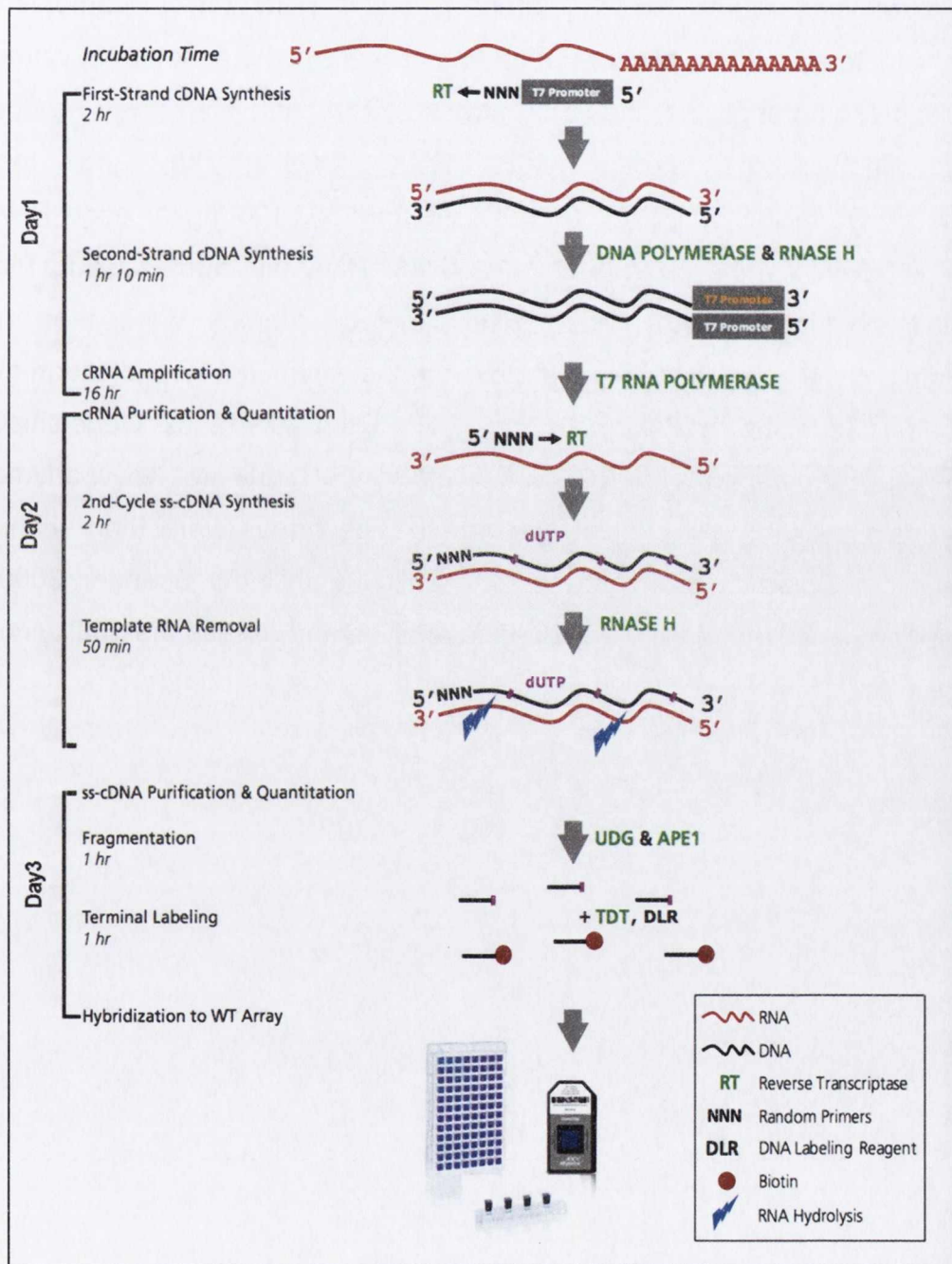


Figure 2.1 **WorkFlow of Whole-Genome Gene Expression Array Analysis.** Samples were prepared as outlined in the illustration and described in detail in the text.

## **2.10 microRNA Expression Array Analysis**

Sample preparation for this experiment is outlined in Figure 2.2. As mentioned in the previous section above (Section 2.9) that the concentration and quality of all of the RNA samples applied in the Gene and microRNA array were assessed by NanoDrop 2000 and using the 6000 Nano kit (Agilent Technologies) in an Aligent 2100 Bioanalyzer instrument. The RNA integrity number (RIN) for our samples was 9-10 which is indicating the quality of our samples where is the acceptable value for gene array expression analyses should be above 7. The microRNA array was carried out using Flash tag<sup>TM</sup> Biotin HSR RNA labeling kit and the 'Prop' Affymetrix<sup>®</sup>GeneChip<sup>®</sup>miRNA 3.0 Array (Affymetrix). 1000ng of each RNA sample was spiked with spike control oligos and the RNA tail labeled using Flash tag<sup>TM</sup> Biotin HSR Ligation (Affymetrix). The labeled samples were then hybridized according to the manufacturer's instruction in the Affymetrix Hybridization oven using Affymetrix<sup>®</sup>GeneChip<sup>®</sup>miRNA 3.0 Array. Then the Affymetrix GeneChip<sup>®</sup> fluidics station 450(Affymetrix) and AGCC fluidics control software ([www.affymetrix.com](http://www.affymetrix.com)) were used to wash and staining the arrays. The arrays were then scanned using GeneChip<sup>®</sup> Operating software in Affymetrix GeneChip<sup>®</sup> Scanner 3000 and the expression console software was used to analyse and assess the quality control.

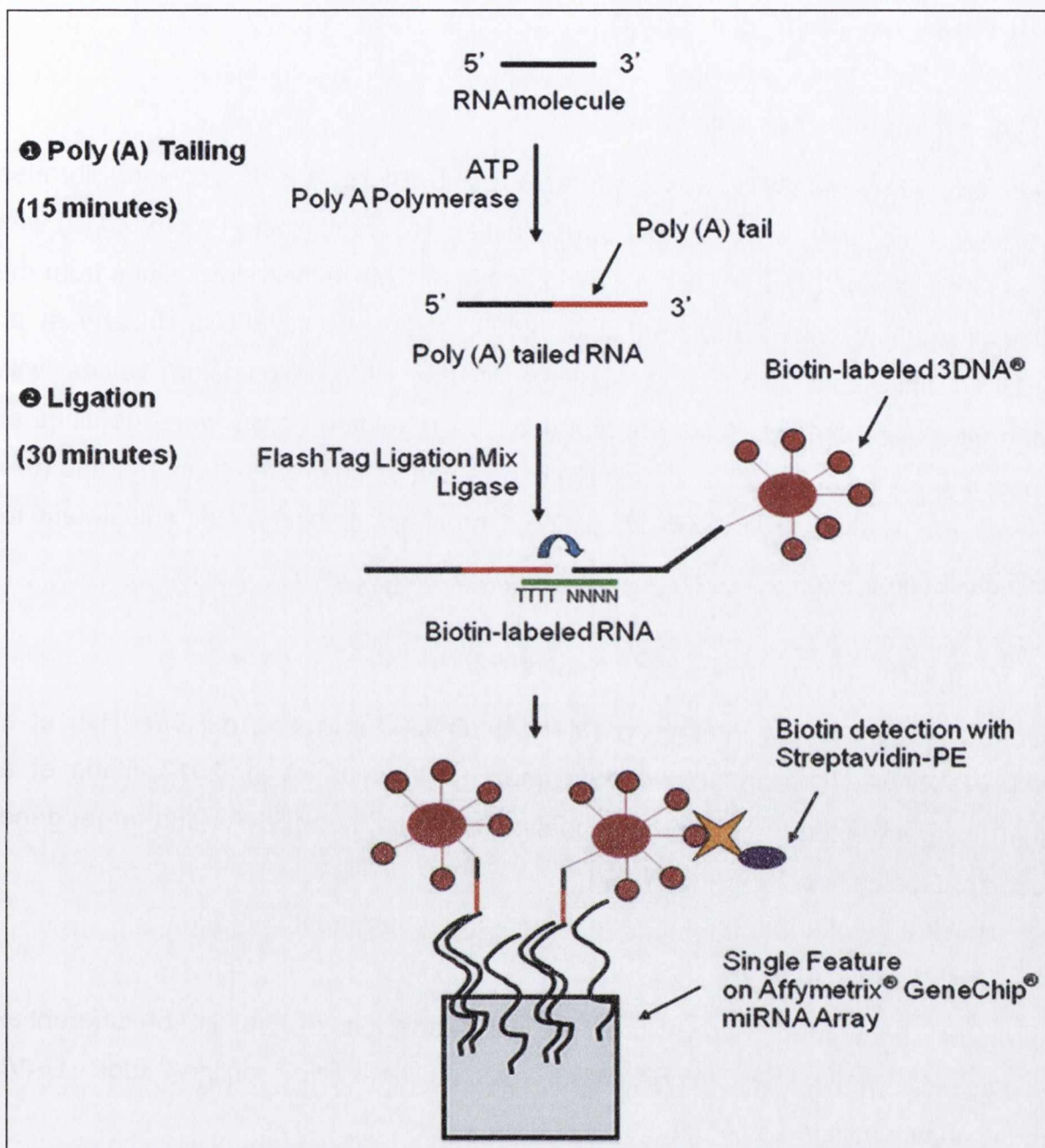


Figure 2.2. **WorkFlow of Whole-Genome MicroRNA Expression Array Analysis.** Samples were prepared as outlined in the illustration and described in detail in the text.

## 2.11 Gene Array Data Analysis

### 2.11.1. Affymetrix Data Analysis

Affymetrix array analysis was performed using Bioconductor software libraries (<http://www.bioconductor.org>). The **oligo** package (Carvalho and Irizarry 2010) was used to process Affymetrix CEL files and compute RMA expression values from the original intensity values (Bolstad et al. 2003, Irizarry et al. 2003a, Irizarry et al. 2003b). Differential expression analysis of the RMA expression values was performed using limma (Ritchie et al. 2015). De-regulated genes were identified as those with (a)  $\log_2$ -based fold-change in expression value greater than **1.0**, and (b) a significance p-value less than the defined threshold of **0.05**, after adjustment for multiple testing.

### 2.11.2. miRNA-Target Interaction Analysis

Several miRNA-Target Interaction (MTI) databases, including miRTar (Hsu et al. 2011) miRWalk (Dweep et al. 2011) and StarBase (Li et al. 2013, Yang et al. 2010) were queried to identify relationships between the miRNAs and target genes found to be significantly de-regulated.

### 2.11.3. Pathway Analysis

Gene set enrichment analysis, or pathways analysis of the list of differentially expressed genes was performed using the free online tool DAVID (<https://david.ncifcrf.gov/> Huang et al 2009).



## Chapter 3.

# Peptide Inhibition of MyD88 Leads to Differentiation of 2102Ep cells

### 3.1.1. Introduction

Forcing differentiation upon cancer stem cells (CSCs) removes their tumorigenic potential and as such is a potential anti-cancer therapy (Ffrench et al 2015, 2014, Reya et al 2001). However, CSCs can resist differentiation to maintain a pool of undifferentiated tumorigenic CSCs during tumorigenesis. The nullipotent 2102Ep CSC line is capable of producing a tumour while completely resisting differentiation. As such, this is a very good model in which to study CSC differentiation resistance. Previous work in our group demonstrated that loss of MyD88 in combination with addition of retinoic acid (RA) resulted in differentiation of 2102Ep cells (Cooke 2013). However, this did not occur consistently. This, it was proposed, was best addressed by improving the efficiency of the siRNA protocol used to knockdown MyD88. It was hypothesised that improving the MyD88 knockdown protocol or switching to a Peptide Inhibitor (PepInh) protocol could consistently demonstrate a relationship between loss of MyD88 and differentiation in these cells. In this chapter, effort resulting in a considerable improvement of the siRNA knockdown protocol will be described. Ultimately, these efforts proved insufficient to achieve a consistent differentiation. However, the switch to a MyD88 PepInh drug proved very successful. Finally, we will describe how MyD88PepInh+RA treated cells appeared to be differentiated but did not alter markers of the undifferentiated state at a molecular level. These conflicting results led to a novel hypothesis, which is tested in Chapter 4.

### 3.1.2. Demonstrating Stem Cell Differentiation

In Chapter 1, the asymmetric division properties of stem cells and CSCs were described in detail (Section 1.2). Experimentally, there is no single assay that can definitively demonstrate the undifferentiated or differentiated state. In contrast, three different assays are generally employed as proof of stem cell status: morphology,

cellular proliferation rate and molecular marker expression. As such, all three tests were used in the analysis described in this chapter.

It is well described that all stem cells and CSCs alter their morphology or phenotype considerably when differentiating (Andrews 2002, Andrews et al 2005). In the undifferentiated state, stem cells and CSCs generally form as cluster of cells in adherent cell culture. These clusters are generally round and demonstrate a concave morphology. The edge of these concave clusters is often described as a bright halo. Upon differentiation, this halo quickly disappears and the clusters form a more flattened than concave morphology. At higher power, these clusters of undifferentiated cells can be seen to contain large number of tightly packed cells, while differentiated cells appear flat and almost transparent (Figure 3.1). As differentiation continues, cells become larger and denser. Specifically, embryonal carcinoma (EC) cells treated with RA tend to appear as neural-like cells. As such, the researcher can easily visualise indications of differentiation in this model, even without performing complex molecular analysis. This is very useful in optimising differentiation protocols as the researcher can quickly call cells as undifferentiated or differentiated during optimisation.

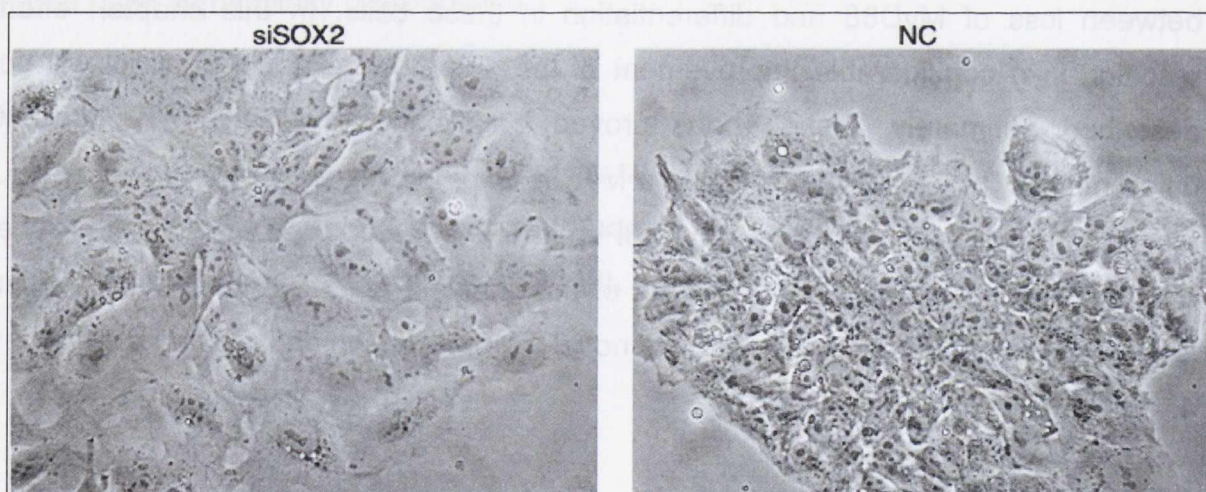


**Figure 3.1. Typical undifferentiated and differentiated morphologies of 2102Ep cells.** Our group has previously demonstrated that loss of Sox2 through siRNA treatment differentiates 2102Ep cells (Vencken et al 2014). For illustrative purposes, the phenotype of differentiated ('siSOX2') and control ('NC') 2102Ep cells is reproduced from this paper. At high power, undifferentiated 2102Ep cells have a tightly-packed cluster morphology. Cells become larger and almost transparent upon differentiation.

Secondly, stem cells and CSCs are known to exit the cell cycle during differentiation (Ffrench et al 2015, 2014). This results in a decrease in the cellular proliferation of differentiating cells when compared to undifferentiated cells. In cell culture, this is a very useful differentiation status indicator for the researcher. In our experience, cells plated with RA or another differentiation stimulus will be undistinguishable from controls for two to three days. However, once the cells are expanded to a larger flask upon reaching confluence at day two to three, the difference between undifferentiated and differentiated cells becomes apparent. Control cells tend to rapidly proliferate in the new space provided by the new flask, and reach confluence in another two to three days. In contrast, this new space appears to further differentiate differentiating cells, where cells become larger. Differentiating cells often reach 'confluence' but this is due to an expansion in cell size rather than cell number. These cells can remain in the same flask while controls must be expanded. Differentiated cells demonstrate very low levels of cell death (floating cells for example) upon reaching 'confluence'. As such, monitoring cell proliferation during expansion of these cells in cell culture is a very useful indicator of stem cell differentiation status.

Finally, in order to confirm stem cell differentiation status, the expression of molecular markers must be assessed. 2102Ep cells are nullipotent and express similar markers to pluripotent cells. At a gene expression level, Oct4, Sox2 and Nanog levels are highly expressed in undifferentiated cells and their expression lost during differentiation. Oct4-Sox2-Nanog levels are often demonstrated by qPCR. At a protein level, Alkaline Phosphatase (AP) and Stage Specific Embryonic Antigen 4 (SSEA4) are well characterised pluripotency markers. Both AP and SSEA4 are highly expressed in undifferentiated cells and their expression lost during differentiation. Alkaline Phosphatase levels are generally demonstrated using commercially available Elisa kits, while SSEA4 is generally used as a flow cytometry marker. Together, morphology, cellular proliferation rate, and bio-marker expression levels provide a validation of stem cell differentiation status. This is an 'all or nothing' process. As such, it has never been reported that stem cells or CSCs would provide conflicting data from across these assays. Undifferentiated cells will always produce positive results in all assays, while differentiated results will always produce negative results.

### **3.1.3. Inhibition of MyD88 via Peptide Inhibitor**

Peptide inhibitors (PepInh) are relatively new research tools and are becoming increasingly more commercially available for specific proteins of interest. Peptide inhibitors are designed to block the function of a protein of interest rather than its expression, as is the case with a traditional inhibitor such as a siRNA. Peptide inhibitors are reported to have a broad range of efficiencies, with some working extremely well and others acting very poorly. The MyD88 PepInh used in this thesis is a commercially available PepInh from InvivoGen. This particular MyD88PepInh was chosen as it was the only commercially available MyD88PepInh at the time that was provided with a negative control PepInh ('CtrlPepInh').

The mode of action of the MyD88PepInh is illustrated in Figure 3.2. MyD88 functions as a homodimer, where binding occurs at the TIR (Toll/Interleukin-1 Receptor) domain (O'Neill et al 2013). The MyD88PepInh efficiently binds to the MyD88 TIR domain, which competitively blocks MyD88 homodimerisation and thus MyD88 signaling (Figure 3.2). Once MyD88 signaling has been blocked, cells generally switch to MyD88-independent TLR Signaling, as described in Chapter 1 (Section 1.7). The MyD88PepInh has been successfully used in a limited number of studies to date (Derossi et al 1994, Ioiarro et al 2005, Toshchakov et al 2005) but has not been used in human EC cells to our knowledge. As a caveat, we noted that it would not be easy to demonstrate successful inhibition by the PepInh as it does not affect MyD88 gene or protein expression, which rules out the use of standard procedures such as qPCR and western blot analysis. This would not be an issue if the protocol worked efficiently as the differentiation of the cells should be obvious. However, if considerable optimisation was required, this could have necessitated a more complex assay to demonstrate MyD88 inhibition efficiency.

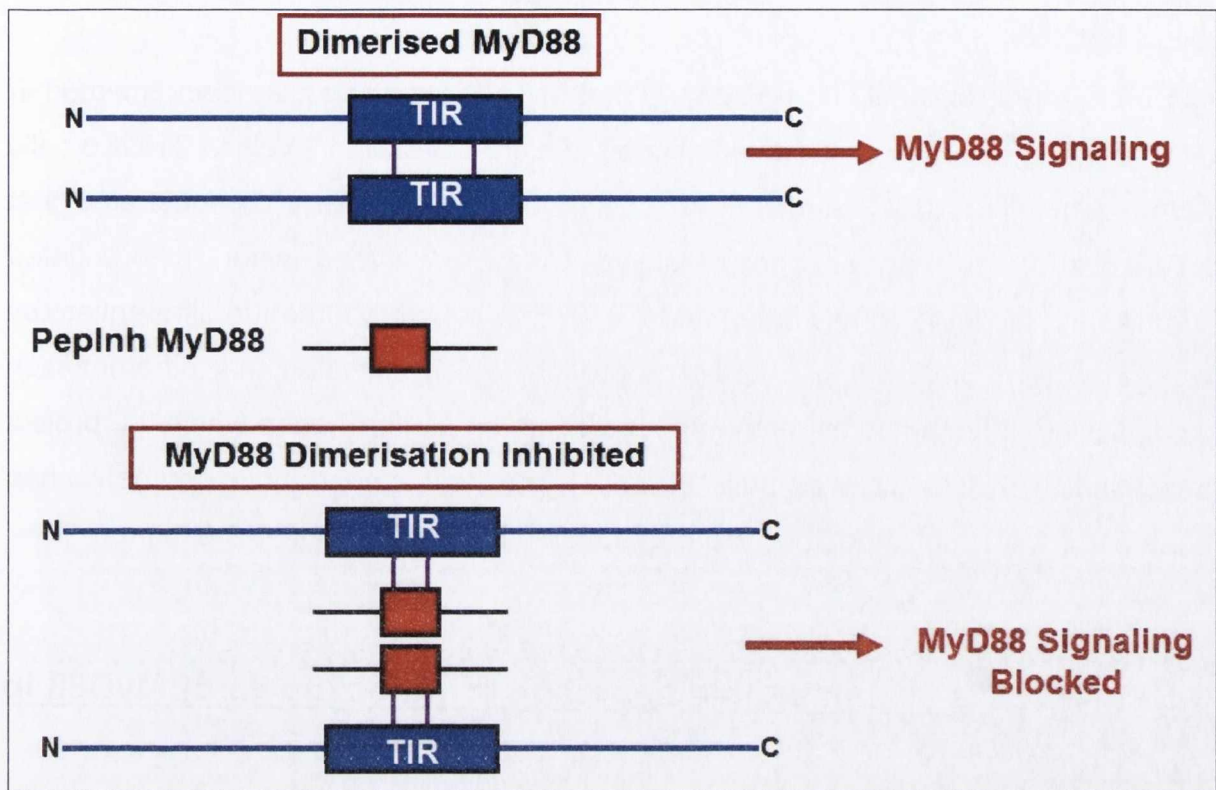


Figure 3.2. **Mode of Action of MyD88 Peptide Inhibitor.** The MyD88 protein functions through homo-dimerisation at the Toll/Interleukin-1 Receptor (TIR) domain. During MyD88-dependent signaling, homo-dimerisation occurs. The MyD88 Peptide Inhibitor (Peplnh) competitively binds to the TIR domain of MyD88 proteins, which inhibits homo-dimerisation and thus blocks MyD88-dependent signaling. It is generally thought that this results in a switch to MyD88-independent TLR signaling.

### **3.1.4. Aims and Hypothesis**

As previously stated, earlier work in our group had identified an association between loss of MyD88 and differentiation of human EC cells. However, this differentiation was inconsistent and as such very difficult to characterise. Addressing this, the aim of this Chapter was to generate a consistent differentiation protocol, which would allow this mechanism to be studied. Specifically, the main aim was to generate a consistent MyD88 knockdown or inhibition protocol. It was hypothesised that this was the crucial step that would permit consistent differentiation of the cells in response to addition of RA. It was hypothesised that an improved siRNA protocol could facilitate consistent and efficient knockdown of MyD88. As a contingency, we hypothesised that a MyD88Peplnh could be employed to inhibit MyD88.

### **3.2. Materials and Methods**

All materials and methods related to this chapter are described in chapter 2.

### **3.3. Results**

Our group has previously demonstrated that MyD88 expression is downregulated in differentiating NTera2 cells and maintained at high expression levels in 2102Ep cells (d'Adhemar et al 2014). Additionally, our group has previously demonstrated that NTera2 and 2102Ep cells downregulate Oct4-Sox2-Nanog when differentiated (Vencken et al 2014). In this latter study, 2102Ep cells were forced to differentiate by knocking down Sox2 using a siRNA approach, which indicated that differentiation was possible. These key experiments represented a platform upon which the project described in this thesis was built. However, as these important experiments had been previously published, they are not repeated for illustration in this Chapter.

#### **3.3.1. siRNA is an unsuitable approach for knockdown of MyD88 in 2102Ep cells**

In the last decade, siRNAs have been successfully used by many groups to knockdown the expression of many different genes of interest. At the outset of this project, several previous siRNA experiments had been attempted but failed to demonstrate consistent knockdown of MyD88 in 2102Ep cells. It was hypothesized that further optimisation of the siRNA protocol would allow consistent demonstration of the MyD88-driven differentiation phenotype. Addressing this, a panel of novel siRNA experiments was performed to further optimise siRNA MyD88 knockdowns. These optimisations investigated different transfection reagents, media, time-points and siRNAs. In each experiment, cell samples were harvested from siRNA treatments and appropriate controls, RNA isolated, and the percentage gene expression knockdown assessed by qPCR. Displaying data from all of these experiments is beyond the scope of this thesis but several examples are now shown in Figures 3.3-3.9. These experiments improved the original transfection protocol and achieved up to 90% knockdown of MyD88 in 2102Ep cells, which would be sufficient for the study of most genes. However, in this case, these levels of knockdown proved to be insufficient for consistent differentiation of 2102Ep cells. It appears that a mere 10% expression of MyD88 is sufficient to maintain MyD88-dependent mechanisms that promote differentiation-resistance in these cells. As siRNAs are not appropriate to achieve 100% absolute removal of a protein of

interest, it was concluded that a siRNA approach was not an appropriate technique for our study and other experimental options were considered. The optimisations carried out for siRNAs are now described, after which an alternative approach is described in Section 3.3.2.

Optimisation of the siRNA protocol began with an assessment of the utility of different concentrations of the siRNA used in previous work and using the already established protocol. An example of this optimisation is shown in Figure 3.3, which indicated that a concentration of 5nM was optimal ( $72.24 \pm 1\%$  knockdown, p-value 0.036), while all other concentrations did not show statistically significant changes. However, it was noted that this protocol did not give substantial knockdown of MyD88. As such, further optimisations were carried out. Based on this data, concentrations of 5nM and 7.5nM were used in future work.

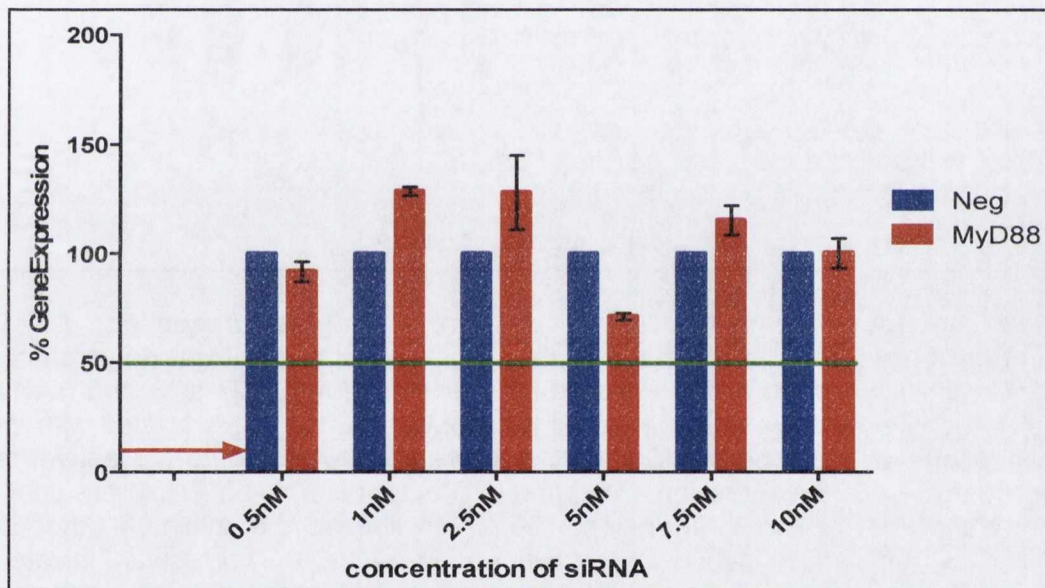


**Figure 3.3 Knockdown of MyD88 in 2102Ep Cells Using Different siRNA Concentrations.** The bar chart shows the percentage gene expression of MyD88 in 'siMyD88' treated 2102Ep cells, as measured by qPCR at 72h (n=3). Using a negative siRNA control (blue) as a calibrator (100%), cells treated with increasing concentrations of siMyD88 (red) were assessed for MyD88 expression. The green line represent 50% expression (-2.0 fold change) and the red arrow represents 90% knockdown, the minimum knockdown we predicted as sufficient to induce differentiation of these cells. The data shows that no substantial knockdown of MyD88 was achieved. However, 5nM siRNA was identified as optimal, statistically significant (p-Value 0.036) and carried forward for further optimisations. All other concentrations showed no statistically significant change.

As a second step in optimisation, a new siRNA (which was referred to as 'siRNA #2'), which targets a different part of the MyD88 transcript, was purchased and its effect assessed. Figure 3.4 demonstrates the effect of siRNA#2 on the knockdown of

MyD88 in 2102Ep cells. The data shows that, at 7.5nM concentrations, siRNA#2 improved upon the previous data. The data also showed that a 72 hour knockdown was optimal, after which cells recovered MyD88 expression. However, this improvement resulted in only a  $46\% \pm 2$  knockdown (p-value 0.05), which was insufficient for our purposes. As such, further optimisations were carried out. From this point on, 7.5nm siRNA#2 for 72 hours was used in all work.

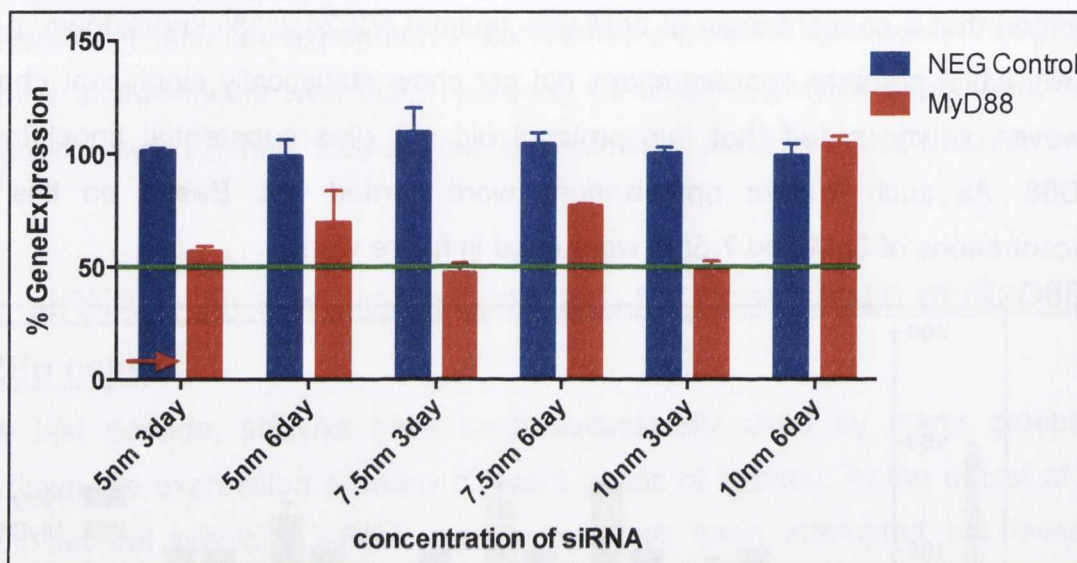


**Figure 3.4 Knockdown of MyD88 in 2102Ep Cells Assessed At Different Concentrations Over Time.** The bar chart shows the percentage gene expression of MyD88 in siMyD88 treated 2102Ep cells, as measured by qPCR at 3 and 6 days (n=3). Using a negative siRNA control (blue) as a calibrator (100%), cells treated with increasing concentrations of a second siMyD88 (i.e. a different siRNA to figure 3.3 above, red) were assessed for MyD88 expression. The green line represents 50% expression (-2.0 fold change) and the red arrow represents 90% knockdown, the minimum knockdown we predicted as sufficient to induce differentiation of these cells. The results indicate that this siRNA approach was not efficient at knocking down MyD88 at these concentrations and over a longer time period. This indicated that further optimisation was required.

The third step in optimisation involved a re-assessment of the transfection reagent used. Upon investigation, the recommendations from the supplier companies had changed, in light of recent developments and publications. A new list of cell types and suggested reagents indicated that better results might be obtained from the use of 'Lipofectamine RNAiMax' ('RNAiMax'). The newly optimised protocol described in Figure 3.4 was repeated using RNAiMax, the data for which is shown in Figure 3.5. The data show that a consistent knockdown of approximately 70% was obtained across time-points from 24-72 hours (24h:  $33\% \pm 10.9$ , p-value 0.016; 48h:  $37\% \pm 7.6$ , p-value 0.05; 72h:  $40\% \pm 7.2$ , p-value 0.03). As this represented a substantial improvement on the previous protocol, RNAiMax was used in all future work.



However, as 70% knockdown was insufficient for our purposes, further optimisation was carried out.

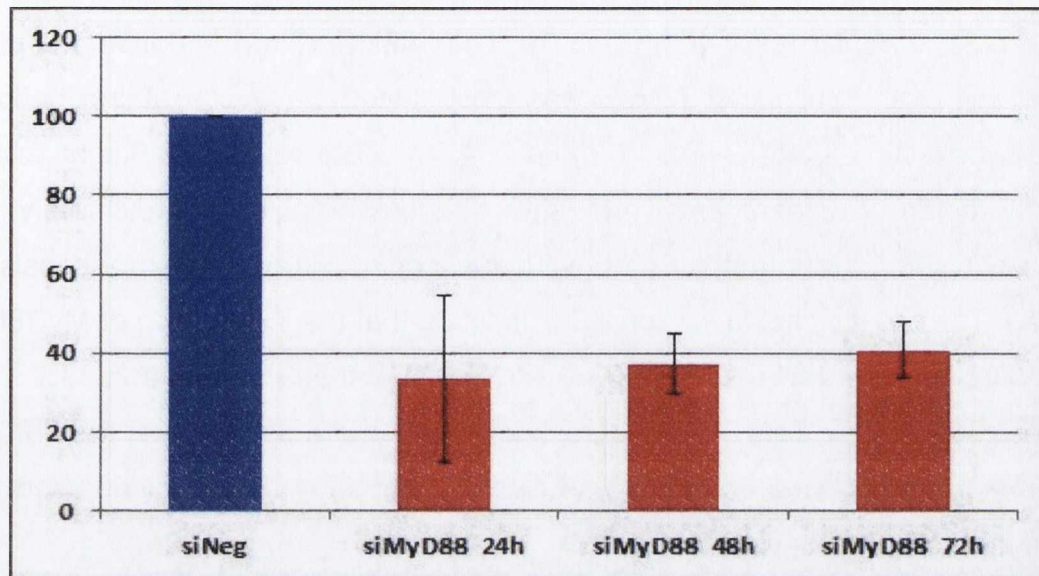


**Figure 3.5. Lipofectamine RNAiMax improves MyD88 knockdown in 2102Ep cells.**

The bar chart shows the percentage gene expression of MyD88 in siMyD88 treated 2102Ep cells, as measured by qPCR at 24-72 hours (n=3). Using a negative siRNA control (blue) as a calibrator (100%), cells treated with increasing concentrations of siMyD88#2 and transfected with 'Lipofectamine RNAiMax', were assessed for MyD88 expression. The results indicate that Lipofectamine RNAiMax improves the MyD88 knockdown in these cells. However, as the knockdown still did not reach 90%, it was concluded that further optimisation was required. All data is statistically significant (p-Values: 24h 0.016, 48h 0.0052, 72h 0.0037)

As a fourth optimisation, the transfection media was assayed for improved efficiency of the protocol. Previously, 2102Ep cells were grown at all times in standard hEC media in the absence of antibiotics, which are well-known to interfere with siRNA transfections. Our group was very cautious about changing this media, as it contains serum, which is a key factor in the switch from undifferentiated to differentiated growth in stem cells generally. Our concern was that moving to a serum-free media might compromise the state-stability of the cells. However, as it had been reported for many cell types that incubations in serum free media such as 'OptiMEM' substantially improved transfection efficiency, this media was assessed in 2102Ep cells.

To test this in 2102Ep cells, transfections were carried out and the cells grown for 4 hours in OptiMEM media. OptiMEM was then removed and cells returned to standard hEC media. It was noted that OptiMEM did not result in any proliferation or

morphological changes that would indicate spontaneous differentiation of the cells. Data from these experiments are shown in Figures 3.6 and 3.7. This data indicated that the switch to OptiMEM media has a substantial improvement upon transfections carried out in hEC media (Figure 3.6). The data further demonstrated that a concentration of 1.8 $\mu$ l of RNAiMax was best suited to OptiMEM incubation for knockdowns lasting up to 72 hours (Figure 3.7). The data in Figure 3.6 is an example of many different experiments and shows knockdown of approximately 90%. However, it is important to state that this degree of knockdown was not consistently obtained. The results shown in Figure 3.7 indicate that the expression of MyD88 was 48%  $\pm$  5.02, p-value 0.01 at 24h, 32%  $\pm$  3.22, p-value 0.005 at 48h, and 37%  $\pm$  3.09, p-value 0.001 at 72h. This 70-80% knockdown was more reflective of the data from multiple experiments. As OptiMEM was clearly a superior media, it was used for all subsequent optimisations.

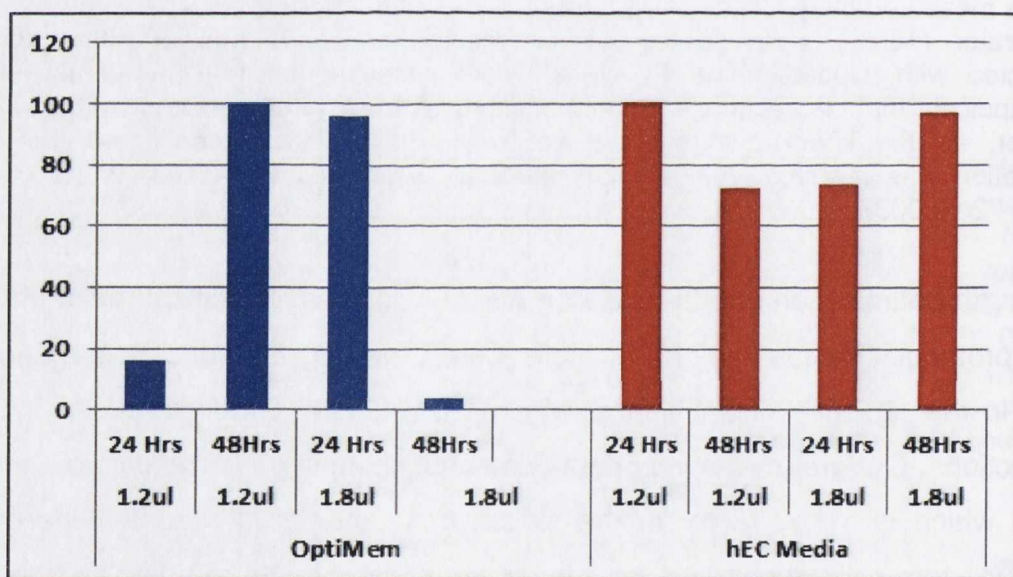


**Figure 3.6. 'OptiMEM' media further enhances transfection efficiency.** The bar chart shows the percentage gene expression of MyD88 in siMyD88 treated 2102Ep cells, as measured by qPCR at 24 and 48 hours. Using a specific negative siRNA control for each different treatment (not shown) as a calibrator (100%), cells were transfected with siMyD88#2 in either 1.2ul or 1.8ul of RNAiMax. These cells were then incubated for 24-48 hours in hEC media, either with (blue) or without (red) an initial 4 hour OptiMEM incubation. The results indicate that OptiMEM substantially improves upon hEC as a transfection media for this experiment. This experiment was carried as n=1 for cost-limitation purposes and the optimized protocol repeated at n=3 as shown in Figure 3.7.

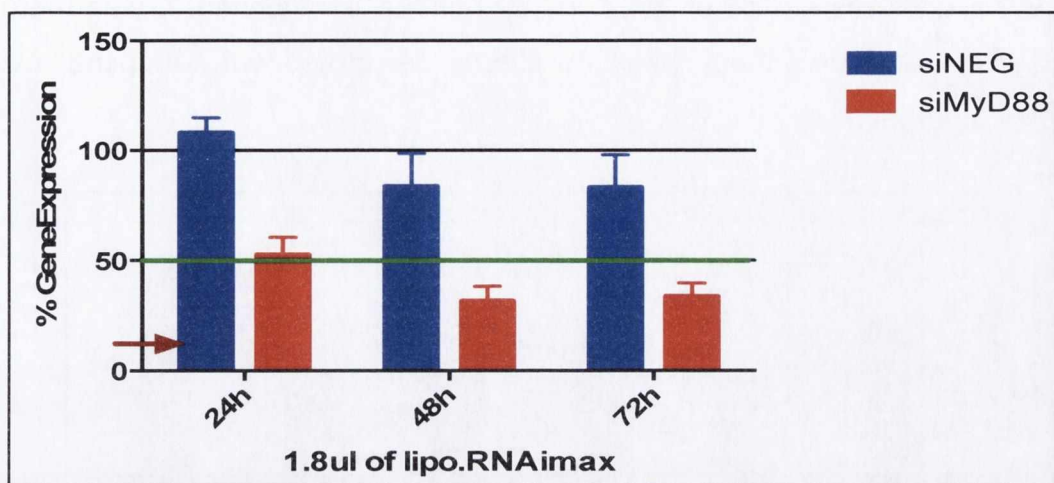


**Figure 3.7. Transfection of 2102Ep cells with siMyD88 using Lipofectamine RNAi max in OptiMEM media.** The bar chart shows the percentage gene expression of MyD88 in 7.5nM siMyD88#2 (RNAiMax) treated 2102Ep cells, as measured by qPCR over 72 hours (n=3). Following transfection, cells were incubated in OptiMEM for 4 hours before changing to hEC media. Using a negative siRNA control (blue) as a calibrator (100%), cells were assessed for MyD88 expression. The green line represents 50% expression (-2.0 fold change) and the red arrow represents 90% knockdown, the minimum knockdown we predicted as sufficient to induce differentiation of these cells. The data shows that this protocol gives an improved knockdown, the expression of MyD88 was 48% ± 5.02, p-value 0.01 at 24h, 32% ± 3.22, p-value 0.005 at 48h, and 37% ± 3.09, p-value 0.001 at 72h. However, the knockdown achieved was not sufficient for our needs and further optimisations were required.

Finally, an alternative approach to transfection was carried out as a comparison to the above work, which was a so-called ‘forward transfection’ approach. This term refers to an approach where cells are plated overnight and the transfection components (siRNA, transfection reagent and transfection media) added post-adherence. An alternative approach, which is known as a ‘reverse transfection’, involves the addition of the transfection components to the cells at the point of plating. The efficiency of either protocol appears to be cell specific according to the literature. 2102Ep cells were reverse transfected using an otherwise similar protocol to above. The only other difference was a longer (16 hour) incubation in OptiMEM, which was suggested by the supplier. This data is shown in Figure 3.8 and indicates that the knockdown had similar efficiency to the forward approach. However, as the reverse protocol takes one day less to perform it was preferable from a user point of view.

As another alternative, a combination reverse + forward transfection was carried out. In this approach, cells are initially reverse transfected and then forward transfected the next day following adherence of the cells. The data for this experiment is shown

in Figure 3.8 and was not as efficient as the reverse transfection. It was therefore concluded that any further optimisations should be carried out using the reverse transfection approach.

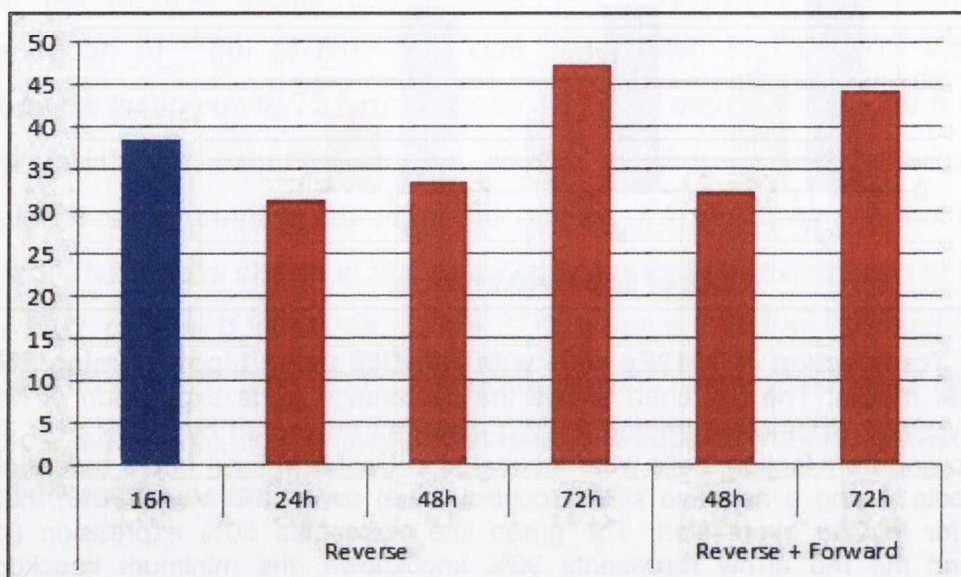


**Figure 3.8. A comparison of reverse and forward+reverse transfection approaches.** The bar chart shows the percentage gene expression of MyD88 in 7.5nM siMyD88#2 (RNAiMax) treated 2102Ep cells, as measured by qPCR over 72 hours. Using a specific negative siRNA control as a calibrator in each case (100%, not shown), cells were assessed for MyD88 expression (red). As an additional control, cells transfected for only 16 hours in OptiMEM are included (Blue). This data indicated that the reverse+forward protocol did not improve the efficiency of the experiment. The data also shows that the reverse approach gives comparable results to the forward protocol used in the data shown in the figures above. This experiment was carried as n=1 for cost-limitation purposes and the optimized protocol repeated at n=3 as shown in Figure 3.9.

### **3.3.2. Loss of MyD88 does not Affect Oct4-Sox2-Nanog Expression**

From previous work (Cooke 2013) there was conflicting data in relation to the effect of loss of MyD88 upon Oct4, Sox2 and Nanog expression. While some data suggested a statistically significant decrease in Oct4-Sox2-Nanog expression when a knockdown of greater than 90% was generated, the data was sporadic and unconvincing: differentiation appeared to occur rarely, randomly and with no relationship to percentage knockdown. Addressing this, the effect of loss of MyD88 expression on Oct4-Sox2-Nanog levels was assessed using the newly optimised protocol. While this protocol routinely produced 70-80% knockdown, occasional samples with greater than 90% knockdown were obtained. These samples were selected and their expression of Oct4-Sox2-Nanog assessed by qPCR (Figure 3.9). The data shows that loss of MyD88 results in a statistically significant

downregulation of Oct4 ( $43.9\% \pm 4.3$ ,  $p$ -value 0.05), but has no effect on Sox2 or Nanog. As the downregulation of Oct4 is not substantial, as would be expected for differentiating cells, we concluded that MyD88 was not a direct regulator of Oct4-Sox2-Nanog. However, this question is visited again in Chapter 5, at which point a more definitive mechanism is described.

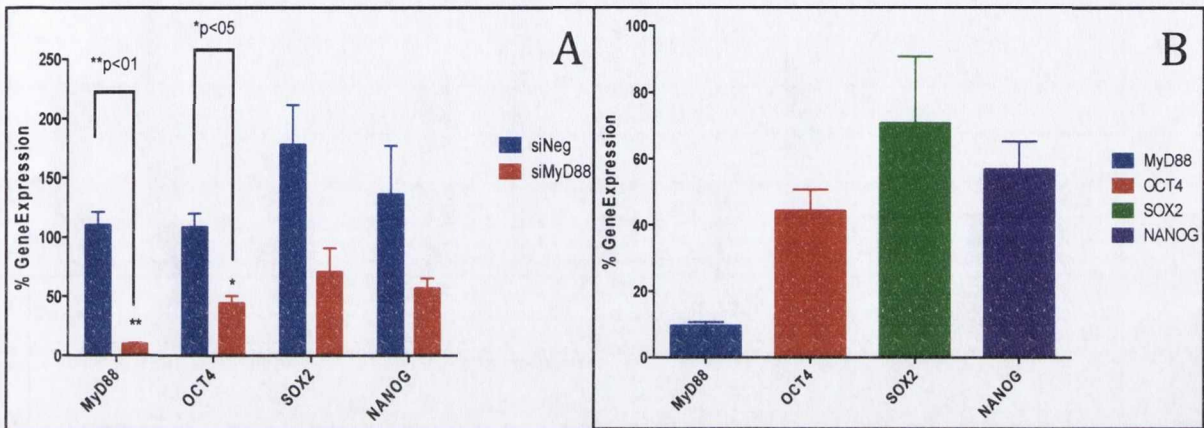


**Figure 3.9. The effect of knocking down MyD88 on Oct4-Sox2-Nanog Expression in 2102EP cells.** During the course of our optimisations, greater than 90% knockdowns were achieved in some biological replicates. These replicates were taken and assessed for expression of Oct4, Sox2 and Nanog, which should be downregulated in differentiated 2012Ep cells. A) Using a negative siRNA control (blue) as a calibrator (100%), the effect of siMyD88 treatment (red) on MyD88, Oct4, Sox2 and Nanog expression was assessed by qPCR. Loss of MyD88 did not result in differentiation but was linked to downregulation of Oct4 ( $43.9\% \pm 4.3$ ) expression in a significant manner ( $p$ -value 0.05). While this loss of Oct4 would not be expected to be sufficient to differentiate the cells, the data suggests an association between Oct4 and MyD88. The same data is represented in B for illustrative purposes.

### **3.3.3. siRNA-Knockdown of MyD88 does not Permit Differentiation of 2102Ep Cells in Response to Retinoic Acid**

Having optimized the siRNA protocol to a substantial degree, RA was added to cells transfected via this optimised protocol, to determine whether differentiation could be induced. Despite knockdowns of between 70-95%, the addition of RA did not stimulate differentiation of these cells. This protocol was attempted in two different approaches. In the first approach, siRNA treated cells were incubated for 3 days, at which point RA was added. These cells continued to proliferate with an obviously undifferentiated phenotype (data not shown). In a second approach, cells were treated with RA for one or two weeks, at which point transfections were carried out (Figure 3.10). In the latter approach, cells were subsequently harvested and the effect on MyD88, Oct4, Sox2 and Nanog expression assessed (Figure 3.11). From

these data it was clear that the siRNA approach was insufficient for our purposes and alternatives had to be considered. This work is described in the next section.

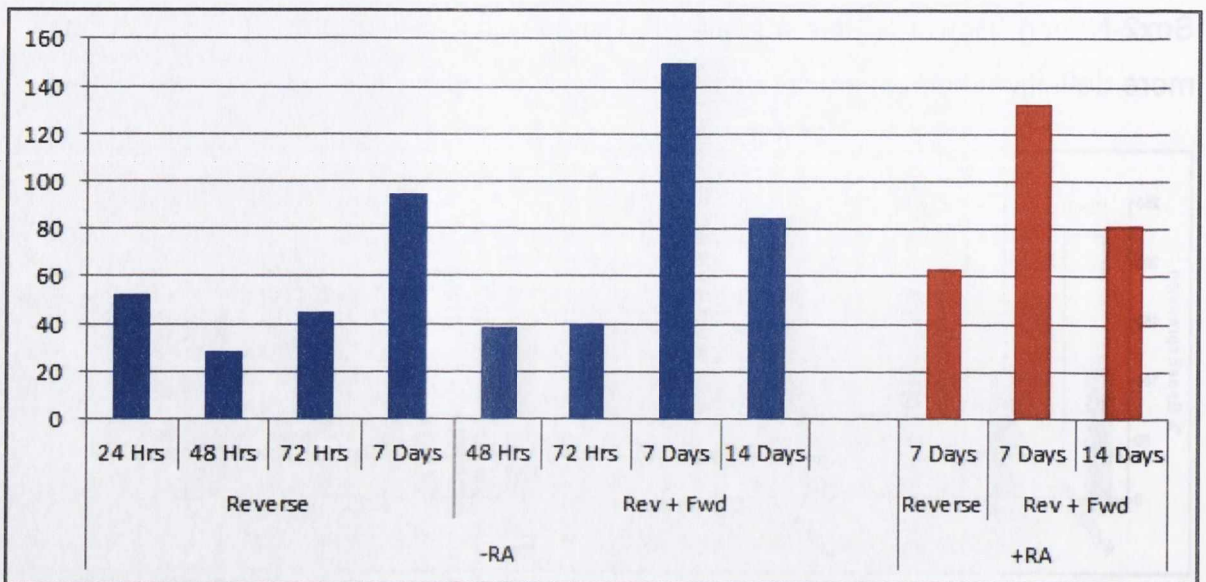


**Figure 3.10. Pre-Treatment of 2102Ep cells with Retinoic Acid does not Affect Knockdown Efficiency.**

The bar chart shows the percentage gene expression of MyD88, as measured by qPCR over time. Using a specific negative siRNA control as a calibrator in each case (100%, not shown), cells were assessed for MyD88 expression. As additional controls, cells transfected with no retinoic acid (-RA) using both the reverse and reverse+forward approaches are included. Cells pre-treated with RA (+RA, red) were subsequently transfected using the reverse and reverse+forward approaches, and their expression of MyD88 assessed by qPCR. The data demonstrate that RA does not affect siRNA knockdown efficiency in these cells.

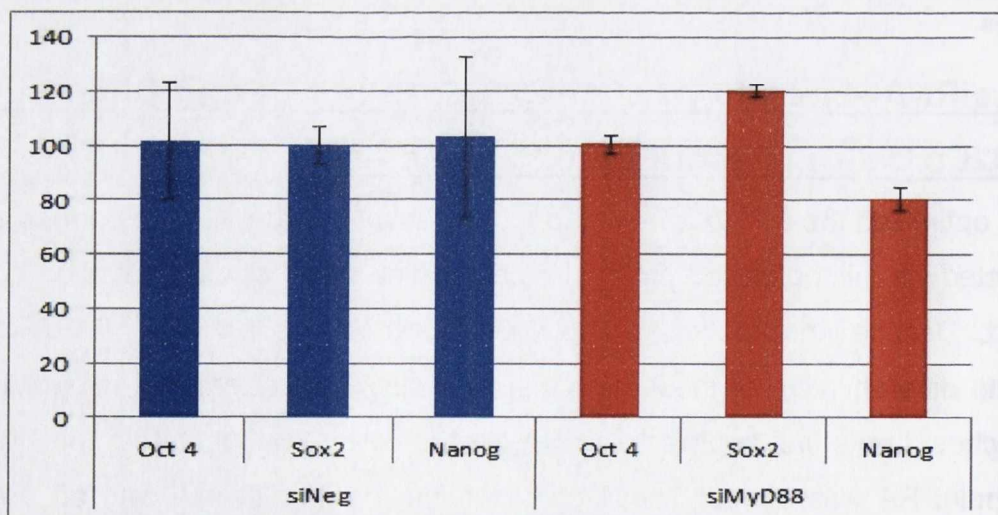


**Figure 3.11. The Addition of Retinoic Acid to siMyD88 Transfected Cells does not Induce Differentiation via Changes in Oct4, Sox2, Nanog Expression.** In this experiment, 2102Ep cells were first treated with a siRNA for MyD88 (siMyD88) or a negative control siRNA (siNeg), after which RA was added. After 6 days treatment, no substantial

change in Oct4 ( $100.5\% \pm 3.5$ ), Sox2 ( $120.2\% \pm 2.1$ ) or Nanog ( $80.6\% \pm 4.5$ ) expression was detected via qPCR analysis of RNA from these samples. All experiments were n=3.

### **3.3.4. MyD88 Peptide Inhibitor Facilitates Retinoic Acid-Induced Differentiation of 2102Ep Cells.**

Consideration and discussion was given to the options of continued use of a siRNA approach or a move to a PepInh approach. While siRNAs were available from other companies, it was decided that it was unlikely that a siRNA approach would yield the total loss of MyD88 that appeared to be required for this differentiation mechanism. As such, a decision was made to attempt a MyD88 PepInh approach, after which results would be assessed and future strategy decided upon. From its first use, the MyD88 PepInh approach pushed 2102Ep cells into an obviously differentiated state, which could be visualized during the experiment and confirmed using stem cell state markers after the experiment. As such, the MyD88 PepInh approach was adopted and used for the remainder of the project.

The MyD88PepInh was added to the cells at a concentration of 5uM, which was the lowest concentration recommended by the supplier (InvioGen). The recommended procedure suggested a 6 hour MyD88PepInh treatment, after which experiments could be undertaken. However, two factors were incorporated into the 2102Ep protocol. First, the siRNA experiments suggested that near-total inhibition of MyD88 was required throughout the course of the experiment. Second, 2102Ep cells required a minimum of 7 days to differentiate. Therefore, after 6 hours MyD88PepInh treatment, RA was added for an overnight incubation. Subsequently, old media was removed each morning and new 'MyD88PepInh+RA' media added. This was continued for 8-12 days. As controls, cells were also treated with A) a control peptide inhibitor (CtrlPepInh), B) 'CtrlPepInh+RA, C) MyD88PepInh-RA, D) -RA, and E) +RA.

MyD88PepInh+RA treatment facilitated differentiation of 2102Ep cells in all but one of more than 20 experiments. While this was strong evidence that the MyD88PepInh was indeed inhibiting MyD88, it was important for publication that this be demonstrated. As described above (Section 3.1.3.) the PepInh does not affect MyD88 gene or protein expression, which ruled out the use of qPCR or western blot

analysis to demonstrate successful inhibition. Instead, cells were treated with the MyD88 or Ctrl PepInh (6 hours) and subsequently with interleukin 1 $\beta$  (IL-1 $\beta$ ), which can only operate MyD88-dependently, and the effect upon the final target of TLR Signaling, NF- $\kappa$ B, assessed. In CtrlPepInh treated samples, the active component of NF- $\kappa$ B, phosphorylated I- $\kappa$ B $\alpha$ , was shown to be present at high levels (Figure 3.12). In contrast, MyD88PepInh treated cells showed a significant decrease in phosphorylated I- $\kappa$ B $\alpha$ , demonstrating inhibition of MyD88-dependent signaling in response to IL-1 $\beta$ , and thus inhibition of MyD88. This, coupled with the differentiation phenotype observed, was strong evidence that differentiation was due to actual inhibition of MyD88 by the MyD88PepInh rather than an off-target effect.

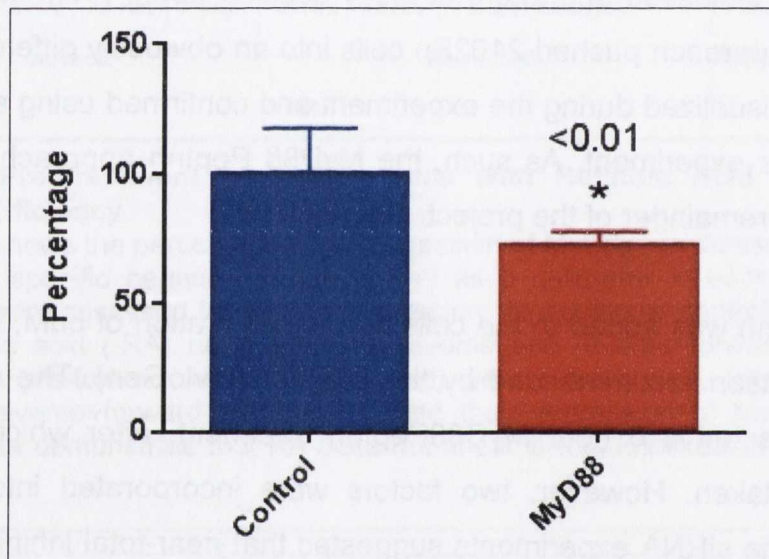
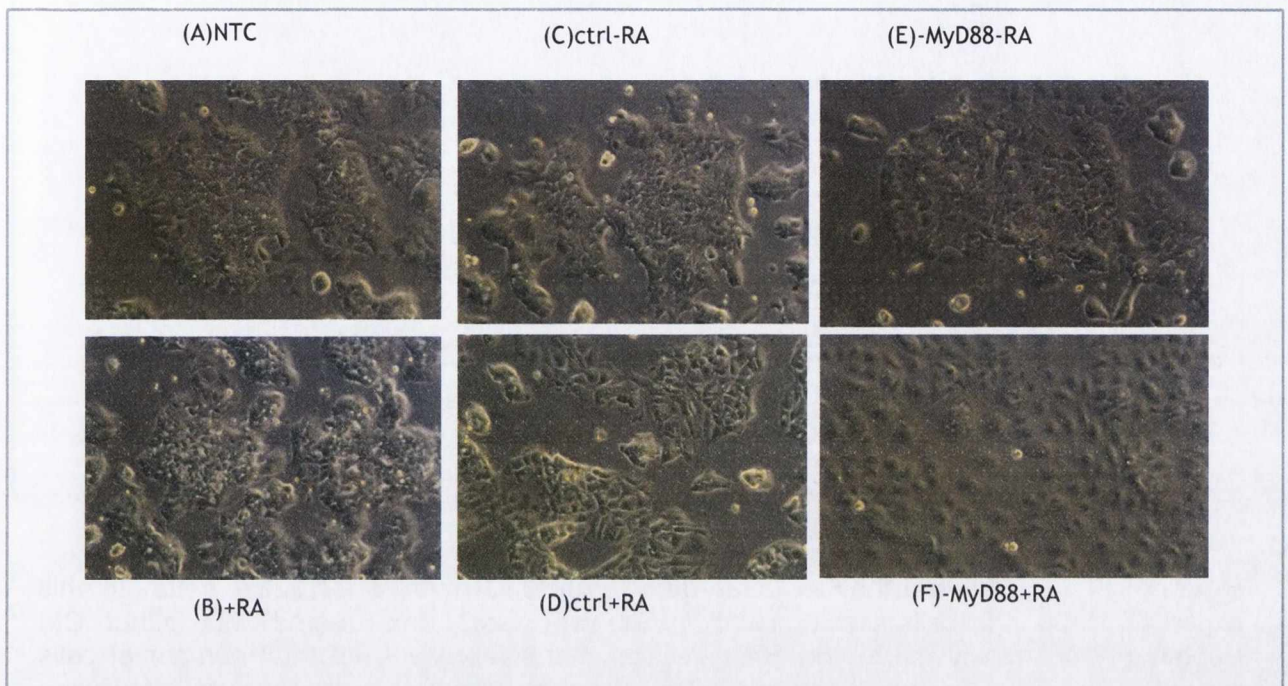


Figure 3.12. **The MyD88 Peptide Inhibitor Inhibits MyD88-dependent TLR Signaling.** TLR Signaling targets NF- $\kappa$ B, which results in an increase of its active form, phosphorylated I- $\kappa$ B $\alpha$ , in the cell. In this experiment, cells were treated with either the Ctrl (blue) or MyD88 (red) PepInh for 6 hours and subsequently with IL-1 $\beta$ , which can only act MyD88-dependently, for 30 minutes. Cells were then assessed for phosphorylated I- $\kappa$ B $\alpha$  by elisa. The results demonstrate that the percentage expression of phosphorylated I- $\kappa$ B $\alpha$  (Y-axis) was significantly higher in CtrlPepInh treated cells than in MyD88PepInh treated cells. This data indicates that MyD88 activity is inhibited by the MyD88PepInh, which decreases MyD88-dependent TLR Signaling.

As stated above (Section 3.1.2.), there is no single test to demonstrate differentiation. Therefore, morphology, proliferation and changes in stem cell markers were assessed. Phenotypically, cells were larger, which is indicative of differentiation (Figures 3.13). Growth rate (cell count) data demonstrated that MyD88 PepInh+RA treated cells stopped proliferating (1.05 million cells  $\pm$ 0.07) compared to



control cells (9.77 million cells  $\pm$ 0.22), which continued to grow: this is also indicative of differentiation (p-Value 0.0001, Figure 3.14).



**Figure 3.13. MyD88PepInh+RA Treatment Induces a Differentiation Phenotype:** These photographs show that MyD88 PepInh+RA treatment induced 2102Ep cells into a differentiated phenotype, which was not observed in controls. All treatments were carried out for 12 days, which was required to complete differentiation. NTC: Non-treated cells, RA: retinoic acid, Ctrl: Control scrambled PepInh drug, -MyD88: MyD88 PepInh Drug.

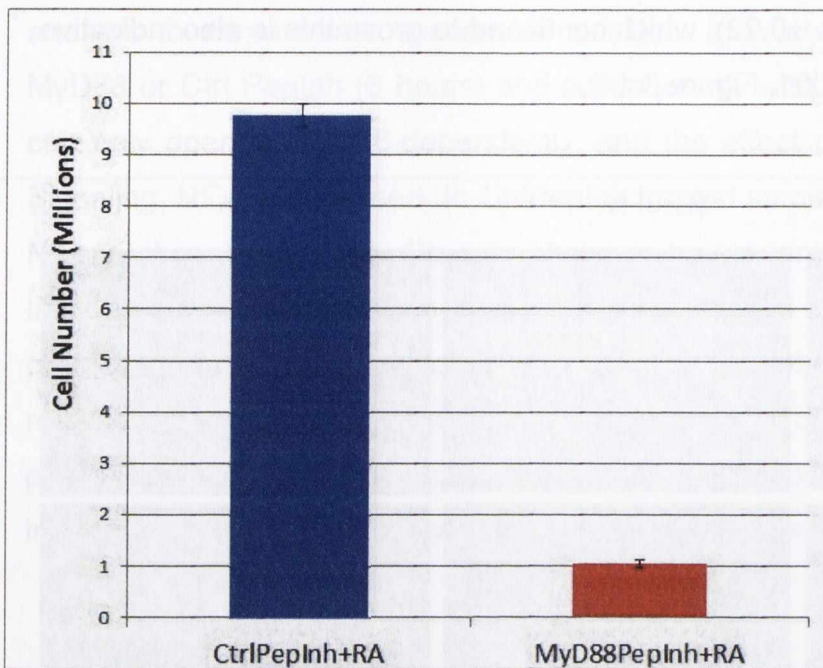


**Figure 3.14. MyD88PepInh+RA Treatment Inhibits Growth of 2102Ep cells.** In this experiment, 50,000 cells were plated in 24-well plates and treated with either CtrlPepInh+RA or the MyD88PepInh+RA. The bar charts represent the total number of cells present after 12 days of each treatment. The presence of substantially fewer cells following MyD88PepInh treatment is characteristic of differentiation. Data represent n=3 (CtrlPepInh) and n=9 (MyD88PepInh), p-Value 0.0001.

At a molecular level, a decrease in Oct4-Sox2-Nanog levels is a very strong indicator of differentiation, as was detailed in Chapter 1 (Section 1.3). When assessed, qPCR data demonstrated decreases in Oct4 ( $60.8\% \pm 2.2$ , p-value  $<0.01$ ) Sox2( $44.8\% \pm 2.4$ , p-value  $<0.01$ ) and Nanog( $48.2\% \pm 0.7$ , p-value  $<0.05$ ) in the MyD88 PepInh+RA cells but not in controls (Figure 3.15). However, suspicions were arisen at this point as the changes in Oct4, Sox2 and Nanog were not as strong as would be expected with differentiated EC cells, which is incompatible with the morphology and growth rate results observed. Addressing our suspicions, a quick Elisa-based assay was employed to determine whether these cells were in the undifferentiated or differentiate state. This assay demonstrated that undifferentiated 2102Ep maker Alkaline Phosphatase (AP) was not statistically significantly downregulated in MyD88 PepInh+RA cells, despite their differentiated phenotype (Figure 3.16). Again, this was incompatible with the morphology and growth rate results observed.

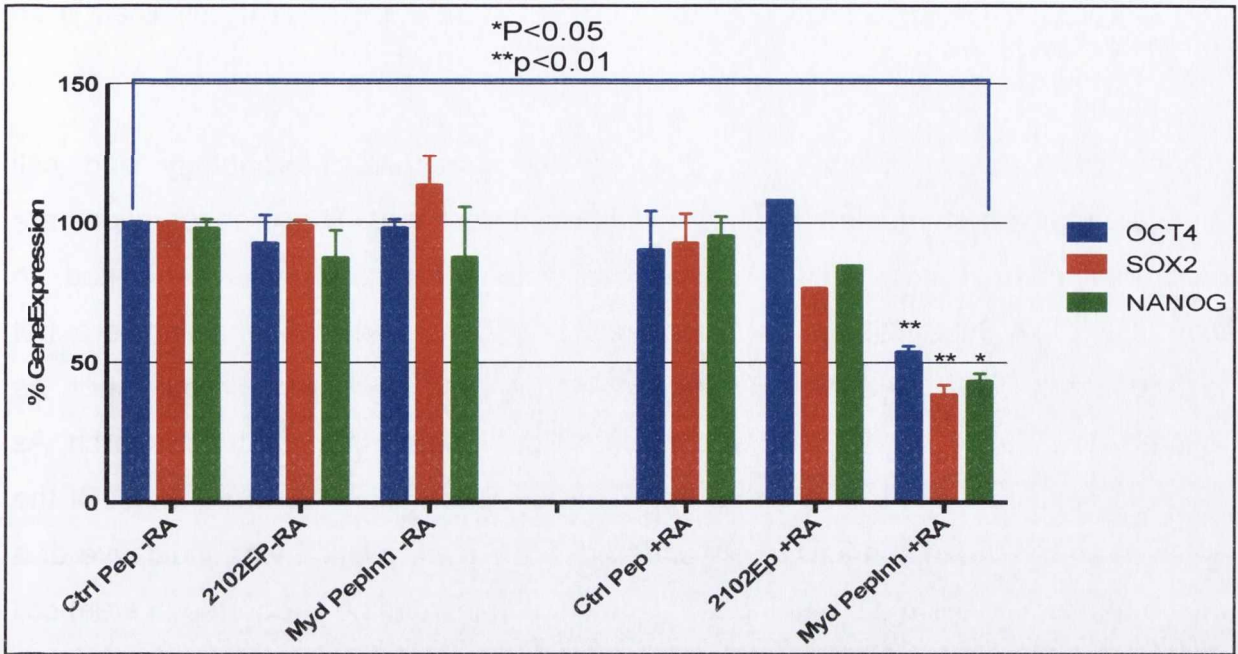


**Figure 3.15. MyD88PepInh+RA Treatment Reduces Oct4-Sox2-Nanog Expression.** This chart shows qPCR result as percentage expression of Nullipotency Genes (Oct4 in blue, Sox2 in red and Nanog in green) in untreated (2102Ep±RA), control treated (CtrlPep±RA) and MyD88PepInh treated (-MyD88±RA) 2102Ep cells. Only -MyD88+RA treated 2102Ep cells show downregulation of nullipotency Genes Oct4 (60.8% ± 2.2), Sox2 (44.8% ± 2.4) and Nanog (48.2% ± 0.7). However, a greater degree of downregulation would be expected if differentiation was truly being observed.

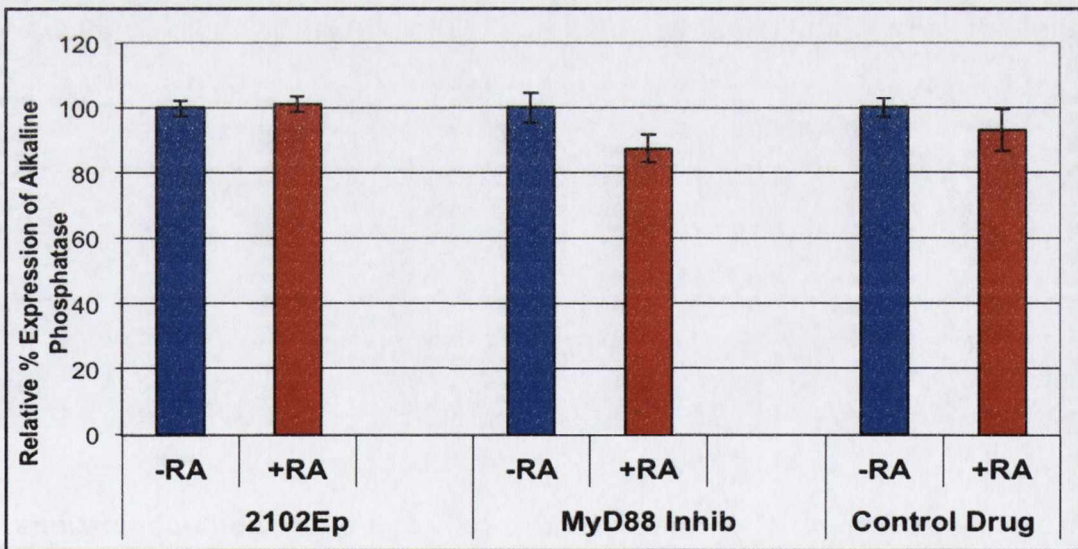


**Figure 3.16. Alkaline Phosphatase (AP) Expression Indicates that MyD88PepInh+RA Treated 2102Ep cells are in an Undifferentiated State.** After 12 days of MyD88PepInh or control treatment, cells were harvested and assessed for alkaline phosphatase expression, which is a marker of stem cell state. The bar chart indicates that no substantial loss of

alkaline phosphatase was observed, which indicates that these all cells remained in an undifferentiated state.

These four pieces of data provided conflicting results. Morphology and cell proliferation data suggested that the cells had differentiated. These observations are very difficult to discount, even when conflicting molecular data is generated. In contrast, Oct4-Sox2-Nanog and AP levels suggested that these cells were not differentiated. The idea that Oct4-Sox2-Nanog and AP levels would not be decreased in differentiated cells would contradict 20 years of stem cell research. As such, an explanation that validated both sets of observations was required. Of the several possible explanations, we wondered if this contradiction was indicative of a two-population system, something that is becoming increasingly reported in stem cell research. Addressing this hypothesis, morphology images from the MyD88PepInh experiments were re-examined to assess whether two types of cell were present. Figure 3.17 demonstrates that there appear to be two cell types in the flasks containing MyD88PepInh+RA treated cells, which support this 2 sub-population hypothesis.



**Figure 3.17. MyD88PepInh+RA Treated 2102Ep cells appear as 2 sub-populations.** The image shows cells treated with MyD88PepInh+RA for 5 (left) and 12 (right) days. The blue arrows indicate cells with an undifferentiated morphology, which adopt a standard clustering formation. The red arrows indicate cells with a differentiated morphology, which adopt a separated, pebble-like morphology. This supports the 2 sub-population hypothesis.

We noted that this 2 sub-population hypothesis would also provide a potential explanation for the high expression of phospho-I- $\kappa$ B $\alpha$  in MyD88PepInh treated cells: we hypothesised that one population of the cells did not take up the MyD88PepInh while the other population did. As the MyD88PepInh was refreshed each day to avoid uptake efficiency issues, this additionally suggests that one population of 2102Ep cells could resist MyD88 inhibition. In order to test this new hypothesis, a single-cell based approach such as flow cytometry was required. These experiments are described in Chapter 4 and demonstrated the presence of two sub-populations within 2102Ep cells. One of these populations remains undifferentiated throughout the experiment while the other differentiates in MyD88PepInh+RA conditions.

### **3.4. Discussion**

At the outset of this study, preliminary data indicated that MyD88 was a functional component of pluripotency/nullipotency in human NTera2 and 2102Ep EC cells respectively. Specifically, loss of MyD88 appeared to allow differentiation of the otherwise nullipotent 2102Ep cell line but only in the presence of the differentiation morphogen RA. However, the experimental demonstration of this mechanism was sporadic. Perhaps more worryingly, when previous work compared siMyD88 treated cells to that of a negative control siRNA by whole genome gene expression arrays, the samples did not cluster in to any extent (Cooke 2013). This experiment indicated that the samples, despite a considerable difference in MyD88 expression, were indistinguishable at a molecular level. This considerable conundrum was addressed to some extent in this chapter. The data presented demonstrated that inhibition of MyD88 using a PepInh allowed consistent experimental differentiation of 2102Ep cells, but again only in the presence of RA. In parallel with the previous gene array data, however, the data was muddled: some assays indicated the presence of a clearly differentiated cell type and others the presence of an undifferentiated cell type. This led to the hypothesis that the 2102Ep cell line contains two sub-populations. The first sub-population appears to remain nullipotent throughout the experimental approach. The second sub-population differentiates when MyD88 is inhibited and RA is present. Addressing this hypothesis required a different, single-cell approach, such as flow cytometry, which is described in detail in Chapter 4. As the elucidation of this mechanism builds through Chapters 4 and 5, the overall mechanism and implications are principally discussed in the 'General Discussion' (Chapter 6). In this section, the implications of these initial experiments will be briefly discussed.

#### **3.4.1. The Relationship Between Self-Renewal and Differentiation**

The most fundamental mechanism in stem cell and CSC biology is the relationship between the self-renewal and differentiated states. Self-renewal is often misunderstood as cellular proliferation. However, self-renewal involves two processes. First, self-renewal controls the continued proliferation of the undifferentiated stem cell. Secondly, self-renewal involves multiple regulatory systems that, together, inhibit differentiation. As such, self-renewal is a two-

mechanism process. In contrast, differentiation involves the reverse of these two mechanisms. Once differentiation begins, self-renewal mechanisms of cellular proliferation are inhibited and mechanisms that drive lineage (endoderm, mesoderm and/or ectoderm) differentiation are promoted. As such, stem cell and CSC states are a balance between the promotion and inhibition of self-renewal and differentiation mechanisms (Figure 3.18).

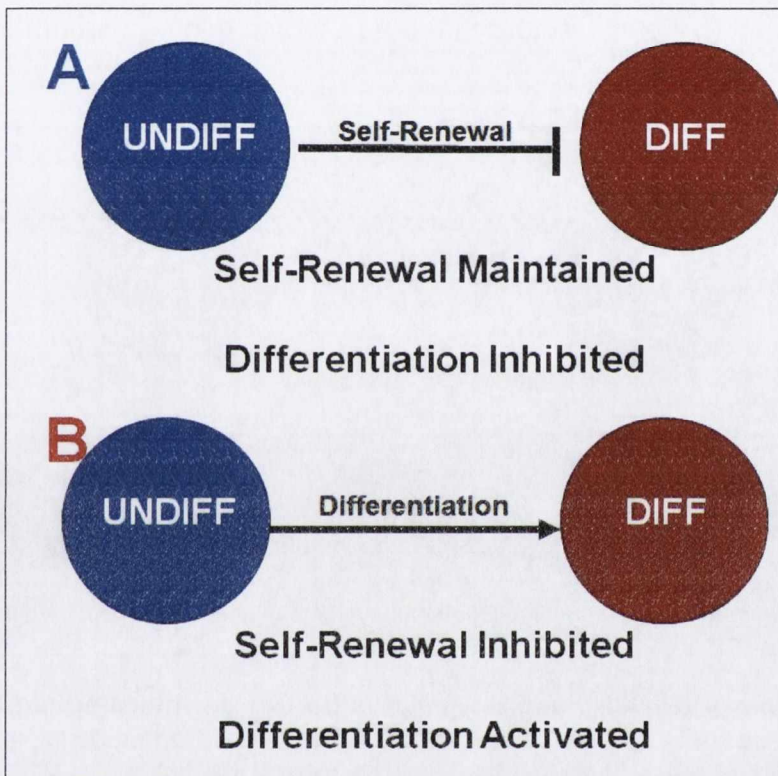


**Figure 3.18. The Relationship Between Self-Renewal and Differentiation.** The relationship between self-renewal and differentiated stem cell and CSC states is tightly balanced. Self-renewal involves the maintenance of self-renewal mechanisms and the inhibition of lineage differentiation mechanisms (A). In contrast, differentiation involves the inhibition of self-renewal mechanisms and the promotion of lineage differentiation mechanisms. The correct balancing of these mechanisms is required to ensure maintenance of the undifferentiated stem cell pool.

Mechanistically, exit from the self-renewal state is a cell cycle exit process. Historically, exit from the self-renewal state and differentiation were considered to be a single coupled process (Figure 3.19). More recently, this concept has been challenged by models that attempt to model a transition state between the two. The work described in this chapter offers an interesting parallel, where loss of MyD88 defines such a transition state (Figure 3.19). This concept has been most

prominently addressed by Austin Smith's work on mouse embryonic stem (mES) cells, which was described in Chapter 1 (Section 1.3). Smith's laboratory has produced a series of papers that indicate that mES cells exist in a 'ground' or 'naïve' state, which is thought to represent the basal pluripotent state found in the cells of the inner cell mass of the developing embryo (Figure 3.19). Ground state mES cells can transition to a primed state, which is known as an 'EpiSC' state due to its similarities to cells of the epiblast stage of the mouse embryo. EpiSCs are capable of lineage differentiation, which, along with mES to EpiSC transition, is governed by the presence of specific growth factors in the embryonic microenvironment.

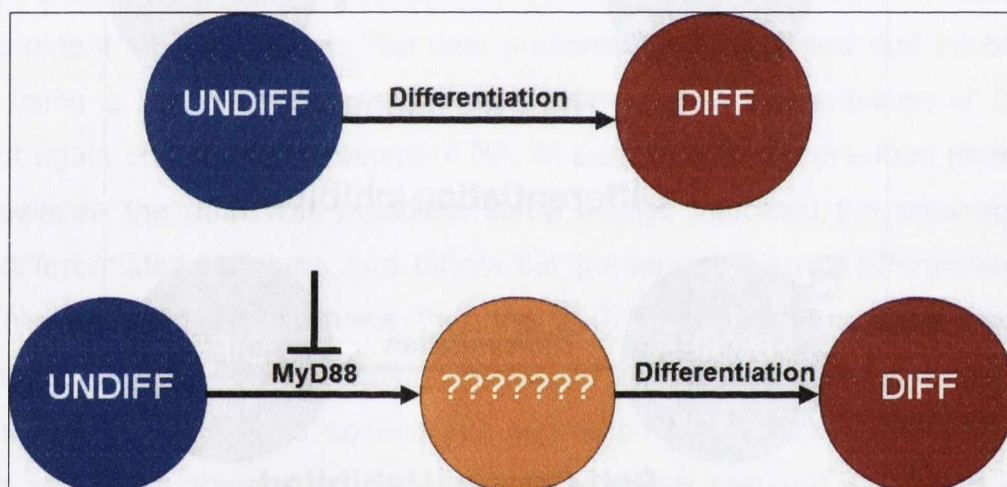


**Figure 3.19. Loss of MyD88 Facilitates Transition to an Intermediate Stem Cell State.** Historically, exit from the self-renewal state and lineage differentiation were considered to be a single, coupled process, as illustrated at the top of the figure. In 2102Ep cells, loss of MyD88 appears to transition some cells in to an as yet undefined transition state, which is primed for differentiation in response to the morphogen retinoic acid. This model is an interesting parallel to the Ground State model, which is described in Figure 3.20.



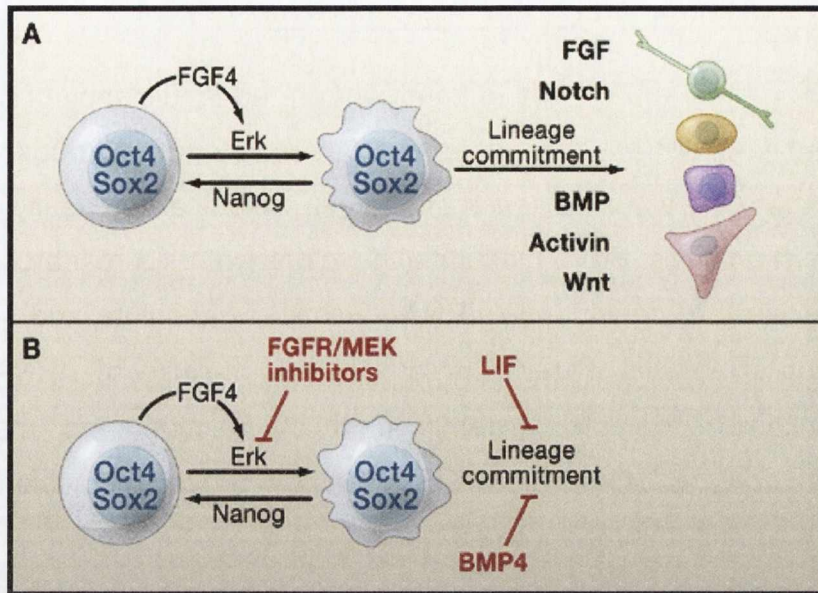


**Figure 3.20. The 'Ground State' Model of Pluripotency.** Several years of research from Austin Smith's lab has resulted in a model where mouse embryonic stem (mES) cells can exist in a 'Ground' or 'Naïve' state, which transitions to an epiblast 'EpiSC' state, which is primed for lineage differentiation. This model indicates that the presence of key growth factors facilitate mES to EpiSC and EpiSC to lineage differentiation states (A). In the laboratory, blocking of these mechanisms is achievable using specific growth factor inhibitors (B). This is an interesting parallel to the MyD88 model presented in Figure 3.18. (Smith and Silva 2008).

The MyD88 model proposed here (Figure 3.18) offers many parallels to that of Smith's Ground State model. This is very interesting, as the Ground State hypothesis has not, to our knowledge, been demonstrated in human pluripotent cells. The first similarity is that loss of MyD88 in our system appears to move some 2102Ep cells in to a transition state. Secondly, this state appears to be stable in the self-renewal state in the absence of a morphogen such as RA. Thirdly, as the main function of MyD88 (via TLR Signaling) is to determine the exact profile of chemokines and cytokines secreted by the cell, this mechanism is also determined by the cellular microenvironment. Fourthly, this MyD88-regulated self-renewal state appears to be primed for lineage differentiation in a similar fashion to the Ground State model. Of course, this speculation requires further testing. The testing of these hypotheses and models are presented in Chapter 4 and the mechanisms involved further discussed in Chapters 4, 5 and 6.

### **3.4.2. A Technical Comment on the use of siRNAs.**

Before concluding, it is appropriate to comment on the inefficiency of siRNAs in this study. For some time, siRNAs have been widely used by many groups to knockdown the expression of many different genes of interest, which can be easily confirmed via qPCR or western analysis. From their initial development as a research tool, siRNAs have been criticized for 'leakiness': siRNAs are never absolute and some residual gene expression is always present. In most cases, the use of siRNAs displays a sufficient knockdown to permit identification of function and mechanism by comparison with controls. However, this leaky system proved insufficient in our study and a PepInh approach proved more efficient.

In considering the use of siRNA alternatives, the use of a PepInh drew one principle concern: this drug affects protein function rather than protein expression so it would not be possible to demonstrate drug efficiency using gene or protein expression as a readout. This would have been a considerable problem if extensive optimisation was required, which was the experience from the siRNA work. In this case, differentiation was efficiently achieved, which could serve as a readout. Moreover, differentiation was immediately achieved with the first concentration suggested by the suppliers. From our experience, it appears that the PepInh approach is highly effective with limited optimisation required, advantages that promote their use ahead of siRNAs.

### **3.5 Conclusion**

In this Chapter, the elucidation of regulation of EC pluripotency/nullipotency by MyD88 was continued. After considerable attempts to demonstrate differentiation using a siRNA approach, the decision was made to attempt alternatives, the first of which was peptide inhibition. The use of the PepInh immediately facilitated differentiation of the cells, according to certain observations. In contrast, other observations clearly indicated that undifferentiated cells persisted. This has led to the hypothesis that the 2102Ep cell line contains two sub-populations. One of these sub-populations appears to remain nullipotent while the other readily differentiated when MyD88 is inhibited and RA present. The loss of MyD88 appears to transition these 2102Ep cells in to a self-renewal state that is primed for lineage differentiation in response to RA. This is an interesting and exciting observation that is further elucidated in Chapters 4 and 5. In conclusion, at the end of this Chapter a significant

step had been made towards to elucidation of the MyD88 mystery inherent in these cells. In the context of human pluripotency, it appears that whatever is happening in these cells is highly unusual, unpredicted in the literature and of potential enormous importance.

## Chapter 4.

# MyD88 is a Retinoic Acid Differentiation Gate-Keeper in 2102Ep hEC cells.

### 4.1 Introduction

In the previous Chapter, a two sub-population hypothesis for MyD88-regulated differentiation in 2102Ep cells was proposed. This was based on conflicting data from cells treated with both a MyD88 inhibitor and retinoic acid (RA). Morphology and cellular proliferation data suggested the presence of differentiated cells, which had an altered phenotype and growth rate. In contrast, expression of the Alkaline Phosphatase, Oct4, Sox2 and Nanog pluripotency/nullipotency markers was higher than would be expected for differentiated cells, which suggested the presence of undifferentiated cells. At the time, these conflicting observations presented quite a conundrum. However, other projects underway in the group at the time had elucidated the presence of multiple different Cancer Stem Cell (CSC) types in another cell line of interest. This led to the hypothesis that a similar mechanism might be present in the 2102Ep cell line. Specifically, the data presented in Chapter 3 suggested the presence of two sub-populations within the cell line. The first sub-population appeared to remain nullipotent through the experiment. In contrast, the second sub-populations readily differentiated in the presence of a MyD88 peptide inhibitor (PepInh) and retinoic acid (RA). This Chapter describes the testing of this two sub-population hypothetical model, which was achieved through single-cell analysis using flow cytometry. As will be described, these experiments confirmed the presence of two sub-populations within the 2102Ep cell line, with characteristics as hypothesised.

The conflicting data from Chapter 3 suggested that there might be 2 sub-populations within the 2102Ep cell line, one of which is fully nullipotent. The other sub-population appears to be partially Nullipotent and capable of differentiation in MyD88PepInh +RA conditions. This hypothesis was tested in this section using flow cytometry analysis of SSEA4, a protein marker that can be used to discriminate between undifferentiated and differentiated nullipotent cells.

#### **4.1.1. Cripto-1 Expression Marks Two Sub-Populations of NTera2 Pluripotent Embryonal Carcinoma Cells**

The concept of multiple CSC populations within well-established cancer and CSC cell lines is becoming increasingly more reported in recent years (Ffrench et al 2014, 2015). This appears to be related to the hierarchical structure of stem cells and CSCs within tissues and tumours respectively, which was described in Chapter 1 (Section 1.2). In this model, an apex stem cell sits at the top of a tree like structure, where it primarily resides in a quiescent state. When required for growth and repair, the apex stem cell is 'awakened' and re-enters the cell cycle to produce intermediary stem cells known as progenitor cells, after which it returns to quiescence. These progenitor cells are less potent than their apex stem cell parents and carry out the main asymmetric division work required to produce the mature, differentiated cells needed for growth and repair. In this model, quiescence permits the apex stem cell to reside long-term, while progenitor cells are generally short lived. This hierarchical model of stem cell biology is now broadly accepted and indicates the presence of multiple stem and progenitor cells in all tissues and cell lines. In addition, it now appears that more complex tissues contain multiple independent and/or interdependent hierarchies acting side by side. These complex mechanisms are as yet poorly understood. However, this model clearly indicates the presence of multiple different stem, progenitor and differentiated cell types within each tissue of the body. These concepts are described in detail and fully referenced in our group's recent review and book chapter (Ffrench et al 2014, 2015).

From the earliest use of the term 'CSC' in work with Leukaemia stem cells, CSCs were described as hierarchies with similar complexities to those observed in their non-malignant equivalents, namely Haematopoietic and Mesenchymal stem cells (HSCs and MSCs, Bonnet and Dick 1997, Kreso and Dick 2014). Indeed, analysis from another project in our group indicates that there are at least 12 individual CSCs within a hierarchy we have identified in an ovarian cancer cell line model (unpublished). These observations serve to illustrate the complexity involved in CSC biology and lend credit to the two-population hypothesis that has been proposed in this thesis.

In embryonal carcinoma (EC) cells, two sub-populations have previously been described in pluripotent NTera2 cells but not, to our knowledge, in nullipotent 2102Ep cells. In their study, Watanabe et al (2007, 2010) described the presence of two NTera2 sub-populations based on the expression of the 'Cripto-1' gene. Cripto-1 (CR-1) is a Nodal co-receptor, which is a component of the 'Activin' arm of the TGF- $\beta$  Signaling pathway (Watanabe et al 2007). This pathway is specifically involved in left-right axis determination in embryonic patterning, which is essential for correct development. The two NTera2 sub-populations have been designated CR-1<sup>High</sup> and CR-1<sup>Low</sup> cells, where the former are more tumourigenic and express higher levels of Oct2-Sox2-Nanog than the latter (Watanabe et al 2010). While this mechanism, and its functional importance, is as yet poorly understood, it lends more weight to the two-population hypothesis that has been proposed.

#### **4.1.2. Is MyD88 a Retinoic Acid Differentiation Gatekeeper in Embryonal Carcinoma CSCs?**

The results presented in Chapter 3 suggest that MyD88 may be a RA-differentiation gatekeeper in both nullipotent and pluripotent EC cells. The full elucidation of this mechanism is compounded by the potential presence of two sub-populations. As such, the obvious direction in which this study would now proceed was to assess the differentiation status of individual cells. For this purpose, the most useful approach was flow cytometry based on the expression of undifferentiated state marker 'SSEA4'. It is well-established that SSEA4 is expressed on the cell surface of undifferentiated pluripotent cells and lost upon differentiation (Section 1.4). Furthermore, SSEA4 flow cytometry was already a 'tried and tested' approach from other projects within our group.

To test the hypothesis, 2102Ep cells would be treated with MyD88 Peptide Inhibitor (PepInh) and the expression of SSEA4 assessed across individual cells. Our hypothesis predicted that substantial changes in SSEA4 should not be present on any cells until RA is introduced. However, it was possible that loss of MyD88 would transition cells in to a new state that could be distinguished from untreated 2102Ep cells on the basis of SSEA4<sup>High</sup> and SSEA4<sup>Medium</sup> levels. Of course, this and later work with RA treated cells would be based upon the untested assumption that, once

differentiated, 2102Ep cells would transition to SSEA4<sup>Low</sup> levels. As such, as a first experiment, 2102Ep cells would be force-differentiated using a siRNA specific for Sox2, which we have previously shown differentiates 2102Ep cells (Vencken et al 2014). These force-differentiated 2102Ep cells would then be tested to ensure loss of SSEA4 expression. Once this marker had been validated, cells would be treated with MyD88 or control (Ctrl) PepInh with and without RA and the expression of SSEA4 on individual cells assessed by flow cytometry. This experimental plan predicts that populations of SSEA4<sup>High</sup>, SSEA4<sup>Medium</sup> and SSEA4<sup>Low</sup> may be present at different stages of the protocol. As will be described in detail below, this procedure validated our hypothesis through demonstration of the presence of SSEA4<sup>High</sup> and SSEA4<sup>Low</sup> populations, but only when MyD88PepInh and RA are combined. The final advantage of this approach is that the flow cytometry protocol could be easily adapted to cell sorting, which allowed the separation of these different sub-populations for molecular analysis.

#### **4.1.3. Is MyD88 an Absolute Differentiation Gatekeeper in Embryonal Carcinoma CSCs?**

Due to their pluripotency, EC cells are capable of differentiating to produce cells representative of all three germ layers (endoderm, mesoderm and ectoderm). As such, it was important to assess the role of MyD88 in lineage differentiation in EC cells. These experiments would be vital to understanding the MyD88 differentiation mechanism. Specifically, the aim of these experiments was to demonstrate whether MyD88-facilitated differentiation was specific to RA and/or one or more lineage differentiation mechanisms. Apart from contributing to our understanding of differentiation-resistance in CSCs, these results would be of particular interest to regenerative medicine. Experiments addressing this question are included in this Chapter.

The precise mechanisms of lineage differentiation are poorly understood. This is primarily due to the fact that pluripotent stem cells rapidly differentiate, which makes the identification of key early events challenging. The comparison of 2102Ep and NTera2 cells is particularly useful in this regard, as demonstrated by the identification of MyD88. As such, the mechanism under scrutiny in this thesis has particular

potential value to regenerative medicine. Stem cell researchers involved in regenerative medicine aim to produce tissues and organs to patient's exact specifications. However, once stem cells are removed from their *in vivo* niche, the differentiation of stem cells is very difficult to control. In all but a few well-characterised models, pluripotent stem cells tend to produce a multitude of (undesired) tissues when stimulated to produce a desired cell or tissue type. A better understanding of the 'Gatekeepers' of different lineage differentiation mechanisms is vital to regenerative medicine (Smith 2010, Loh and Lim 2011).

While growth factors in the stem cell microenvironment are known to be the key determinants of lineage differentiation, there is debate about the precise mechanisms involved. The 'Ground State' model of mES cells described earlier (Figure 3.19) illustrates how mES cells differentiate in to different lineages depending upon the presence of growth factors such as Fibroblast Growth Factor (FGF), Transforming Growth Factor-beta (TGF- $\beta$ ) and Wnts (Silva and Smith 2008). In contrast, Bing Lim has offered an alternative 'Competition' hypothesis for human ES (hES) cells (Loh and Lim 2011, Figure 1.4). In this review paper, Bing Lim points out that both loss and over-expression of key factors such as Oct4, Sox2 and Nanog cause specific lineage differentiation in hES cells. Modelling this paradox, the Competition model proposes that, in hES cells, each key transcription factor promotes the differentiation of one lineage while inhibiting another. In this way, the presence of all of these transcription factors (Oct4, Sox2, Nanog and others) causes a homeostasis to be reached, which is, in effect, a balanced self-renewal state. Upon differentiation with agents such as RA, for example, all transcription factors are lost, which results in three germ layer differentiation. The key implication of the Competition Model is that generation of specific cells from hES cells must involve systematic alteration of only the precise transcription factors involved in that lineage. In the case of this thesis, it was exciting to investigate whether the Ground State or Competition Models would be supported by the MyD88 differentiation mechanism.



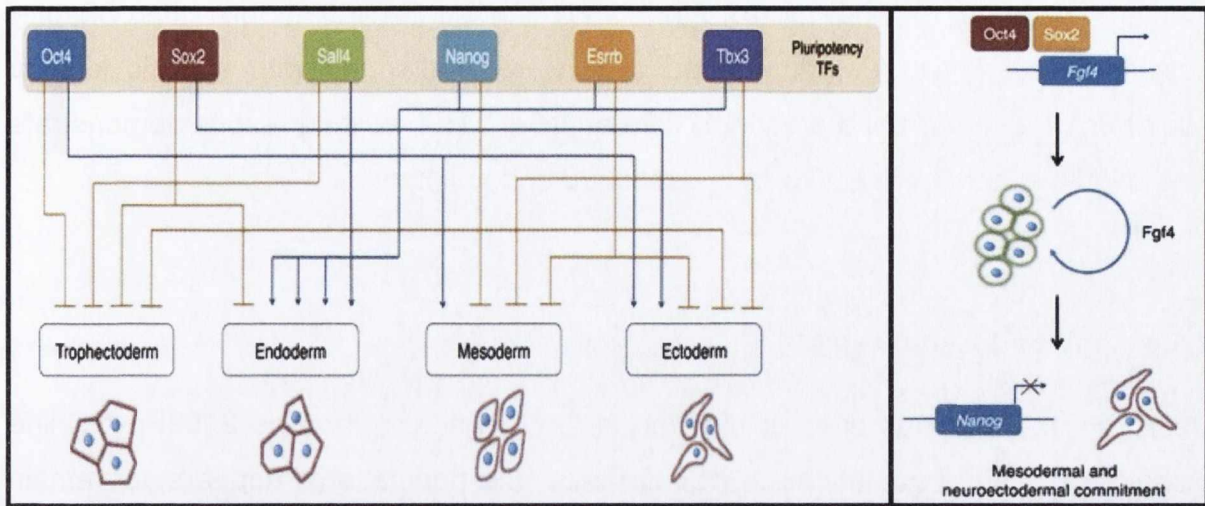


**Figure 4.1. The Competition Model of Human Embryonic Stem Cell Differentiation.** In his review paper, Bing Lim proposed the Competition Model illustrated in response to complex, contradictory differentiation data from human embryonic stem (hES) cells. The paper address the contradictory reports that loss or excessive over-expression of specific transcription factors such as Oct4, Sox2, Nanog and others, leads to specific lineage differentiations in hES cells. The authors propose that each key transcription factor promotes one lineage differentiation while inhibiting another. As such, when all transcription factors are expressed, a homeostasis is reached, where no differentiation occurs, and a stable self-renewal state is maintained. Three germ-layer differentiation, it was argued, arises from loss of expression of all transcription factors in response to a morphogen such as retinoic acid (Left Panel). Once the process of differentiation beings, changes in key transcription factors Oct4 and Sox2 lead to changes in key growth factors such as FGF4, which ultimately leads to commitment to specific lineage differentiation (Right Panel: Loh and Lim 2011).

As the previous paragraph illustrates, differentiating pluripotent cells down specific lineages is complex. However, very recently, lineage differentiation kits have become commercially available. The kits are based largely upon the pivotal paper in this area, which showed that, in human pluripotent cells, Activin-A and TGF- $\beta$ 1 can induce mesoderm differentiation, RA, Epidermal Growth Factor (EGF), BMP-4 and bFGF induce ectoderm (and some mesoderm), and Neural Growth Factor (NGF) and Hepatocyte Growth Factor (HGF) induce ectoderm (and some mesoderm and endoderm) differentiation (Schulinder et al 2000). The general approach to lineage differentiation now is to induce endoderm through treatment with ActivinA and Wnt3a, mesoderm through inhibition of Wnt-regulator GSK3 $\beta$ , and ectoderm through inhibition of BMP and Nodal/Activin Signaling (Sullivan et al 2010, Lam et al 2014, Surmacz et al 2012). These kits are limited in that they cannot produce functional tissues through the differentiation they stimulate. However, these kits are empowering in that they can stimulate pluripotent stem cells down a specific lineage, the effect of which can be assessed by looking at relatively early differentiation

markers such as SSEA4, Oct4, Sox2 and Nanog. Exploiting this, this Chapter describes how MyD88PepInh treated cells were challenged with specific kits for endoderm, mesoderm and ectoderm differentiation. The exciting results demonstrate that MyD88 is not RA-specific, as is described in detail later.

#### **4.1.4 Aims and Hypothesis**

Data from the previous chapter resulted in the hypothesis that the 2102Ep cell line contains two sub-populations. One of these sub-populations appears to remain nullipotent throughout the experiment. The other sub-population appears to be capable of differentiation in response to RA once MyD88 has been inhibited. The aim of this chapter was to use flow cytometry as an approach to assess the differentiation status of individual cells to A) test the two sub-population hypothesis and B) separate and isolate the two sub-populations for molecular analysis. Furthermore, the aim of the chapter was to use molecular marker expression to demonstrate that MyD88PepInh+RA treated cells were indeed differentiated. Additionally, the chapter aimed to address the broader role of MyD88 in pluripotency by assessing the role of MyD88 in endoderm-, mesoderm- and ectoderm-specific lineage differentiation mechanisms. In the final part of the Chapter, it is hypothesised that the regulation by MyD88 of the precise profile of secreted chemokines and cytokines was an important factor in stem cell status regulation in EC cells. Addressing this, the aim of the final section was to assess whether conditioned media from each stem cell state could affect the differentiation status of these cells.

## **4.2 Materials and Methods**

All materials and methods related to this chapter are described in chapter 2.

## **4.3 Results**

### **4.3.1 NTERA2 cells treated with RA can be distinguished by SSEA4, Oct4, Sox2 and Nanog expression.**

It is widely reported that SSEA4 expression can be used to discriminate between undifferentiated (high expressing) pluripotent cells and differentiated (low expressing) cells. As such, undifferentiated and differentiated NTERA2 cells were used as positive and negative controls for the optimisation of flow cytometry protocols. In these experiments, NTERA2 cell differentiation was achieved by incubation in RA for 7 days. As is the case for all flow cytometry data shown in this Chapter, three parameters were used to ensure that only single, live cells were included in analysis (Figure 4.2). The first parameter exploits comparisons of forward and side scatter to identify 'events' that are too small to be live cells, and are thus 'gated' out as cellular debris. The removal of debris from the analysis is important as it can lead to false-positive staining. Secondly, a comparison of scatter and pulse width allows the identification of doublets, which can be gated away from single cells. The removal of doublets is also vital as a doublet 'event' called as positive may actually represent one positive and one negative cell together, which complicates analysis. Finally, a Propidium Iodide (PI) 'dead cell' stain allows the identification of whole live cells. Again, the removal of dead cells is important for analysis as it can lead to false-positive staining. These three parameters are shown in Figure 4.2 and are imposed on all analysis in this Chapter. However, the controls are not shown in each case due to space limitations. Together, these controls ensure that only single, whole, live cells are included in analysis.

Undifferentiated and differentiated NTERA2 cells were assessed for SSEA4 expression by flow cytometry (Figure 4.3). As the data illustrates, undifferentiated cells were 98.83% ( $\pm 1.43$ ) SSEA4<sup>Pos</sup> while differentiated cells were 87.66% ( $\pm 2.55$ ) SSEA4<sup>Neg</sup>. In each case, unstained, 'auto-fluorescence' controls are shown to explain differences in gating between the cell types. Additionally, a bar-chart statistical analysis shows a clear and strong statistical significance within this data (SSEA4<sup>Pos</sup> p-value <0.0001, SSEA4<sup>Neg</sup> p-value =0.00017). Finally, a qPCR analysis of these samples shows high Oct4-Sox2-Nanog expression in undifferentiated and

low expression of Oct4 32.03% ( $\pm$  3.25) Sox2 53.45% ( $\pm$  3.19) and Nanog 8.13% ( $\pm$  0.35) in differentiated cells, which confirms their stem cell status.

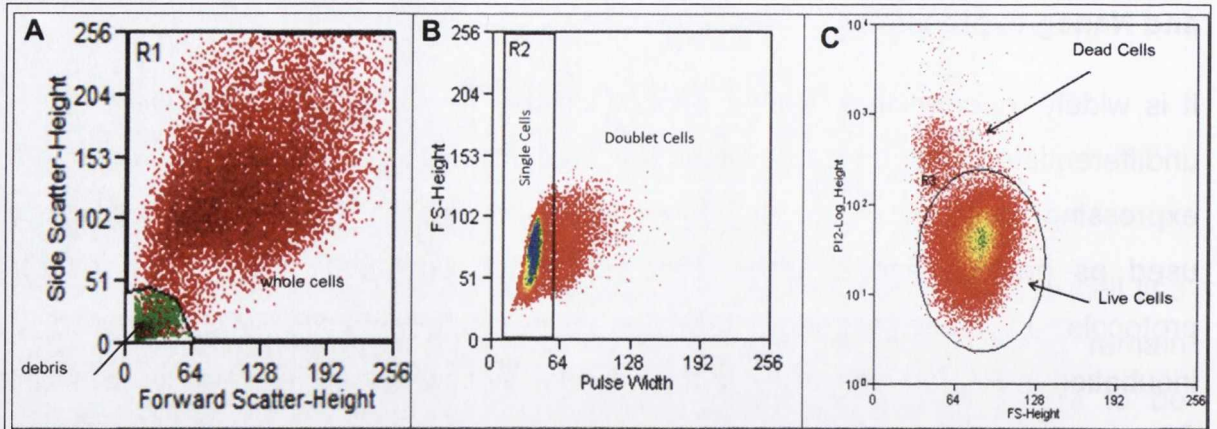


**Figure 4.2. Three Parameters Used in Flow Cytometry Analysis.** All flow cytometry analysis carried out in this chapter was based upon three controls. First, a comparison of forward and side scatter allows identification and removal of cellular debris (A). Second, a comparison of scatter and pulse width allows identification and removal of doublets (B). Third, a PI stain allows identification and removal of dead cells (C). These controls ensure that only whole, live, single cells are included in analysis.

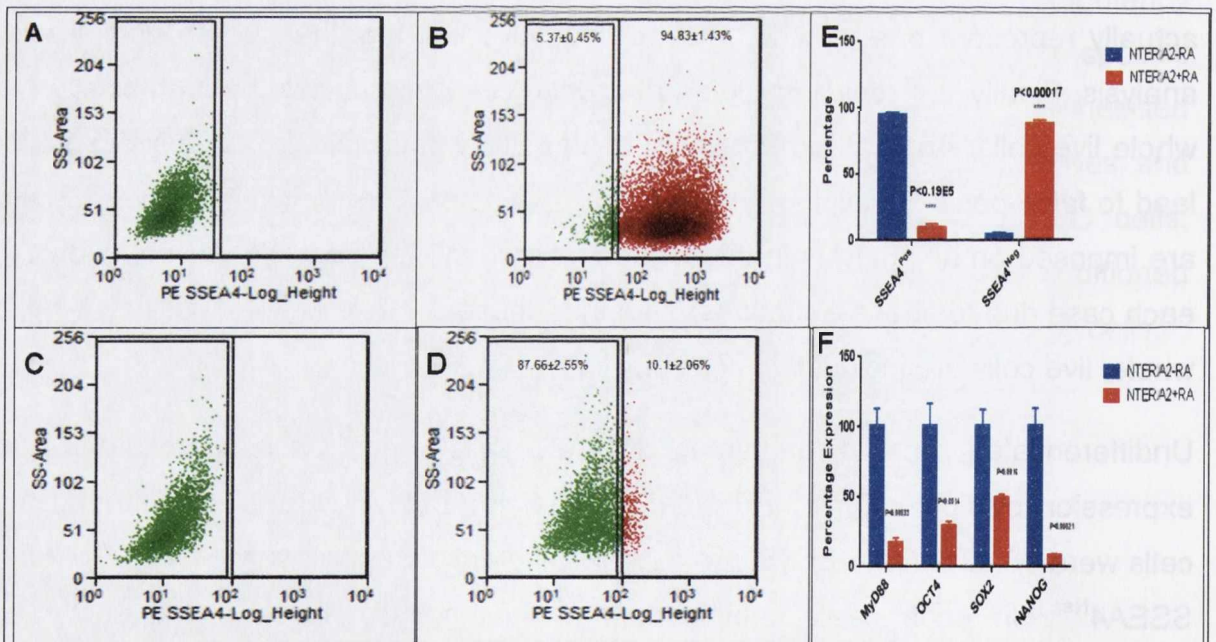


**Figure 4.3. NTERA2 Cells Highly Express SSEA4 in the Undifferentiated State.** In this experiment, NTERA2 cells were treated with (+RA) or without (-RA) retinoic acid (RA) for 7 days. A and C) Unstained control profiles shown illustrate the basis for slightly different gating in each sample. The majority of cells are SSEA4 positive in -RA conditions (B) and SSEA4 negative in +RA conditions (D). The bar-chart (E) demonstrated that these differences were substantial and statistically significant ( $p$ -value = 0.00017). Finally, the

stem cell status of these samples was confirmed through qPCR analysis of Oct4 ( $32.03\% \pm 3.25$ ), Sox2 ( $53.45\% \pm 3.19$ ) and Nanog ( $8.13\% \pm 0.35$ ) expression patterns (F). All experiments  $n=3$ .

#### **4.3.2 Force-Differentiated 2102Ep cells can be distinguished by SSEA4 and Oct4, Sox2, Nanog expression.**

As 2102Ep cells do not normally differentiate, it was decided that a force-differentiated 2102Ep cell sample should be generated. Force-differentiated cells could then be used to confirm that undifferentiated and differentiated 2102Ep cells can be separated via flow cytometry on the basis of SSEA4 expression. Our group has previously shown that knockdown of Sox2, using siRNA, results in differentiation of 2102Ep cells (Vencken et al 2014). Here, a siRNA for Sox2 ('siSox2') was used to generate a population of differentiated 2102Ep cells. Cells were treated with siSox2, which adopted a differentiated cell morphology as previously described (Vencken et al 2014). Undifferentiated and siSox2-differentiated 2102Ep cells were then assessed for SSEA4 expression on flow cytometry, using cells transfected with a scrambled siRNA as a negative control. As an additional control, 2102Ep cells were shown to express similarly high levels of SSEA4 in -RA and +RA conditions (Figure 4.4). Flow cytometry data indicated that  $98.01\% (\pm 0.93)$  of negative control cells were SSEA4<sup>Pos</sup> while  $84.98\% (\pm 1.37)$  of siSox2-differentiated cells were SSEA4<sup>Neg</sup> (Figure 4.5). Additionally, a bar-chart statistical analysis shows a clear and strong statistical significance within this data ( $p$ -value  $<0.0001$ ). This confirmed the suitability of SSEA4 as a flow cytometry marker for discrimination of undifferentiated and differentiated 2102Ep cells.

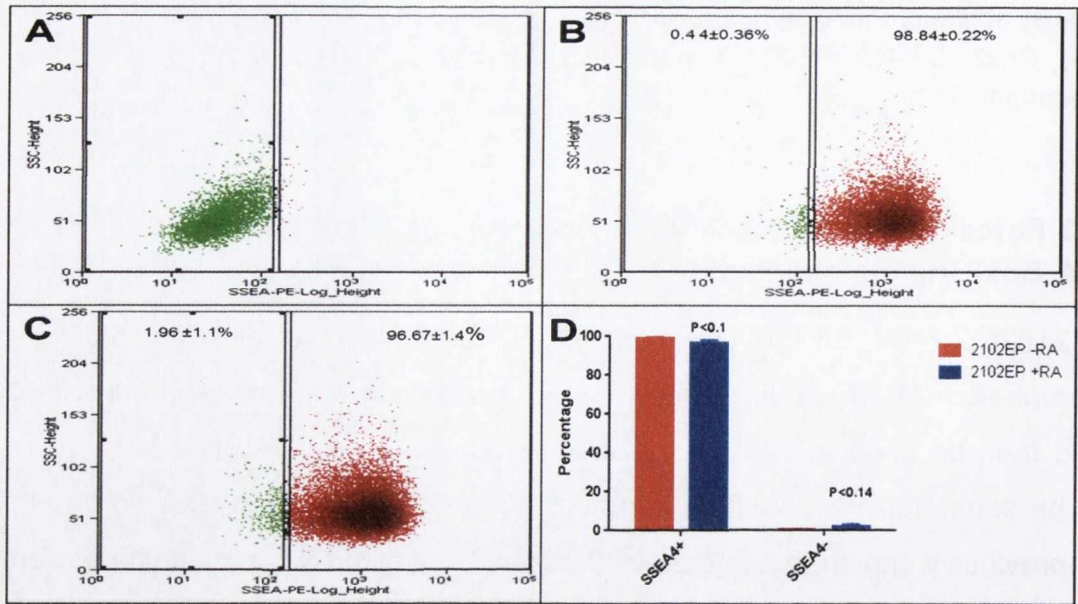


**Figure 4.4. SSEA4 Expression Does Not Discriminate Between 2102Ep Cells in -RA versus +RA Conditions.** In this experiment, 2102Ep cells were treated with (+RA) or without (-RA) retinoic acid (RA) for 12 days. A) Unstained control profiles were identical for both samples, which directed use of identical gating. Flow cytometry data indicates that both -RA (B) and +RA (C) treated samples express similarly high levels of SSEA4. Finally, the bar-chart (D) illustrates that there is no statistically significant difference between the data. All experiments were n=3.

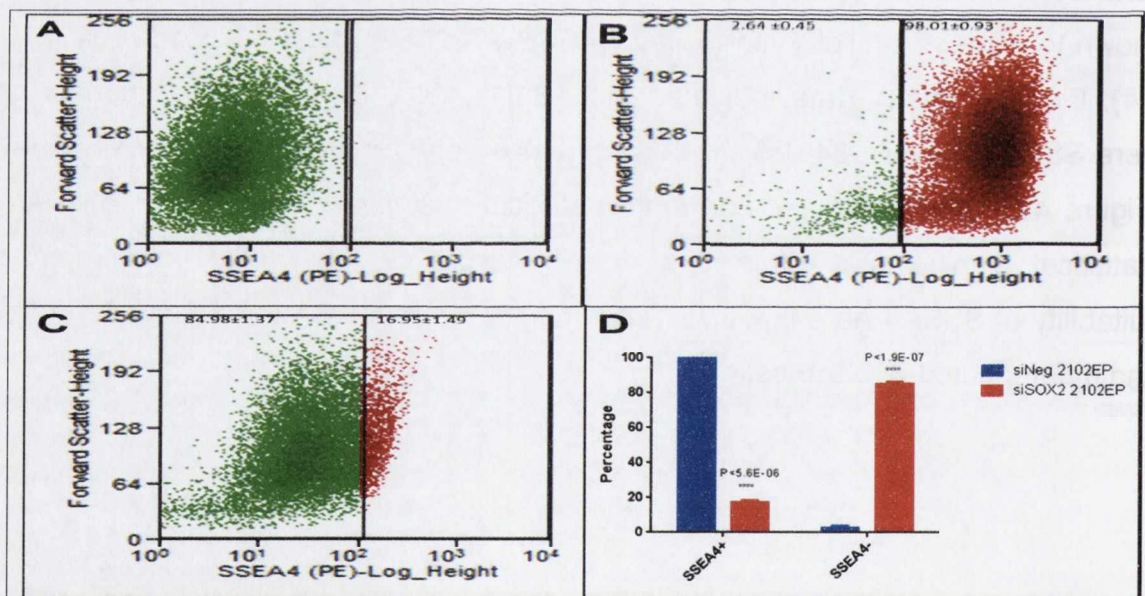


**Figure 4.5. SSEA4 Expression Discriminates Undifferentiated and Differentiated 2102Ep Cells.** In this experiment, 2102Ep cells were treated with a siRNA for Sox2 (siSox2), which we have previously shown differentiates these cells (Vencken et al 2014). Cells treated with a scrambled siRNA were used as a negative control. These figures show distinct patterns of SSEA4 expression in undifferentiated (negative control) and differentiated (siSox2) cells. Finally, the bar-chart illustrates that these data are highly statistically significant (p-value < 0.0001). As such, SSEA4 is suitable for discrimination of undifferentiated and differentiated 2102Ep cells by flow cytometry. All experiments were n=3.

### 4.3.3. Loss of MyD88 Does Not Effect 2102Ep SSEA4 expression.

The two sub-population hypothesis predicts that SSEA4 expression will allow discrimination of undifferentiated and differentiated cells following MyD88PepInh+RA treatment. However, it was unclear if loss of MyD88 alone would affect SSEA4 expression or stem cell status. Addressing this, 2102Ep cells were treated with MyD88PepInh or a negative control PepInh (CtrlPepinh). In each case, cells were re-treated with PepInh daily for 12 days to ensure MyD88 inhibition was maintained and the effect of non-take up of PepInh by cells minimised. After 12 days, cells were assayed for SSEA4 expression by flow cytometry. In MyD88PepInh and CtrlPep treated samples, 98.70% ( $\pm 0.44$ ) and 97.1% ( $\pm 2.9$ ) of cells stained positive for SSEA4 respectively, indicating an undifferentiated state. In each case, unstained, 'auto-fluorescence' controls are shown to explain differences in gating between the cell types. Additionally, a bar-chart statistical analysis shows that there was no statistically significant difference between the MyD88PepInh and CtrlPepInh samples.

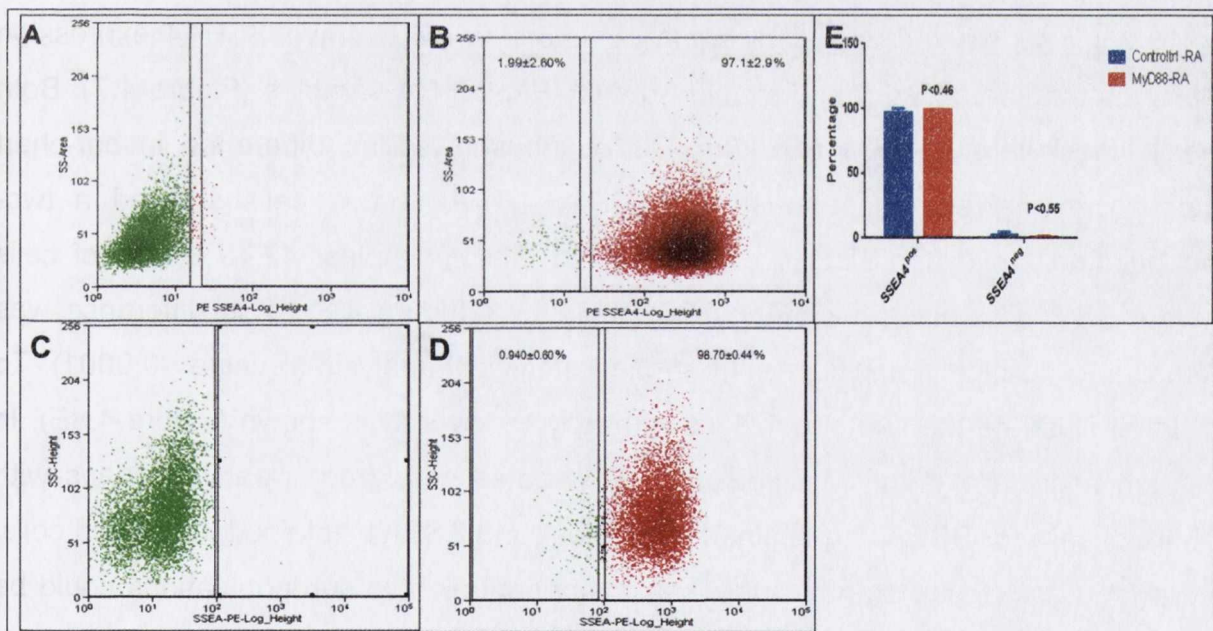


**Figure 4.6. Loss of MyD88 Does Not Effect SSEA4 Expression in 2102Ep Cells.** In this experiment, 2102Ep cells were treated with either a MyD88 Peptide Inhibitor (MyD88PepInh) or a negative control (CtrlPepInh), which was replenished daily for 12 days. The image shows the expression of SSEA4 in the resulting cell samples and indicates that almost 100% of cells remain SSEA4 positive during the experiment (B=CtrlPepInh, D=MyD88PepInh). In each case, unstained 'auto-fluorescence' controls are shown to explain differences between gating between the cell types (A=CtrlPepInh, C=MyD88PepInh). The bar chart (E) represents a statistical analysis, which indicates that there was no difference between the MyD88PepInh and CtrlPepInh treated samples. All experiments were n=3.

#### **4.3.4. 2102Ep cells contain 2 sub-populations, only one of which differentiates in MyD88 PepInh +RA conditions.**

Once loss of MyD88 had been shown to have no effect on differentiation status in these cells, the main aim of the Chapter, namely validation of the two sub-population hypothesis, was addressed. 2102Ep cells were treated with either MyD88PepInh or CtrlPepInh for 6 hours. Retinoic acid was then added to the cells, which were incubated overnight. This media was replenished daily for 12 days, at which point the cells were assessed for SSEA4 expression by flow cytometry. As briefly mentioned above, the take-up of PepInh by all cells was a concern throughout the experiment. In effect, it was possible that the apparent 'two sub-populations' could be due to some cells taking up PepInh and some not. This is a common problem with transfections, for example, where some cells take up the siRNA and others do not. While reporter plasmids could be used for this purpose with transfections, this was not possible with the PepInh. Thus, PepInh media was replenished daily for 12 days. This should dramatically reduce the possibility that any cells would randomly fail to take up the PepInh every day for 12 days.

2102Ep cells treated with CtrlPepInh+RA were found to have SSEA4 expression profiles that were undistinguishable from CtrlPepInh-RA samples (Figure 4.7). Both cell types were 97-98% SSEA4 positive and showed no difference in bar-chart statistical analysis. In contrast, MyD88PepInh+RA treated cells showed a two-population profile for SSEA4 expression. In these samples, 42.49% ( $\pm 4$ ) of cells were SSEA4<sup>Neg</sup> and 55.27% ( $\pm 0.93$ ) SSEA4<sup>Pos</sup> (Figure 4.8). This difference was shown to be highly significant in bar-chart statistical analysis (p-value <0.0001). To further illustrate the two populations, a histogram overlay is shown (Figure 4.8E). In this histogram overlay, MyD88PepInh+RA-treated cells (red) clearly overlaps with control cells for SSEA4<sup>-</sup> (unstained cells, blue) and SSEA4<sup>+</sup> (stained, untreated cells, green). Using these standard flow cytometry controls two sub-populations could be discriminated. We therefore conclude that the two sub-population hypothesis proposed is valid.



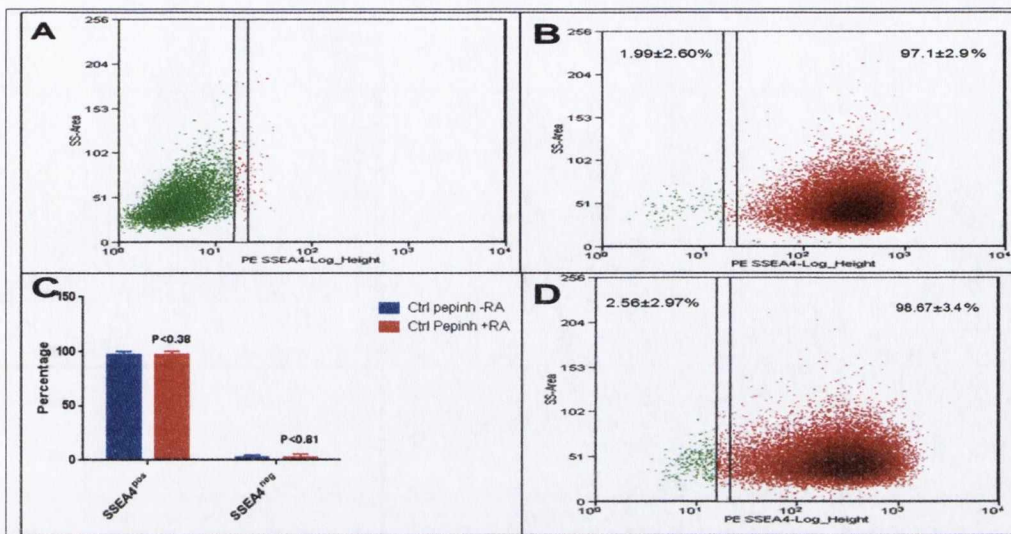


**Figure 4.7. CtrlPepInh Treated 2102Ep Cells Similarly Highly Express SSEA4 in -RA and +RA Conditions.** This experiment acted as a control for testing of the two sub-population hypothesis in Figure 4.8. In this experiment, 2102Ep cells were treated with a negative control (CtrlPepInh) with (+RA) or without (-RA) retinoic acid (RA). The image shows the A) the gating parameters determined by unstained controls, and the expression of SSEA4 in the resulting cell samples (B=-RA, D=+RA) and indicates that almost 100% of CtrlPepInh+RA cells remain SSEA4 positive during the experiment. The bar chart (C) represents a statistical analysis, which indicates that there was no statistically significant difference between the samples. All experiments were n=3.

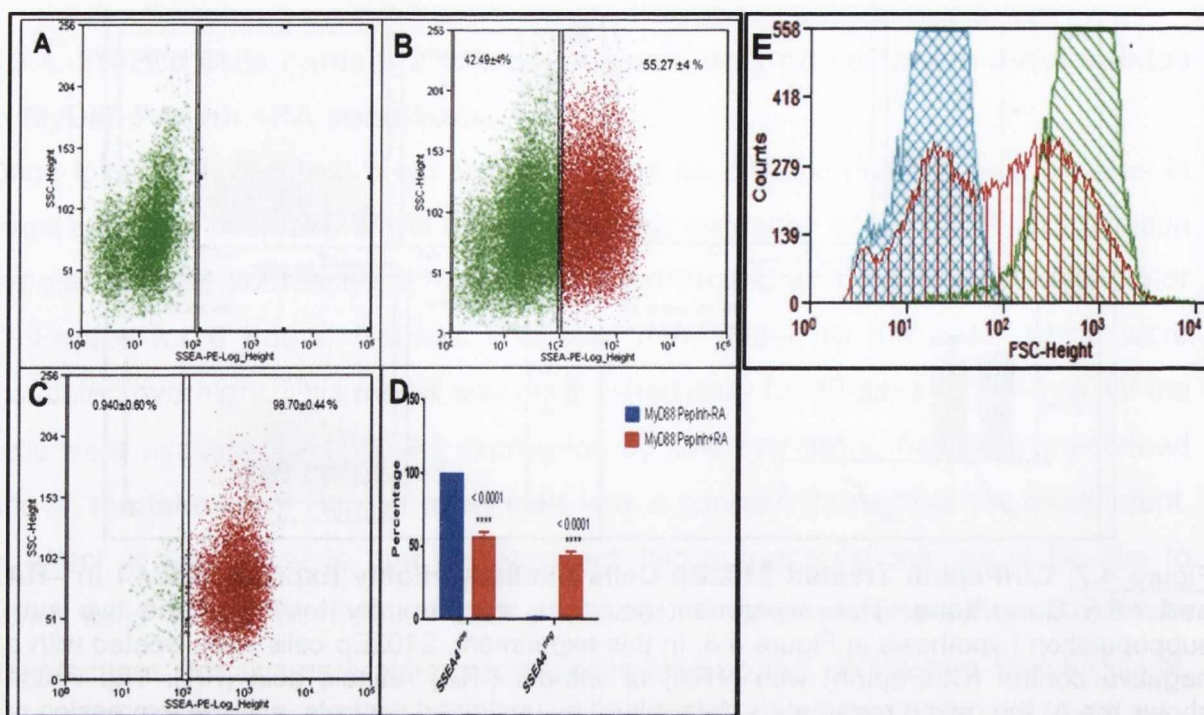


**Figure 4.8. Validation of the Two Sub-Population Hypothesis.** This hypothesis proposes that 2102Ep cells contain two sub-populations, one of which is nullipotent while the other can differentiate in response to loss of MyD88 and the presence of retinoic acid (RA). Testing this, 2102Ep cells were treated with either a MyD88 Peptide Inhibitor (MyD88PepInh) or a negative control (CtrlPepInh) in combination with RA. The CtrlPepInh data is shown in Figure 4.7 and the MyD88PepInh data is shown here. The image shows the gating parameters determined by unstained controls (A) and that (B) MyD88PepInh+RA treated cells displayed a two population-profile. Approximately 45% (Green) of these cells were SSEA4<sup>Neg</sup> and 55% (Red) SSEA4<sup>Pos</sup>. In contrast, MyD88PepInh-RA treated cells were approximately 98% SSEA4 positive (C). The bar chart (D) represents a statistical analysis, which indicates that there was a substantial statistically significant difference between the samples (p-value 0.0001). Finally, E represents a histogram overlay showing how the MyD88PepInh+RA population (Red) contained two populations, which were separated based on the profiles for SSEA4<sup>-</sup> (unstained cells, blue) and SSEA4<sup>+</sup> (stained, untreated cells, green) controls. All experiments were n=3.

#### 4.3.5. Separated SSEA4<sup>Pos</sup> and SSEA4<sup>Neg</sup> MyD88PepInh+RA Treated 2102Ep cells Express Oct4-Sox2-Nanog at High and Low Levels Respectively.

Having validated the two sub-population hypothesis, the next aim of this Chapter was to separate the sub-populations for molecular analysis. 2102Ep cells were treated as described in Section 4.3.4 above. Following treatment, cells were separated, based on the expression of SSEA4, using the modified flow cytometry approach known as 'Fluorescent-Activated Cell Sorting' (FACS). This approach allows the sorting of cells based on their expression of a marker of interest. Cells can then be collected for further analysis. The FACS data for this experiment is shown in Figure 4.9 and validates the data shown in Figure 4.8. Specifically, two sub-populations, one SSEA4<sup>Pos</sup> and one SSEA4<sup>Neg</sup>, were detected, separated and

collected by FACS. Cells were subsequently tested for their expression of Oct4, Sox2 and Nanog by qPCR. This analysis demonstrated that the SSEA4<sup>Pos</sup> sub-population expresses high levels of Oct4, Sox2, Nanog, which validates their apparent continued nullipotency (Figure 4.9). In contrast, the SSEA4<sup>Neg</sup> sub-population expresses Oct4 (33.5% ± 10.9), Sox2 (28.9% ± 10.4) and Nanog 21.3% ± 11.2) at low levels, which validates its differentiation. We can therefore conclude that loss of MyD88 permits differentiation of a sub-population of 2102Ep cells in the presence of RA.

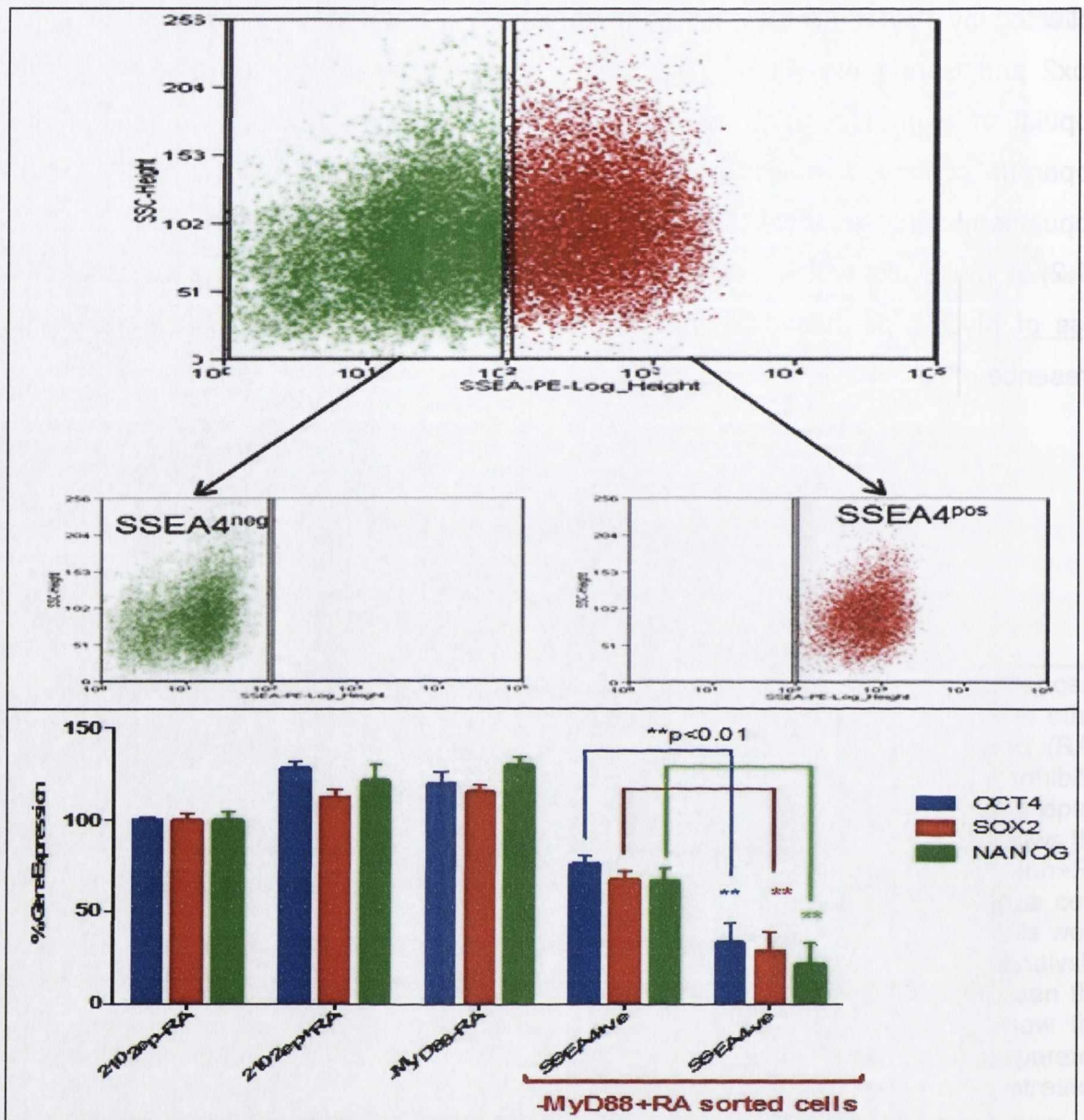


**Figure 4.9. Separation and Molecular Analysis of the Two 2102Ep Sub-Populations.** In this experiment, cells were treated with either MyD88 Peptide Inhibitor (MyD88PepInh) or a negative control PepInh (CtrlPepInh) as described in Section 4.3.4 and Figure 4.4 above. Once again, cells were treated with PepInh for 6 hours, after which retinoic acid (RA) was added to the cells to stimulate differentiation over a period of 12 days. Cells were subsequently separated based on SSEA4 expression by FACS. Separated cells were collected and analysed for expression of Oct4, Sox2 and Nanog by qPCR. In each case, unstained 'auto-fluorescence' controls are shown to explain differences between gating between the cell types. The bar chart represents a statistical analysis, which indicates that there was a substantial statistically significant difference between the samples ( $p$ -value < 0.01). All experiments were  $n=3$ .

#### 4.3.6. MyD88 Inhibition Facilitates Non-RA Lineage Differentiation Mechanisms

Having demonstrated that loss of MyD88 is an essential component for 2102Ep differentiation in response to RA, the next aim of the Chapter was to assess the role of MyD88 in other differentiation lineages. In the experiments described in this section, MyD88PepInh treated cells were treated as previously described. In this case, after 6 hours PepInh treatment, cells were challenged with a differentiation kit instead of RA. These kits contain a differentiation solution, which is a cocktail of growth factors known to stimulate either endoderm, mesoderm or ectoderm differentiation, but the precise nature of which is not disclosed by the supplier. However, the supplier importantly confirmed for us that none of their lineage differentiation kits contain RA.

At this point, a problem emerged with the CtrlPepInh. The combination of A) CtrlPepInh, B) RA and C) the SSEA4 flow cytometry protocol regularly resulted in toxicity issues and large scale cell death. This was a substantial problem for the work described in this Chapter, as EC cells are well-known to spontaneously differentiate in response to high levels of stress. This 'differentiation' rapidly results in cell death. This 'pseudo-differentiation' is accompanied by a loss of SSEA4 expression. Despite the quality results displayed in the example in Figure 4.7 above, this problem occurred regularly enough to cause concerns. This was associated with the fact that the PepInh and Differentiation Kits involved in these experiments are particularly expensive, which meant that extensive repeat experiments were beyond the scope of the project. In addition, when contacted, the supplier confirmed that this was a problem experienced by many users. Their suggestion that the concentration of CtrlPepInh used in experiments be reduced would have substantially delayed the project and was not guaranteed to be successful. In light of these problems, a decision was made to design the lineage differentiation experiments without the CtrlPepInh. Therefore, MyD88PepInh+RA treated cells were exposed to each differentiation kit, using cells exposed to only the differentiation kits as a control. Due to the expenses involved, a shortened 6 day experiment was initially employed instead of the earlier 12 day differentiation protocol. As such, induction of differentiation, rather than differentiation *per se*, was assessed.

2102Ep cells treated with or without MyD88PepInh were exposed to specific endoderm, ectoderm and mesoderm differentiation kits, which had no obvious effect upon cellular morphology after 6 days (Figure 4.10). These cells were then assessed for the presence of SSEA4 by flow cytometry. In the case of all three lineages, treatment resulted in the production of a small population of SSEA4<sup>Neg</sup> cells: Endoderm 2% (Figure 4.11), Ectoderm 3% (Figure 4.12) and Mesoderm 17% (Figure 4.13).

The combination of MyD88PepInh and Endoderm kit resulted in no substantial statistically significant difference between the samples after 6 days (Figure 4.11). This was validated by demonstration by qPCR that these cells expressed Oct4, Sox2 and Nanog at similar levels (Figure 4.11). As such, it appears that MyD88 does not play a role in endoderm differentiation in hEC cells.

The combination of MyD88 PepInh and Ectoderm kit resulted in the production of approximately 10% more SSEA4<sup>Neg</sup> cells than controls after 6 days, a result that was found to be strongly statistically significant (p-value 0.01) (Figure 4.12). Unfortunately, when isolated by FACS, this 10% SSEA4<sup>Neg</sup> population did not yield sufficient RNA for qPCR to be performed. As such, it could only be demonstrated that the SSEA4<sup>Pos</sup> populations from the MyD88 PepInh and Control treatments expressed Oct4, Sox2 and Nanog at similar levels (Figure 4.12). However, this data suggests some role for MyD88 in ectoderm lineage differentiation.

The combination of MyD88 PepInh and Mesoderm kit resulted in the production of approximately 20% more SSEA4<sup>Neg</sup> cells than controls after 6 days, a result that was found to be strongly statistically significant (p-value 0.01) (Figure 4.13). This 20% SSEA4<sup>Neg</sup> population was sufficient for qPCR analysis, which demonstrated that there was a substantial and statistically significant downregulation of Oct4 ( $36.6\% \pm 3.1$ , p-value 0.02), Sox2 ( $17.9\% \pm 4.7$ , p-value 0.02) and Nanog ( $15.3\% \pm 4.6$ , p-value 0.01). In contrast, SSEA4<sup>Pos</sup> cells from the MyD88 PepInh and Control treatments expressed Oct4, Sox2 and Nanog at similarly high levels (Figure 4.13). Together, these data indicate that MyD88 is involved in three germ layer lineage differentiation in 2102Ep cells. This involvement appears to be stronger during mesoderm differentiation. However, longer treatments with higher concentrations of differentiation kit solutions may demonstrate greater roles in endoderm and ectoderm differentiation, as discussed later.

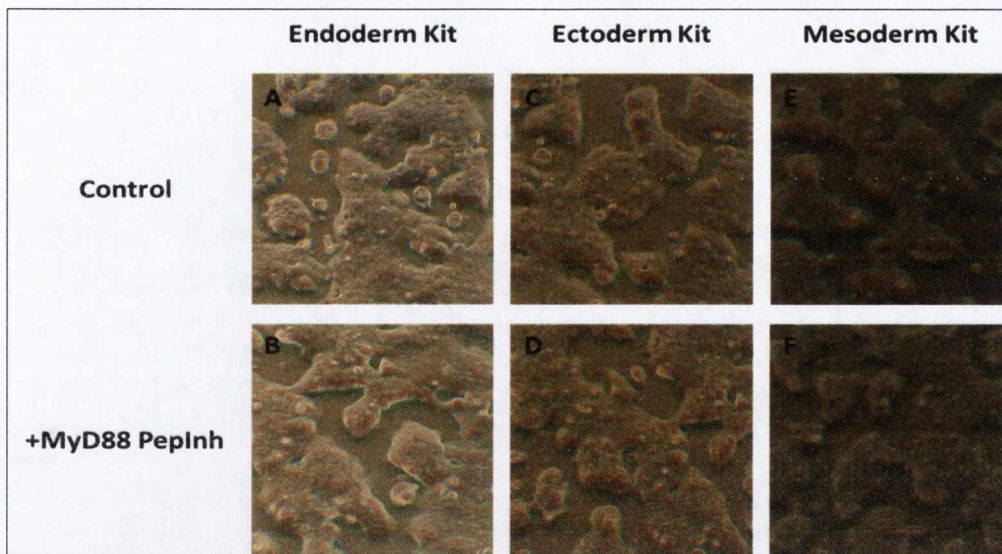


**Figure 4.10. MyD88 inhibition Does not Effect Cellular Morphology of 2102Ep Cells in Lineage Differentiation Conditions.** In this experiment, 2102Ep cells were treated with (+MyD88PepInh) or without (Control) MyD88 Peptide Inhibitor (MyD88PepInh) for 6 hours, after which the cells were exposed to differentiation solutions specific for Endoderm, Mesoderm or Ectoderm lineages. The representative images show that no substantial difference was observed between the samples.

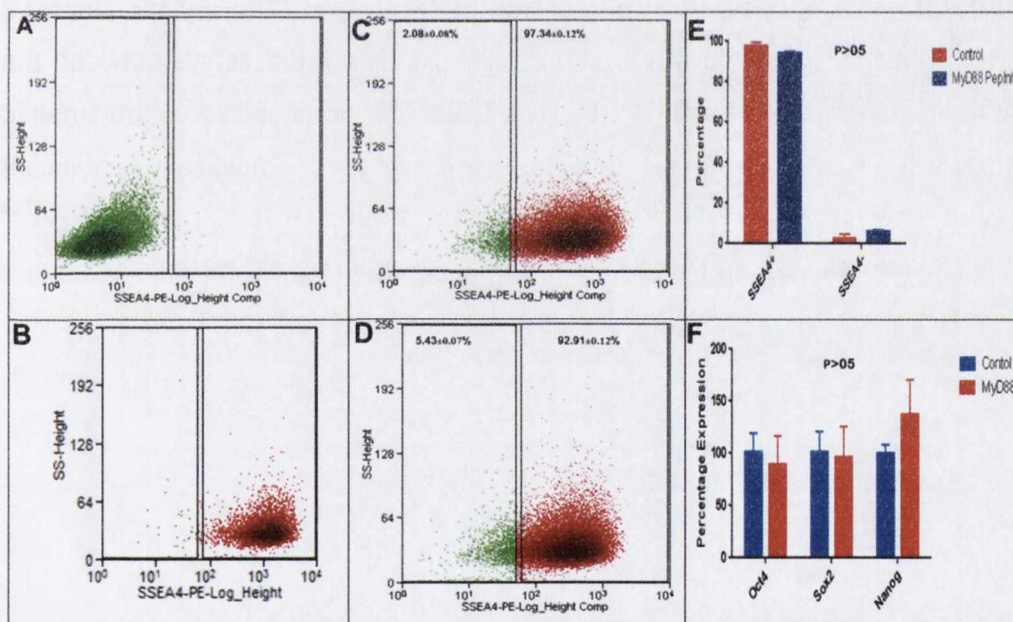


**Figure 4.11. MyD88 inhibition Effects SSEA4 Expression in 2102Ep Cells in Endoderm Lineage Differentiation Conditions.** In this experiment, 2102Ep cells were treated with (D) or without (C) MyD88 PepInh for 6 hours and then with the Ectoderm Differentiation kit for 6 days. The bar-charts indicate that there is no statistically significant difference between the samples SSEA4 (E) Or Oct4-Sox2-Nanog (F) expression patterns. [A] Unstained and B) untreated cell controls]. All experiments were n=3.

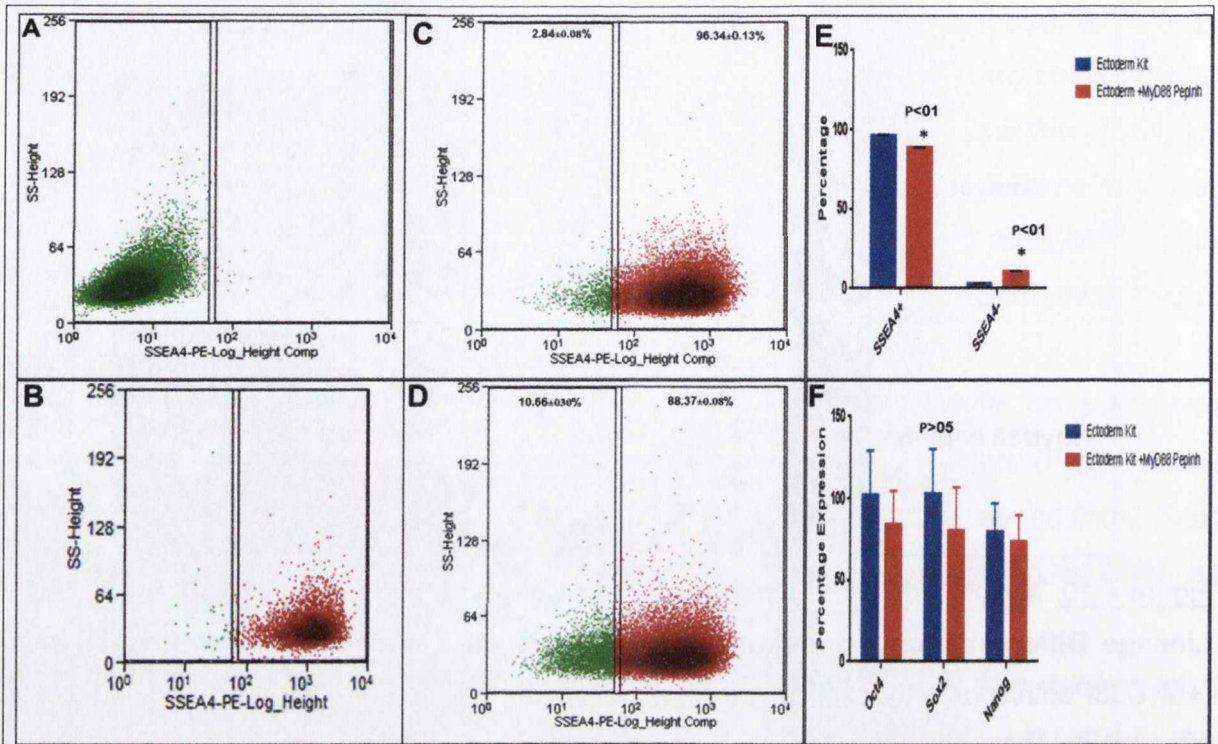


**Figure 4.12. MyD88 inhibition Effects SSEA4 Expression in 2102Ep Cells in Ectoderm Lineage Differentiation Conditions.** In this experiment, 2102Ep cells were treated with (D) or without (C) MyD88PepInh for 6 hours and then with the Ectoderm Differentiation kit for 6 days. The bar-charts indicate that there is a statistically significant difference between the samples SSEA4 expression (p-value < 0.01) (E). The SSEA4<sup>Neg</sup> population was too small to yield sufficient RNA for qPCR analysis. However, there was no statistically significant difference between the Oct4-Sox2-Nanog expression patterns (F) of the SSEA4<sup>Pos</sup> populations. [A] Unstained and [B] untreated cell controls]. All experiments were n=3.



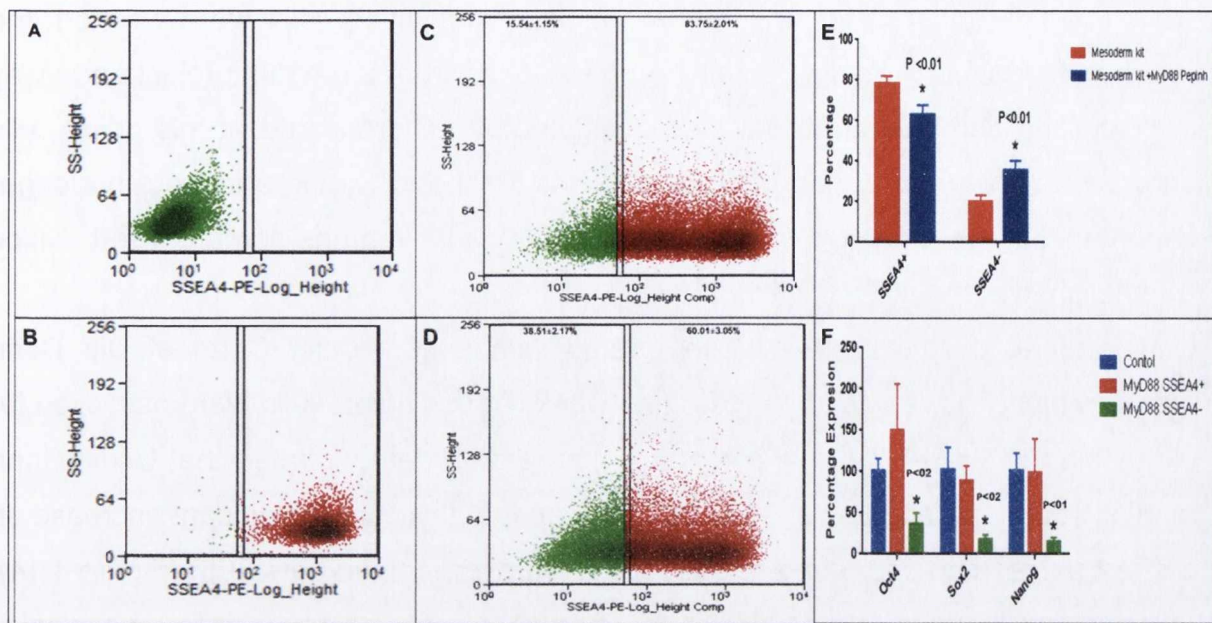


**Figure 4.13. MyD88 inhibition Effects SSEA4 Expression in 2102Ep Cells in Mesoderm Lineage Differentiation Conditions.** In this experiment, 2102Ep cells were treated with (D) or without (C) MyD88 PepInh for 6 hours and then with the Mesoderm Differentiation kit for 6 days. The bar-charts indicate that there was a statistically significant difference between the samples SSEA4 (p-value 0.01) (E) and Oct4 (36.6% ± 3.1, p-value 0.02), Sox2 (17.9% ± 4.7, p-value 0.02) and Nanog (15.3% ± 4.6, p-value 0.01) (F) expression profiles. [A] Unstained and B) untreated cell controls]. All experiments were n=3.

#### 4.3.7. Differentiated Ntera2 Cells Secrete Factors That are Sufficient to Differentiate Undifferentiated Ntera2 Cells.

The main function of MyD88 is reported to be determination of the exact profile of chemokines and cytokines secreted by the cell via TLR Signaling (Sections 1.7-1.8). In terms of the model presented in this thesis, it was hypothesised that these secreted proteins may influence stem cell status in EC cells. Specifically, it was proposed that high expression of MyD88 by undifferentiated Ntera2 cells may promote maintenance of their self-renewal. In contrast, it was proposed that low expression of MyD88 expression by differentiated Ntera2 cells may promote differentiation. To test this proposal, media from undifferentiated and differentiated Ntera2 cells was collected daily for either one or two weeks and pooled. This media was thus 'conditioned' with factors specific to the undifferentiated or differentiated state, which are referred to as 'Undifferentiated Conditioned' (Undiff Conn) and 'Differentiated Conditioned (Diff Conn) media respectively. To ensure that Diff Conn media was not contaminated by the RA used to induce differentiation, Ntera2 cells

were RA-differentiated for one or two weeks, after which cells were washed and returned to standard media containing no RA. Data from a parallel project underway in our group demonstrated that these cells remain differentiated at this point: cells showed reduced expression of SSEA4, Oct4, Sox2 and Nanog and were no longer capable of generating xenograft tumours in immune-compromised mice (unpublished).

Undifferentiated Ntera2 cells were treated with either Undiff Conn or Diff Conn media, which was replaced daily for one week. At this point, cells were assessed for expression of SSEA4 by flow cytometry. These data demonstrated that Undiff Conn media treatment results in a substantial and statistically significant increase in SSEA4 expression compared to untreated control cells (p-value <0.05) (Figure 4.14). However, this increase was observed after only one week and, after two weeks, SSEA4 levels were similarly high in untreated and Undiff Conn treated cells. The cells from the one-week experiment were then assessed by qPCR, which indicated that Undiff Conn media treatment results in a statistically significant difference in Oct4, Sox2 and Nanog expression (p-value <0.05) (Figure 4.14). In a similar experiment, 2102Ep cells were treated with MyD88PepInh as before, but now treated with Diff Conn media as a substitute for RA. The results showed that Diff Conn media can substitute for RA to induce 2 sub-populations, one of which shows reduced SSEA4 ( $50\% \pm 1.5$  and p-value 0.006), Oct4 ( $43.35\% \pm 2.5$  and p-value 0.02), Sox2 ( $22.67\% \pm 1.9$  and p-value 0.0025), and Nanog ( $16.14\% \pm 2.2$  and p-value 0.0023) levels (Figure 4.15). Together, these data give some validation to the hypothesis that MyD88 is involved in the secretion of factors by undifferentiated Ntera2 cells that promote maintenance of the self-renewal state.

In parallel, undifferentiated Ntera2 cells treated with Diff Conn media were shown to express substantially and statistically significantly reduced levels of SSEA4 after one (p-value <0.01) and two weeks (p-value <0.05), which were similar to those observed in +RA control cells (Figure 4.14). These data were associated with substantial and statistically significant reductions in Oct4 ( $27.9\% \pm 8.2$ ), Sox2 ( $11.9\% \pm 4.3$ ) and Nanog ( $5.2\% \pm 1.6$ ) expression (p-value <0.05) by Diff Conn media treated cells (Figure 4.14). Notably, this mechanism appears to be different to the standard RA-induced Ntera2 differentiation mechanism. As detailed in Chapter 1 (Section 1.4), Ntera2 cells regularly maintain high Sox2 levels when differentiated.

In contrast, Diff Conn media treated cells displayed dramatically reduced expression of all three pluripotency factors. These data give partial validation to the hypothesis that MyD88-independent TLR Signaling is involved in the secretion of factors by differentiated NTERA2 cells that are sufficient to promote differentiation. As MyD88-independent signaling is known to produce Type 1 Interferons (IFNs), these are likely candidate components of the DiffConn media. This is supported by the literature, where a correlation between cell cycle exit generally (Bekisz et al 2010), and differentiation of pluripotent cells specifically (Hong and Carmichael 2013, Pare and Sullivan 2014, Irudayam et al 2015), has been described.

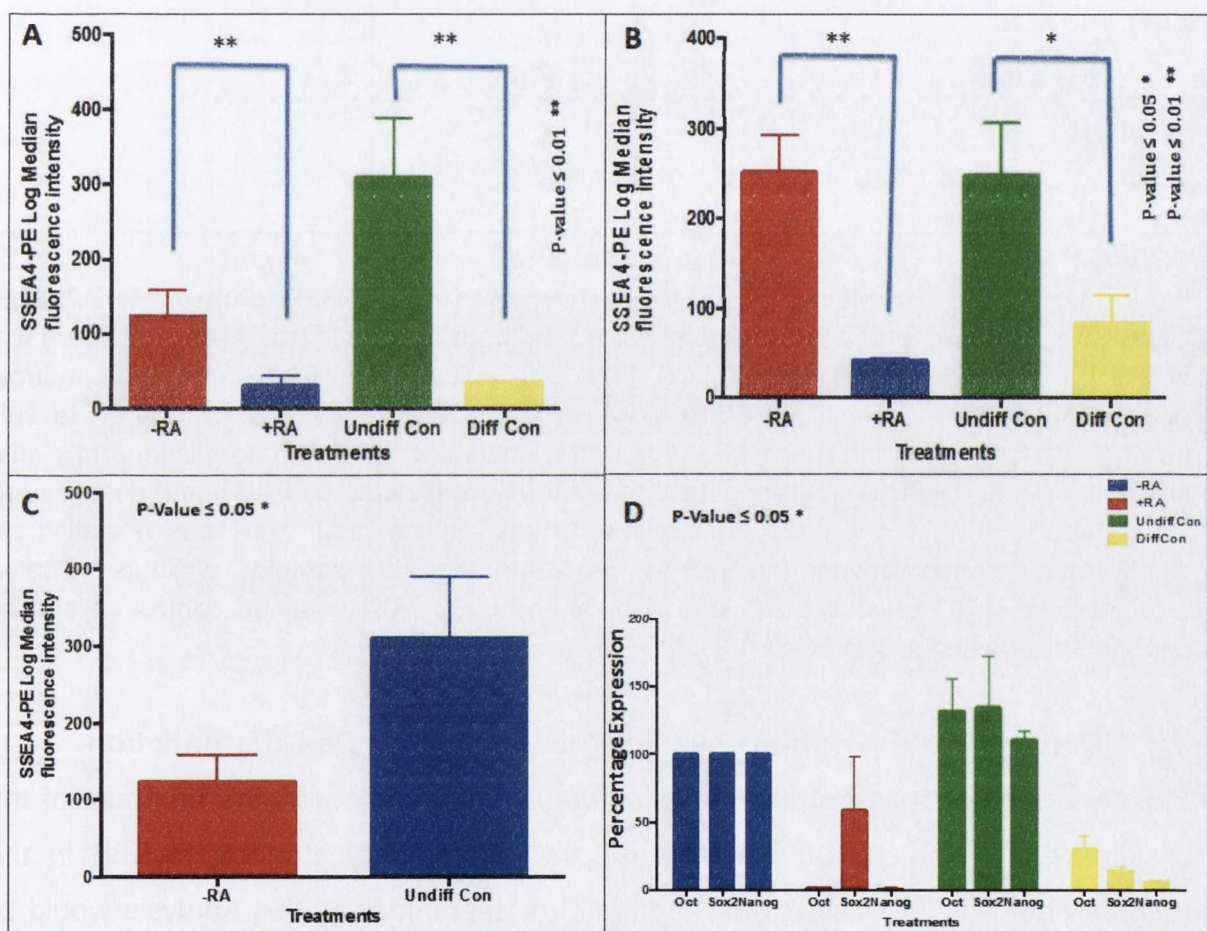


**Figure 4.14. NTERA2 Cells Secrete Stem Cell State Specific Factors That Promote Self-Renewal and Differentiation.** In this experiment, conditioned media from undifferentiated (Undiff Conn) and differentiated (Diff Conn) cells was collected and added to undifferentiated NTERA2 cells, which resulted in a statistically significant difference in SSEA4 expression after 7 (p-value <0.01) (A) and 14 (p-value <0.05) (B) days. This was accompanied by statistically significant increases and decreases (p-value <0.05) in Oct4-Sox2-Nanog in Undiff Conn and Diff Conn treated cells respectively (D). All experiments were n=3.

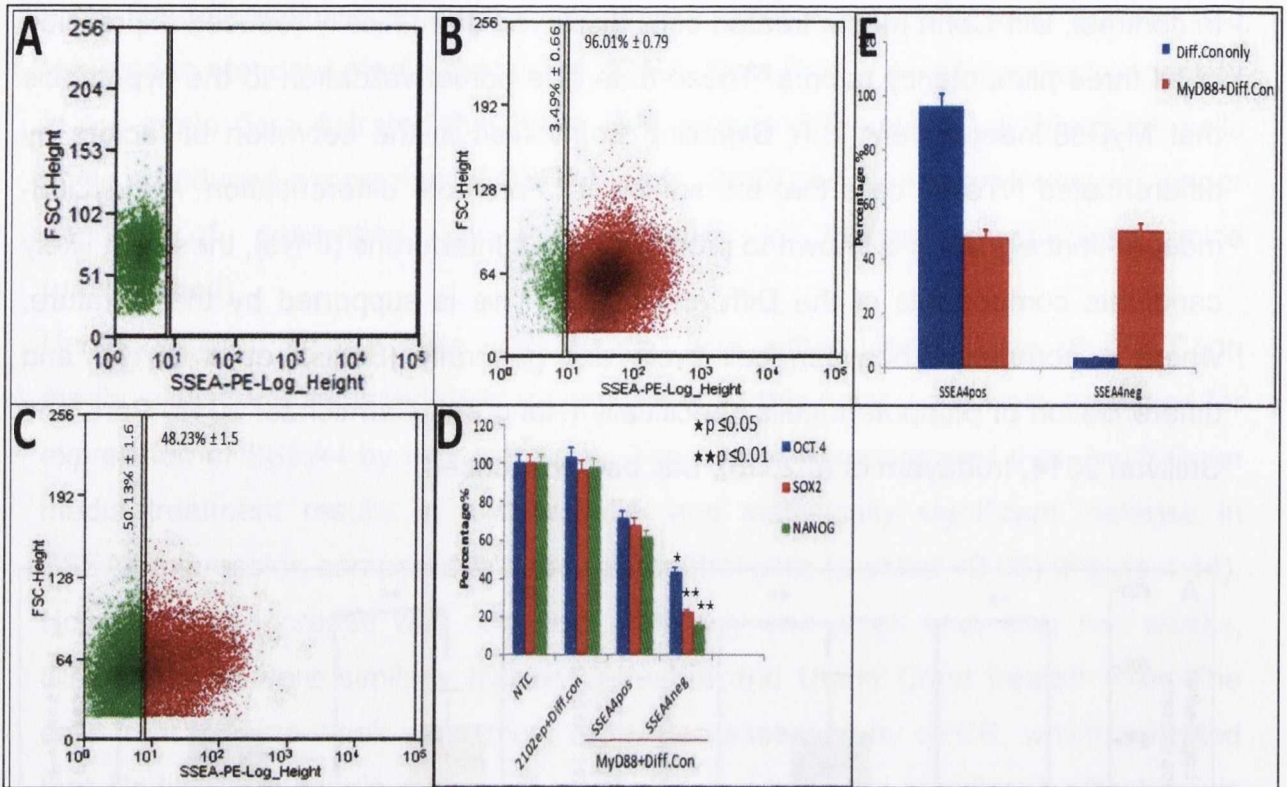


**Figure 4.15. DiffConn Media Induces Differentiation of MyD88PepInh-treated 2102Ep cells.** In this experiment, conditioned media from differentiated Ntera2 cells (DiffConn) was added to MyD88PepInh treated cells. The data shows that DiffConn media induced differentiation, as measured by SSEA4 expression after 12 days (C) compared to cells treated with only DiffConn media (B). Again, the characteristic 2 sub-populations of similar size are present (C). The 2 sub-populations from C were isolated by FACS and assessed for Oct4, Sox2 and Nanog expression. The bar charts indicate that there was a statistically significant difference between the SSEA4 positive and negative samples, which is indicative of differentiation (D p-value  $\leq 0.02$  and E p-value 0.006). [A] Unstained control cells]. This experiments was conducted n=2.

#### 4.3.8. Can the 2102Ep Sub-Populations be Isolated via De-Differentiation.

Following the validation of the two sub-populations hypothesis, the next aim of this project was to molecularly characterise the events regulated by MyD88 in this mechanism. This analysis is described in Chapter 5. Ideally, this analysis would be best achieved if the two sub-populations could be isolated and studied as pure populations. However, the separation of the two cell types would ideally require knowledge of cell surface markers specifically expressed by these cells. SSEA4 was not an appropriate marker as the SSEA4<sup>Neg</sup> population is, by definition, already differentiated and thus cannot be studied in the undifferentiated state.

In this section an experimental approach was designed to attempt to isolate the primed sub-population via 'de-differentiation'. 'De-differentiation' is a general term used in stem cell biology to refer to a process by which differentiating/differentiated cells may return to their immature, self-renewing, stem cell state. Our idea that the two sub-populations could be separated using a de-differentiation approach was based on an observation during the initial optimisation of the MyD88 PepInh protocol, which revealed that removal of the MyD88 PepInh after 5 (rather than 12) days resulted in the cells returning to the self-renewing state or 'de-differentiating'. Exploiting this, 2102Ep cells were treated with MyD88PepInh for 7 days, at which point the two sub-populations could be separated by FACS: the two sub-populations were not observed at 5 days and only became apparent at 6-7 days (Figure 4.16). As this data shows, only 30% of cells were SSEA4 negative after 6-7 days. This represented a very small number of cells, which were returned to cell culture in MyD88 PepInh media, which, it was hypothesised, would permit them to de-differentiate to the primed self-renewal state. These cells initially grew well in 96-well plate format but unfortunately did not survive expansion to 24-well plates, after which they quickly died. The obvious solution to such a problem is to start the experiment with a very large cell number. However, the expense of the MyD88 PepInh was such that a large-scale cell culture experiment for 6-7 days was unrealistic. As such, the de-differentiation protocol was deemed unsuitable for isolation of primed self-renewing cells. Instead, molecular analysis was used to identify potentially suitable bio-markers, experiments that are described in detail in Chapter 5.

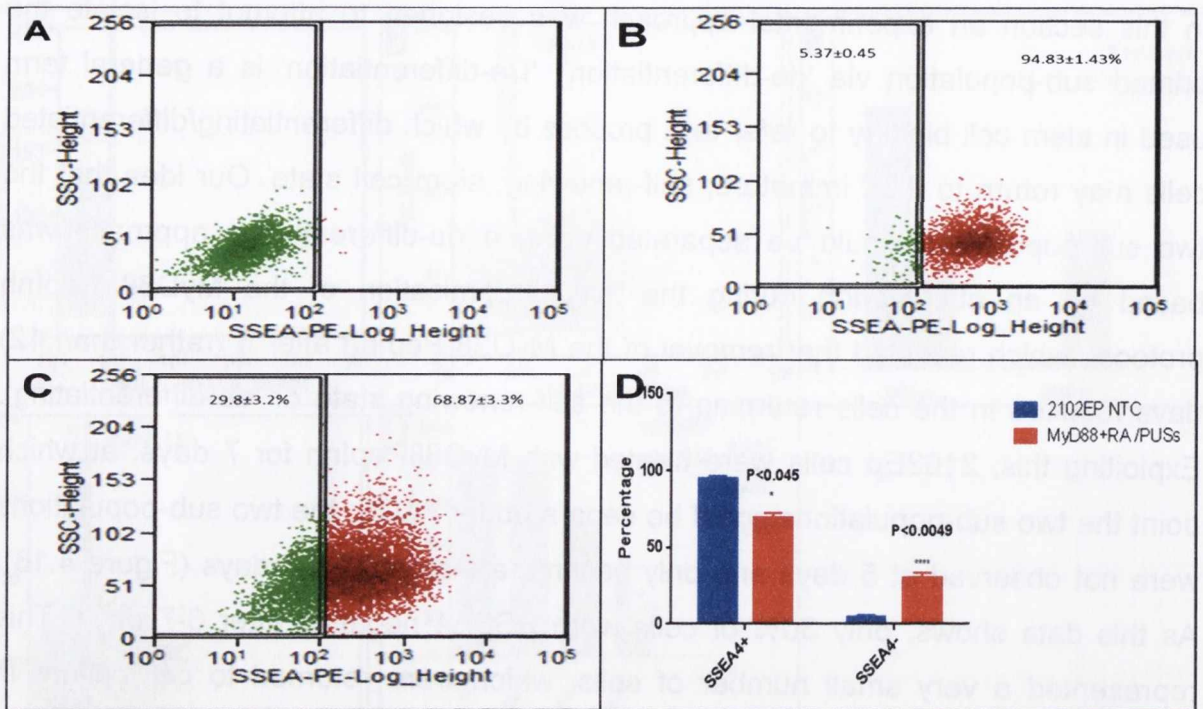


**Figure 4.16. Primed Self-Renewal State 2102Ep Cells can be Isolated via De-Differentiation.** In this experiment, 2102Ep cells were treated with MyD88 Peplnh for 6 days, after which cells were separated by FACS based on SSEA4 expression [Unstained (A) and untreated (B) control cells. CtrlPeplnh+RA (B) and MyD88 Peplnh+RA (D) cells]. The bar-chart (D) indicates that there is a significant difference in SSEA4 expression (p-value < 0.0049) between the samples. All experiments were n=3.

#### 4.3.3. Can the 2102Ep Sub-Populations be Isolated via De-Differentiation?

Following the validation of the two sub-population hypothesis, the next aim of this project was to molecularly characterize the events regulated by MyD88 in this mechanism. This analysis is described in Chapter 5. Ideally, this analysis would be best achieved if the two sub-populations could be isolated and studied as pure populations. However, the separation of the two cell lines would likely require knowledge of cell surface markers specifically expressed by these cells. SSEA4 was not an appropriate marker as the SSEA4<sup>+</sup> population is, by definition, already differentiated and thus cannot be studied in the original undifferentiated state.

## **4.4 Discussion**

At the outset of this Chapter, a two sub-population hypothesis had been proposed to explain ambiguous data generated in Chapter 3. This data indicated that loss of MyD88 in combination with addition of RA resulted in the presence of differentiated and undifferentiated cells. This led to the hypothesis that the 2102Ep cell line contains two sub-populations, only one of which differentiates in MyD88PepInh+RA conditions. Testing this hypothesis required a switch to a single cell analysis assay, which could determine the presence of individual undifferentiated and differentiated cells. Flow cytometry analysis described in this Chapter validated the two sub-populations hypothesis while FACS analysis facilitated isolation of the differentiation-resistant (nullipotent) and differentiated sub-populations. The differentiation status of the sub-population was confirmed via loss of expression of Oct4, Sox2 and Nanog. Furthermore, loss of MyD88 was shown to play a role in non-RA driven lineage differentiation mechanisms. Finally, conditioned media experiments were used to assess the functional role of loss of MyD88, which is known to alter the profile of chemokines and cytokines secreted by the cell. This data indicated that undifferentiated and differentiated cells secrete factors that are sufficient to promote their respective stem cell states. The next step in this study was to molecularly characterise the MyD88 and RA mechanisms and this work is described in Chapter 5. Before proceeding to this Chapter, in this section the implications of the two sub-populations hypothesis are discussed.

### **4.4.1 MyD88 is a Differentiation Gatekeeper in Pluripotent Cells.**

MyD88 is almost exclusively studied in its role as a mediator of Toll-Like Receptor (TLR) Signaling in innate immunity, which was described in Chapter 1 (Section 1.7). Therefore, such an important role for MyD88 in nullipotent/pluripotent differentiation might seem surprising. However, MyD88 was originally described in mice as a modulator of myeloid differentiation (Lord et al., 1990, Liebermann and Hoffman 2002). In fact, the 'D' in MyD88 stands for 'Differentiation', reflecting a long-forgotten role. To our knowledge, a role for MyD88 in stem cell differentiation and in the regulation of Oct4, Sox2 and/or Nanog has not been previously described. Results described in Chapter 3 and 4, were shown as evidence that, in a sub-population of 2102Ep cells, MyD88 inhibition in combination with RA treatment led to a

downregulation of pluripotency markers SSEA4, Oct4, Sox2 and Nanog. In addition, this sub-population displayed differentiated cell morphology and a reduced cellular proliferation in response to this treatment. Together, this is strong evidence for a role for MyD88 in the RA-induced downregulation of Oct4-Sox2-Nanog to facilitate differentiation of these otherwise nullipotent cells. As such, MyD88 appears to be a gatekeeper for RA-Induced differentiation of this sub-population of these cells. The mechanistic implications for this data are discussed in the following sections.

In addition to a role in RA differentiation, loss of MyD88 was shown to play a role in non-RA differentiation mechanisms. This is of critical importance to our understanding of differentiation of pluripotent cells. Once again, it is important to note that a role of MyD88 in pluripotency has never been described to our knowledge. This quite likely reflects the difficulty in studying early, more subtle events regulating exit from the self-renewal state and transition to towards lineage directed differentiation. As will be discussed in detail in the General Discussion in Chapter 6, it is possible that inhibition of MyD88 may facilitate transition to a stable, primed self-renewal state in other pluripotent cell types, which may be helpful in taking more control over lineage differentiation in areas such as organ generation in regenerative medicine.

#### **4.4.2 MyD88 is a Novel Upstream Regulator of Oct4-Sox2-Nanog.**

It is well known that Oct4, Sox2 and Nanog work together to maintain the nullipotent and pluripotent stem cell state and facilitate differentiation (Ffrench et al 2014, 2015). In pluripotent cells, morphogens such as RA activate pathways (in this case the RA Signaling Pathway), which downregulate Oct4, Sox2 and Nanog to facilitate differentiation (Andrews 2002, Andrews et al 2005). In nullipotent cells, poorly-understood factors inhibit this differentiation mechanism, which results in maintained high Oct4-Sox2-Nanog expression, producing a cell type that resists morphogens such as RA and continues to proliferate in the undifferentiated nullipotent state (Andrews 2002, Andrews et al 2005). While the mechanisms acting downstream of Oct4, Sox2 and Nanog are well characterized, the upstream mechanisms are poorly



understood. Indeed, upstream regulators of Oct4, Sox2 and Nanog are some of the most sought after mechanisms in stem cell and CSC biology.

In this study, MyD88 has been identified as a novel upstream regulator of Oct4-Sox2-Nanog driven differentiation of a sub-population of nullipotent cells. So far, the data indicate that loss of MyD88 is a requirement for RA-induced differentiation of nullipotent 2102Ep cells. In addition, loss of MyD88 was shown to play some role in non-RA stimulated differentiation mechanisms in all three germ layer lineages. Although further analysis of non-RA mechanisms was beyond the scope of this project, it appears likely that further optimisation and longer differentiation time courses will demonstrate a strong role for MyD88 in all three lineage-differentiation mechanisms.

#### **4.4.3 Loss of MyD88 Facilitates Transition to a Primed Self-Renewal State.**

Historically, genes identified as playing key functional roles in stem cell status govern spontaneous differentiation of the cells. For example, loss of Oct4, Sox2 or Nanog results in rapid, spontaneous differentiation of pluripotent cells, which does not require the addition of a differentiation morphogen such as RA (Vencken et al 2014). Unusually, loss of MyD88 does not result in spontaneous reduction in levels of Oct4, Sox2 and/or Nanog, as is usual in reported differentiation mechanisms. Instead, loss of MyD88 appears to allow these cells to respond to the differentiation morphogen RA in a way that they otherwise do not. Our data suggests that MyD88 is a gatekeeper to an intermediate state between self-renewal and differentiation, a state that has been hypothesized but only partially demonstrated (Silva and Smith 2008). This concept of two-step differentiation is discussed in detail in the next section. During the completion of this work, the precise mechanism involved will be elucidated. This, it is hoped, will substantially improve our understanding of A) nullipotent resistance to differentiation, B) pluripotent differentiation and C) how CSCs resist differentiation to produce highly aggressive tumours.

#### **4.4.4 Proposed model of MyD88-regulated differentiation in 2102Ep cells.**

At the end of the previous Chapter, a proposed model of MyD88-regulated differentiation was described, which is reproduced in Figure 4.16. As described in

Section 4.1, the self-renewal state is defined by promotion of self-renewal and inhibition of differentiation mechanisms. These mechanisms prevent self-renewing cells from responding to *in vivo* differentiation stimuli, which are ever-present in the stem cell and tumour microenvironment. In Chapter 3, a two sub-population hypothesis for MyD88 regulated differentiation in EC cells was proposed. This model indicated that in one sub-population, loss of MyD88 transitions cells to a transition state, which is stable in the self-renewal state and can respond to RA (Figure 4.16, Bottom). In this Chapter, the two sub-populations hypothesis was validated and is illustrated in Figures 4.17 and 4.18. The data generated in this Chapter indicates that loss of MyD88 permits transition to a new state that will now be referred to as the 'Primed Self-Renewal' (SR<sup>PR</sup>) state. It is noted that this model shows some similarity to the 'Ground State' model of mES differentiation but has never been described in human pluripotent cells.

The implication of this data is that MyD88 can now be labelled as a key differentiation inhibition mechanism in hEC cells. In the self-renewal state, MyD88 is necessary for the maintenance of the self-renewal state. Mechanistically, MyD88 expression is associated with secretion of self-renewal state promoting factors in to the stem cell niche. Upon loss of MyD88, a sub-population of cells transition to the SR<sup>PR</sup> state. This state is defined by an ability to differentiate in response to RA and mesoderm lineage differentiation stimuli, and possibly to endoderm and ectoderm differentiation stimuli. As such, MyD88 may represent a key state-stability factor in pluripotent cells generally. Now that this mechanism has been partially elucidated, the final aim of the project was to molecularly characterise the events controlled by A) MyD88 and B) MyD88+RA. This characterisation is described in Chapter 5.

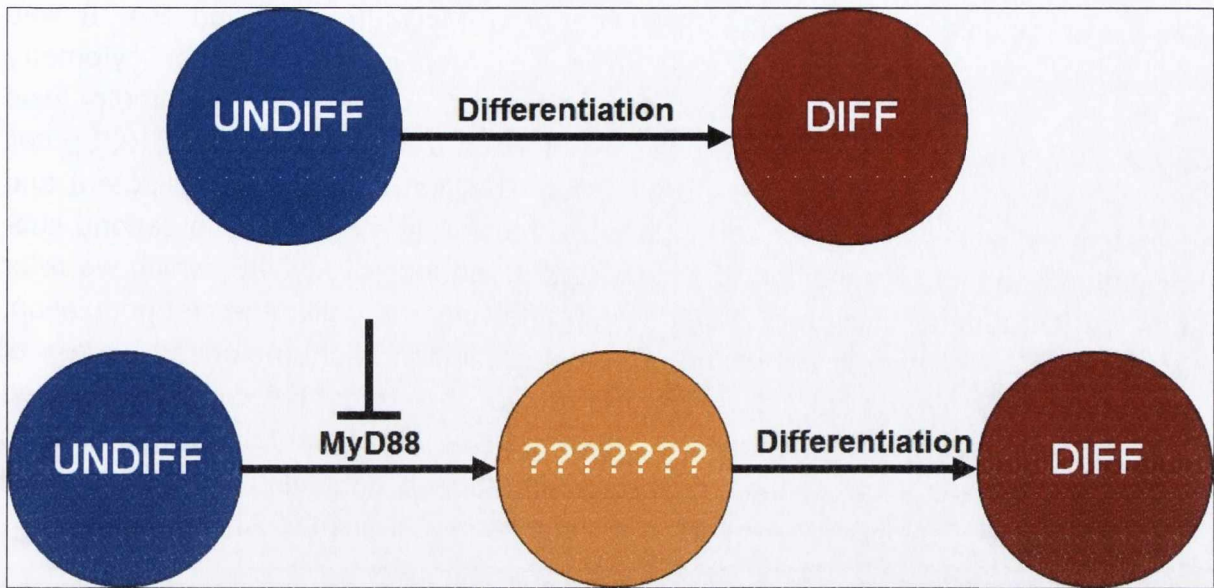


Figure 4.17. **Early Model of MyD88-Regulation Differentiation.** Exit from the undifferentiated start and lineage differentiation have, historically, been considered to be a single couple process (Top). Early data from this project (described in Chapter 3) indicated that loss of MyD88 controls entry into a transition state, which is responsive to differentiation stimuli (Bottom). The previously-unknown nature of this transition state was partially elucidated in Chapter 4, as described in Figure 4.18.

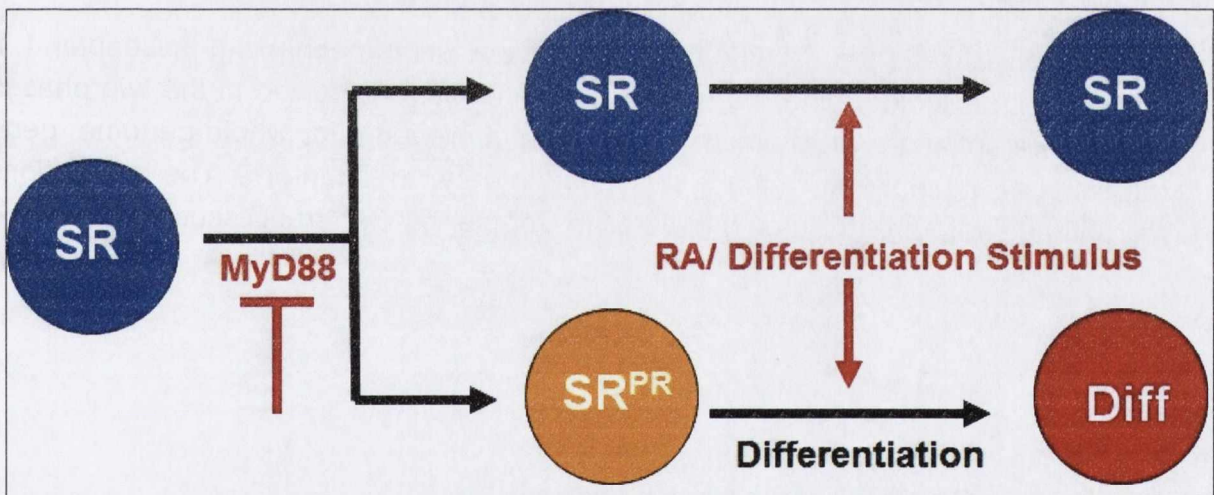


Figure 4.18. **Proposed Model of MyD88-Regulation Differentiation.** Together, data from Chapters 3 and 4 indicate that 2102Ep cells contain two sub-populations. One of these sub-populations transitions to a primed self-renewal state ( $SR^{PR}$ ) upon loss of MyD88, which responds to differentiation stimuli. This unusual state appears to remain stably self-renewing and primed in the absence of MyD88 and a differentiation stimulus.

## 4.5 Conclusion

In the previous Chapter evidence was provided for the presence of 2 sub-populations within the 2102Ep cell line. Based on this hypothesis it was proposed that the first of these sub-populations was nullipotent and that the second could be

stimulated to differentiate in the presence of a MyD88PepInh and RA. It was additionally hypothesised that a single cell analysis technique such as flow cytometry would be required to test this hypothesis. In this chapter, flow cytometry was successfully employed to support these hypotheses. As proposed, the 2102Ep cell line was shown to contain 2 sub-populations. The first of these is nullipotent and maintains SSEA4, Oct4, Sox2 and Nanog expression at all times. The second sub-population appears to transition to a new state upon loss of MyD88, which we refer to as the SR<sup>PR</sup> state. This state is stably self-renewing but, unlike the first population, can respond to RA by differentiating. This differentiation is characterised by loss of SSEA4, Oct4, Sox2 and Nanog. It was additionally shown that RA could be replaced in this mechanism by other growth factors, such as those contained in a specific mesoderm differentiation kit tested. The results allow a conclusion that maintained expression of MyD88 is a differentiation-resistance mechanism in 2102Ep cells.

In addition, the role of MyD88 as a regulator of the profile of proteins secreted by the cell was assessed in this mechanism. These data showed that proteins secreted by self-renewing and differentiated cells were sufficient to promote the self-renewal and differentiated state of Ntera2 cells respectively. This data suggests a mechanism where hEC cells secrete state-specific factors to promote that stem cell state in both themselves and cells in the niche. As MyD88 is a key regulator of the prolif of secreted factors produced by TLR Signaling, this suggests a functional role for MyD88 in this mechanism.

Having demonstrated the validity of the 2 sub-population mechanism in Chapter 4, it was important to next define the molecular mechanisms involved in the two phases of this differentiation mechanism. This was achieved via whole-genome gene expression array analysis, which is described in detail in Chapter 5. The implications of all of these data are discussed in detail in Chapter 6, 'General Discussion'.

## Chapter 5

# MyD88 Inhibition Facilitates Differentiation of 2102Ep Cells Through Activation of Retinoic Acid Signaling

### 5.1. Introduction

#### 5.1.1 Overview

In the previous chapter, we described that loss of MyD88 permits differentiation of a sub-population of 2102Ep cells in response to Retinoic Acid (RA) treatment. This is an unusual mechanism to observe. Historically, it was believed that stem cells and CSCs exit the self-renewal (SR) state and differentiate in one coupled process. This process occurs rapidly, which means it is very difficult to identify some of the earlier and more subtle events involved in exit from the SR state. The mechanism we have identified allows us to step inside this coupled process, as it appears to be uncoupled in our model. To exploit this, in this Chapter we used gene and microRNA (miRNA) array analysis to characterise the molecular events involved in A) MyD88 inhibition and B) differentiation induced by MyD88 inhibition and RA treatment.

The results below describe in detail the molecular events involved in our model. As expected, loss of MyD88 led to several molecular changes indicative of activation of MyD88-Independent TLR signaling (Section 1.7). Perhaps surprisingly, no alterations in RA signaling or stemness pathways such as Sonic Hedgehog (Shh), TGF- $\beta$ , Notch or Snail signaling were observed in cells treated with the MyD88 Peptide Inhibitor (PepInh). Instead, inhibition of MyD88 activates expression of a number of HOX genes, which are well-known regulators of differentiation and development (Section 5.1.2.). In parallel, the other main molecular events controlled by MyD88 appear to be decreases in the expression of Taste and Olfactory Receptors. This seemingly unusual result is in line with several recent publications, as described in the sections below (Sections 5.1.3 and 5.1.4). This mechanism appears to permit 2102Ep cells to activate all levels of RA signaling (Section 1.6) in response to RA treatment, which results in differentiation of these cells. These results are described in Section 5.3 ('Results') and their implications detailed in Section 5.4 ('Discussion').

### 5.1.2 Hox Genes are Key Developmental/Differentiation Regulators

The Hox genes are a subgroup of homeobox genes that encode a set of important transcription factors, which regulate development processes and play a major role in anterior–posterior patterning of the developing embryo. As pluripotent stem cell differentiation is essentially the beginning of embryonic development, Hox genes have been unsurprisingly shown to be key components of differentiation from pluripotent cells. There are a total of 39 Hox genes in humans, arranged in 4 distinct clusters (A-D), each localized to a different chromosome (HOXA at 7p14, HOXB at 17q21.2, HOXC at 12q13, and HOXD at 2q31. Alharbi et al 2013, Lappin et al 2006, Quinonez and Innis 2014. Figure 5.1).

Functionally, specific roles for each Hox cluster (A, B, C or D) have not been described. In contrast, the roles of specific Hox genes have been described in detail. Roles for Hox genes have been reported in abnormal development and malignancy, where the normal expression of Hox genes is disrupted. This leads to changes in the expression of one or more target pathways, which results in tumour growth. Three mechanisms have been proposed to explain the deregulation of Hox genes in cancer. The first two mechanisms, ‘temporal-spatial deregulation’ and ‘gene dominance’, occur when the expression of Hox genes is associated with oncogenesis. The third mechanism, ‘epigenetic deregulation’, is obvious in tissues where Hox genes normally function as tumour suppressors (Shah and Sukumar 2010).

It is well known that Hox genes are altered in response to RA treatment. In human embryonic stem (hES) cells, the HoxA group is altered when the cells are induced to differentiate in response to RA (Atkinson et al 2008). In addition, a large number of HOX genes were upregulated during RA-induced differentiation of human ‘NTera2’ embryonal carcinoma (hEC) cells (Unpublished data from our group). However, data described in this Chapter is the first indication of a relationship between Hox genes and MyD88/TLR signaling, and has not been previously described.

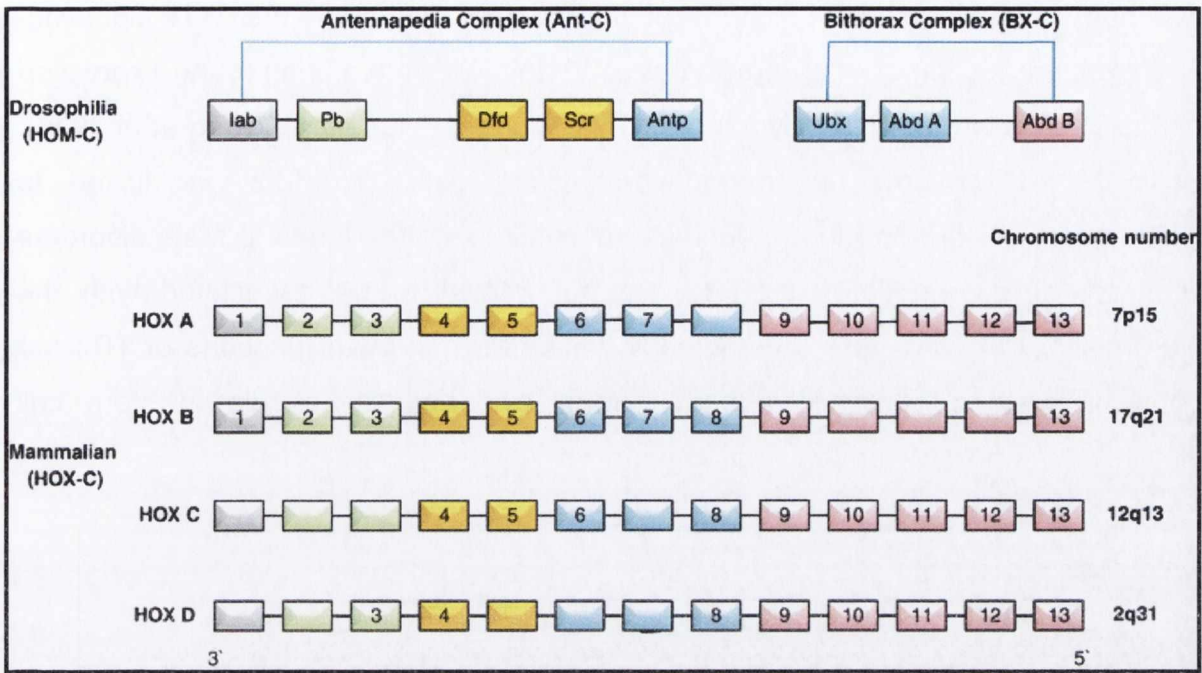


**Figure 5.1. Hox Gene Family Organisation.** In humans, HOX genes are assembled in to the A-D families, which are structurally related and associated with loci on separate chromosomes (Alharbi et al 2013).

### 5.1.3 Taste Receptor Family 2

The detection of the 5 taste sensations (sweet, bitter, sour, salty and umami) is achieved through combinations of a subclass of the superfamily of G protein-coupled receptors (GPCRs), known as Taste Receptors (TRs). Functionally, TRs are primarily known to play a key taste sensation role within the cells of taste buds, as a component to detect target chemical signals. These signals are converted into molecular responses, which facilitate the sensation of taste (Figure 5.2.). Taste receptors are arranged into two different types according to the function. Sweet is primarily detected by Type 1 Taste Receptors (T1Rs) and bitter primarily detected by Type 2 Taste Receptors (T2Rs), while the other sensations are detected though combinations of T1Rs and T2Rs (Adler et al 2000, Nelson et al 2001).

In recent years, TRs of many types have been found in non-taste cells (Li 2013). In terms of non-taste functions, T2Rs have been best studied in spermatogenesis (Xu et al 2013). Although the mechanism is poorly understood, it is clear that T2Rs play a role in determining the ratio of self-renewing and differentiating cells present at different stages of spermatogenesis. A relationship between TLR signaling and TRs has been described in a small number of recent studies. In mouse taste cells, T1Rs

have been shown to achieve many of their functions through the TLR signaling-dependent production of TNF- $\alpha$  (Feng et al 2012). TLRs have been found expressed in endocrine cells that originally express TRs and taste signaling (Wang et al 2014). Additionally, it is now understood that some taste disorders are linked to inflammation and that the therapeutic use of cytokines often leads to taste disorders (Wang et al 2014). To date, TRs are not known to be associated with the differentiation of pluripotent cells. Clearly, while the non-taste functions of TRs are poorly understood, there is already strong evidence for a role in stem cell differentiation and TLR-driven inflammation.

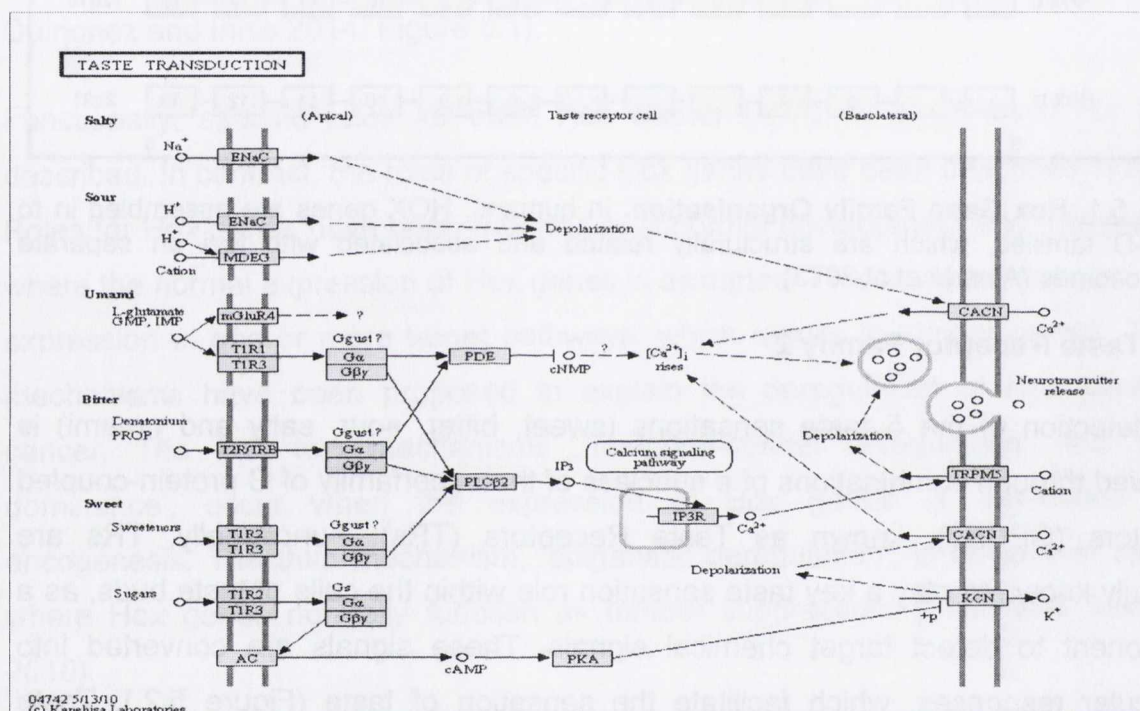


**Figure 5.2. The Taste Sensation Signaling Pathway.** The sensation of taste occurs as a result of specific chemical signaling binding to the specific taste receptor (T1R/T2R) where it blocks or permits entry in to ion channels of receptor cells. This leads to depolarization, which facilitates signal transmission (www.genome.jp).

### 5.1.4 Olfactory Receptors

Olfactory Receptors (ORs) are the key smell receptors, which are involved in the detecting and processing of odour and pheromone signals for transmission to the brain. ORs are a large family whose mechanism is well-described in olfactory tissues. In recent years, ORs have been shown to be widely expressed in several non-sensory tissues such as in the testis and sperm, kidneys, prostate, erythroid cells and notochord (Barnea et al 2004, Kaupp 2010). Like expression of TRs in non-



sensory tissues, this discovery was surprising and the role of ORs in non-sensory tissues remains poorly explained.

In the nose, the binding of an odorant to the OR leads to activation of the heterotrimeric G protein 'G $\alpha$ olf and G $\beta\gamma$ ', which appears to be the key functional event. Once olfactory G $\alpha$ olf is stimulated, it activates type 3 adenylyl cyclase (AC3), leading to the production of cyclic AMP (cAMP) from ATPs, which activate the olfactory cyclic nucleotide-gated channel (CNGC) and a Ca<sup>2+</sup>-activated Cl<sup>-</sup> channel (CaCC). Activation of both channel types finally leads to depolarization, which facilitates signal transmission (DeMaria and Ngai 2010, Figure 5.3).

Although it is poorly characterised, a relationship between ORs and RA signaling has been described for some time. ORs are particularly associated with neural differentiation and we have found alterations in OR expression during NTera2 RA-induced differentiation (Section 5.3.14). RA is necessary to maintain progenitor populations during the development of the olfactory epithelium and to sustain olfactory neurogenesis through the expression of several neural-specific molecules that may induce the differentiation of OR neurons once the initial morphogenesis of the OE is complete (Whitesides et al 1998, Paschaki et al 2013). While the data described in this Chapter is the first description of a relationship between ORs and MyD88, a recent study had described a relationship between ORs and TLR signaling in *Drosophila* (Ward et al 2015). Specifically, TLR signaling appears to be involved in OR-related patterning during *Drosophila* development.

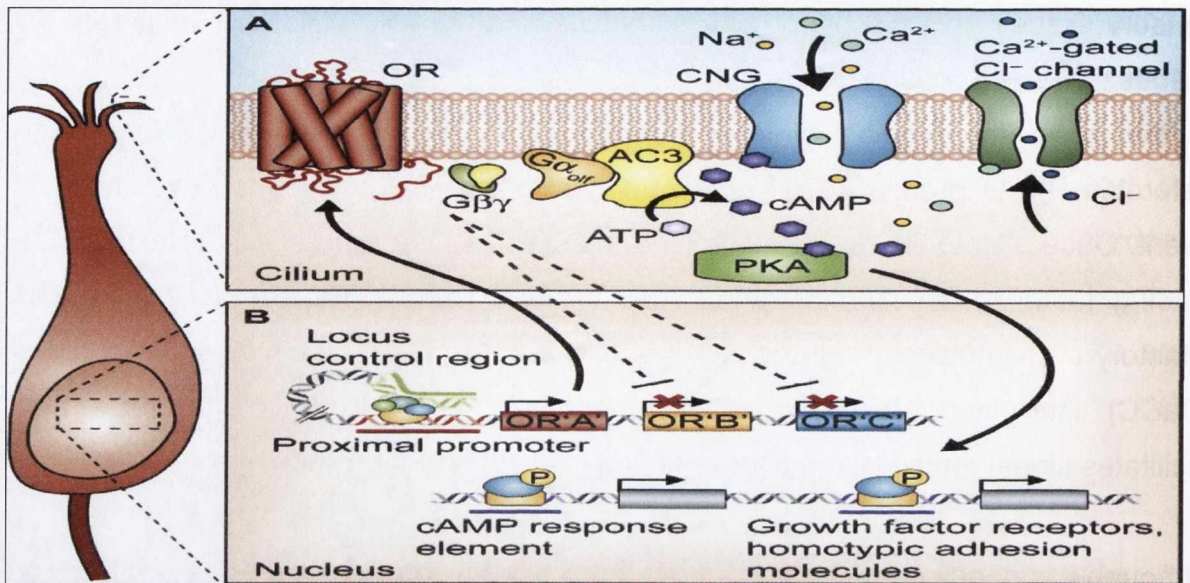


**Figure 5.3. Olfactory Receptor Signaling.** (A) The association of odorous ligands with specific receptors on Olfactory Sensory Neurons (OSNs) regulates the activation of G proteins 'G $\alpha$ olf' and 'G $\beta\gamma$ ' in OSNs. The activation of G $\alpha$ olf stimulates type III adenylyl cyclase (AC3) and an increase in cyclic AMP (cAMP), which leads to opening of the cyclic nucleotide-gated (CNG) ion channel to allow the influx of Na<sup>+</sup> and Ca<sup>2+</sup> into the cilia. This leads to depolarisation of the cell, which facilitates signal transmission. (B) Neuron identity is a key component of OR signaling, where the selection of one type of OR for expression results in the silencing of all other OR genes in that OSN via an OR-dependent feedback loop. This process involves protein kinase A (PKA), which is activated via cAMP, regulates the transcriptional of cAMP response element binding protein (CREB)-dependent gene expression via CREB's phosphorylation (DeMaria, and Ngai 2010).

### 5.1.5. MicroRNAs

MicroRNAs (miRNAs) are short single-stranded endogenous non-coding RNAs that consist of approximately 20-22 nucleotides and play an important role in the regulation of several cellular, physiological, pathological and developmental processes (Divya Lenkala et al 2015). Specific populations of miRNA are expressed in undifferentiated and differentiated stem cells and CSCs. Additionally, several miRNAs have been shown to directly regulate key stem cell components such as Oct4-Sox2-Nanog and various components of stemness signaling pathways such as Wnt, Sonic Hedgehog, Notch and TGF- $\beta$  (Ffrench et al 2015). MicroRNAs play an important role in the development and progression of cancer through regulation of the expression of a number of oncogenes and tumour suppressors (Ffrench et al 2015). Several studies have indicated that miRNAs are involved in many different types of cancer such as breast, colon, gastric, lung, prostate and thyroid cancers (Ffrench et al 2015).

MicroRNAs are initially made from pri-miRNAs through a process that begins in the nucleus (Figure 5.4). The pri-miRNA is transcribed from specific miRNA genes by the enzyme RNA polymerase II. Once the pri-miRNA is created, it is exported into the cytoplasm by exportin-5 (Exp5) and ras-related nuclear protein-GTP complex (Ran-GTP). Then, in the cytoplasm, the RNA polymerase III 'Dicer' forms a specific complex, which leads to generation of the mature miRNA (Yi et al 2003, Lee et al 2004, Bao et al 2012).

The function of most miRNAs is to 'post-transcriptionally' regulate target mRNAs. In this model, target mRNAs are bound by miRNAs through a key sequence known as the 'seed region', which is located in the 3' untranslated region (UTR) of the target mRNA. Once bound, the miRNA suspends the mRNA transcript within the cell, where it is neither degraded nor translated. Upon receiving an appropriate signal, the miRNA can release bound mRNAs and present them to the ribosome for translation. As such, miRNAs regulate the timing at which specific transcripts are presented for translation.

It is well established that different populations of miRNAs play important roles in RA and TLR signaling as well as the stem cell, cancer and CSC roles described above. Our group has previously shown that miRNA signatures expressed in 2102Ep cells are differentially expressed in A) high-grade ovarian tumour samples (Gallagher et al 2009) and B) primary versus recurrent ovarian tumour samples (Gallagher et al 2012). Additionally, we have shown that miRNAs are associated with the role of MyD88 as an ovarian cancer bio-marker (d'Adhemar et al 2014). Complementing this, in this Chapter we described the specific regulation of a defined population of miRNAs by MyD88 during 2102Ep differentiation.

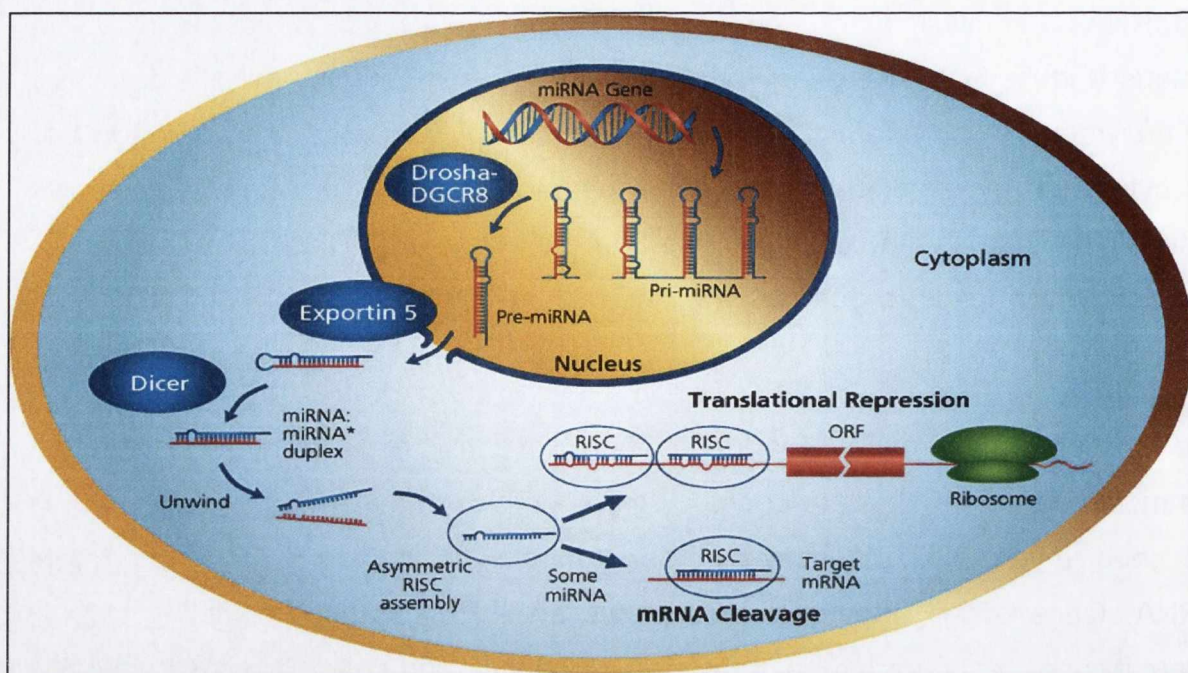


**Figure 5.4. MicroRNA Biogenesis.** The primary miRNA (pri-miRNA) is transcribed by polymerase II, and processed in to a 'pre-miRNA' in the nucleus by the microprocessor complex Drosha-DGCR8. The Pre-miR is then exported into the cytoplasm by the exportin-5-Ran-GTP complex. In the cytoplasm, the RNase Dicer forms a specific complex, which leads to generation of the mature miRNA. This initiates the formation of the RNA- induced silencing complex (RISC), which facilitates post-transcriptional regulation of the target mRNA ([www.sigma.com](http://www.sigma.com)).

### 5.1.6. Aims & Hypotheses

In the previous chapter, we described how MyD88 is a differentiation gatekeeper during RA-induced differentiation of a sub-population of 2102Ep cells. The aim of this chapter was to characterise the mechanism controlled and driven by MyD88. Specifically, genes and miRNAs regulated by MyD88 are identified through array analysis. Additionally, the downstream gene events that facilitate RA-induced differentiation following MyD88 inhibition are also characterised. We hypothesise that the elucidation of this mechanism will provide novel insight in to the regulation of pluripotency, RA signaling, TLR signaling, cancer and CSC resistance to differentiation.

## 5.2 Materials and Methods

All materials and methods related to this chapter are described in chapter 2.

## **5.3 Results**

Our data indicate that 2102Ep cells maintain high MyD88 expression levels to facilitate differentiation-resistance or 'Nullipotency'. The aim of the work presented in this chapter was to characterise the mechanism involved in A) MyD88-driven nullipotency and B) differentiation in response to a combination of MyD88 inhibition and RA treatment. Whole genome gene and microRNA expression arrays were used to characterise the mechanism involved. In this section, results related to MyD88 inhibition are presented first. This analysis involved comparison of MyD88 Peplnh Inhibitor (PepInh) and Control (Ctrl) PepInh treated samples. Subsequently, results related to RA-induced differentiation are presented. To facilitate this analysis, SSEA4<sup>Neg</sup> (differentiated) cells isolated by FACS are compared to MyD88 PepInh treated samples. The aim of this analysis was to identify molecular events that occur upon MyD88 inhibition separate to those that subsequently drive differentiation in response to RA treatment. These results are combined in the Discussion (Section 5.4) to arrive at a model of MyD88-RA-driven differentiation. Finally, the results section will conclude with a comparison between PUS and NTera2 differentiation and the identification of putative Primed Self-Renewal (SR<sup>PR</sup>) state marker genes. Large genelists such as 'Top 20s' are shown in appendices as cited while full genelists are listed as 'Supplementary (S) Tables, and are contained in a compact disc at the back of the thesis.

### **5.3.1. Defining the MyD88 Inhibition Mechanism: Comparison of MyD88PepInh and CtrlPepInh Treated 2102Ep cells.**

#### **5.3.1.1. An Overview of Gene Array Analysis of the MyD88 Inhibition Mechanism**

In this first set of analysis, we aimed to identify the genes, pathways and microRNAs regulated by MyD88 to maintain nullipotency. To identify these molecular events, cells treated with MyD88 PepInh for 12 days were compared to cells treated with the Ctrl PepInh for 12 days. This is referred to as the 'MyD88 vs Ctrl PepInh' comparison, and was used to identify molecular events associated with MyD88 inhibition. Other cell samples available for comparison were MyD88PepInh and Ctrl PepInh +RA treatments as well as FACS-separated SSEA4<sup>Neg</sup> (differentiated) and SSEA4<sup>Pos</sup> (undifferentiated) samples. The comparison of these treatments and controls is illustrated in Figure 5.5 and were used to answer specific questions, as

described below. As such, gene events described below are those that occurred in tester sample but not in controls.

Whole-genome analysis passed all quality control checks and demonstrated clear separation of MyD88 and Ctrl PepInh treated samples (Figure 5.6). Hierarchical clustering (Figure 5.6) shows that Ctrl PepInh treated cells are most similar to cells treated with Ctrl PepInh and RA, while MyD88 PepInh cells are most similar to cells treated with MyD88 PepInh and RA. This indicates that any changes made by 2012Ep cells in response to the control drug and/or RA are small in comparison to those made by MyD88 PepInh and/or RA treatment.

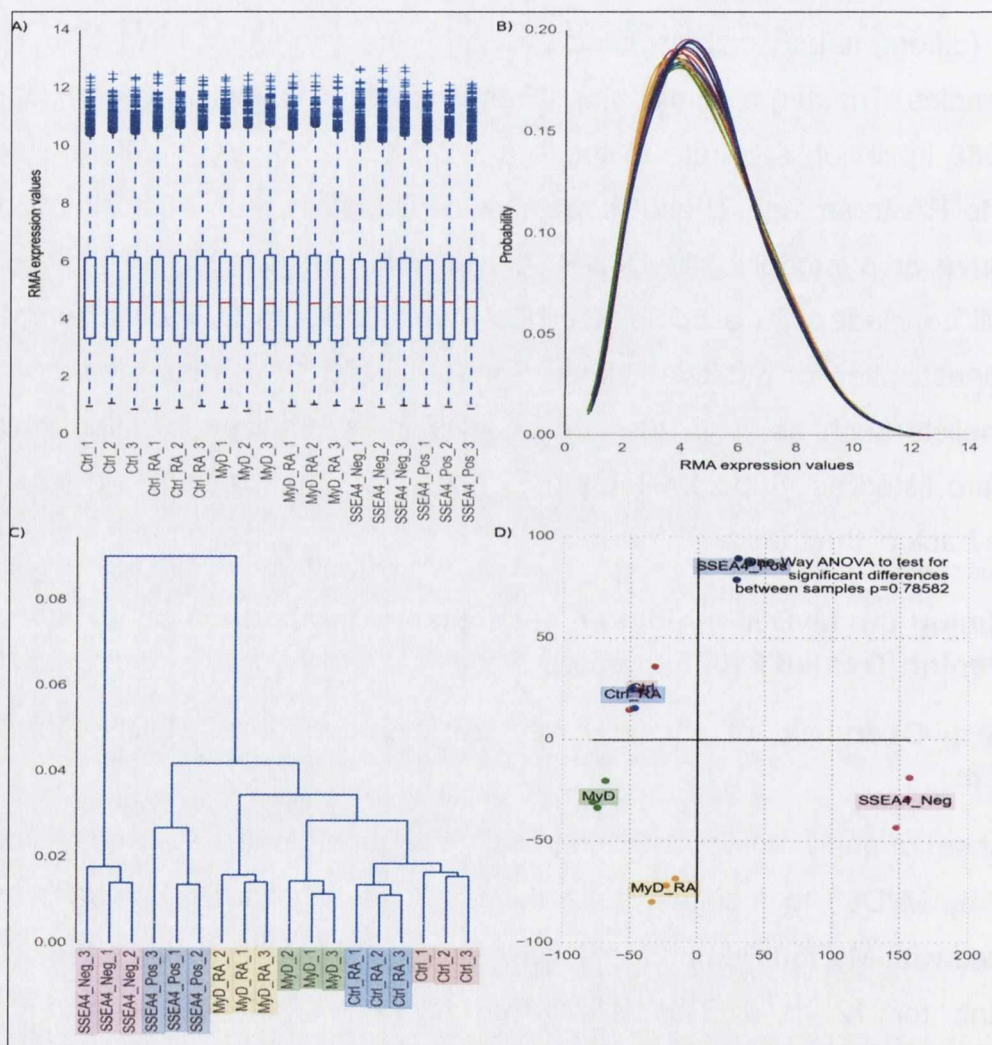


**Figure 5.5. Overview of Gene Expression Array Analysis in Chapter 5.** In this experiment, 2102Ep cells from various aspects of the MyD88 differentiation protocol were arrayed for whole genome gene expression analysis. Samples included were treated with a MyD88 (MyD) or Control (Ctrl) PepInh with (\_RA) or without retinoic acid for 12 days. Additionally, cells FACS separated on the basis of SSEA4 expression at the end of the experiment are also included (differentiated=SSEA4\_Neg, undifferentiated=SSEA4\_pos).

The images show data from three individual biological replicates for each treatment, which passed all quality controls (A and B). The data show strong separation of the samples in to their treatment groups by hierarchical clustering (C), which was found to be strongly statistically significant (D).

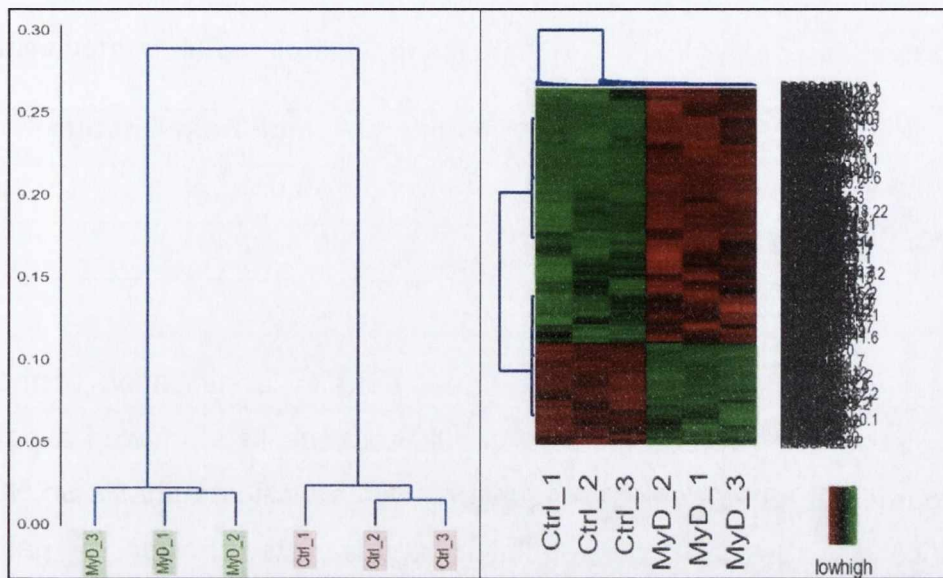


**Figure 5.6. Gene Expression Array Analysis of MyD88PepInh and CtrlPepInh Samples.** In this experiment, 2102Ep cells were treated with either MyD88PepInh (MyD) or CtrlPepInh (Ctrl) for 12 days, RNA isolated and gene expression arrays performed. The image shows data from three individual biological replicates for each treatment. The data show strong separation of the samples in to their treatment groups by hierarchical clustering (left panel) and a bias towards downregulated genes by heat map (right panel).

### 5.3.1.2. Loss of MyD88 Affects HOX, Taste Receptor and Olfactory Receptor Genes

Loss of MyD88 resulted in 295 downregulated and 119 upregulated genes at fold change maximums of -47.1 to +8.0 (Table 5.1). As such, in the nullipotent state, MyD88 maintains the expression of twice as many genes as it inhibits and at a much higher level. The top 20 downregulated genes do not contain any known stemness regulators (Appendix 1). In comparison, the top upregulated genes contain several HOXA family members, which are key developmental/differentiation regulators (Section 5.1.3). This indicates that, in the nullipotent state, MyD88 is responsible for repression of HOXA genes. Other genes of note include downregulation of development regulator Early growth response 1 (Egr1) and key oncogene Fos, as both Egr1 and Fos (AP-1) are known to be activated by MyD88 in response to detection of bacteria (Kenzel et al 2009). Additionally, the induction of Egr1 by RA is long-established (Larsen et al 1994). In parallel, histone modification genes, which

are known to play a role in chromatin remodelling in stem cell differentiation, were upregulated. Stemness signalling pathways such as Sonic Hedgehog, TGF- $\beta$ , Snail and Notch were not altered in these samples.

**Table 5.1. Comparison of MyD88 PepInh Samples to Control PepInh treated samples**

Treatment	Gene Number	Max Fold Change
<b>MyD88 PepInh Upreg</b>	119	8.0
<b>MyD88 PepInh Downreg</b>	295	-47.1

'DAVID' is an online bio-informatics tools that permits identification of molecular relationships in gene array data sets. Upregulated gene lists showed a pattern of many developmental (differentiation) regulators, with specific emphasis on HOX and histone-modification genes. Downregulated genes lists showed a pattern of emphasis on sensory perception of chemical stimuli, with specific emphasis on Taste Receptor Type 2 (T2R) and Olfactory Receptor (OR) genes. With these results in mind, each of these processes was studied in greater detail. Due to their importance, we will first discuss A) Oct4-Sox2-Nanog, B) TLR signaling and C) RA signaling in detail.

### **5.3.1.3. Inhibition of MyD88 does not Affect Expression of Pluripotency Markers Oct4-Sox2-Nanog**

The most important molecular events controlled by MyD88 are Oct4, Sox2 and Nanog. These key pluripotency regulators were shown to be independent of MyD88 regulation in the previous chapters. In this analysis, MyD88 PepInh treated cells showed statistically significant changes in expression of all three pluripotency markers. However, these changes were below the  $\pm 2.0$  fold change imposed in the study (Oct4=1.2, Nanog=1.3, Sox2=-1.1 fold change, all FDR<0.05: Table S1). As such, regulation of Oct4, Sox2 and Nanog clearly requires RA in addition to loss of MyD88. This matches the undifferentiated phenotype of MyD88 PepInh treated cells.



#### **5.3.1.4 Inhibition of MyD88 Appears to Activate MyD88-Independent TLR Signaling**

Inhibition of MyD88 is likely to activate MyD88-independent TLR Signaling. MyD88-independent signaling is primarily achieved through TLR3 with some tentative indications of a role for TLR4 (Section 1.7). In line with this, TLR3 was significantly upregulated upon inhibition of MyD88, but only to 1.3 fold (Table S1). One of the main adaptor molecules for TLR3 in MyD88-independent signaling is TRAM and TRAM2 was significantly upregulated (1.4 fold) in MyD88 inhibited cells. In parallel, one of the main products of MyD88-dependent signaling, AP-1, was downregulated in MyD88 PepInh treated cells (Fos: -4.9, Jun: -1.7). Together, these results suggest de-activation of MyD88-dependent signaling and activation of TLR3-mediated MyD88-independent signaling in these cells upon loss of MyD88, as expected.

#### **5.3.1.5 MyD88 Inhibition Does Not Alter RA Signaling Genes**

In this comparison (MyD88PepInh vs Ctrl PepInh), no cells experienced RA treatment. Due to the RA-induced differentiation mechanism described in the previous chapter, it was possible that MyD88 inhibition altered aspects of the RA signaling pathway. However, no RA signaling pathway genes were found to be altered upon loss of MyD88 (Table S1). As such, loss of MyD88 does not affect RA signaling in the absence of RA.

#### **5.3.1.6 MyD88 Regulates Taste and Olfactory Receptor Gene Expression**

From DAVID functional relationship analysis, two sets of receptors were highlighted as being downregulated in cells treated with MyD88 PepInh, namely Taste and Olfactory (smell) receptor signaling (Table S2). A large number (6 above and another 2 below the 2.0 fold change cut-off) of Taste Receptor Type 2 (T2R) family members were significantly downregulated by MyD88 inhibition (Table 5.2). Five Olfactory Receptor (OR) genes are also downregulated by MyD88 inhibition (Table 5.2). The TR and OR signaling pathways have been primarily studied at the bio-chemical, protein level. At a molecular level, these pathways are as yet poorly defined but none of the other known members of the taste signaling cascade were downregulated on our arrays. At first glance, these mechanisms appear to be unrelated to pluripotency or CSC biology. However, as described in the introduction to this chapter, TRs and

ORs are now known to be expressed in non-sensory organs with as yet poorly-defined functions. Additionally, links between TRs and TLR signaling and ORs and RA signaling has been demonstrated (Section 5.1.3). This data indicates that in 2102Ep cells, MyD88 functions to maintain high expression of TRs and ORs during nullipotency.

**Table 5.2. Taste and Olfactory Receptors altered in MyD88PepInh versus Ctrl**

MyD88PepInh vs Ctrl PepInh			
Description	Gene Name	Fold Change	p-Value
Olfactory receptor, family 56, subfamily A, member 1	OR56A1	-3.3	0.01
Taste receptor, type 2, member 50	TAS2R50	-2.8	0.02
Taste receptor, type 2, member 46	TAS2R46	-2.8	0.01
Taste receptor, type 2, member 13	TAS2R13	-2.8	0.003
Taste receptor, type 2, member 43	TAS2R43	-2.8	0.01
Taste receptor, type 2, member 31	TAS2R31	-2.7	0.0039
Olfactory receptor, family 56, subfamily A, member 4	OR56A4	-2.6	0.008
Taste receptor, type 2, member 14	TAS2R14	-2.3	0.002
Olfactory receptor, family 5, subfamily P, member 2	OR5P2	-2.22	0.04
Olfactory receptor, family 7, subfamily A, member 5	OR7A5	-2.05	0.01
Taste receptor, type 2, member 20	TAS2R20	-2	0.13
Olfactory receptor, family 3, subfamily A, member 1	OR3A1	2.64 □	0.0022

### 5.3.1.7. Loss of MyD88 Activates HOX Gene Expression

As mentioned above, HOXA genes were identified as Top 20 upregulated genes in MyD88 PepInh treated cells. On closer inspection, HOXA1, 2, 4 and 13 are upregulated by loss of MyD88 (Table 5.3). As such, it appears that one of the roles of MyD88 in nullipotent cells is to inhibit differentiation by suppressing HOXA gene expression. As HOX genes are important regulators of development/differentiation, this is likely to represent an important aspect of the MyD88 mechanism.

**Table 5.3. HOX genes altered in MyD88PepInh versus Ctrl**

<b>MyD88PepInh vsCtrl PepInh</b>			
<b>Description</b>	<b>Gene Name</b>	<b>Fold Change</b>	<b>p-Value</b>
Homeobox A1	HOXA1	3.38	0.0017
Homeobox D13	HOXD13	2.8	0.0020
Homeobox A2	HOXA2	2.41	0.0052
Homeobox A4	HOXA4	2.30	0.0030

#### **5.3.1.8. Summary of MyD88 Inhibition Data**

To summarise, loss of MyD88 results in upregulation of HOXA and histone modification genes in parallel with downregulation of Taste and Olfactory Receptor Genes. This suggests a mechanism where the role of MyD88 in 2102Ep cells is to maintain nullipotency by suppression histone-modification and HOXA genes while promoting expression of Taste and Olfactory Receptor genes. As we will see in the next sections, this mechanism produces a cell type that is capable of responding to RA thorough upregulation of RA signaling.

#### **5.3.2. Identification of the MyD88 Inhibition Facilitated RA Differentiation Mechanism: Comparison of MyD88PepInh Treated and SSEA4<sup>Neg</sup> Cells**

##### **5.3.2.1. Loss of MyD88 in the Presence of RA Facilitates Differentiation of 2102Ep cells via Upregulation of RA Signaling**

Once MyD88 has been inhibited, RA-treatment stimulates one population of 2102Ep cells to differentiate (Chapter 4). In this section, the genes and pathways involved in RA-induced differentiation were assessed. According to our model, these genes are altered by SR<sup>PR</sup> state cells to facilitate differentiation. For this analysis, a MyD88 PepInh vs SSEA4<sup>Neg</sup> comparison was undertaken. This comparison identified molecular events that follow MyD88 inhibition to permit differentiation upon RA

treatment. The full list of samples available for comparison is shown in Figure 5.5. Whole-genome analysis passed all quality control checks and demonstrated clear separation of MyD88 PepInh treated, SSEA4<sup>Pos</sup> and SSEA4<sup>Neg</sup> samples (Figure 5.7). As expected, SSEA4<sup>Neg</sup> (differentiated) cells were shown to be the most diverse sample by hierarchical clustering (Figure 5.5). Notably, SSEA4<sup>Pos</sup> cells did not show more similarity to Ctrl PepInh treated cells than MyD88 PepInh treated cells. This suggests that SSEA4<sup>Pos</sup> cells are not the same population as the parent 2102Ep cells, as discussed in detail later.

Differentiation of SR<sup>PR</sup> state cells involved high fold change alterations in a large number of genes (Table 5.4, Appendix 2, Table S3). This large gene list, which includes non-coding RNAs and unknown genes, reflects a considerable difference between the cell types. SSEA4<sup>Neg</sup> cells showed characteristic downregulation of Nanog, Sox2 (both -7.2 fold) and Oct4 (-1.8 fold), confirming their differentiation (Table 5.5).

Molecular relationships involved in the response of MyD88 inhibited cells to RA were identified using DAVID analysis (Table S4). This revealed upregulation of TLR, Jak-Stat and MAPK signaling as well as genes associated with membrane remodelling and transcription factor binding. In parallel, genes associated with chromosome remodelling and the cell cycle, with specific emphasis on spindle and centriole associated genes, were downregulated in SSEA4<sup>Neg</sup> cells. Notably, 'Pathways in Cancer' was highlighted as a substantial component of both up- and downregulated gene lists. Together, this indicates that SSEA4<sup>Neg</sup> cells are displaying gene events associated with exit from the cell cycle and morphological changes associated with differentiation. These are typical differentiation-associated changes that would be expected for SSEA4<sup>Neg</sup> cells.

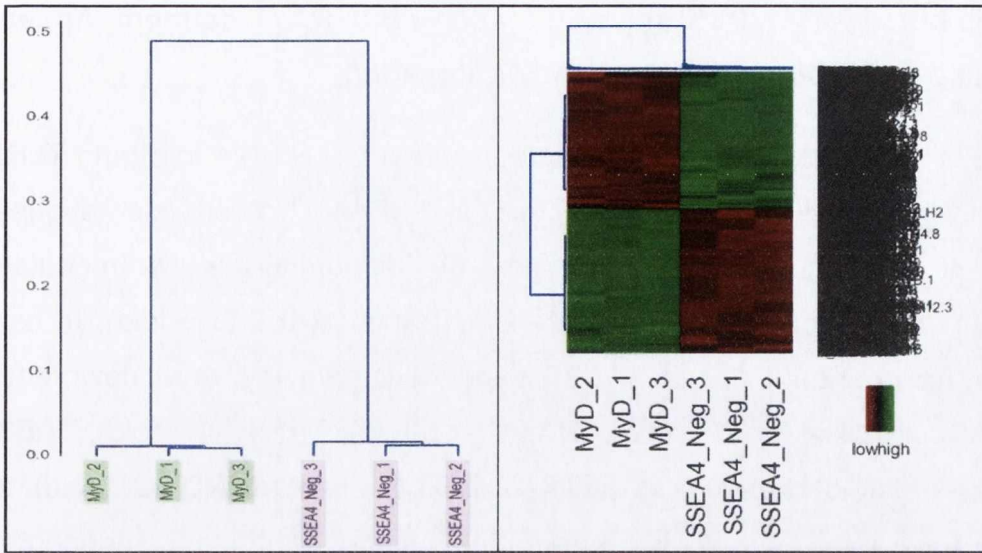


**Figure 5.7. Gene Expression Array Analysis of MyD88PepInh and SSEA4<sup>Neg</sup> Samples.** In this experiment, 2102Ep cells were treated with MyD88PepInh (MyD) for 12 days. Subsequently, undifferentiated SSEA4<sup>Pos</sup> and differentiated SSEA4<sup>Neg</sup> samples were separated by FACS. RNA was isolated from these samples and gene expression arrays performed. The image shows data from three individual biological replicates for each treatment. The data show strong separation of the samples into their treatment groups by hierarchical clustering (left panel) and similar levels of upregulated and downregulated genes by heat map (right panel).

**Table 5.4. Comparison of SSEA4<sup>Neg</sup> Samples to MyD88 PepInh treated samples**

Treatment/Sample	Gene Number	Max Fold Change
SSEA4Neg Upreg	1794	+66
SSEA4Neg Downreg	1697	-330

**Table 5.5. Downregulation of Oct4, Sox2 and Nanog in SSEA4<sup>Neg</sup> cells**

Description	Gene Name	Fold Change	p-Value
POU class 5 homeobox 1	OCT4 (POU5F1)	-1.8	0.01
SRY (sex determining region Y)-box 2	SOX2	- 7.2	2.89E-06
Nanog homeobox	NANOG	- 7.2	1.89E-05

### 5.3.2.2. Inhibition of MyD88 in Combination with RA Treatment Appears to Further Activate MyD88-Independent TLR Signaling

Screening for TLR signaling identified upregulation of TLR7 (24 fold) and TLR3 (3.2 fold) and downregulation of TLR4 (-2.5 fold) in SSEA4<sup>Neg</sup> cells, which suggests an active MyD88-independent pathway (Table 5.6). Supporting this, two modulators of this pathway are also altered, TRAF4 (1.4 fold) and TRAF6 (1.3 fold). In contrast, several key components of the MyD88 dependent pathway were downregulated: TRAF5 (-3.5 fold), IRAK4 (-1.8 fold), IRAK1 (-1.5 fold), TAB1 (-1.4 fold), TAB3 (-2.6 fold), FOS (-13.7 fold), FOSB (-21.2 fold), JUNB (-5.4 fold), JUND (-2.7 fold), JUN (-1.8 fold). However, it should be noted that several of these components (e.g. FOS/JUN) can be activated by alternative cascades. TLR3 and TLR7 are primarily known for detection of viral nucleotides. However, in recent years, the role of TLR3 and TLR7 in human pluripotent cells has become a topical 'mystery' (Pare and Sullivan 2014). For example, it has been demonstrated that self-renewing pluripotent cells have a diminished response to viral nucleotides, which is enhanced in differentiated cells (Hong and Carmichael 2013, Pare and Sullivan 2014). As yet, the mechanism behind this observation is not understood.

**Table 5.6. TLR genes altered in SSEA4<sup>Neg</sup> cells versus MyD88PepInh treated cells**

SSEA4 <sup>Neg</sup> cells vs MyD88			
Description	Gene Name	Fold Change	p-Value
Tol-like Receptor 7	TLR7	24	6.2E-07
Tol-like Receptor 3	TLR3	3.2	1.57E-05
Tol-like Receptor 4	TLR4	-2.5	0.00055

### 5.3.2.3. MyD88 Inhibition Permits 2102Ep Activation of RA Signaling in Response to RA

Nullipotent 2102Ep cells do not differentiate in response to RA treatment, which is associated with a failure to upregulate RA signaling. In comparison, NTera2 cells terminally differentiate in response to RA signaling, which involves upregulation of all levels of RA signaling from cellular reception by STRA6, through cytoplasmic reception by CRABPs and finally nuclear reception by RARs and RXRs (Section 1.6). Following loss of MyD88, RA treatment was found to upregulate all of these parts of RA signaling in SSEA4<sup>Neg</sup> cells (Table 5.7). Retinoic Acid Receptors (RARs)  $\alpha$  (2.2 fold),  $\beta$  (8.8 fold) and  $\gamma$  (1.4 fold) and RXR $\alpha$  (1.4 fold) as well as STRA6 (2.3 fold) and CRABP2 (2.2 fold), were all upregulated in SSEA4<sup>Neg</sup> cells, which indicates upregulation of RA Signaling in these differentiated cells. As such, the role of MyD88 in 2102Ep cells is to maintain nullipotency by suppressing activation of RA signaling in response to RA treatment.

**Table 5.7. RA signaling genes altered in SSEA4<sup>Neg</sup> cells versus MyD88PepInh treated cells**

SSEA4 <sup>Neg</sup> cells vs MyD88			
Description	Gene Name	Fold Change	p-Value
Stimulated by retinoic acid 6	STRA6	2.3	0.00017
Cellular retinoic acid binding protein 2	CRABP2	2.2	0.00015
Cellular retinoic acid binding protein 1	CRABP1	-2.0	0.001
Retinoic acid receptor, alpha	RARA	2.2	0.00038
Retinoic acid receptor, beta	RARB	8.8	1.68-E06
Retinoic acid receptor responder (tazarotene induced)3	RARRES3	2.3	6.6E-06
Retinoic acid induced 14	RAI 14	2.6	3.6E-05
Bone morphogenetic protein/retinoic acid inducible neural-specific 1	BRINP1	-3.8	0.00022

### 5.3.2.4. Inhibition of MyD88 in Combination with RA Treatment Appears to Rescue Taste and Olfactory Receptor Gene Expression

In Section 5.3.5, it was noted that TRs and ORs were altered by MyD88 inhibition in these cells. It was, therefore, important to identify any further changes in TR and/or OR signaling once the MyD88 PepInh treated cells had been differentiated.

Interestingly, all of the T2R family member and OR genes downregulated in the MyD88PepInh vs CtrlPepInh comparison earlier were now upregulated in SSEA4<sup>Neg</sup> cells. A SSEA4<sup>Pos</sup> vs SSEA4<sup>Neg</sup> comparison indicated no difference in the expression of the T2Rs or ORs, which demonstrated that T2R levels have returned to those seen in the nullipotent cell (Table S5). This suggests a mechanism where loss of T2Rs and ORs is important for the SR<sup>PR</sup> state and their high expression required for the nullipotent and differentiated states. The potential roles of T2Rs and ORs in hEC cells are discussed in section 5.4.3.

### 5.3.2.5. Loss of MyD88 Facilitates Upregulation of HOX Genes During RA Treatment

In Section 5.3.6, it was shown that HOXA/D family member genes were upregulated in response to loss of MyD88. Following on from this, it was noted that SSEA4<sup>Neg</sup> cells upregulate the expression of a large number of HOX A, B and C family member genes (Table 5.8). As such, the nullipotency-maintenance role of MyD88 in 2102Ep appears to involve suppression of HOX gene expression activity in response to RA treatment.

**Table 5.8. HOX genes altered in SSEA4<sup>Neg</sup> cells versus MyD88PepInh treated cells**

SSEA4 <sup>Neg</sup> cells vs MyD88			
Description	Gene Name	Fold Change	p-Value
Homeobox A1	HOXA1	6.8	3.08E-06
Homeobox A2	HOXA2	3.7	2.77E-05
Homeobox A3	HOXA3	2.4	0.0015
Homeobox A5	HOXA5	3.4	1.77E-05
Homeobox B1	HOXB1	4.2	9.53E-06
Homeobox B3	HOXB3	7.2	2.71E-06
Homeobox B4	HOXB4	4.9	2.93E-05
Homeobox B5	HOXB5	3.3	3.04E-05
Homeobox C8	HOXC8	2.4	0.0023
Homeobox C13	HOXC13	2.9	0.00015
Homeobox D13	HOXD13	-4.2	1.2E-05

### 5.3.2.6. Summary of SSEA4<sup>Neg</sup> Differentiation Data

In summary, our data indicates that, following MyD88 inhibition, 2102Ep cells can respond to RA treatment with an upregulation of RA signaling. Associated with this is a differentiation phenotype, which involves loss of Oct4-Sox2-Nanog expression, cell cycle exit, changes in genes associated with morphological alterations and



upregulation of HOX genes as well as MyD88-independent TLR, Jak-Stat and MAPK signaling. This characterisation can be combined with MyD88 PepInh-specific data to build a picture of the differentiation mechanism we have elucidated. This is discussed in detail in the Discussion (Section 5.4).

### **5.3.3. MicroRNA Array Analysis Identifies Several Cancer and Stem Cell/Differentiation miRs Associated with MyD88 Inhibition**

MicroRNAs have been shown to be important regulators of stem cells, cancer and CSCs. To complement the gene array analysis described above, MyD88 and Ctrl PepInh treated cell samples were assessed for their expression of a large panel of miRNAs using a miRNA array. The aim of this study was to identify the population of miRNAs (and other non-coding RNAs) regulated by MyD88. MicroRNAs downregulated in MyD88Pepinh treated samples are likely to be involved in maintenance of the nullipotent and/or pluripotent state. In contrast, miRNAs upregulated in MyD88Pepinh treated samples are likely to be involved in priming hEC cells for lineage differentiation. Characterisation of the miRNAs involved in this mechanism provides an important resource for future projects that will assess their functional role in nullipotency and/or pluripotency and as potential clinical biomarkers.

As with the gene arrays, miRNA array data passed all quality control tests and showed good hierarchical clustering (Figure 5.8). Using cut-offs of  $\pm 2$  (fold change) and 0.05 (p-value), 24 miRNAs were upregulated to a maximum of 5.1 fold and 59 downregulated to a maximum of -14.23 fold in MyD88PepInh treated cells (Table S6). The top ten up and downregulated miRNAs are shown in Table 5.9 and 5.10 respectively. It was noted that several of the top ten miRNAs has very high numbers (miR-1246\*, miR-4521\* etc), which reflects their relatively recent discovery. These newly discovered miRNAs are thus unlikely to have known functions or targets.

On the advice of our bio-informatician, validated and predicted targets were identified using the 'miRWalk' and 'TargetScan' resources. Of the numerous target prediction resources available, TargetScan was chosen as it allows predicted targets to be ranked based on the likelihood of being true targets. Validated targets were identified for several of the top miRNAs. Of note were regulators of cell cycle genes (miR-519c-3p\*, miR-654-3p\*) and miR-3687\*, which is known to regulate Retinoic Acid

Induced 1 (RAI1). Predicted targets did not reveal strong potential for binding key genes identified above such as MyD88, HOX, Oct4-Sox2-Nanog or any components of TLR, T2R, OR or RA signaling pathways. This suggests an indirect mechanism involving intermediates. Finally, literature searches were undertaken to identify any known functions for these miRNAs. These are listed in Tables 5.9 and 5.10 along with the PubMed Identification (PMID) number of the appropriate reference. Several miRNAs were found to be commonly expressed in many different malignancies (references too numerous to display). Several miRNAs were found to regulate neural differentiation, which suggests a potential role in RA-induced differentiation. The most notable miRNA on the list is the highly-studied miR-27a\*\*. miR-27 family members have a long-established role in many different cancers and are known to regulate inflammation/immunity and to suppress RARs, RXRs and Oct4. As such, miR-27a\*\* is a potential key component of the MyD88 mechanism we have uncovered.

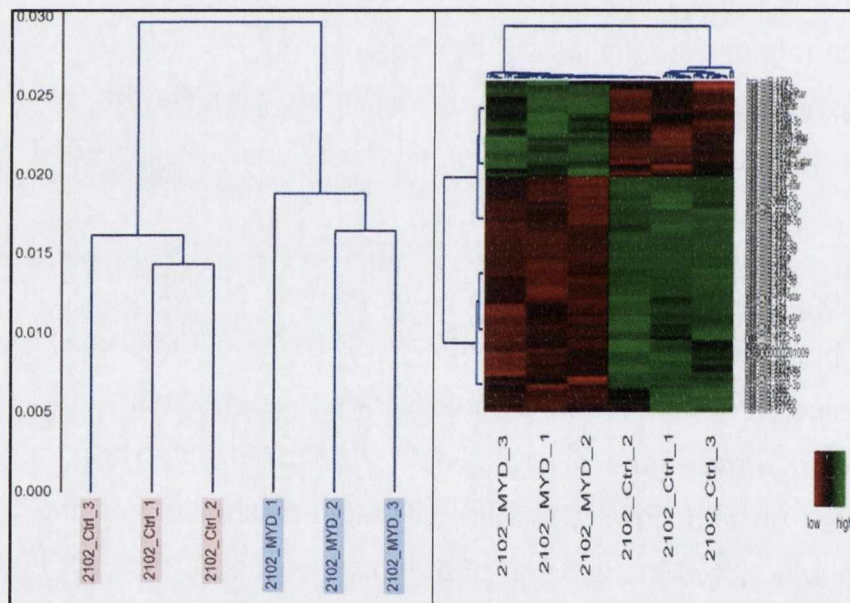


**Figure 5.8. MicroRNA Expression Array Analysis of MyD88PepInh and CtrlPepInh Samples.** In this experiment, 2102Ep cells were treated with either MyD88PepInh (MyD) or CtrlPepInh (Ctrl) for 12 days, RNA isolated and microRNA expression arrays performed. The image shows data from three individual biological replicates for each treatment. The data show strong separation of the samples in to their treatment groups by hierarchical clustering (left panel) and a bias towards downregulated microRNAs by heat map (right panel).

**Table 5.9. Top miRNAs upregulated in MyD88 PepInh treated cells**

Name	Fold Change	Validated Targets*	Predicted Targets**	Function	Ref (PMID)
miR-1246*	5.1	CFTR	FAM53C, CREBL2, ANTXR2	Chemoresistance in Pancreatic CSCs. Expressed in several cancers	25117811
miR-4521*	3.8	None	GABARA PL2, VPS13C, CLIC2	Neural differentiation. Expressed in Colon CSCs	26049006 23007737
miR-335*	3.7	None	FLT1, LMX1A, PGM3	Inhibition of pluripotent genes. Metastasis	26206603 26236665
miR-181a-2**	3.5	None	ZNF781, ZNF439, ZNF594	Known TLR regulator. Promotes cell cycle in leukaemia	23516523 26113450
miR-1269b*	3.2	None	MINA, MXRA7, FOXO1	TGF- $\beta$ and metastasis	25872451
miR-3128*	2.8	None	EGLN1, SLC5A3, OSTF1	Unknown	
miR-1290*	2.7	KIF13B MYC	EHHADH, SYNPO2, OSBPL6	Neural differentiation. Expressed in lung CSCs	26049006 25783528
miR-27a**	2.5	None	GXYLT1, PLK2, AKIRIN1**	Regulates inflammation. Suppresses RAR and RXR. Silences Oct4	24835395 25915942 25519956
miR-519c-3p*	2.5	ABCB1, ABCG2, AKT1, ATP8A2, CDKN1A, ELAVL1, HGF, HIF1A, PTEN, SF4, TIMP2	Not in 'Target Scan'	p21 regulator	22547681
miR-527*	2.5	cJun	CCR6, JRKL, AKAP11	Expressed in colorectal cancer. Regulates cJun	25687380 22797068

\*= Validation database miRwalk

\*\*= Ranked prediction from Targetscan database

**Table 5.10. Top miRNAs downregulated in MyD88 PepInh treated cells**

Name	Fold Change	Validated Targets*	Predicted Targets**	Function	PMID
miR-4730*	-14.23	None	C9ORF27 Ythdc1 Sec14l2	Unknown	
miR-431*	-10.21	None	ATB2B1 ZNF280C CAMTA1	Promotes TGF- $\beta$ -driven differentiation' mES primed state	26215566 22201644
miR-3647-5p*	-9.97	None	C18orf26 SLC25A2 6 C10orf118	Unknown	
miR-4793-3p*	-8.83	None	AFF3 RNF169 COPS2	Unknown	
miR-654-3p*	-7.03	CDKN1A, DICER1, PAK3, PBRM1	KLF12 RARP11 SORBS1	Expressed in lung Cancer. Expressed in prostate Cancer	25702651 24166498
miR-493*	-6.25	None	MRVI1 WDR33 NCKAP1L	Common cancer biomarker	Several
miR-543*	-6.0	SYNE1	PDE5A ANO5 PER3	Neural differentiation. mES primed state	26049006 22201644
14qll-14*	-5.94	None	Not in 'Target Scan'	Neural development	24945811 19656775
miR-3687*	-5.91	KIAA035 PPARGC 1B, RAI1	MTA2 NCS1 RBMS1	Expressed in several cancers	
miR-411*	-5.67	None	ELFN1 SLC4A7 C16orf52	Glioblastoma. Expressed in several cancers	21912681

\*= Validation database miRwalk

\*\*= Ranked prediction from Targetscan database

### **5.3.4. SR<sup>PR</sup> Differentiation is similar, but not identical, to RA-Induced NTera2 Differentiation**

A direct gene array comparison between SR<sup>PR</sup> differentiation and NTera2 RA-induced differentiation was beyond the scope of this study. However, gene array data for 3 day RA-differentiated NTera2 cells was available in the group and was used to compare these two differentiation mechanisms (Table S7). The principle difference between these comparisons is the level of MyD88 downregulation. In NTera2 cells, MyD88 is substantially downregulated but is still detectably expressed (d'Adhemar et al 2014). As we discussed in Chapter 3, low levels of MyD88 have considerable effects on differentiation in hEC cells. In contrast, in SR<sup>PR</sup> state cells, MyD88 is inhibited to a much greater extent. Despite these differences, a similar activation of RA signaling was observed in NTera2 RA-differentiated cells: RAR $\alpha$  (4.0 fold), RAR $\beta$  (4.7 fold), CRABP2 (11.1 fold) and STRA6 (3.7 fold). Additionally, there was upregulation of a large number of HOX genes and no change in T2R or OR gene expression in RA NTera2 cells, which mirrors RA treated SR<sup>PR</sup> state cells. DAVID analysis suggested a similar pattern of differentiation, with specific emphasis on alteration of cellular remodelling genes. In contrast, no significant changes in TLR signaling were observed in RA-differentiated NTera2 cells, which may reflect the different differentiation time-points between the studies. Within the limitation of this comparison, this data indicates that the SR<sup>PR</sup> model we have identified in 2102Ep cells is similar to standard RA-induced differentiation in NTera2 cells, but contains key differences.

### **5.3.5. Identification of Putative SR<sup>PR</sup> Markers**

In Chapter 4, we interpreted our data to suggest the presence of a SR<sup>PR</sup> cell, which is characterised by loss of MyD88, self-renewal characteristics and the ability to differentiate in response to RA treatment. To test this hypothesis, it would be important to isolate SR<sup>PR</sup> state cells from the mixed population that results from MyD88 inhibition. While this was not possible within the scope of this project, it was possible to identify potential SR<sup>PR</sup> markers for future work. In this section, genelists from gene expression array experiments were screened for potential markers of SR<sup>PR</sup> state cells. Specifically, proteins expressed on the cell surface (e.g. receptors)

were identified, as they could be exploited to isolate SR<sup>PR</sup> state cells via flow cytometry.

Two assumptions were the basis for this analysis. First, SR<sup>PR</sup> markers should be upregulated in MyD88PepInh vs CtrlPepInh cells and, second, SR<sup>PR</sup> markers should be lost following RA-treatment. We therefore identified a list of cell surface expressed markers that were upregulated in the MyD88PepInh vs CtrlPepInh comparison and also downregulated in the SSEA4<sup>neg</sup> vs MyD88PepInh comparison.

Eight cell surface expressed proteins showed upregulation at the gene level in MyD88PepInh vs CtrlPepInh comparison (Appendix 1). Of these, only 1 (Basp1) was eliminated from our analysis as it was not downregulated in the SSEA4<sup>neg</sup> vs MyD88PepInh comparison. The 7 remaining putative SR<sup>PR</sup> markers are shown in Table 5.11.

**Table 5.11. Identification of putative SR<sup>PR</sup> Markers (upregulated in SR<sup>PR</sup> cells)**

Description	Gene	MyD88PepInh vs Ctrl PepInh		MyD88PepInh vs SSEA4 <sup>Neg</sup>	
		Fold Change	p-Value	Fold Change	p-Value
Olfactory Receptor, Family 3, Sub-family A, Member 1	Or3a1	2.64	0.0022	3.85	0.00003
Cadherin 2	Cdh2	2.44	0.0028	3.73	0.00001
CD97 Molecule	CD97	2.38	0.0065	2.12	0.0003
Protocadherin Beta 11	PCDHB11	2.27	0.005	2.12	0.0018
Aldehyde Dehydrogenase Family 1, Member L2	Aldh1l2	2.2	0.0028	6.12	0.00005
Endothelin Receptor Type A	EDNRA	2.11	0.015	2.05	0.0056
PRAME Family member 20	PRAMEF20	2.06	0.0032	2.3	0.0002

An additional 19 cell surface expressed proteins showed downregulation at the gene level in MyD88PepInh vs CtrlPepInh comparison (Appendix 1). Of these, 5 potential markers (UPK1A, RYR3, EPHA3, TMEM45A and NPY1R) were eliminated as they were not upregulated in the SSEA4<sup>neg</sup> vs MyD88 PepInh comparison and one (BASP1) eliminated as its expression pattern was not significantly downregulated in MyD88vs SSEA4<sup>Neg</sup>. The 13 remaining putative SR<sup>PR</sup> markers are shown in the

(Table 5.12). Although isolation of SR<sup>PR</sup> cells was beyond the scope of this project, these 20 putative markers are now available for the group to carry out this work in future.

**Table 5.12. Identification of putative SR<sup>PR</sup> Markers (downregulated in SR<sup>PR</sup> cells)**

Description	Gene Name	MyD88PepInh vs Ctrl PepInh		MyD88PepInh vs SSEA4 <sup>Neg</sup>	
		Fold Change	p-Value	Fold Change	p-Value
Olfactory receptor, family 56, subfamily A, member 1	OR56A1	-3.3	0.01	-2.23	0.003
Taste receptor, type 2, member 50	TAS2R50	-2.8	0.02	-2.34	0.01
Taste receptor, type 2, member 46	TAS2R46	-2.8	0.01	-2.18	0.009
Taste receptor, type 2, member 13	TAS2R13	-2.8	0.003	-2.75	0.001
Taste receptor, type 2, member 43	TAS2R43	-2.8	0.01	-2.78	0.001
Taste receptor, type 2, member 31	TAS2R31	-2.7	0.0039	-1.72	0.008
Olfactory receptor, family 56, subfamily A, member 4	OR56A4	-2.6	0.008	-2.31	0.003
Taste receptor, type 2, member 14	TAS2R14	-2.3	0.002	-2.24	0.0004
Olfactory receptor, family 5, subfamily P, member 2	OR5P2	-2.22	0.04	-2.20	0.01
Protocadherin 11 X-linked	PCDH11X	-2.22	0.01	-1.80	0.01
CD163 molecule-like 1	CD163L1	-2.13	0.04	-2.04	0.01
Olfactory receptor, family 7, subfamily A, member 5	OR7A5	-2.05	0.01	-1.54	0.004
Taste receptor, type 2, member 20	TAS2R20	-2	0.13	-2.09	0.05

## **5.4 Discussion**

In the previous chapters MyD88 was identified as a critical factor in 2102Ep nullipotency. Inhibition of MyD88 permitted some 2102Ep cells to differentiate in response to RA. This demonstrated that A) 2102Ep nullipotency is determined by maintained high expression of MyD88 before and during RA-treatment, and B) MyD88-independent TLR Signaling is necessary for differentiation. In this chapter, gene array analysis was employed to characterise the mechanisms controlled by MyD88 in 2102Ep cells. Gene array analysis was divided in to two categories. First, the mechanisms controlled by MyD88 were characterised by comparing samples treated with MyD88 PepInh to samples treated with Ctrl PepInh. Second, the mechanisms controlled by RA treatment were characterised by comparison of MyD88Pepinh treated cells with to several controls. These data, which were described in the results section, present a three-stage mechanism: nullipotent, MyD88 inhibited SR<sup>PR</sup>, and SSEA4<sup>Neg</sup> differentiated cells.

According to our data, 2102Ep nullipotency is characterised by MyD88-dependent TLR Signaling, high expression of T2Rs and ORs, Oct4-Sox2-Nanog, SSEA4 as well as low expression of HOXA genes and low activity of RA Signaling. MyD88-inhibited 2102Ep (SR<sup>PR</sup>) cells are characterised by MyD88-independent TLR signaling, high expression of HOXA/D genes, Oct4-Sox2-Nanog, SSEA4 and low expression of T2R and OR genes. Finally, 2102Ep cells differentiated by MyD88 inhibition and RA treatment are characterised by TLR3/TLR7-driven MyD88-independent TLR signaling, high expression of HOXA and B, T2R and OR genes, high RA signaling activity as well as low levels of SSEA4 and Oct4-Sox2-Nanog. Together, this analysis suggests a mechanism where constitutive expression of MyD88 in 2102Ep cells maintains high expression of T2Rs and ORs while inhibiting HOXA/D genes, which prevents these cells from differentiating in response to RA. To emphasise the importance of this data, apart from the well-known role of HOX genes, none of the other molecular events identified have been previously modelled as components of the differentiation of nullipotent/pluripotent cells.



#### 5.4.1 MyD88 Promotes Nullipotency by Preventing the 2102Ep Response to RA

At the outset of this Chapter, the mechanism through which MyD88 maintained nullipotency was not understood. The data described above indicate that the primary function of MyD88 in nullipotency is to inhibit the response of these cells to RA. In the MyD88PepInh vs CtrlPepInh experiment, no changes in RA signaling genes were observed. As such, loss of MyD88 does not prime 2102Ep cells for RA-induced differentiation by increasing the expression of RA signaling genes. Additionally, CtrlPepInh+RA treated cells show no increase in RA signaling genes, which indicates that nullipotent cells do not activate RA signaling. However, cells treated with MyD88PepInh+RA (SSEA4<sup>Neg</sup> cells) show increases in expression at all levels of RA signaling. RA is received at the cell surface by the STRA6 receptor, which is upregulated in these cells. RA is then transported through the cytoplasm of the cell by CRABP2, which is also increased in these cells. RA is then received at the nucleus by RAR and RXR receptors, both of which are also increased in these cells.

Importantly, these cells are differentiated, which indicates that RA signaling is functional downstream of MyD88. For example, RA signaling in response to RA treatment leads to decreases in Oct4-Sox2-Nanog expression in SSEA4<sup>Neg</sup> cells, which is in concordance with the EC literature (Andrews 2002, Andrews et al 2005). As such, loss of MyD88, which induces MyD88-independent TLR signaling, is necessary for RA-induced differentiation of these cell. By extrapolation, we can conclude that the primary determinant of 2102Ep nullipotency is maintained high expression of MyD88, which blocks these cells' ability to respond to RA-treatment by initiating RA signaling driven differentiation. It is noted that this mechanism has not been previously described. Finally, it is important to note that some 2102Ep cells can remain nullipotent in spite of MyD88PepInh+RA treatment (SSEA4<sup>Pos</sup> cells). This indicates that the MyD88 mechanism reported here is not applicable to all 2102Ep cells, as will be discussed later (Chapter 6).

#### 5.4.2. MyD88 Promotes Nullipotency By Inhibiting HOXA/D Family Gene Expression

Once it was established that MyD88 promotes nullipotency by blocking activation of RA signaling, it was important to understand how this was achieved. When MyD88PepInh samples were interrogated it was expected that a stem cell process would be highlighted. For example, it was hypothesised that loss of MyD88 might activate Shh, TGF- $\beta$  or Notch signaling. Although none of these common stemness pathways were involved in this mechanism, HOXA/D genes were highlighted as being upregulated upon inhibition of MyD88. As described earlier (Section 5.1.2) HOX genes are well known regulators of stem cell differentiation and development. Specifically, HOX genes are involved in 'head to tail' patterning during embryonic development. In this role, they are key regulators that ensure that the correct differentiation process (tissue-generation for example) takes place in the correct location. In addition, HOX genes have an established relationship with RA and OR signaling (Section 5.1.2). As HOXA/D family gene expression was the only stemness process highlighted in our array analysis it is reasonable to suggest that these HOXA/D genes are the primary link between MyD88 and differentiation.

Although HOX genes occur in clusters (A-D), individual HOX gene expression is usually independent of genomic arrangement (Mallo and Alonso 2013). In effect, this means that some genes from HOX families A-D are generally expressed together rather than only HOXA or only HOXB etc. genes. As such, it is unusual that the MyD88 mechanism that has been described primarily involves only HOXA family members. The expression of HOX genes is primarily determined by histone modification/epigenetic status (Schuettengruber et al 2007, Mallo and Alonso 2013). For example, embryonic stem cells (ESCs) do not express HOX genes due to the presence of H3K27m3 and absence of H3K4m3 histone methylation marks, a situation that is reversed during early RA-induced embryonic development (Reviewed in Mallo and Alonso 2013, Ffrench et al 2015).

Histone modification by Polycomb group (PcG) proteins is catalysed by Enhancer of Zest Homologues 1 and 2 (EZH1 and EZH2). EZH1, which is downregulated in MyD88PepInh treated cells, is known to regulate genes (including Hoxa11) as an essential component of pluripotency maintenance and differentiation in ESCs (Shen

et al 2008). Thus, it is likely that the regulation of EZH1 by MyD88 is a key component of the activation of HOXA genes in 2102Ep cells. Together, this data suggests a model where 2102Ep nullipotency is maintained by MyD88-dependent expression of EZH1 and repression of HOXA/D family genes. As such, it is unsurprising that a set of stemness genes such as these are involved in the MyD88 mechanism. However, this is the first report of a relationship between MyD88 and HOX genes. Furthermore, the parallels with ESCs suggest that MyD88 may be a key regulator in ESC differentiation that has not been highlighted to date.

#### **5.4.3. Taste and Olfactory Receptors Are Novel Regulators of Nullipotency/Pluripotency**

In parallel to the inhibition of HOX genes, MyD88 was found to promote the expression of T2Rs and ORs. At first glance, the promotion of sense receptors as a mechanism through which differentiation is resisted is surprising. However, a thorough literature review revealed that TRs and ORs are now being shown to have non-sense roles in non-sense cells. A relationship between ORs and RA-induced differentiation is long established and TLR signaling has been linked more recently to both TRs and ORs (Section 5.1.3-5.1.4). However, this is the first report linking MyD88, TRs and ORs to exit from the pluripotent self-renewal state.

Mechanistically, the authors of studies linking TRs and ORs to TLR signaling have proposed models related to a function in inflammation. For example, one study proposed that the response of TRs to TLR4 ligand LPS was indicative of a role for TRs in the 'sensing' of bacteria (Feng et al 2012). This is an obvious and reasonable interpretation of the data. In contrast, our data indicates a non-sensory role for T2Rs and ORs. In our model, maintained expression of MyD88 results in maintained expression of T2Rs and ORs despite the absence of an obvious sense ligand (taste/smell/LPS). In parallel, our data does not indicate downstream activity of T2R or OR signaling in response to MyD88 inhibition. As such, our data suggest that this mechanism relates to receptor function rather than signal transduction.

There are two broad categories of ligand that these T2Rs and ORs are likely to be receiving in nullipotent cells. The first ligand is RA. If T2R and/or ORs can receive RA it is possible that they may compete with RA cellular receptor STRA6, which could block RA signaling in the cell. In this case, downregulation of T2Rs and ORs

following MyD88 inhibition may prime the cells for RA signaling in response to RA treatment. We note that both T2Rs and ORs ultimately return to high levels of expression in SSEA4<sup>Neg</sup> cells. This suggests that T2Rs and ORs play different roles at different stages of RA-induced differentiation. This is in line with temporal and geographical expression patterns shown by T2Rs and ORs in other systems (Section 5.1.3-5.1.4).

The second ligand that T2Rs and ORs may be receiving in the nullipotent state are those secreted by MyD88-dependent TLR signaling. The main function of TLR signaling is to determine the profile of pro-inflammatory signaling molecules (chemokines and cytokines) secreted by the cell (Section 1.8). In our model, nullipotent cells express MyD88-dependent TLR signaling while SR<sup>PR</sup> and SSEA4<sup>Neg</sup> (differentiated) cells express MyD88-independent TLR signaling. As such, nullipotent and differentiating 2102Ep cells produce different profiles of chemokines and cytokines. This may indicate that the function of T2Rs and ORs in the nullipotent state is to receive ligands (chemokines and cytokines) produced by MyD88-dependent TLR signaling to promote the nullipotent state, while loss of MyD88 may reverse this mechanism to facilitate differentiation. This hypothesis is supported by conditioned media experiments that were described in Chapter 4. In our model, a switch to MyD88-independent TLR signaling may result in a downregulation of these ligands to which the cell responds in turn by downregulating these receptors. This may be a normal function of these cells in RA-differentiation in NTera2 cells.

Regardless of whether one or either of these models proves to be correct, our study highlights a new role for T2Rs and ORs in the maintenance of nullipotency and RA-induced differentiation of pluripotent cells. T2Rs and ORs are maintained at high levels of expression by MyD88 in the nullipotent state and are substantially downregulated upon MyD88 inhibition as part of a differentiation mechanism. We note that this is the first description of any involvement for T2Rs in the Oct4-Sox2-Nanog controlled differentiation of nullipotent/pluripotent cells and as such will be of topical interest to many pluripotency researchers. Additionally, our data will be of highly topical interest to the many groups that are investigating the role of taste and olfactory receptor signaling in non-sensory cells.

#### 5.4.4 MyD88-Independent TLR Signaling Drives Differentiation of 2102Ep Cells

In the second piece of gene array analysis described in this chapter, we identified the molecular events that occur downstream of MyD88 inhibition, which facilitate differentiation. The data clearly indicate a standard differentiation mechanism where all aspects of RA signaling are activated to drive a differentiation transition that is driven by loss of Oct4-Sox2-Nanog expression. It was notable that stemness mechanisms such as Shh, TGF- $\beta$ , Notch and Snail signaling were not altered in our analysis. Instead, upregulation of the key differentiation regulator HOX genes appears to be the key driver of differentiation. Together, this data form a new model where MyD88-dependent TLR signaling is necessary for nullipotency and MyD88-independent TLR signaling is necessary for differentiation. This model is illustrated in Figure 5.9.

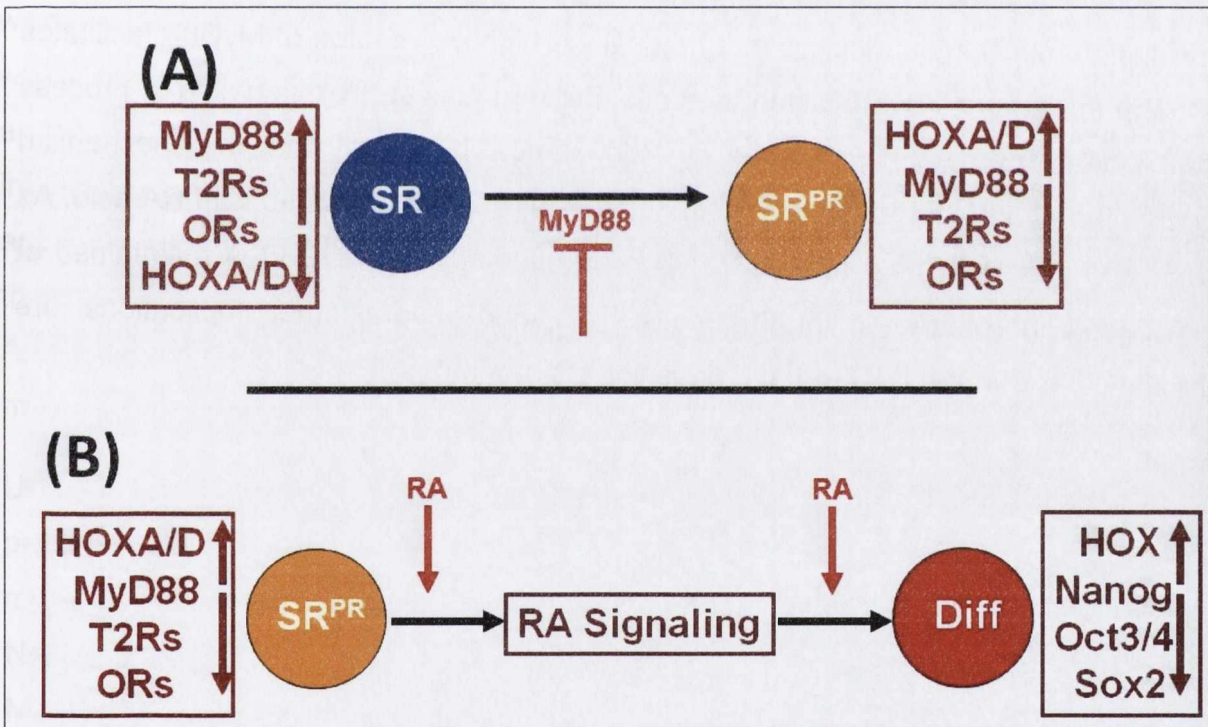


**Figure 5.9. Proposed Model of Differentiation Regulated by MyD88-Independent TLR Signaling.** According to our gene array data, the nullipotent self-renewal (SR) state is characterised by MyD88-dependent TLR signaling, high expression of Taste Receptor Family 2 (T2R) and Olfactory Receptor (OR) genes and low expression of HOXA/D family genes. Inhibition of MyD88 activates MyD88-independent TLR signaling to produce a Primed Undifferentiated State (PUS), which is associated with increase in HOXA/D expression and decreases in T2R and OR expression. This permits the cells to activate retinoic acid (RA) signaling in response to RA, which results in a differentiated phenotype that is characterised by low expression of Oct4-Sox2-Nanog and high expression of HOX genes.

## **5.5 Conclusion**

In the previous Chapter, we identified a differentiation mechanism in 2102Ep cells that is controlled by MyD88. Upon treatment with MyD88PepInh, two sub-populations of 2102Ep cells emerged. The first sub-population appears to retain nullipotency. The second sub-population can differentiate in response to the addition of RA to the cells. In this Chapter, we aimed to identify the mechanism, hypothesising that a pluripotent stemness process may be involved. Through gene array analysis, this process was highlighted as HOX gene regulation of differentiation. Upon loss of MyD88, HOXA/D family genes are upregulated, which is part of a larger process involving downregulation of so-called sense receptors (T2Rs and ORs). These changes are associated with the cells ability to then differentiate in response to RA signaling. Our data revealed that, upon addition of RA to the cells, RA signaling is activated at all levels and HOX genes are further recruited. In conclusion, our results indicate that maintained high expression of MyD88 facilitates 2102Ep nullipotency by inhibiting the cells ability to activate RA signaling, a process that appears to involve regulation by HOX genes. It is likely that this mechanism mirrors the events that spontaneously occur in NTera2 cells treated with RA acid. As such, the important next step is to try to understand how MyD88 is maintained at high levels in RA-treated 2102Ep cells. This, and several other implications, are discussed in Chapter 6 'General Discussion'.

## Chapter 6

### General Discussion

#### 6.1 Overview

Inducing Cancer Stem Cell (CSC) differentiation is a potential avenue for development of new anti-cancer treatments due to the fact that differentiated CSCs lose their ability to generate tumours (Ffrench et al 2014, 2015). In this study, the role of MyD88 in differentiation resistance was assessed in the nullipotent 2102Ep human embryonal carcinoma (hEC) CSC cell line, a role that had been tentatively suggested in earlier work. As the MyD88-induced differentiation mechanism had only been sporadically observed in previous work, this project initially aimed to develop a stable and consistent model in which the role of MyD88 in the mechanism could be studied. In Chapters 3 and 4, the establishment of such a model was described. This model involves inhibition of MyD88 protein function using a Peptide Inhibitor (PepInh) approach. Additional experiments demonstrated that loss of MyD88 opened these cells to induction of differentiation through retinoic acid (RA) treatment. Additionally, MyD88 inhibition facilitates mesoderm differentiation strongly and may play a role in endoderm and ectoderm differentiation (Chapter 4).

Unexpectedly, it was found that this cell line model contains two sub-populations, only one of which expresses the MyD88<sup>-</sup>RA<sup>+</sup> differentiation mechanism. This sub-population differentiates through a standard Oct4-Sox2-Nanog mechanism that has not been previously associated with MyD88. Mechanistically, this is due to regulation of Hox, Taste Receptor Family 2 (T2R) and Olfactory Receptor (OR) genes by MyD88. When MyD88 is expressed, Hox genes are inhibited and T2R and OR genes promoted, which results in a nullipotent/pluripotent state. Upon loss of MyD88, Hox genes are activated and T2R and OR genes inhibited, which permits the cells to activate RA signaling in response to RA treatment. In Chapter 4, it was demonstrated that this mechanism is most likely regulated by different factors secreted by

MyD88-Dependent and MyD88-Independent Toll-Like Receptor (TLR) signaling.

These data are previously undescribed and have implications for our understanding of stem cell/CSC biology, CSC differentiation-resistance, the use of Forced-Differentiation of CSCs as a potential clinical intervention and regenerative medicine research with pluripotent cells. These implications are now discussed in detail. In addition, it is important to note that these results have not been reported in any other model systems and as such a comprehensive comparison of this model to other models is, unfortunately, not possible. Instead, the implications of our model for the one comparative model, the naïve ground state model, and for our understanding of Oct4-Sox2-Nanog are discussed.

## **6.2 MyD88 is a Novel Upstream Regulator of Oct4-Sox2-Nanog**

One of the main problems with molecular biology is that it is very difficult to identify upstream regulators of mechanisms of interest. While it is possible to use functional analysis such as siRNA or PepInh treatments to identify downstream events regulated by Oct4, Sox2 and Nanog in pluripotency, it is not easy to identify those events that regulate the Oct4-Sox2-Nanog complex. As an example of the complexity involved, Bing Lim and colleagues identified some upstream regulators of Oct4-Sox2-Nanog by randomly targeting the entire genome using tens of thousands of siRNAs in multiplex (Chia et al 2010. PMID: 20953172). As such, our identification of MyD88 as a key upstream regulator is of particular importance to our understanding of the events regulating Oct4, Sox2 and Nanog.

It is noteworthy that MyD88 does not appear to have been suggested as a key player in pluripotency by any group, at any time to our knowledge. There are two obvious reasons for this. First, MyD88 does not appear to directly target Oct4-Sox2-Nanog, and as such it would not have been identified through 'pull-down' type assays that have identified other regulators of this complex. Secondly, this reflects the difficulty in identifying the early, subtle events involved in pluripotent differentiation. Pluripotent cells readily and rapidly



commence differentiation once they are removed from the *in vivo* niche. In fact, 20 years of research has largely focused upon identifying growth factors that can be added to cell culture media to mimic the *in vivo* niche, which could maintain pluripotent cells in the self-renewing state. While much progress has been made in this regard in mouse Embryonic Stem (mES) cells (Silva and Smith 2008), this has proved much more difficult in human ES (hES) and induced pluripotent stem (iPS) cells. Interestingly, the main known function of MyD88 is to regulate self-secretion of such factors in to the cells' microenvironment. It seems likely that our description of the role of MyD88 in maintaining the pluripotent self-renewal state will attract interest from hES and iPS cell researchers.

Our original discovery of MyD88 was neither fortunate nor accidental but strategic. At the start of the study ten years ago, a decision was made to carry out whole-genome analysis on early differentiation of hEC cells. This was based on the original hypothesis that early differentiation could identify upstream regulators of Oct4-Sox2-Nanog and that the earliest genes altered during differentiation were likely to be important regulators of self-renewal. This experiment was only possible because of the choice of hEC CSCs as a model system. From addition of RA, hEC cells differentiate in a uniform fashion, which permits molecular analysis at early time points. In contrast, hES cell cultures tend to differentiate in a more diverse fashion, which means that molecular analysis is generally carried out later (7 days), at which point hES cells have uniformly differentiated. During genelist analysis of this dataset, MyD88 was highlighted based on the alteration of a number of TLR genes on the array. Subsequent testing of MyD88 identified only tentative data, which could reasonably have been abandoned. However, the application of stem cells approaches described in this thesis has resulted in an important contribution to the research area. This includes an understanding that CSC cell lines can contain multiple different types of stem and progenitor cell and that these must be assessed using single cell analysis. Ultimately, the results described in this thesis justify several choices such as the cell line model and approach. It is clear that without these

strategic decisions, the role of MyD88 in pluripotency may have remained uncovered.

### **6.3 Differentiation from Pluripotent Cells is not a Single-Coupled Process**

It has previously been discussed that, historically, exit from the self-renewal state and lineage differentiation were considered to be a single, coupled process. In effect, this hypothesis envisaged that these two processes occurred together and dependently so that self-renewal state exit could not occur without direct differentiation. In Chapters 3 and 4, data and analysis were provided that identified MyD88 as a key player in the transition of pluripotent stem cells to a transition state between self-renewal and differentiation. This transition state has been labelled the 'Primed Self-Renewal' ( $SR^{PR}$ ) state by our group. This model is not dissimilar to the 'Ground State' model of mES differentiation but has not been described in human cells (Silva and Smith 2008).

When considering this mechanism, it is important to keep in mind that both the Ground State and  $SR^{PR}$  models are artificial states generated in cell culture. As caricatures, rather than direct representations, of the events that occur in the developing mouse embryo and human embryonal carcinoma, it is important to consider what actually occurs *in vivo*. Importantly, Austin Smith and colleagues have produced some *in vivo* data that supports the Ground State model's relevance to the mouse embryo (Smith 2010). When considering the process of differentiation from ES or EC cells, it seems likely that several key factors regulate maintenance of the self-renewal state. In an environment where different differentiation stimuli are present at different times, it is vital that ES cells maintain the self-renewal state and differentiate in the correct lineage and at the correct time in order to produce the functional embryo. This process appears to involve complete differentiation of ES cells as ES cells have not been identified either late in embryonic development or in the adult. In contrast, 2102Ep cells can resist differentiation throughout tumour development, to generate a highly-malignant, undifferentiated tumour. In the case of differentiating ES cells, which are the non-malignant equivalent

of NTera2 cells (Andrews 2002, Andrews et al 2005), it seems likely that the 'normal' response to some, if not all, differentiation stimuli is downregulation of MyD88. Downregulation of MyD88 appears to then activate a cascade that results in differentiation via a standard Oct4-Sox2-Nanog mechanism. It seems reasonable to extrapolate that the *in vivo* differentiation process involves several subtle steps, which together ensure that only the correct differentiation processes are activated at the appropriate time. In contrast, the maintained expression of MyD88 in 2102Ep cells may represent a type of mechanism through which CSCs have adapted to ensure that at least some CSCs resist differentiation to retain a self-renewing CSC population at all times. This has important clinical implications, as will be discussed later.

#### **6.4 A New Model of NTera2 Differentiation**

NTera2 cells, like all pluripotent cells described to date, readily respond to differentiation stimuli such as RA. As such, it is difficult to identify some of the earlier, more subtle molecular events involved in the exit from the SR state before lineage differentiation. The nullipotent property of 2102Ep cells allows us to further elucidate differentiation of pluripotent cells in response to RA. Our analysis indicates strong evidence that the MyD88 mechanism we have observed in 2102Ep cells is similar or perhaps identical to that which occurs spontaneously in RA-treated NTera2 cells. Together, our nullipotent (2102Ep) and pluripotent (NTera2) data suggests a new model for lineage differentiation. In this model, the pluripotent SR state is characterised by stable expression of Oct4-Sox2-Nanog, which we have demonstrated is at least in part due to high expression of MyD88. Upon addition of RA to pluripotent cells, MyD88 is downregulated, which results in downregulation of T2Rs and ORs as well as upregulation of HOXA/D genes. These changes allow the cells to activate RA signaling, which results in downregulation of Oct4-Sox2-Nanog, further upregulation of HOX A and B genes and the return of T2R and OR expression. This results in upregulation of stemness signaling pathways such as Shh, TGF- $\beta$ , Wnt, Notch and Snail, which drive lineage differentiation. Due to their similarity to hEC cells, it is interesting to speculate that similar mechanisms will be found in hES and/or iPS cells.

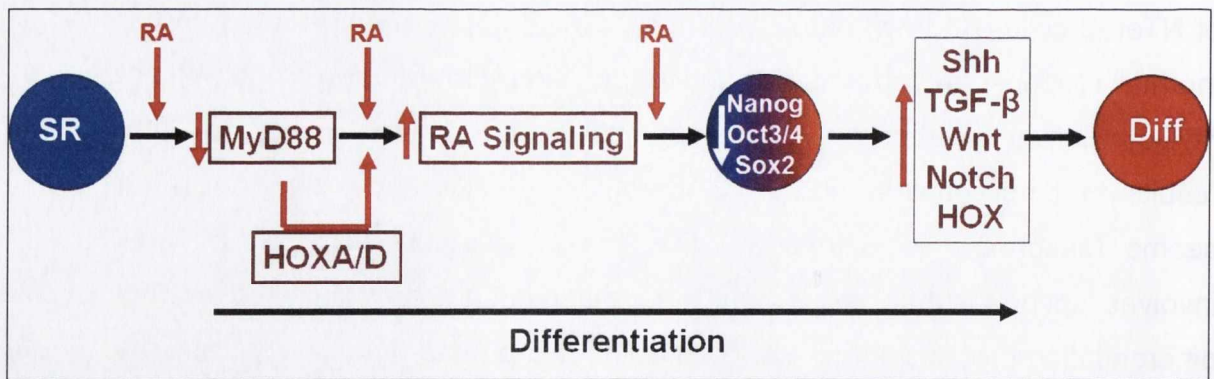


**Figure 6.1. A Unified Model of RA-Induced Differentiation of Ntera2 hEC Cells.** When our data from 2102Ep and Ntera2 hEC cells is combined, a unified model of RA-induced differentiation emerges. In this model, the pluripotent Ntera2 self-renewal (SR) state is dependent upon MyD88-dependent TLR signaling. Upon stimulation with retinoic acid (RA), Ntera2 cells spontaneously downregulate MyD88, which leads to an increase in HOXA/D genes and a decrease in taste (T2R) and olfactory (OR) receptor genes. These molecular events facilitate an increase in RA signaling, which results in differentiation of Ntera2 cells through the standard Oct4-Sox2-Nanog downregulation mechanism. Further work from our group has demonstrated that this mechanism involves increased in Sonic Hedgehog (Shh), TGF- $\beta$ , Wnt and Notch Signaling. This is the first report of such a role for TLR signaling in pluripotency.

## 6.5. Are the 2102Ep Sub-Populations a Stem-Progenitor Cell Hierarchy?

The concept of hierarchical organization of stem cells was described in detail in Chapter 1. To briefly review, it is now becoming clear that most, if not all, stem cell populations are organized as Stem-Progenitor-Differentiated cell hierarchies. In this model, a highly potent stem cell produces an array of differentiated cells through the production of intermediary progenitor cells (Ffrench et al 2015, 2014). These progenitors are themselves stem cells, but are less potent than the stem cell at the top of the hierarchy. The result described in Chapters 3 and 4 indicate that the 2102Ep cell line consists of two sub-populations with very different stem cell potencies. These results can be interpreted as evidence of a 2102Ep Stem-Progenitor cell hierarchy. If this is true, the SR<sup>PR</sup> sub-population identified may in fact represent a progenitor population produced by parent 2102Ep cells *en route* to the production of differentiated cells (Figure 6.2). If this model holds true, MyD88 is again the differentiation gatekeeper, a role for MyD88 that has not been previously described or hypothesized. Additionally, some data has been generated that

indicates that the SR<sup>PR</sup> state is reversible through restoration of MyD88 (Figure 6.2). In future, further characterization of this mechanism should facilitate a better understanding of the precise nature of the novel 2102Ep sub-population.

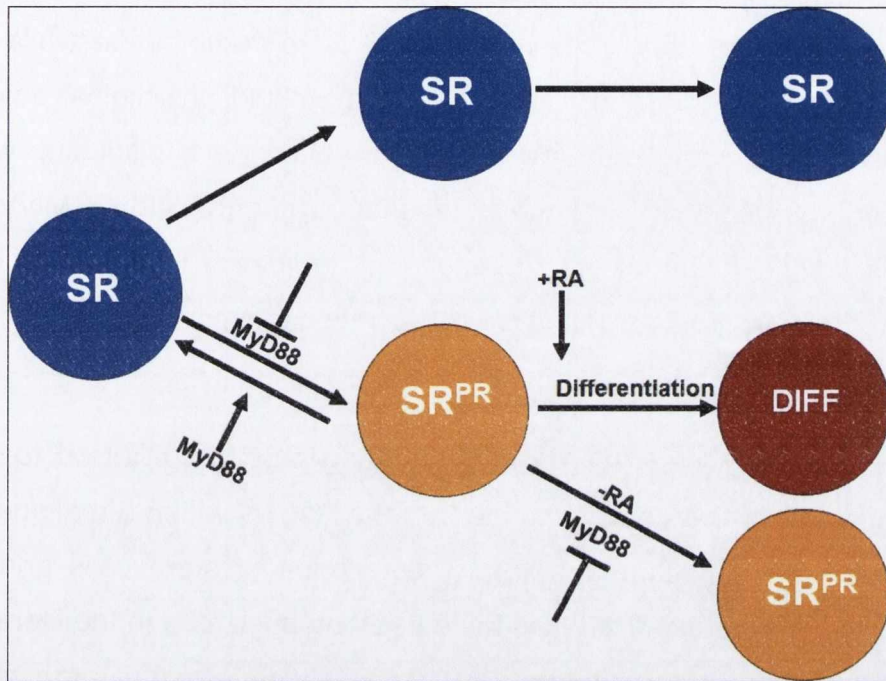


**Figure 6.2 The Primed Self-Renewal State Stem Cell Hierarchy Model.** In recent years stem cells have been shown to be organized as Stem-Progenitor-Differentiated cell hierarchies. Our data can be interpreted to fit a hierarchical model as illustrated. In this model, parent 2102Ep cells can produce Primed Self-Renewal State progenitor cells, which can differentiate in response to retinoic acid treatment. In parallel, 2102Ep cells self-renew to maintain an undifferentiated stem cell pool.

## 6.6 Differentiation Gate-Keepers May Facilitate Differentiation-Resistance in CSCs

Despite being obvious clinical targets in malignancy, achieving clinical targeting of CSCs had proved challenging. To date, clinical attempts to target CSCs can be broadly divided into two categories. The first approach is targeting specific mechanisms that have are expressed by specific CSCs identified in specific malignancies. This has been extensively reviewed in our group’s recent review paper and book chapter (Ffrench et al 2014, 2015). A strong example of this is targeting of Notch Signaling in ovarian and pancreatic cancers (McAuliffe et al 2012, Yabuuchi et al 2013). Notch signaling is dependent upon the gamma-secretase enzyme, which can be targeted using gamma secretase inhibitors (GSIs) to block Notch signaling (McAuliffe et al 2012, Yabuuchi et al 2013). Surprisingly, GSIs high levels of

efficiency are not due to targeting the CSC *per se*. Instead, GSIs dramatically increase the response of these malignancies to chemotherapy drugs gemcitabine (pancreas) and cisplatin (ovary), to which these malignancies are otherwise refractory (McAuliffe et al 2012, Yabuuchi et al 2013, Ffrench et al 2014, 2015). Even more surprisingly, these approaches only effective in combination while treatment with GSIs or chemotherapy had little effect. In a striking pre-clinical animal study, ovarian cancer was completely eliminated by GSIs and cisplatin, which was elegantly demonstrated using magnetic resonance imaging (MRI, McAuliffe et al 2012). This is a typical example of an increasing number of studies, which have led to the broad opinion that targeting of CSC mechanisms can be used to treat refractory disease.

The second broad approach to clinically targeting CSCs is referred to as 'Global Targeting'. The aim of this approach is to target all CSCs within a malignancy with a single drug. In light of the contemporary description of stem cells and CSCs as hierarchies, global targeting strategies have been pursued less in the literature. Such approaches require a strong understanding of the CSCs to be targeted, which is simply highly difficult when multiple stem and progenitor cells are present. Historically, one of the original global targeting approaches was RA-treatment, which it was believed would force-differentiate CSCs to reduce or eliminate tumourigenic potential. Several pre-clinical studies demonstrated that RA-treatment was a highly efficient anti-cancer treatment. However, this efficiency did not translate in to the clinic (Ffrench et al 2014, 2015). Instead, RA-treatment was only effective in specific patients with specific malignancies (Castaigne et al 1990, Foster et al 2009, Ffrench et al 2014, 2015). This has led to RA-treatment being abandoned in all but a select type of cancer patient.

The MyD88 mechanism that has been described is an obvious potential explanation for the failure of RA-treatment in some patients. In light of the data presented in this thesis, it is reasonable to hypothesise that some CSCs within a malignancy can maintain high expression of a specific 'Differentiation Gate-Keeper', even in the presence of a force-differentiation treatment such as RA. In the model presented here, the Gate-Keeper has been identified as MyD88. However, it is likely that different proteins act as differentiation gate-keepers in each malignancy. If this is true, it should be possible to identify malignancy-specific differentiation gate-keepers

by employing a similar approach to that employed in this thesis. Once identified, the implication of our model is that a two-target approach is likely to be more successful than RA-treatment alone. The proposition is that pre-treatment with a differentiation gate-keeper inhibitor should increase the number of CSCs that can be globally targeted. A caveat to this is that, in the model presented here, a sub-population of CSCs can retain differentiation-resistance even in the presence of MyD88 PepInh. As such, it is likely that the dual-targeting approach suggested would not eliminate all CSCs. However, the elimination of a substantial number of CSCs is likely to substantially improve patient outcome. The development of these concepts in this and other models within our group is a strong legacy of this project with important potential clinical implications.

## **6.7 The Potential Importance of MyD88 to Regenerative Medicine**

To conclude, it seems appropriate to discuss the potential relevance of this project to regenerative medicine. Although it was not the main aim of the project to address this research area, the results produced have important potential relevance to the area of regenerative medicine. Since the first isolation of mES cells in the early 1980s, regenerative medicine has been attempting to capture their potential (Evans and Kaufman 1981, Thompson 1999, Evns 2011). The aim of these efforts is to use pluripotent ES or induced Pluripotent Stem (iPS) cells to A) repair injured tissues and B) generate *de novo* tissues and organs for patients requiring transplants. Despite considerable efforts, controlling differentiation of pluripotent cells in culture has proved challenging. *In vivo*, ES cells are governed by a complex set of factors present in the stem cell niche, which is both difficult to completely characterise and, as a result, replicate in culture. As a result, ES and iPS cells tend to spontaneously differentiate to produce undesired cells and tissues during cell culture differentiation protocols. These difficulties have severely hampered regenerative medicine and must be addressed with future research.

In this thesis, MyD88 has been described as a differentiation gate-keeper governing transition to a SR<sup>PR</sup> state. Due to their similarity with EC cells, it is likely that a similar mechanism exists in ES cells, whether this is governed by MyD88 or a different, ES-

specific gate-keeper (Andrews 2002, Andrews et al 2005, Josephson et al 2007). If this is true, it may be possible to transition ES and iPS cells to a  $SR^{PR}$  state through inhibition of a gate-keeper such as MyD88. In this  $SR^{PR}$  state, we hypothesise that ES and iPS cells may be more receptive to lineage differentiation in a controlled fashion. If this hypothesis ultimately holds true, attempts to harness the power of ES and iPS cells for regenerative medicine may be substantially improved. While this was not an intended outcome of the PhD project, it is an important potential legacy that, it is hoped, will be furthered by regenerative medicine researchers following publication of this study.

## **Section 6.8 Future Work**

The results presented in this thesis offer several avenues through which future work could further expand our understanding of CSCs. In this section, several potential future work projects are suggested and their importance discussed.

### **6.8.1 Validation of the $SR^{PR}$ Model: Isolation of $SR^{PR}$ cells**

Unfortunately, isolation of  $SR^{PR}$  cells was not possible within the scope of this project. The models proposed in this thesis can be further validated if it is possible to isolate a pure population of  $SR^{PR}$  cells from 2102Ep cells. This will be one of the main focuses of future work. In this section, we describe two approaches that have been identified through which  $SR^{PR}$  cells may be isolated and the approach through which putative  $SR^{PR}$  cells will be validated.

The first approach will expand upon the de-differentiation approach that was described in Chapter 4. As described earlier, this approach proved successful to a point, after which cells died in cell culture. It is reasonable to assume that some adjustments in the cell culture protocol will allow improved cell survival. The second approach to isolating  $SR^{PR}$  cells is based upon the identification of 20 putative markers (Section 5.3.15.). Initially, all 20 markers will be screened for antibody availability and then, where possible, specific antibodies tested in flow cytometry. It is hypothesised that true  $SR^{PR}$  markers will show a two sub-population result in flow cytometry. The marked population will then be isolated by FACs for further validation. We hypothesise that several of these putative markers will highlight the same sub-population.



Once isolated, putative  $SR^{PR}$  cells will be validated through a three-tiered cell culture protocol as described in Figure 6.3. Firstly, due to the de-differentiation observation described above, we suspect that  $SR^{PR}$  cells may de-differentiate back to a nullipotent 2102Ep state upon removal of MyD88PepInh. This will be tested by removal of MyD88PepInh for several days, which our hypothesis suggests will render the cells unresponsive to RA (Figure 5.10.A). Secondly, we hypothesise that  $SR^{PR}$  cells should remain stably self-renewing and capable of differentiation in response to RA. To test this, putative  $SR^{PR}$  cells will be maintained in MyD88PepInh media for several passages and a sample routinely tested for its ability to differentiate in response to RA (Figure 6.3.B). Thirdly, putative  $SR^{PR}$  cells should readily respond to RA by differentiating (Figure 6.3.C). Through this process, we believe validated  $SR^{PR}$  cells can be isolated for further analysis.

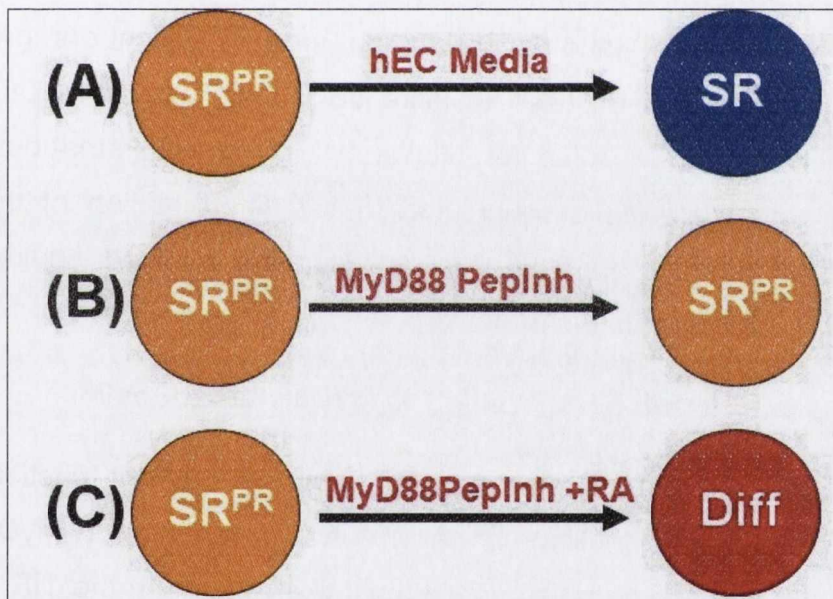


**Figure 6.3. Validation of Putative  $SR^{PR}$  cells.** Putative  $SR^{PR}$  cells will be identified and isolated through de-differentiation or use of potential  $SR^{PR}$  markers identified in gene array analysis. Once isolated,  $SR^{PR}$  cells will be validated based on three defining properties. A)  $SR^{PR}$  cells may return to the original self-renewal (SR) state when cultured in standard (hEC) media. B) PUS cells should remain stable in media containing MyD88 peptide inhibitor (PepInh). C)  $SR^{PR}$  cells should differentiate (Diff) in media containing MyD88PepInh and retinoic acid (+RA).

### 6.8.2. Validation of the $SR^{PR}$ Molecular Mechanism

In Chapter 5, gene array analysis was used to identify several molecular mechanisms, which were proposed as a  $SR^{PR}$  model of 2102Ep differentiation. We

propose that this model could be further validated by functional assessment of the mechanisms developed as future work. Specifically, we hypothesise that inhibition of the specific T2Rs and ORs identified may facilitate RA differentiation of 2102Ep cells in the absence of MyD88 inhibition. In addition, we hypothesise that over-expression of specific HOX genes may facilitate RA differentiation of 2102Ep cells in the absence of MyD88 inhibition. Finally, a RA Receptor Element (RARE) reporter assay could be employed to validate the proposed activation of the RA Signaling pathway. Together, we propose that this work could substantially advance the SR<sup>PR</sup> model of 2102Ep differentiation.

### **6.8.3. Can Nullipotent Cells be Induced to take up Peplnh?**

Our data suggests that the first of the 2 sub-populations (nullipotent cells) does not take up MyD88Peplnh, which facilitates their continued nullipotency. We hypothesise that technologies such as nano-diamonds (an area in which our group has a collaboration partner) could be used to increase the delivery of MyD88Peplnh to these cells, which may induce full differentiation. We hypothesise that better delivery of MyD88Peplnh to these cells could lead to full differentiation of the cell line. Subsequently, any uptake or drug-efflux mechanism involved could be further assessed to build the mechanism further.

### **6.8.4. Are the 2 Sub-Populations Related to MyD88 Mutations?**

We have proposed in this thesis that the MyD88Peplnh may not function in the first of the two sub-populations (nullipotent cells) due to a mutation in MyD88 in those cells. We propose that this mutation would most likely reside in the TIR domain and would change the ability of the Peplnh to bind. This model would suggest that mutated MyD88 proteins in this cell are constantly in homo-dimerisation without competition. This could be tested by sequencing of the TIR domain of MyD88. We hypothesise that this may be the case, and propose that this should be tested in future work.

#### **6.8.5. Is MyD88 Expression Directly Linked to SSEA4 Expression?**

It is noted that, within the scope of this project, it was not possible to provide direct evidence that the differentiated SSEA4<sup>Neg</sup> cells detected at the end of the differentiation protocol are cells in which MyD88 has been inhibited. While the data described here is strong indirect evidence, it is important that some future work to demonstrate this directly be proposed. One option for future work is that MyD88PepInh-treated cells could be double-stained for expression of SSEA4 and MyD88. In this scenario, it would be expected that SSEA4<sup>Pos</sup> cells would be MyD88 positive and SSEA4<sup>Neg</sup> cells would be MyD88 negative. However, as the MyD88PepInh does not affect MyD88 protein expression, this assay would require either A) use of an siRNA, which we have shown is highly inefficient, and/or B) double-staining for SSEA4 and phospho-i-κ-B-α, the detection of which may be technically challenging. As an alternative, it may be possible to demonstrate this through double-staining via immuno-histochemistry. While this work will be technically challenging, it is important that this future work be completed if possible.

#### **6.8.6. The Role of MyD88 in Non-Malignant Human Pluripotent Cells.**

It is noted that further assessment of MyD88 in human pluripotent stem cells could provide important insights for regenerative medicine. In assessing how this would be best studied, it became clear that MyD88 does not play a similar role in murine pluripotency. According to our data, MyD88 knockouts should not be viable, as embryonic development should be substantially diminished. However, several MyD88 knockout mouse models have been described in the literature, which are viable apart from some inflammation defects (DaSilva et al 2014, Salcedo et al 2010, Hou et al 2008, Kawai et al 1999). As such, the role of MyD88 should be studied in human cells and alternative differentiation gate-keepers investigated in mES cells. Although it would be interesting to know whether MyD88 plays a similar role in hES cells, these are not used by our group for ethical and legal reasons. However, it would be possible to investigate the role of MyD88 in iPS cells. While this is not an area of interest to our group, we hope that this will be followed up by iPS researchers following publication of our study.

### **6.8.7. What is the function of TLR7?**

Pluripotency researchers are intrigued by TLR7, which has made it highly topical. On the one hand it is being repeatedly reported that TLR7 is involved in the differentiation of pluripotent cells by many researchers (O'Neill 2012). On the other hand, TLR7 is primarily known as a mediator of TLR Signaling in response to viral nucleotides. Debate continues as to whether TLR7 plays two independent roles, and the MyD88 2102Ep differentiation mechanism described in this thesis could be exploited to address this question. Specifically, TLR7 is 24 fold upregulated upon addition of RA to MyD88 inhibited 2102Ep cells. As such, we propose two further TLR7 experiments. Primarily, it is proposed that TLR7 be knocked down by siRNA in MyD88 PepInh treated cells, which would then be challenged to differentiation via RA. If TLR7 is necessary for this differentiation mechanism, then siTLR7 treatment should stop differentiation from occurring. In addition, we propose to treat 2102Ep cells with a TLR7 over-expression plasmid, which may facilitate differentiation in the absence of MyD88 inhibition. Together, these experiments will allow determination of whether TLR7 is necessary or sufficient for differentiation of 2102Ep cells.

### **6.8.9. What are the roles of the microRNAs?**

In the course of this study, a collection of miRNAs were identified as being specific regulators of A) MyD88 inhibition and B) RA-induced differentiation. As our lab has extensive experience in functional and mechanistic assessment of miRNAs, we propose to select a panel of the top differentially expressed miRNAs for functional assessment. Using 'anti-miR' and 'pre-miR' technologies in previously optimised protocols, specific miRNAs could be assessed, and miRNAs necessary and/or sufficient for the process selected for further functional analysis.

### **6.8.10. A Comparison of NTera2 and 2102Ep Differentiation Mechanisms.**

In Chapter 4 it was shown that incubation of MyD88 inhibited 2102Ep cells with DiffConn media from NTera2 cells was sufficient for differentiation. Adding to this, it was shown in Chapter 5 that NTera2 differentiated cell gene arrays had strong differences to MyD88PepInh+RA induced SSEA4<sup>Neg</sup> cells. In future work, we propose that it would be interesting to analyse whether Diff Conn media induced SSEA4<sup>Neg</sup> 2102Ep differentiation using a mechanism that was more similar to

NTera2. This would allow further understanding of the differences between these cell lines, which appear to simply be their differentiation potential. This experiment may answer a fundamental question about whether 2102Ep cells can differentiate using an NTera2 mechanism under any circumstances, which is important in our efforts to understand differentiation-resistance during tumourigenesis.

#### **6.8.12. Pluripotent Differentiation of 2102Ep and NTera2 cells.**

In Chapter 4, it was noted that 2102Ep cells could partially respond to differentiation kits specific for endoderm, mesoderm or ectoderm lineage differentiation. As a final piece of future work, we propose that it would be interesting to further assess lineage differentiation in both 2102Ep and NTera2 cells. Specifically, we propose that with further optimisation it may be possible to demonstrate that MyD88 is a regulator of all 3 lineages in 2102Ep cells. In addition, optimisation of these protocols for NTera2 cells would demonstrate if any negative result is specific to that lineage or to both hEC cell types. Once optimised, we propose that gene array analysis of each lineage differentiation protocol in each cell type could provide important information for regenerative medicine researchers attempting to generate such lineages consistently from iPS cells.

## References

Note: Our group has recently published comprehensive reviews of stem cell and cancer stem cell theory and background (Ffrench et al 2014, 2015). These references are used for all general background citation in the thesis.

Akira. 2006. TLR signaling. **Current Topics in Microbiology and Immunology**. 311: 1-16.

Al-Hajj et al 2003. Prospective identification of tumorigenic breast cancer cells. **Proceedings of the National Academy of Sciences, USA**. 100(7): 3983-3988.

Alder et al 2000. A novel family of taste receptors. **Cell**. 100(6): 693-702. PMID: 10761934.

Alharbi et al 2013. The role of HOX genes in normal hematopoiesis and acute leukemia. **Leukemia**. 27: 1000-1008.

Andrews et al 1980. A comparative study of eight cell lines derived from human testicular teratocarcinoma. **International Journal of Cancer**. 26: 269-280.

Andrews et al 1982. Cell-surface antigens of a clonal human embryonal carcinoma cell line: morphological and antigenic differentiation in culture. **International Journal of Cancer**. 29: 523-531.

Andrews et al. 1984a. Pluripotent embryonal carcinoma clones derived from the human teratocarcinoma cell line Tera-2. **Laboratory Investigations**. 50(2): 147-162.

Andrews et al. 1984b. Three monoclonal antibodies defining distinct differentiation antigens associated with different high molecular weight polypeptides on the surface of human embryonal carcinoma cells. **Hybridoma**. 3(4): 347-361.

Andrews et al 1990. Different patterns of glycolipid antigens are expressed following differentiation of TERA-2 human embryonal carcinoma cells induced by retinoic acid, hexamethylene bisacetamide (HBMA) or bromodeoxyuridine (BUdR). **Differentiation**. 43: 131-138.

Andrews 2002. From teratocarcinomas to embryonic stem cells. **Philosophical Transactions of the Royal Society of London B Biological Sciences**. 357:405–417.

Andrews et al 2005. Embryonic stem (ES) cells and embryonal carcinoma (EC) cells: opposite sides of the same coin. **Biochemical Society Transactions**. 33(Pt6): 1526-1530.

Atkinson et al 2008. Epigenetic marking prepares the human HOXA cluster for activation during differentiation of pluripotent cells. **Stem Cells**. 26(5): 1174-1185.

Bao et al 2012. Targeting CSC-related miRNAs for cancer therapy by natural agents. **Current Drug Targets**. 13(14): 1858-1868. PMID: 23140295.

Barnea et al 2004. Odorant receptors on the axon termini in the brain. **Science**. 304(5676): 1468.

Barton and Kagan 2009. A cell biological view of Toll-like receptor function: regulation through compartmentalisation. **Nature Reviews Immunology**. 9(8): 532-542.

Beutler 2007. Neo-ligands for innate immune receptors and the etiology of sterile inflammatory disease. **Immunological Reviews**. 220: 113-128.

Bekisz et al 2010. Antiproliferative properties of Type I and Type II interferon. **Pharmaceuticals**. 3: 994-1015.

Bolstad et al 2003. A comparison of normalisation methods for high density oligonucleotide array data based on variance and bias. **Bioinformatics**. 19(2): 185-193.

Bonham et al 2014. A promiscuous lipid-binding protein diversifies the subcellular sites of toll-like receptor signal transduction. **Cell**. 156: 705-716.

Bonnet and Dick 1997. Human acute leukemia is organised as a hierarchy that originates from a primitive hematopoietic cell. **Nature Medicine**. 3(7): 730-737.

Carvalho and Irizarry 2010. A framework for oligonucleotide microarray preprocessing. **Bioinformatics**. 26(19): 2363-2367.

Chambon 1996. A decade of molecular biology of retinoic acid receptors. **The FASEB Journal**. 10:949 -954.

Chambers et al 2003. Functional expression cloning of Nanog, a pluripotency sustaining factor in embryonic stem cells. **Cell**. 113: 643-655.

Chen et al 2007. Suppression of ES cell differentiation by retinol (vitamin A) via the overexpression of Nanog. **Differentiation**. 75, 682-693.

Cooke, A. MyD88: A key regulator of chemoresistance, differentiation and hypoxia resistance in cancer stem cells? 2013. **PhD Thesis**, University of Dublin, Trinity College Dublin.

Copley et al 2012. Hematopoietic Stem Cell heterogeneity takes centre stage. **Cell Stem Cell**. 10: 690-697.

Cunningham and Deuster 2015. Mechanisms of retinoic acid signaling and its roles in organ and limb development. **Nature Reviews Molecular Cell Biology**. 16: 110-123.

D'Adhemar et al 2014. The MyD88+ phenotype is an adverse prognostic factor in epithelial ovarian cancer. **PLoS One**. 9(6): e100816.

DaSilva et al 2014. MyD88 knockout mice develop initial enlarged periapical lesions with increased numbers of neutrophils. **International Endodontic Journal**. 47: 675-686.

DeRossi et al 1994. The third helix of the Antennapedia homeodomain translocates through biological membranes. **Journal of Biological Chemistry**. 269: 10444-10450.

DiGioia and Zanoni 2015. Toll-like receptor co-receptors as master regulators of the immune response. **Molecular Immunology**. 63: 143-152.

DeMaria and Ngai 2010. The cell biology of smell. **Journal of Cell Biology**. 191(3): 443-452.

Das et al 2014. Retinoic acid signaling pathways in development and diseases. **Bioorganic and Medicinal Chemistry**. 22(2): 673-683.

Duran et al 2001. Hybrids of pluripotent and nullipotent human embryonal carcinoma cells: partial retention of a pluripotent phenotype. **International Journal of Cancer**. 93: 324-332.

Dweep et al 2011. miRWalk-Satabase: prediction of possible miRNA binding sites by 'walking the genes of three genomes'. **Journal of Biomedical Informatics**. 44(5): 839-847.

Evans 2011. Discovering pluripotency: 30 years of mouse embryonic stem cells. **Nature Reviews Molecular Cell Biology**. 12(10): 680-686.

Evans and Kaufman 1981. Isolation of pluripotent cells from mouse embryos. **Nature**. 292(5819): 154-156.

Feng et al 2012. Expression and secretion of TNF- $\alpha$  in mouse taste buds: a novel function of a specific subset of type II taste cells. **PLoS ONE**. 7(8): e43140.

Gallagher et al 2009. Regulation of microRNA biosynthesis and expression in 2102Ep embryonal carcinoma stem cells is mirrored in ovarian serous adenocarcinoma patients. **Journal of Ovarian Research**. 2:19.

Gallagher et al 2012. Suppression of cancer stemness p21-regulating mRNA and microRNA signatures in recurrent ovarian cancer patient samples. **Journal of Ovarian Research**. 5: 2.

Hashimoto et al 1988. The Toll gene in *Drosophila*, required for dorsal-ventral embryonic polarity, appears to encode a transmembrane protein. **Cell**. 52: 269-279.

Hong and Carmichael 2013. Innate immunity in pluripotent human cells: attenuated response to interferon- $\beta$ . **Journal of Biological Chemistry**. 288(22): 16196-16205.



- Hou et al 2008. Toll-like receptors activate innate and adaptive immunity by using dendritic cell-intrinsic and –extrinsic mechanism. **Immunity**. 29: 272-282.
- Hu et al 2011. miRTar: an integrated system for identifying miRNA-target interactions in human. **BMC Bioinformatics**. 12(1): 330.
- Huang et al 2009. Systematic and integrative analysis of large gene lists using DAVID bioinformatics resources. **Nature Protocols**. 4:44-57.
- Ioiarro et al 2005. Peptide-mediated interference of TIR domain dimerization in MyD88 inhibits interleukin-1-dependent activation of NF- $\kappa$ B. **Journal of Biological Chemistry**. 280: 15809-15814.
- Irudayam et al 2015. Characterisation of type 1 interferon pathway during hepatic differentiation of human pluripotent stem cells and hepatitis C virus infection. **Stem Cell Research**. 15(2): 354-364.
- Irizarry et al 2003a. Summaries of affymetrix GeneChip probe level data. **Nucleic Acids Research**. 31(4): e15.
- Irizarry et al 2003b. Exploration, normalisation and summaries of high density oligonucleotide array probe level data. **Biostatistics**. 4(2): 249-264.
- Janssens and Beyaert 2002. A universal role for MyD88 in TLR/IL-1R-mediated signaling. **Trends in Biochemical Sciences**. 27(9): 474-482.
- Josephson R, Ording CJ and Liu Y et al. Quantification of embryonal carcinoma 2012E as a reference for human embryonic stem cell research. *Stem Cells*. 2007; 25: 437-446.
- Kaupp 2010. Olfactory signaling in vertebrates and insects: differences and commonalities. **Nature Reviews Neuroscience**. 11: 188-200.
- Kannagi et al 1983. Stage-specific embryonic antigens (SSEA-3 and -4) are epitopes of a unique globo-series ganglioside isolated from human teratocarcinoma cells. **The EMBO Journal**. 2(12): 2355-2361.
- Kawai et al 1999. Unresponsiveness of MyD88-deficient mice to endotoxin. **Immunity**. 11(1): 115-122.
- Kelly et al 2006. TLR-4 signaling promotes tumor growth and paclitaxel chemoresistance in ovarian cancer. **Cancer Research**. 66(7): 3859-3868.
- Kenzel et al 2009. Egr1 Role of p38 and early growth response factor 1 in the macrophage response to group B streptococcus. **Infection and Immunity**. 77(6): 2474-2481.
- Kleinsmith and Pierce 1964. Multipotentiality of single embryonal carcinoma cells. **Cancer Research**. 24; 1544-1551.

Kreso and Dick 2014. Evolution of the cancer stem cell model. **Cell Stem Cell**. 14(3): 275-291. PMID: 24607403.

Lam et al 2014. Rapid and efficient differentiation of human pluripotent cells into intermediate mesoderm that forms tubules expressing kidney proximal tubular markers. **Journal of the American Society of Nephrology**. 25(6): 1211-1225.

Lappin et al 2006. Hox genes: seductive science, mysterious mechanisms. **Ulster Medical Journal**. 75(1): 23-31.

Larsen et al 1994. Retinoic acid induces expression of early growth response gene-1 (Egr-1) in human skin *in vivo* and in cultured skin fibroblasts. **The Journal of Investigative Dermatology**. 102(5): 730-740.

Lee et al 2004. MicroRNA maturation: stepwise processing and subcellular localisation. **EMBO Journal**. 21(17): 4663-4670.

Lee et al 2012. Activation of innate immunity is required for efficient nuclear reprogramming. **Cell**. 151(3): 547-558.

Li 2013. Taste perception: from the tongue to the testis. **Molecular Human Reproduction**. 19(6): 349-360.

Li et al 2013. starBase v2.0: decoding miRNA-ceRNA, miRNA-ncRNA and protein-RNA interaction networks from large-scale CLIP-Seq data. **Nucleic Acid Research**. 42(D1): D92-D97.

Liebermann and Hoffman 2002. OMyeloid differentiation (MyD) primary response genes in hematopoiesis. **Oncogene**. 21: 3391-3402.

Livak and Schmittgen 2001. Analysis of relative gene expression data using real-time quantitative PCR and the 2-ddCt method. **Methods**. 25: 402-408.

Loh and Lim. 2011. A precarious balance: pluripotency factors as lineage specifiers. **Cell Stem Cell**. 8: 363-369.

Lord et al 1990. Complexity of the immediate early response of myeloid cells to terminal differentiation and growth arrest includes ICAM-1, Jun-B and histone variants. **Oncogene**. 5: 387-396.

Lu et al 2008. LPS/TLR4 signal transduction pathway. **Cytokine**. 42(2): 145-151.

McAuliffe et al 2012. Targeting Notch, a key pathway for ovarian cancer stem cells, sensitises tumors to platinum therapy. **Proceedings of the National Academy of Sciences USA**. 109(43): E2939-E2948.

Mallo and Alonso 2013. The regulation of Hox gene expression during animal development. **Development**. 140: 3951-3963.

Marletz et al 2006. Retinoic acid signaling and the evolution of chordates. **International Journal of Biological Sciences**. 2(2): 38-47.

Matin et al 2004. Specific knockdown of Oct4 and beta2-microglobulin expression by RNA interference in human embryonic stem cells and embryonic carcinoma cells. **Stem Cells**. 22(5): 659-668.

Medzhitov et al 1997. A human homologue of Drosophila toll protein signals activation of adaptive immunity. **Nature**. 388(6640): 394-397.

Nelson et al 2001. Mammalian sweet taste receptors. **Cell**. 106(3): 381-390.

Nelson et al 2015. dsRNA released by tissue damage activates TLR3 to drive skin regeneration. **Cell Stem Cell**. 17: 139-151.

O'Neill 2012. Transflammation: when innate immunity meets induced pluripotency. **Cell**. 151(3): 471-473.

O'Neill et al 2013. The history of Toll-like receptors-redefining innate immunity. *Ature reviews immunology*. 13(6): 453-460. PMID: 23681101.

Pare and Sullivan 2014. Distinct antiviral responses in pluripotent versus differentiated cells. **PLoS Pathology**. 10(2):e1003865.

Paschaki et al 2013. Retinoic acid regulates olfactory progenitor cell fate and differentiation. **Neural Development**. 8: 13-23.

Patel et al 2012. Toll-like receptors in ischaemia and its potential role in the pathophysiology of muscle damage in critical limb ischaemia. **Cardiology Research and Practice**. 2012: 121237.

Quinonez and Innis 2014. Human Hox gene disorders. **Molecular Genetics and Metabolism**. 111(1): 4-15.

Reya et al 2011. Stem cells, cancer and cancer stem cells. **Nature**. 414 : 105-111.

Ritchie et al 2015. Limma powers differential expression analysis for RNA-sequencing and microarray studies. **Nucleic Acids Research**. 43(7) : e47.

Rizzino 2013. The Sox2-Oct4 Connection : Critical players in a much larger interdependent network integrated at multiple levels. **Stem Cells**. 31(6) : 1033-1039.

Schuettengruber et al 2007. Genome regulation by polycomb and trithorax proteins. **Cell**. 128(4): 735-745.

Salcado et al 2014. MyD88-mediated signaling prevents development of adenocarcinomas of the colon: role of interleukin 18. **Journal of Experimental Medicine**. 207 (8): 1625-1636.

Schulinder et al 2000. Effects of eight growth factors on the differentiation of cells derived from human embryonic stem cells. **Proceedings of the Academy of Sciences, USA**. 97(21): 11307-11312.

Shah and Sukumar 2010. The Hox genes and their roles in oncogenesis. **Nature Reviews Cancer**. 10(5): 361-371.

Silva and Smith. 2008. Capturing pluripotency. **Cell**. 132: 532-538.

Simeone et al 1991. Differential regulation by retinoic acid of the homeobox genes of the four HOX loci in human embryonal carcinoma cells. **Mechanisms of Development**. 33(3): 215-227.

Shen et al 2008. EZH1 mediates methylation on histone H3 lysine 27 and complements EZH2 in maintaining stem cell identity and executing pluripotency. **Molecular Cell**. 32: 491-502.

Solter and Knowles 1979. Developmental stage-specific antigens during mouse embryogenesis. **Currents Topics in Developmental Biology**. 13 (1): 139-165.

Stefkova et al 2015. Alkaline Phosphatase in Stem Cells. **Stem Cells International**. 2015: 628368.

Sullivan et al 2010. Generation of functional human hepatic endoderm from human induced pluripotent stem cells. **Hepatology**. 51(1): 329-335.

Surmacz et al 2012. Directing differentiation of human embryonic stem cells towards anterior neural ectoderm using small molecules. **Stem Cells**. 31(7): 1446.

Takahashi et al. 2007. Induction of pluripotent stem cells from adult human fibroblasts by defined factors. **Cell**. 131: 1-12.

Takeda et al 2003. Toll-like receptors. **Annual Review of Immunology**. 21: 335-376.

Thomson et al 1998. Embryonic stem cell lines derived from human blastocysts. **Science**. 282: 1145-1147.

Toshchakov et al 2005. Differential involvement of BB loops of Toll-IL-1 resistance (TIR) domain-containing adapter proteins in TLR4- versus TLR2-mediated signal transduction. **Journal of Immunology**. 175: 494-450.

Vencken et al 2014. An integrated analysis of the Sox2 microRNA response program in human pluripotent and nullipotent stem cells. **BMC Genetics**. 15: 711.

Wang et al 2009. Toll-like receptors and cancer: MyD88 mutation and inflammation. **Frontiers in Immunology**. 5(367): 1-10.

Wang et al 2011. Rapid and efficient reprogramming of somatic cells to induced pluripotent stem cells by retinoic acid receptor gamma and liver receptor homolog 1. **Proceedings of the National Academy of Sciences USA**. 108(45): 18283-18288.

Ward et al 2015. Toll receptors instruct axon and dendrite targeting and participate in synaptic partner matching in a Drosophila olfactory circuit. **Neuron**. 85(5): 1013-1028.

Watanabe et al 2007. Requirement of glycosylphosphatidylinositol anchor of Cripto-1 for trans activity as a nodal co-receptor. **Journal of Biological Chemistry**. 282(49): 35772-35786.

Watanabe et al 2010. Cripto-1 is a cell surface marker for a tumorigenic, undifferentiated subpopulation in embryonal carcinoma cells. **Stem Cells**. 28(8): 1301-1314.

Whitesides et al 1998. Retinoid signaling distinguishes a subpopulation of olfactory receptor neurons in the developing adult mouse. **The Journal of Comparative Neurology**. 394: 445-461.

Xu et al 2013. Functional characterisation of bitter-taste receptors in the mammalian testis. **Molecular Human Reproduction**. 19(1): 17-28.

Yabuuchi et al 2013. Notch Signaling pathway targeted therapy suppresses tumor progression and metastatic spread in pancreatic cancer. **Cancer Letters**. 335: 41-51.

Yamamoto and Takeda 2010. Current views of toll-like receptor signaling pathways. **Gastroenterology Research and Practice**. 2010: 240365.

Yang et al 2010. StarBase: a database for exploring microRNA-mRNA interaction maps for Argonaute CLIP-Seq and degradome-Seq data. **Nucleic Acids Research**. 39: D202-D209.

Yi et al 2003. Exportin-5 mediates the nuclear export of pre-microRNAs and short hairpin RNAs. **Genes and Development**. 17(24): 3011-3016.

Appendix 1.

Top 20 Up and Downregulated genes MyD88 vs Ctrl (Ref Section 5.4)

MyD88Peplnh vs Ctrl Peplnh Upregulated genes				MyD88Peplnh vs Ctrl Peplnh downregulated genes			
Description	Gene	Fold Change	p-Value	Description	Gene	Fold Change	p-Value
histone cluster 1, H3h	HIST1H3H	3.982	0.0028	early growth response 1	EGR1	-12.53	0.0006
poly(A) binding protein interacting protein 2	PAIP2	3.72	0.00079	RNA, U6 small nuclear pseudogene	RNU6-679P	-6.00	0.00086
homeobox A1	HOXA1	3.38	0.0017	Rho-associated, coiled-coil containing protein kinase 1 pseudogene 1	ROCK1P1	-5.80	0.0044
arylacetamide deacetylase-like 3	AADA3L3	3.19	0.00099	FBJ murine osteosarcoma viral oncogene homolog	FOS	-4.91	0.00095
histone cluster 1, H2aj	HIST1H2AJ	2.98	0.01078	RNA, 5S ribosomal pseudogene 311	RNA5SP311	-4.84	0.0091
molybdenum cofactor sulfurase	MOCOS	2.91	0.0031	coiled-coil domain containing 129	CCDC129	-4.72	0.001
tripartite motif containing 49B	TRIM49B	2.80	0.0047	RNA, U6 small nuclear pseudogene	RNU6-522P	-4.66	0.003
homeobox D13	HOXD13	2.79	0.0020	neurtin 1	NRN1	-4.65	0.0006
annexin A3	ANXA3	2.69	0.0018	ubiquitin specific peptidase 17-like family member 15	USP17L15	-4.569	0.0017
chromosome 9 open reading frame 129	C9orf129	2.67	0.0023	RNA, 5S ribosomal pseudogene 311	RNA5SP311	-4.244	0.007

MyD88PepInh vs Ctrl PepInh Upregulated genes				MyD88PepInh vs Ctrl PepInh downregulated genes			
Description	Gene	Fold Change	p-Value	Description	Gene	Fold Change	p-Value
annexin A1	ANXA1	2.66	0.0017	RNA, 5S ribosomal pseudogene 311	RNA5SP31	-4.10	0.0096
olfactory receptor, family 3, subfamily A, member 1	OR3A1	2.64	0.0022	G antigen 2A	GAGE2A	-3.87	0.0079
taxilin gamma pseudogene, Y-linked	TXLNGY	2.55	0.00281	nuclear paraspeckle assembly transcript 1 (non-protein coding)	NEAT1	-3.57	0.0011
methyl-CpG binding domain protein 3-like 3	MBD3L3	2.45	0.0022	ribosomal modification protein rimK-like family member A	RIMKLA	-3.40	0.0015
zinc finger, CCHC domain containing 12	ZCCHC12	2.44	0.018	RNA, U6 small nuclear 620, pseudogene	RNU6620P	-3.35	0.0033
cadherin 2, type 1, N-cadherin (neuronal)	CDH2	2.44	0.0028	uropod protein 1A	UPK1A	-3.32	0.00079
apelin receptor early endogenous ligand	APELA	2.43	0.0030	olfactory receptor, family 56, subfamily A, member 1	OR56A1	-3.29	0.011
RNA, U1 small nuclear 122, pseudogene	RNU1-122P	2.42	0.0022	RNA, 5S ribosomal pseudogene 98	RNA5SP98	-3.28	0.0023
homeobox A2	HOXA2	2.41	0.0052	REX1, RNA exonuclease 1 homolog (S. cerevisiae)-like 1, pseudogene	REXO1L1P	-3.278	0.038
CD97 molecule	CD97	2.38	0.0064	REX1, RNA exonuclease 1 homolog (S. cerevisiae)-like 8, pseudogene	REXO1L8P	-3.249	0.0049

## Appendix 2.

### Top 20 Up and Downregulated genes SSEA4<sup>neg</sup> vs MyD88PepInh (Ref Section 5.3.8)

SSEA4 <sup>neg</sup> vs MyD88PepInh Upregulated genes				SSEA4 <sup>neg</sup> vs MyD88PepInh downregulated genes			
Description	Gene	Fold Change	p-Value	Description	Gene	Fold Change	p-Value
mucin 15, cell surface associated glycoprotein hormones, alpha polypeptide	MUC15	328.0	3.41E-07	secreted frizzled-related protein 2	SFRP2	-24.8	6.81E-07
endogenous retrovirus group FRD, member 1	CGA	301.5	8.73E-08	Zic family member 3	ZIC3	-19.3	6.05E-07
vestigial-like family member 1	ERVFRD-1	138.96	8.73E-08	protein tyrosine phosphatase, receptor-type, Z polypeptide 1	PTPRZ1	-15.96	7.66E-07
interferon-induced protein 44-like	VGLL1	86.18	8.73E-08	lysophosphatidic acid receptor 4	LPAR4	-15.2	7E-07
cytochrome P450, family 26, subfamily A, polypeptide 1	IF144L	85.40	8.73E-08	kinase insert domain receptor (a type III receptor tyrosine kinase)	KDR	-14.1	8.25E-07
low density lipoprotein receptor-related protein 2	CYP26A1	81.72	1.0E-07	brain expressed, X-linked 1	BEX1	-12.9	7.28E-06
GATA binding protein 3	LRP2	54.66	1.0E-07	metallothionein 1M	MT1M	-12.74	6.13E-07
nuclear receptor subfamily 2, group F, member 2	GATA3	45.28	1.29E-07	TIMP metalloproteinase inhibitor 4	TIMP4	-12.64	9.32E-07
FYN binding protein	NR2F2	44.52	1.15E-06	Neurotensin	NTS	-12.3	2E-06
	FYB	42.87	4.69E-07	metallothionein 1L (gene/pseudogene)	MT1L	-12.0	3.22E-05



SSEA4 <sup>neg</sup> vs MyD88PepInh Upregulated genes					SSEA4 <sup>neg</sup> vs MyD88PepInh downregulated genes				
Description	Gene	Fold Change	p-Value	Description	Gene	Fold Change	p-Value		
oxidized low density lipoprotein (lectin-like) receptor 1	OLR1	42.55	3.40E-07	ectonucleotide pyrophosphatase/phosphodiesterase 2	ENPP2	-11.69	6.24E-07		
2'-5'-oligoadenylate synthetase 2, 69/71kDa	OAS2	39.72	2.93E-07	apelin receptor early endogenous ligand	APELA	-11.66	3.03E-06		
lectin, galactoside-binding, soluble, 16	LGALS16	39.65	1.88E-06	pipecolic acid oxidase	PIPOX	-11.47	1.15E-06		
urothelial cancer associated 1 (non-protein coding)	UCA1	39.56	1.09E-07	dihydropyrimidinase-like 3	DPVSL3	-11.04	1.05E-06		
keratin 23 (histone deacetylase inducible)	KRT23	36.32	2.0E-06	insulin-like growth factor binding protein-like 1	IGFBP11	-10.45	1.07E-05		
interferon-induced protein with tetratricopeptide repeats 3	IFIT3	35.59	6.24E-07	EGF-like repeats and discordin 1-like domains 3	EDIL3	-10.21	1.56E-06		
endoplasmic reticulum protein 27	ERP27	35.31	4.69E-07	nudix (nucleoside diphosphate linked moiety X)-type motif 11	NUDT11	-10.18	1.68E-06		
interferon induced with helicase C domain 1	IFIH1	31.50	6.57E-07	C-type lectin domain family 4, member D	CLEC4D	-10.16	1.15E-06		
glial cells missing homolog 1 (Drosophila)	GCM1	31.38	3.18E-07	coiled-coil domain containing 172	CCDC172	-10.15	2.78E-06		
growth regulation by estrogen in breast cancer-like	GREB1L	29.22	3.25E-07	calbindin 1, 28kDa	CALB1	-9.94	1.27E-06		